DOI: *http://dx.doi.org/10.22122/johoe.v10i3.1208* *Published by Vesnu Publications*

Received: 09 Mar. 2021 **Accepted: 05 May 2021**

ABO blood group phenotypes and dental disorders-Is there any relation? A cross sectional study in Haridwar, Uttarakhand, India

Acharya Balkrishna D Litt (Yoga)[1], Kuldeep Singh BDS[2], Abhishek Sharma MDS[3], Vinay Kumar Sharma PhD[4], Swami Narsingh Chandra Dev PhD[4], Gurpreet Oberoi BDS[5], Paran Gowda PhD[6]

Original Article

Abstract

BACKGROUND AND AIM: Research has focused on relating ABO blood group systems and different systemic disorders in recent years. Studies showing relation between dental disorders and ABO blood groups, to date, are limited. The current study was undertaken to explore whether blood group affects dental diseases, especially dental caries.

METHODS: 346 patients who attended the Dental Clinic and Research Center, Patanjali Ayurved Hospital, Haridwar, India, were randomly selected for the study. Patients who showed their blood group test performed in a registered pathological laboratory or in our pathobiology laboratory were included in the study. Dental caries were recorded based on the Decayed, Missing, and Filled Teeth (DMFT) index issued by the World Health Organization (WHO).

RESULTS: The prevalence of caries among the adults and older people was within 100% both in Yerevan and its regions. The most common dental disorder was dental caries among all blood groups. Dental caries were more prevalent in blood group B, followed by O, A, and AB. No significant correlation was found between the DMFT index score and blood groups.

CONCLUSION: Further studies are required on a larger population to conclude any correlation between the ABO blood group phenotypes and dental disorders.

KEYWORDS: Dental Caries; Dental Attrition; Dental Disease; ABO Blood Group System

Citation: Balkrishna A, Singh K, Sharma A, Sharma VK, Chandra SN, Oberoi G, et al. **ABO blood group phenotypes and dental disorders-Is there any relation? A cross sectional study in Haridwar, Uttarakhand, India.** J Oral Health Oral Epidemiol 2021; 10(3): 122-7.

Oral diseases pose a major public health burden worldwide.[1] Dental caries are one of the most prevalent oral diseases which occur due to demineralization of enamel.[2] Likewise, periodontitis is the main cause of tooth loss, which occurs due to inflammatory disruption of periodontal tissues.[3] Additionally, periodontium is also damaged due to the persistent movement of the mobile tooth in oral function, which further accelerates the disease progression implying tooth loss.[4] Food consistency and muscle strength affect occlusal attrition (OA), while the interproximal attrition results from the adjacent teeth differential movement.[5,6] The amount of attrition varies with age, gender, and type of tooth and depends on the tooth's position in size and morphology in the jaw.[7,8] Abrasion is a pathological process that occurs due to abrasive substances on the tooth surface or any item found continually on the

1- Vice Chancellor, University of Patanjali, Haridwar, Uttarakhand, India
2- Dental Officer, Dental Clinic and Research Centre, Patanjali Ayurved Hospital, Haridwar, Uttarakhand, India
3- Assistant Professor, Public Health Dentistry, RUHS College of Dental Sciences (Government Dental College and Hospital), Jaipur, Rajasthan, India
4- Assistant Professor, Patanjali Research Institute, University of Patanjali, Haridwar, Uttarakhand, India
5- Instructor, Dental Clinic and Research Centre, Patanjali Ayurved Hospital, Haridwar, Uttarakhand, India
6- Professor, Patanjali Research Institute, University of Patanjali, Haridwar, Uttarakhand, India
Address for correspondence: Abhishek Sharma MDS; Assistant Professor, Public Health Dentistry, RUHS College of Dental Sciences (Government Dental College and Hospital), Jaipur, Rajasthan, India; Email: drabhi712@gmail.com

teeth or between them.[9,10]

The ABO system was first discovered by Landsteiner and Weiner[11] and had 4 different blood types: O, A, B, and AB. Blood group O erythrocytes do not possess any antigen, but O-serum possesses antibodies to A and B antigens. Erythrocytes of blood groups A and B bear the A and B antigens respectively and make antibodies to the other groups. Type AB erythrocytes have both A and B antigens and do not make antibodies.[12,13] Interestingly, numerous researchers have reported that the blood group variation occurs in different areas and races.[14,15]

For years, scientists have been engrossed in finding the relationship between blood type and well-being. Recent research has provided major advances, indicating a strong relationship between different blood types and diseases varying from infertility to diabetes mellitus (DM). A correlation has been observed between the blood group type and various diseases like dental caries, salivary gland tumors, chickenpox, malaria, oral carcinoma, hematological cancer, cardiac diseases, and cholera. Individuals gallstones, colitis, and tumors of the pancreas as well as ovary, coronary artery disease (CAD), DM.[16-27]

A limited amount of work has been reported in the field of dental research except for few reports on periodontal diseases,[12,16,28-32] dental caries, and salivary gland tumors. Therefore, the present study was carried out with the aim to find any relation between the ABO blood group phenotypes and dental disorders.

Methods

Ethical approval and consent: Approval for the study was obtained from the Institutional Ethics Committee, Haridwar, India. Data were collected from the patients who visited the Dental Clinic and Research Centre, Patanjali Ayurved Hospital, Haridwar. The patients were also informed about the method and purpose of the study and consent was obtained from them. They were instructed to submit their blood group record from certified laboratories.

Inclusion criteria: The study subjects with at least 20 teeth were included. Patients aged between 20 to 60 years, both males and females, participated in the study. Patients who submitted their blood group certificate were selected for the study.

Exclusion criteria: Individuals who refused to give consent for the study, those with uncooperative behavior, and pregnant woman were excluded from the study.

Data collection: A total of 346 patients suffering from oral disorders were included in the study. Oral examination was carried out, and the interview was conducted on behavior and socioeconomic background. The data was collected using oral health examination card, designed by the Dental Research Centre, Haridwar, based on the guidelines provided by the World Health Organization (WHO). Oral health of the patients was assessed while they were sitting on a dental chair using a mouth mirror, a standard WHO probe, and adequate illumination (WHO, 1997). The DMFT index was recorded according to the WHO guidelines. Qualified dentists diagnosed oral disorders of the subjects through visual clinical examination.

The chi-square test was performed using SPSS software (version 20, IBM Corporation, Armonk, NY, USA). Descriptive statistics were carried out to calculate the mean and standard deviation (SD). The analysis of variance (ANOVA) test was performed for dental caries (DMFT score) to show its relation with the ABO group.

Results

239 (69%) and 107 (31%) of the study participants were respectively men and women with a mean age of 38.00 ± 13.74 years. Among the subjects, the most prevalent blood group was B (39%), followed by O (36%), A (17%), and AB (8%) (Figure 1). Dental caries were the most common dental disorder among the subjects (Figure 2 and Table 1).

Table 1. Distribution of different dental disorders among the blood groups

Dental disorders	Blood group A (n = 59)	Blood group AB (n = 29)	Blood group B (n = 133)	Blood group O (n = 125)
	n (%)	n (%)	n (%)	n (%)
Dental caries	34 (57.63)	20 (68.97)	85 (63.91)	79 (63.20)
Missing teeth	23 (38.98)	10 (34.48)	56 (42.11)	40 (32.00)
Filled teeth	17 (28.81)	6 (20.69)	37 (27.82)	37 (29.60)
Mobile teeth	5 (8.47)	11 (37.93)	9 (6.77)	3 (10.40)
Impacted teeth	3 (5.08)	0 (0)	11 (8.27)	13 (5.60)
Cervical abrasion	8 (13.56)	3 (10.34)	14 (10.53)	7 (18.40)
Attrition	1 (1.69)	1 (3.45)	15 (11.28)	23 (16.00)

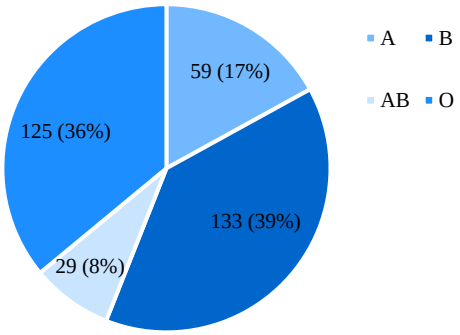

Figure 1. Distribution of blood groups among the subjects

Out of the 346 individuals, 336 had dental caries decayed, missing, or filled components. There was no statistically significant difference among different blood groups in relation to the DMFT score (Table 2).

Table 2. Dental caries [Decayed, Missing, and Filled Teeth (DMFT) index] associated with blood groups

Blood group	n	DMFT (Mean ± SD)	P (ANOVA)
Blood group A	57	2.91 ± 2.30	0.97 (NS)
Blood group AB	28	2.92 ± 2.90	
Blood group B	129	2.99 ± 2.60	
Blood group O	122	3.10 ± 2.40	
Total	336	3.01 ± 2.80	

P value < 0.05 was considered as statistically significant.
NS: Not Significant; DMFT: Decayed, Missing, and Filled Teeth; ANOVA: Analysis of variance

Discussion

For a long time, dental caries have been the most prevalent disease in the history of dentistry. The major etiological factors for dental caries are plaque, dietary factors, and oral hygiene; however, the role of genetics, e.g. blood groups, cannot be ruled out. The ABO blood group has a major role in blood transfusion process, organ transplantation procedures, and in many gastric and physiological processes.[12,33] Similarly, a study[34] elaborated the relation between the ABO blood group and their propensity to chronic disease. Later on, a number of trials were performed to establish the relationship of the ABO blood group with various diseases; however, only a few of them are related to dental diseases. Most of these dental diseases are periodontal or dental caries; interestingly, there is no consistency in the reports on dental disease.[12,35] This inconsistency of the results was maybe due to the region or the population to which they belong.[29,36]

In the present study, no significant correlation was found between the ABO blood group and dental caries, which is similar to the findings of other studies.[34,37,38]

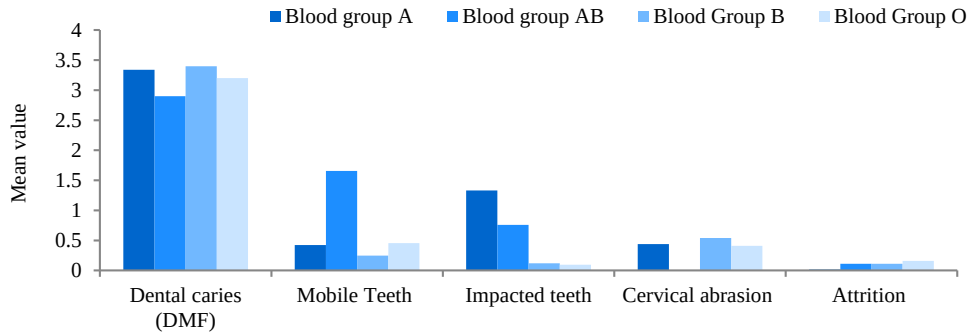

Figure 2. Distribution of dental disorders among the blood groups

Dental caries were more prevalent among individuals with blood group B. Similarly, we also observed that the AB group is more prevalent than the other groups, followed by B, A, and O in other dental diseases like mobile teeth. In the case of impacted teeth, the most prevalent group is O, followed by B and A; however, in our study, none of the AB group patients had impacted teeth.

In a study,[39] the DMFT score was more in the A and B blood groups, followed by the AB group, with the least score being in the individuals with O blood type. However, in our study, blood group B was the most prevalent, followed by O, A, and AB blood groups, which contradicts the result of the above study. The association of blood group phenotypes with dental caries (DMFT score) can be elaborated by the secretion of blood group substance in saliva, which may aggregate the microorganisms, and subsequently moving out them from the oral cavity. It is suggested that the release of ABO antigens into saliva may hamper microbes' capability to bind with tooth surface as lectins being ABO specific, which they use for binding. In one of the studies, no association between the DMFT scores and the ABO and MN system was observed.[34,40] In contrast, Roark and Leyschon[41] observed a significant association between the MN blood group and dental caries. In another study, the lowest and highest mean values of the DMFT index were in blood groups B and AB as 3.9 and 4.9, respectively;[38] however, no difference was observed between them (P = 0.09). These results further strengthen our view that though the ABO blood group was proven crucial in correlation with various diseases, it can still not be correlated with dental diseases like dental caries in a small number of patients. Large multicentric epidemiological trials are required to find out the correlation between the ABO group and dental disease, especially in the case of dental caries.

As our results reflect findings on patients from dental health care center from a specific region, these should be interpreted cautiously. The limited and specific type of the study population was one of the limitations of the study. Geographical, racial, and ethnic diversity can affect these findings. In addition, the Rhesus (Rh) factor could not be considered. Salivary factors were also not taken into account.

Conclusion

Dental caries were more prevalent in blood group B, followed by O, A, and AB. Mobility of teeth was higher in the AB blood group. Individuals with blood group O had more number of impacted teeth. No statistically significant correlation was found between ABO blood groups and dental caries.

Conflict of Interests

Authors have no conflict of interest.

Acknowledgments

The authors would like to appreciate His Holiness Swami Ramdev Ji for his blessings. Dr. Vandana Chauhan and Dr. Archana Rawat, who supported us in data collection and data entry, Mr. N. Karthikeyan for helping in data analysis, and also the patients, Haridwar, for their participation in the study are also appreciated.

References

1. Petersen PE, Bourgeois D, Ogawa H, Estupinan-Day S, Ndiaye C. The global burden of oral diseases and risks to oral health. Bull World Health Organ 2005; 83(9): 661-9.
2. Abid A, Maatouk F, Berrezouga L, Azodo C, Uti O, El-Shamy H, et al. Prevalence and severity of oral diseases in the Africa and Middle East region. Adv Dent Res 2015; 27(1): 10-7.
3. Serio FG. Clinical rationale for tooth stabilization and splinting. Dent Clin North Am 1999; 43(1): 1-6, v.
4. Davies SJ, Gray RJ, Linden GJ, James JA. Occlusal considerations in periodontics. Br Dent J 2001; 191(11): 597-604.
5. Wolpoff MH. Interstitial wear. Am J Phys Anthropol 1971; 34(2): 205-27.
6. Hinton RJ. Differences in interproximal and occlusal tooth wear among prehistoric Tennessee Indians: Implications

for masticatory function. Am J Phys Anthropol 1982; 57(1): 103-15.
7. Van-reenen JF. The effects of attrition on tooth dimensions of San (Bushmen). In: Kurten B, editor. Teeth: Form, function and evolution. New York, NY: Columbia University Press; 1982. p.182-203.
8. Galbany J, Dotras L, Alberts SC, Perez-Perez A. Tooth size variation related to age in Amboseli baboons. Folia Primatol (Basel) 2010; 81(6): 348-59.
9. Yap AU, Neo JC. Non-carious cervical tooth loss: Part 1. Dent Update 1995; 22(8): 315-8.
10. Landsteiner K, Wiener AS. An agglutinable factor in human blood recognized by immune sera for rhesus blood. Proc Soc Exp Biol Med 1940; 43(1): 223.
11. Goldstein R, Curtis J, Farley B, Siranli S, Clark W. Abfraction, abrasion, attrition, and erosion. In: Goldstein R, Curtis J, Farley B, Siranli S, Clark W, editors. Ronald E. Goldstein's esthetics in dentistry. 3rd ed. Hoboken, NJ: Wiley; 2018. p. 692-719.
12. Al Ghamdi AS. Association between ABO blood groups and severity of chronic periodontitis. JKAU Med Sci 2009; 16(3): 31-4.
13. Hakomori S. Antigen structure and genetic basis of histo-blood groups A, B and O: their changes associated with human cancer. Biochim Biophys Acta 1999; 1473(1): 247-66.
14. Kolmakova GN, Kononova LL. The prevalence of ABO blood groups among persons of native nationality in Buryatia. Sud Med Ekspert 1999; 42(2): 15-6. [In Russian].
15. Kaya H, Gundodu M, Akarsu E, Kiki I, Tekin B. The distribution of blood groups in. Erzurum. Med J Atatürk Univ 1999; 31: 20-2.
16. Demir T, Tezel A, Orbak R, Eltas A, Kara C, Kavrut F. The effect of ABO blood types on periodontal status. Eur J Dent 2007; 1(3): 139-43.
17. Pinkston JA, Cole P. ABO blood groups and salivary gland tumors (Alabama, United States). Cancer Causes Control 1996; 7(6): 572-4.
18. Chakravartti MR, Chakravartti R. ABO blood groups and chicken pox in an Indian population. Acta Genet Med Gemellol (Roma) 1977; 26(3-4): 297-8.
19. Singh N, Shukla MM, Uniyal VP, Sharma VP. ABO blood groups among malaria cases from district Mandla, Madhya Pradesh. Indian J Malariol 1995; 32(2): 59-63.
20. Vijay Raghavan MR, Bailoor DN, Jhansi Rani P. Incidence of ABO blood groups in oral cancer in South Kanara District. J Indian Dental Associatio 1986; 58: 305-8.
21. Janardhana V, Propert DN, Green RE. ABO blood groups in hematologic malignancies. Cancer Genet Cytogenet 1991; 51(1): 113-20.
22. Whincup PH, Cook DG, Phillips AN, Shaper AG. ABO blood group and ischaemic heart disease in British men. BMJ 1990; 300(6741): 1679-82.
23. Glass RI, Holmgren J, Haley CE, Khan MR, Svennerholm AM, Stoll BJ, et al. Predisposition for cholera of individuals with O blood group. Possible evolutionary significance. Am J Epidemiol 1985; 121(6): 791-6.
24. Jesch U, Endler PC, Wulkersdorfer B, Spranger H. ABO blood group. Related investigations and their association with defined pathologies. ScientificWorldJournal 2007; 7: 1151-4.
25. Henderson J, Seagroatt V, Goldacre M. Ovarian cancer and ABO blood groups. J Epidemiol Community Health 1993; 47(4): 287-9.
26. Biswas J, Islam MA, Rudra S, Haque MA, Bhuiyan ZR, Husain M, et al. Relationship between blood groups and coronary artery disease. Mymensingh Med J 2008; 17(2 Suppl): S22-S27.
27. Okon UA, Antai AB, Osim EE, Ita SO. The relative incidence of diabetes mellitus in ABO/Rhesus blood groups in South-Eastern Nigeria. Niger J Physiol Sci 2008; 23(1-2): 1-3.
28. Koregol AC, Raghavendra M, Nainegali S, Kalburgi N, Varma S. ABO blood groups and Rhesus factor: An exploring link to periodontal diseases. Indian J Dent Res 2010; 21(3): 364-8.
29. Arowojolu MO, Dosmu EB, Adingbola TS. The relationship between juvenile and non-juvenile periodontitis, ABO blood groups and haemoglobin types. Afr J Med Med Sci 2002; 31(3): 249-52.
30. Pai GP, Dayakar MM, Shaila M, Dayakar A. Correlation between "ABO" blood group phenotypes and periodontal disease: Prevalence in south Kanara district, Karnataka state, India. J Indian Soc Periodontol 2012; 16(4): 519-23.
31. Demir T, Uslu H, Orbak R, Altoparlak U, Ayyildiz A. Effects of different blood groups on the reproduction of periodontal pocket bacteria. Int Dent J 2009; 59(2): 83-6.
32. Gautam A, Mittal N, Singh TB, Srivastava R, Verma PK. Correlation of ABO blood group phenotype and rhesus factor with periodontal disease: An observational study. Contemp Clin Dent 2017; 8(2): 253-8.
33. Skripal' IG. ABO system of blood groups in people and their resistance to certain infectious diseases (prognosis). Mikrobiol Z 1996; 58(2): 102-8.
34. Singla S, Verma A, Goyal S, Singla I, Shetty A. Correlation of dental caries and blood group in Western Punjab population in India. Indian J Multidiscip Dent 2015; 5(2): 59-61.

35. Roberts JA. Blood groups and susceptibility to disease: A review. Br J Prev Soc Med 1957; 11(3): 107-25.
36. Vivek S, Jain J, Simon SP, Battur H, Supreetha S, Haridas R. Association of ABO blood group and rh factor with periodontal disease in a population of Virajpet, Karnataka: A cross-sectional study. J Int Oral Health 2013; 5(4): 30-4.
37. Mazumdar P, Das UK, S. Correlation between blood group and dental caries in 20-60 years age group: A study. Int J Adv Res 2014; 2(11): 413-24.
38. Haertig A, Krainic K, Vaillant JM, Derobert L. Medicolegal identification: teeth and blood groups (author's transl). Rev Stomatol Chir Maxillofac 1980; 81(6): 361-3. [In French].
39. Walker AR, Dison E, Walker BF, Hart S, Jenkins T. Dental caries and blood groups in South African blacks. Community Dent Oral Epidemiol 1985; 13(1): 42-3.
40. Janghorbani M, Akhavan-Mahdavi S, Masoudi HR. The pelationship between ABO blood groups and Rh factor with dental caries in soldiers of a military base in Kerman. J Kerman Univ Med Sci 1996; 3(2): 87-91. [In Persian].
41. O'roark WL, Leyschon C. Dental-caries prevalence as related to blood groups. J Dent Res 1963; 42: 1530.

MEDWIN PUBLISHERS
Committed to create value for Researchers

Journal of Natural & Ayurvedic Medicine
ISSN: 2578-4986

Phytochemical, Botanical and Biological Paradigm of Astavarga Plants- The Ayurvedic Rejuvenators

Balkrishna A[1,2], Mishra RK[1], Sharma N[2], Sharma VK[2] and Misra L[2]*

[1]Dravyaguna Department, Patanjali Bhartiya Ayurvigyan Avum Anusandhan Sansthan, India

[2]Patanjali Research Foundation, India

Review Article

Volume 2 Issue 6

Received Date: July 06, 2018

Published Date: August 24, 2018

***Corresponding author.** Laxminarain Misra, Patanjali Research Foundation, Haridwar, Uttarakhand 249405, India, Tel: 91-1334240006; Email: laxmisra@hotmail.com

Abstract

Astavarga is nature's most extravagant group of flowering plants found in Himalayan region. As the name Astavarga indicates, it contains eight medicinal plants belonging to Zingiberaceae, Orchidaceae and Liliaceae family viz, Kakoli, Kshirakakoli, Meda, Mahameda, Jeevak, Risbhaka, Riddhi and Vridddhi. As per Ayurveda this group of medicinal plants is classified as Rasayana (Rejuvenation) and is important constituents of preparations like Chyawanprasha rasayan, Ashtavarga churna, Brimhanigutika and Vajikaraghrita, etc. Astavarga plants are mostly used to treat sexual disorders, physical weakness, body pain, strengthen the immune system and as an overall tonic. The plants under this group have been the subject of limited biochemical phytochemical and biological activities investigations. Taking into consideration the therapeutic significance of Astavarga plants as described in the ancient Ayurvedic system of medicine, the detailed phytochemical and pharmacological studies appear imperative to scientifically validate the ancient claims. Thus, the present review article provides detailed information on the Ayurvedic uses, habit and habitats, botanical descriptions, chemical constituents and biological activities reported for this important group of plants. The chemical structures of the isolated compounds from these plants and their reported biological activities in the literature have also been included. The information provided in the present review may stimulate the researchers to explore their phytochemical and pharmacological properties which have not yet been attempted, comprehensively. It will generate the interest on "reverse pharmacology" approach to validate the knowledge that has been known from ancient times.

Keywords: Astavarga; Ayurvedic Uses; Botanical Description; Phyto-Constituents; Biological Activities

Introduction

Ayurveda is the eternal science of life [1]. It is associated with the noble, excellent and great tradition of Indian ancient Rishis (sages) and is a part of its prosperous and glorious history. Starting from Lord Brahma, various Rishis and Maharishis in the tradition of Daksha, Asvini Kumars, Indra, Atreya, Punarvasu, Dhanvantri, Bharadwaja, Nimi, Kasyapa and other humanists have enriched and protected the prosperous tradition of Ayurveda. It still continues to flow well from ancient times [2]. The Samhitas of Ayurveda are conveyors of this eternal tradition. Lord Dhanvantri described that Ayurveda is the science of life. It is the Veda of life (beneficial, non-beneficial, happy and unhappy factors of life). The main purpose of Ayurveda is to protect the fitness of a healthy person and to mitigate the disorders of a patient [3,4]. Around 80% of the population of developing countries relies on traditional medicines, mostly from plants, for their primary health care needs. Modern pharmacopeia has around 25% plant based drugs as well as synthetic analogues based on the pharmacophore from the plants [5,6]. India holds the highest proportion of medicinal plants known for their medicinal value as compared to any country in the world as the Indians have been using plants to cure diseases since ancient times [7]. As the name Astavarga indicates, this important group contains eight medicinal plants belonging to Zingiberaceae, Orchidaceae and Liliaceae family. In Ayurveda this group is reffered to as Rasayana (Rejuvenation) as they display the properties of Jivaniya (Vitality promoter), Vayasthapana (Age-sustainer), Swasthya Vardhaka (Health promoting), Rogapratirodhaka ksamata vardhaka (Immuno modulator), Shukrajanan (Spermatogenic) [8-11].

The actual identification of these plants became uncertain and illusory due to lack of doctumented literature, sparse knowledge of natural habitat and incorrect identification. Many of these plants have become rare and endangered due to climatic changes also some of them are usually growing in smaller niches and are not visible over larger areas. This is the reason why the Astavarga plants were passing through confusion and anonymity regarding their proper identification. Recent extensive surveys by Acharya Balkrishna have confirmed that the Astavarga is constituted by: Habenaria intermedia D. Don (Riddhi), Habenaria edgeworthii Hook. f. ex Collett (Vriddhi), Crepidium acuminatum (D. Don) Szlach [12]. (Jeevak), Malaxis muscifera Kuntze (Rishbhak), Polygonatum cirrhifolium Royle (Mahamedha), Polygonatum verticillatum Allioni (Medha), Roscoea purpurea Smith (Kakoli) and Lilium polyphyllum D. Don (Kshirkakoli). Among them four belong to the Orchidaceae (H. intermedia, H. edgeworthii, C. acuminatum, M. muscifera), three to the Liliaceae (P. cirrhifolium, P. verticillatum, L. polyphyllum) and one (R. purpurea) to Zingiberaceae family (Table 1). In continuation of our interest in investigating and reviewing some of the Ayurvedic plants, we have taken up the phytochemical, botanical and biological paradigm of Astavarga group to inculcate fresh interest in nurturing and protecting them from extinction [13-21].

SN	Sanskrit Name	Botanical Name	Family	Common Name
1	Kakoli	Roscoea purpurea Smith	Zingiberaceae	Roscoe's lily, roscoe's purple lily, purple roscoea, cinnamon stick, hardy ginger
2	Kshirakakoli	Lilium polyphyllum D. Don	Liliaceae	White Himalayan lily, white lily, many leaved lily
3	Jeevak	Crepidium acuminatum (D. Don) Szlach.	Orchidaceae	The gradually tapering malaxis
4	Rishbhak	Malaxis muscifera (Lindl.) Kunt	Orchidaceae	Adder mouth orchid, snake mouth orchid
5	Meda	Polygonatum verticillatum (Linn.) Allioni	Liliaceae	Whorled solomon's seal
6	Mahameda	Polygonatum cirrhifolium (Wall.) Royle	Liliaceae	King's solomon's seal, tendril leaf solomon's seal, coiling leaf solomon's seal, coiling leaf Polygonatum
7	Riddhi	Habenaria intermedia D. Don	Orchidaceae	Intermediate Habenaria, white wild orchid, the in between Habenaria, Raindeer orchid;
8	Vriddhi	Habenaria edgeworthii Hook. f. ex Collett	Orchidaceae	Edgeworth's habenaria

Table 1: Members of Astavarga.

Discussion

All the Astavarga plants contain various phenolic compounds such as catechin (1), gallic acid (2), p-coumaric acid (3), ferulic acid (4), vanillic acid (5), 4-hydroxybenzoic acid (6) phloridizin, caffeic acid, chlorogenic acid, 3-hydroxycinnamic acid, ellagic acid, rutin, and trans-cinnamic acid etc., having strong antioxidant potential with ability to prevent DNA damage from oxidative stress, thus are used for strengthening vitality [22]. Astavarga plants are used to increase body fat, restore fractures and cure fever, diabetese and seminal weakness and build up immunity. Due to immense therapeutic potential, these plants are used in different forms, e.g. taila (oil), ghritam (medicated clarified butter), churna (powder) and formulations, including the popular health tonic chyavanprasha, in the traditional medicinal system (TMS) [23-25]. The identification and differentiation of Astavarga plants in terms of botanical description and habitat, a large number of views and publications have appeared [8,11,23,26-29]. Astavarga is also a subject of extensive biochemical investigation but very little is known about phytochemicals present in most of them. Taking the great medicinal importance of Astavarga plants into consideration, bioactivity guided phytochemical investigations have not been properly attempted and it is definitely the need of the hour to scientifically validate the ancient claims. With this idea, here in the present review article, we provide concise information on the Ayurvedic uses, botanical aspects, chemical constituents and biological activities observed for this traditionally important group of plants.

Ayurvedic Uses of Integrated Astavarga Plants

- The pseudobulbs are sweet, aphrodisiac, and haemostatic, antidiarrhoeal, styptic, antidysenteric, febrifuge, cooling and tonic. It is useful in sterility, vitiated conditions of pitta and vata, semen related weakness, internal and external hemorrhages, dysentery, fever, emaciation, burning sensation and general debility [30-32].
- These medicinal plants are Jivaniya (vitality promoter) and maintain the balance between three doshas of Vatta, Pitta and Kapha. This increases the energy, body strength, glow and other properties of the body [10].
- They are Bramhaniya (body mass promoters) and are described within the Bemhaniyavarga. The Kakoli and Ksir Kakoli from Astavarga plants fall in this category [10].
- The Astavarga plants mitigate the disorder of the body and specifically alleviate Tridosaja disorder in the body to increase the Ayusya (longevity) and slow down the process of aging [10].
- Mahamayurghrita processed with Jivaka and other herbs, is useful in rasaraktadidhatugatvikara, srotaradiindriyavikarasvarabhransa (Aphesia), asthma, cough, facial paralysis, vaginal diseases, blood disorders and semen related problems [33].
- The intake of powder prepared from Jivaka and other herbs mixed with proper quantity of honey and crystal sugar is useful in cough and cardiac diseases [33].
- Vacadi taila processed with Jivaka and other herbs used as anuvasanavasti, is beneficial for gulma, distention, vata associated disorders and urinary incontinence [3].
- Jivaniyagh Rita processed with Jivaka is useful for the whole body vitiated with gout and vata associated disorders [34].
- Citrakadi taila processed with Jivaka and other herbs is useful in vata associated disorders, sciatica, limping, kyphosis, gout and urinary disorders [3].
- Mahapadma taila processed with Jivaka and other herbs is useful in gout and fever [34].
- Jivaniya ghrita processed with Jivaka and other herbs, can be effective in treating gout and other chronic vata associated disorders [34].
- Asthapanavasti processed with Jivaka and other medicinal herbs is useful in treating gulma, metrorrhagia, anaemia, malaria [3].
- The intake of ghrita processed with Devadaru, Kakoli, Jivaka and other medicinal herbs given in proper dose is useful in child emaciation [3].
- Himavanaagada prepared with the powder of Pancavalkala, Jivaka and other herbs, mixed with honey to make a paste and external application of this paste on snake bite reduces the toxicity. It also alleviates other symptoms like oedema, erysipeles, boils, fever and burning sensation [33].

Botanical Description and Ayurvedic Uses

A summary of the taxonomical details of Astavarga plants have been included in Table 2 and their habitat in Table 3. Their botanical descriptions have been given in Table 4. Since some of the plants are no more available, their substitutes, currently employed in the commerce, have been covered in Table 5 [35-37]. The current status of their availability is summarized in Table 6 [29,38,39]. The chemical structures of some of the common compounds, isolated from these plants and their biological activities tested so far, have been depicted in Table 7. However, these tested biological activities are associated with the individual compounds and are not related to the Astavarga plants directly.

	Kakoli	Kshira-kakoli	Jeevak	Rishbhak	Meda	Mahameda	Riddhi	Vriddhi
Kingdom	Plantae	Plantae	Plantae	Plantae	Plantae	Plantae	Plantae	Plantae
Division	Tracheophyta	Tracheophyta	Tracheophyta	Tracheophyta	Tracheophyta	Tracheophyta	Tracheophyta	Tracheophyta
Class	Liliopsida	Liliopsida	Liliopsida	Liliopsida	Liliopsida	Liliopsida	Liliopsida	Liliopsida
Order	Zingiberales	Liliales	Asparagales	Asparagales	Liliales	Liliales	Asparagales	Asparagales
Family	Zingiberaceae	Liliaceae	Orchidaceae	Orchidaceae	Liliaceae	Liliaceae	Orchidaceae	Orchidaceae
Genus	Roscoea	Lilium	Crepidium	Malaxis	Polygonatum	Polygonatum	Habenaria	Habenaria
Species	purpurea	polyphyllum	acuminatum	muscifera	verticillatum	cirrhifolium	intermedia	edgeworthii
Author name	Smith	D. Don	(D. Don) Szlach.	(Lindl.) Kunt	(Linn.) Allioni	(Wall.) Royle	D. Don	Hook.f. ex Collett

Table 2: Taxonomic Position of Astavarga.

SN	Name	Habitat
1	Roscoea purpurea Smith	**Uttarakhand**- Mussoorie- Jaberkhet, Mussorrie, Kyarphulli, Company Bagh, Deoban, Tehri- Nagtibba West of Dhanolti; Uttarkashi- Jamuna Valley, Kharshali, Har-ki-Dun, Chamoli- Valley of flowers, Gobindghat, Khirsu, Pithoragarh-Tejam jankhola vally, Kalivalley, Sarju Valley, Nainital- Nainital, Bhowali, Ramgarh, Fatehgarh, Above Malli Tal; Almora-Binsar, Almora, Lorakhet, Ranikhet to Chaubatia.
2	Lilium polyphyllumD. Don	**Himachal Pradesh-**Hatto peak, Narkanda forests, Chail (Solan district), Sungari-Bahli on Rampur Road. **Jammu & Kashmir-** Gulmarg, Liddar valley. **Uttarakhand-** Gangotri, Rainthal, Amardhar, Kedarnath, Madmaheshwar.
3	Crepidium acuminatum (D. Don) Szlach.	**Himachal Pradesh-** Simla-Glen, Boileaugunj, Elysium Hill in forests way to Rani forest, way from Khajjar to Chamba, Chail, Hattoo, Narkanda. **Uttarakhand**- Dehradun- Camel back road, Below Mussoorie bypass road, above barlowgunj, chakrata, jaunsar, Tehri (Magra); Pauri-Pode khal, Chamoli- Nagnath, Ukhimath, Gopeshwar, Pithoragarh- Sarju Valley, Berenag, Thal Kedar; Nainital, Bhowali, Ramagarh, Almora-Ranikhet, between Ranikhet-Chaubatia.
4	Malaxis muscifera (Lindl.) Kunt	**Himachal Pradesh-** Shimla (Mashobra, Fagu, Hatto forests) Rahala forest, Dhanchoo, Sangla, Chamba. **Jammu & Kashmir-** Gulmarg, Datni, Leh**. Uttarkhand-**Pithoragarh- Tejum Haya, Bakariudiyar, Ralam Valley, Palangarh, Ralam, Almora-Dwali, Dehradun chakrata, Deoban Tehri-Masartal, Bokhills, Dhanolti, Way to Nagtibba; Chamoli- Vasukital, Bajmora, Jumma area, Dunagiri.
5	Polygonatum verticillatum (Linn.) Allioni	**Himachal Pradesh-** Shimla, Narkanda, Hattoo, Churdhar, Janjelli, Sikari Tibba, Kamarunagh. **Jammu & Kashmir-**Trikuta Hills, Udhampur, Doda area. **Uttarakhand**- Ponwalikanta, Tali, Amardhar, Ganganani dhar, Rainthal, Kedarnath, Gangotri, Madmaheshwar.
6	Polygonatum cirrhifolium (Wall.) Royle	**Himachal Pradesh-** Shimla, Matiana, Narkanda. **Uttarakhand-** Mussoorie, Chakrata, Gaurikund, Rambara, Harshal, Ganganani, Devban, Rainthal, Mandakini Ghati, Bhilangana Ghati, Ponwali, Kalimath.
7	Habenaria intermedia D. Don	**Himanchal Pradesh**- Koti (Shimla) Summer Hill, Indian Institute of Advance study, Kamana Hill), Rwanda and Kamarunag (Karsog), Rewalsar hills (Mandi), Shimla (Fagu), Dalhousie (Chamba), Kinnaur. **Jammu & Kashmir-** Azmabad, Poonch, Pirpanjal Range. **Uttarakhand-** Dehradun- Mussoorie (Jaberkhet), Camel back road, Company bagh, Bhatta Fall, Kampty fall; Tehri (Nagtibba) Suakholi, Chamoli- on way to kedarnath, jangal chatti, way to valley of flowers, Gaurikund (Rambera); Utarrkashi Tons valley, Bhagirathi valley and way to Dodital.

8	Habenaria edgeworthi Hook.f. ex Collett	**Himachal Pradesh**- Summer Hills, Shimla, Mountains near Manali, Rahala Forest, Kothi, Manali, Saraha, Nirmand- Annu, Rwanda, Kamarunag peak, Saptasar above Rawalsar (Mandi), Chansel, Churdhar, Jangtoo, Chamba, Narkanda. **Uttarakhand**- Mussoorie- Jaberkhet, Mussorrie, Kyarphulli, Company Bagh, Deoban, Tehri- Nagtibba West of Dhanolti; Uttarkashi- Jamuna Valley, Kharshali, Har-ki-Dun, Chamoli- Valley of fl owers, Gobindghat, Khirsu, Pithoragarh- Tejam jankhola vally, Kalivalley, Sarju valley, Nainital- Nainital, Bhowali, Ramgarh, Fatehgarh, above Malli Tal; Almora- Binsar, Almora, Lorakhet, Ranikhet to Chaubatia.

Table 3: Specific Habitat of Astavarga plants.

SN	NameTaxonomic features
1	**Roscoea purpurea Smith**: Vegetative Characters: 35-50 cm tall, perennial, herb. Rhizome slightly blackish in colour. Root fibres thick, fleshy, fascicled, slightly light brown in colour. Stem purple coloured, leafy, elongate, erect and robust. Leaves 5-6, lanceolate, 15 cm long, 1.2-2.5 cm wide, at flowering time sheath broad, imbricated leaf-sheath green or purple-red with spots. Flowers few, orchid like in a sessile spike. Bracts oblong, hidden in the sheaths of the upper leaves. Calyx green, 3.8 cm long, slit deeply down one side as the flower expands. Corolla tube not longer than the calyx, dilated upwards, limb purple rarely pale lilac or white, upper segments about 2.5 cm long, obovate-cuneate while lower lanceolate, decurved, lip broad deeply bifid. Staminode oblanceolate, unguiculate, half as long as the upper segment. Fertile stamen as long as the staminode. Anther tails 0.4 cm long. Capsule cylindrical, 2.5-3.8 cm long. Seeds ovoid, minute, arillate. Flowering June-July. Fruiting August-September [40] .
2	**Lilium polyphyllum D. Don:** A narrow bulbous herb with fleshy scales long narrow, subequal. Stem 60-120 cm erect, slender. Leaves alternate, lower whorled, lanceolate to linear-lanceolate, 5-13 cm long and 0.5-1.5 cm wide, acute, margin hairy. Raceme 4-10 flowered. Bracts whorled. Flowers pendulous, fragrant. Pedicel 4-10 cm long, slightly drooping. Tepals dull yellow or greenish outside, white within with purple streaks, 3-4 cm long, oblanceolate. Stamens exserted. Anthers 1.3 cm long. Style very declinate. Fruit capsule. Flowering/fruiting August-Lilium polyphyllum D. Don: A narrow bulbous herb with fleshy scales long narrow, subequal. Stem 60-120 cm erect, slender. Leaves alternate, lower whorled, lanceolate to linear-lanceolate, 5-13 cm long and 0.5-1.5 cm wide, acute, margin hairy. Raceme 4-10 flowered. Bracts whorled. Flowers pendulous, fragrant. Pedicel 4-10 cm long, slightly drooping. Tepals dull yellow or greenish outside, white within with purple streaks, 3-4 cm long, oblanceolate. Stamens exserted. Anthers 1.3 cm long. Style very declinate. Fruit capsule. Flowering/fruitingAugust-November[40].
3	**Crepidium acuminatum (D. Don) Szlach:** Terrestrial, sometimes epiphytic orchid. Stem cylindric, 1.5-7 cm long, 4-6 mm in diameter, fleshy with several nodes, mostly enclosed in sheath. Leaves 3-5, obliquely ovate, ovate-oblong or sub-elliptical, 4-12 × 2.5-6 cm long and wide, base contracted into a sheath-like, amplexicaul 2-4 cm long petiole, apex acuminate. Peduncle 12-43 cm, wingless. Rachis erect, 3-16 cm long, 10 or more flowered. Floral bracts lanceolate, 3-6 mm long. Flowers purple red, 1.5 cm in diameter. Pedicel and ovary 7-10 mm. Dorsal sepal narrowly oblong or broadly linear, 8-9 × 2 mm size, 3-veined, margin revolute, apex obtuse. Lateral sepals oblong, 6-7 × 3-3.5 mm size, margin revolute, apex obtuse. Petals narrowly linear, 8-9 × 0.8 mm size, margin revolute. Lip (labellum) superior, ovate-oblong or obovate-oblong in outline, 10-11 × 6-7 mm size, shallowly bilobed. Auricles narrowly ovate, 1/5-2/5 length of lip. Column 1-1.5 mm, stout. Capsule obovoid-oblong, 1.8 × 1 cm size. Fruiting pedicel 7 mm long. Flowering and fruiting May-July (111) [41].
4	**Malaxis muscifera (Lindl.) Kunt**: A terrestrial herb upto 40 cm tall. Pseudobulb small, ovoid. Stem flexuous. Leaves 3-5, unequal, approximate blade of larger leaves 2-10 x 1-4 cm long and wide while blade of smaller 1.5-6 x 0.5-3 cm long and wide, elliptic to oblong or oblong- lanceolate, obtuse or acute or sub-acuminate. Sheathing petiole 2-6 cm long. Inflorescence 2.5-25 cm long. Flowers yellowish-green. Bracts slightly shorter than pedicelled ovary. Sepals subequal, 2-2.3 mm long, oblong-lanceolate. Dorsal sepal directed downwards, laterals upwards. Petals linear, spreading. Labellum fleshy, broadly ovate, 2 mm long, basal portion excavated, obscurely angled on either side of base, apex acuminate. Column very short, anthers sessile on its top. Pollinia ovoid and

	free. Pedicelled ovary up to 3 mm long, pedicel twisted. Fruit capsule, 6-8 mm long, broadly ovoid-oblong, ribbed and of light yellow colour. Flowering- fruiting August- November [40].
5	**Polygonatum verticillatum (Linn.)** Allioni: Rhizome usually shortly branched, tuberous terete, very rarely moniliform, 0.7-1.5 cm thick. Stem erect, 20-80 cm long, glabrous. Leaves in whorls of 3, occasionally alternate near base of stem, sometimes opposite near apex of stem, subsessile, oblong-lanceolate to linear, 6-10 × 0.5-3 cm long and wide, apex acute to acuminate, not cirrose. Inflorescences 1-4 flowered. Flowers pendulous. Peduncle 1-2 cm long. Bracts small or absent. Pedicel 3-10 mm long. Perianth pale purple or white or pale yellow, but probably only when dry, cylindric, 0.8-1.2 cm long. Tepals connate into a tube, 2-3 mm long. Stamens 6, with bare stamens, epipetalous. Filaments 0.5-2 mm long, papillose. Anthers 2.5 mm long. Ovary 3 mm. Style 2.5-3 mm long. Berries red, 6-9 mm in diameter, 6-12 seeded. Flowering May-June and fruiting August-October [40,41].
6	**Polygonatum cirrhifolium (Wall.) Royle:** Rhizome moniliform or tuberous, terete, 1-2 cm thick. Stem erect or scandent, 30-90 cm long, glabrous. Leaves in whorls of 3-6, rarely a few alternate in proximal part of stem, sessile, narrowly linear to linear-lanceolate, very rarely oblong-lanceolate, margin entire, 4-12 cm × 2-15 mm long and wide, tip usually cirrose at anthesis. Inflorescences usually 2-flowered. Flowers pendulous. Peduncle 0.3-1 cm long. Bracts 1-2 mm, scarious, veinless or bract absent. Pedicel 3-8 mm. Perianth white, greenish or pale purple, subcylindric, slightly constricted in middle, 8-11 mm long. Tepals 2 mm long. Filaments 0.6-0.8 × 0.15 mm size, papillose. Anthers 2-2.5 mm. Ovary 2.5 mm. Style 2 mm. Berries red or purple-red, 8-9 mm in diameter, 4-9-seeded. Flowering May-July and fruiting September-October [40,41].
7	**Habenaria intermedia D. Don:** Plants turning black when dried, 23-30 cm tall. Tubers ellipsoid, 1.5-3 × 1-2 cm size, fleshy. Stem erect, terete, stout. Leaves 3-5, laxly arranged. Leaf blade ovate-lanceolate, 3.5-8 × 2-4 cm long and wide, base amplexicaul, apex acute. Raceme 1-4-flowered, 6-15 cm long. Flowers large, green and white. Floral bracts ovate, 4-5 cm long, nearly as long as ovary, apex acuminate. Ovary twisted, terete, including pedicel 3.8-4.5 cm long. Flowers white or greenish. Sepals ciliate, green. Dorsal sepal erect, ovate-oblong, concave, 2.2 × 1.2 cm size, 7-veined, apex acute. Lateral sepals reflexed, obliquely falcate-lanceolate, 3 × 0.6 cm size, 7-veined, apex acute. Petals white, forming a hood with dorsal sepal, erect, white, obliquely subovate-falcate, 2.2 × 0.8 cm size, 5-veined, margin ciliate, unlobed, apex acute. Lip pale or yellowish-green, 2.8-3 cm size, base spurred, deeply 3-lobed above base, lobes ciliate. Lateral lobes linear, outer margin with 10 filiform lobules. Mid-lobe linear, 18-20 mm long, slightly shorter than lateral lobes, apex acute. Spur pendulous, cylindric, 7-8.5 cm long, much longer than ovary, slightly dilated near end, apex obtuse. Connective 2 mm wide. Pollinia ovoid. Caudicles linear. Viscidia orbicular, small. Rostellum with elongate arms. Stigmas clavate. Flowering July[40,41].
8	**Habenaria edgeworthii Hook.f. ex Collett:** A terrestrial, leafy herb with unidivided, oblong tubers and fleshy root fibres. Stem with the raceme 30-47 cm long, leafy from about 5 cm upwards, internodes ensheathed by leaf bases. Leaves erect, 4-9 x 0.8-1.2 cm, lanceolate, setaceously acuminate, acute, indistinctly 5-7 veined, bases sheathing. Flowers 1.5 cm broad when spread out, in elongated terminal racemes. Peduncles as long as the racemes with about two leafy, sterile, acuminate bracts. Floral bracts leafy, 2.4 x 1.1 cm long and wide, broadly lanceolate-ovate, acuminate, acute, initially 3-5-veined but soon branching to give a 9-veined appearance. Dorsal sepal 6 x 4 mm size, oblong-ovate, obtuse, 3-veined, lateral veins branching. Lateral sepals 7 x 4 mm size, broadly and obliquely ovate, obtuse, 3-veined, the lateral veins branching giving a 5-7-veined appearance. Petals 7 x 2 mm size, yellowish-green, bilobed, lobes variable in length and breadth. Upper lobe lanceolate, about half as long as the lower linear lobe, incurved, 2-veined. Lip 5 x 2 mm, purple, inserted at the base of the column, broadly 3-lobed, fleshy, lobes variable in length, obtuse. Spur 1.7 cm long, narrowly clavate, mouth provided with a ligule. Column 3.4 mm high, 3 mm broad, with a small, triangular rostellum and two viscid, sausage-shaped stigmas. Anthers lateral, adnate to the column, 2-loculed. Pollinia 2, granular, golf club-shaped, stalked, 1.3-1.6 x 0.6 mm size, each with a long slender caudicle 2.2-2.4 mm long, attached to a minute gland. Staminodes short and fleshy, arising from the sides of the column and protruding above as granular masses. Ovary with pedicel 2 cm long [40].

Table 4: Botanical features of Astavarga plants.

SN	Name	Substitute	Reference
1	Roscoea purpurea Smith	Aswagandha (Withania somnifera (L.) Dunal) and Kali musali (Curculigo orchioides Gaertn)	[35-37]
2	Lilium polyphyllum D. Don	Aswagandha (Withania somnifera (L.) Dunal), Safed musali (Chlorophytum arundinaceum Baker), Fritillaria roylei Hook. Fritillaria oxypetala D. Don.	[35,36]
3	Crepidium acuminatum (D. Don) Szlach.	Vidarikand (Pueraria tuberose (Wild.) DC), Safed behmen (Centaurea behen Linn.) and Guduchi (Tinospora cordifolia (Willd.) Miers, Malaxis cylindrostachya (Lindl.) Kuntze and Malaxis mackinnoni (Duthie) Ames)	[35,36]
4	Malaxis muscifera (Lindl.) Kunt	Vidarikand (Pueraria tuberose (Willd.) DC.) and Lal behmen (Centaurium roxburghii (D. Don) Druce	[35,36]
5	Polygonatum verticillatum (Linn.) Allioni	Satavari (Asparagus racemosus Willd.), Salam mishri (Eulophia campestris Wall.)	[35,36]
6	Polygonatum cirrhifolium (Wall.) Royle	Satavari (Asparagus racemosus Willd.), Nagbala (Sida veronicifolia Lam.), Shakakul mishri (Polygonatum multiflorum (L.) All.) and Prasarani (Paederia foetida L.).	[35,36]
7	Habenaria intermedia D. Don	Varahikand, Bala (Sida cordifolia L.) and Chiriya musali (Asparagus filicinus Buch-Ham. ex D. Don)	[35,36]
8	Habenaria edgeworthii Hook.f. ex Collett	Varahikand (Tacca integrifolia Ker Gawl.), Salam panja (Dactylorhiza hatagirea (D. Don) Soo) and Mahabala (Sidaacuta Burm.f.). Habenaria griffithii Hook.f.	[35,36]

Table 5: Substitutes of Astavarga Plants in commerce.

SN	Name	Status	Reference
1	Roscoea purpurea Smith	Commonly available	[29,38]
2	Lilium polyphyllum D. Don	Endangered	[39]
3	Crepidium acuminatum (D.Don) Szlach.	Rare	[39]
4	Malaxis muscifera (Lindl.) Kunt	Rare, Threatened	[39]
5	Polygonatum verticillatum (Linn.) Allioni	Threatened	[39]
6	Polygonatum cirrhifolium (Wall.) Royle	Rare	[39]
7	Habenaria intermedia D. Don	Commonly available	[39]
8	Habenaria edgeworthii Hook.f. ex Collett	Rare	[39]

Table 6: Current Status of Astavarga Plants.

Name	Chemical Structure	Biological activities
Catechin (1)	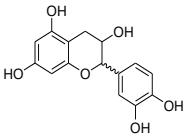	Neuroprotection,anticancer, antioxidant,antiobesity, antidiabetic,cardioprotection, antiangiogenic [42-48]
Gallic acid (2)	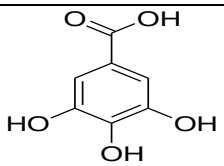	Antidepressant, antiparkinson, antidiabetic, antimalarial, diuretic, cardioprotective, antiviral, antifungal, wound healing, anthelmintic, anxiolytic, anticancer [49-61]
p-Coumaric acid (3)	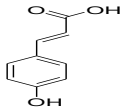	Antioxidant, anti-inflammatory, anxiolytic, antimicrobial, antidiabetic and antihyperlipidemic, anticancer [62-71]
Ferulic acid (4)	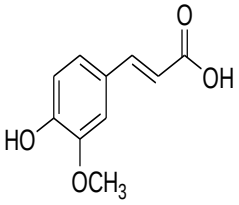	Antioxidant, antiallergic, hepatoprotective, anticarcinogenic, anti-inflammatory, antimicrobial, antiviral, vasodilatory effect, antithrombotic, and helps to increase the viability of sperms antidiabetic and anti-ageing agent, anticancer, improve the structure and function of the heart, blood vessels, liver, and kidneys in hypertensive rats, β-secretase modulator [72-85].
Vanillic acid (5)	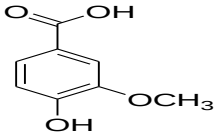	Cognitive improvement, ulcerative colitis [86,87].
Hydroxy benzoic acid (6)	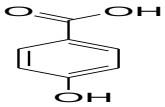	Antimicrobial [88]
Scopoletin (7)	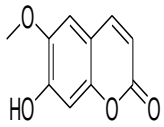	Cognition-enhancing properties, anti-inflammatory, antiproliferative agent, inhibitor of nitric oxide synthase, prostaglandin synthase and monoamine oxidase, antioxidant and radical scavenger [89-97]
Mescaline (8)	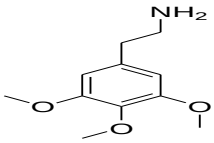	Hallucinogenic [98]
Cetyl alcohol (9)	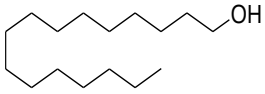	Antimicrobial, emollient [99-100]

Limonene (10)	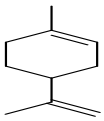	Anticancer, dissolve gall stones, heartburn and gastroesophageal re-flux disorder (gerd) [101-106]
Eugenol (11)	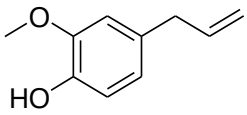	Antioxidant activity, anti-inflammatory, antibacterial and antiviral [107-109]
Citronellal (12)	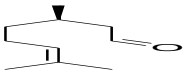	Relaxant effect in smooth muscle of trachea [110]
1, 8- Cineole (13)	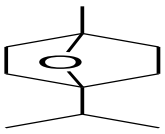	Mucolytic and spasmolytic action on the respiratory tract benefits in inflammatory airway diseases, such as asthma and chronic obstructive pulmonary disease (COPD), antiseptic anthelmintic, anti-inflammatory, antimicrobial [111-116]
Piperitone (14)	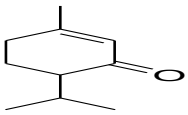	Antimicrobial [117-118]
p-Cymene (15)	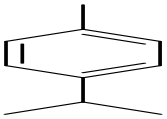	Antioxidant, antinociceptive & anti-inflammatory, anti cancer [119-127]
Diosgenin (16)	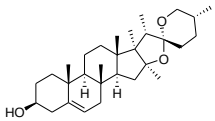	Antidiabetic, antiobesity, anti-inflammatory, anticancer [128-130]
β- Sitosterol (17)	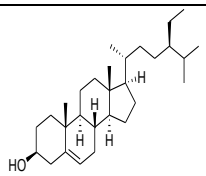	Anti-inflammatory, inducing apoptosis, chemoprotective, hypocholesterolemic, angiogenic, analgesic, anthelminthic and anti-mutagenic, immunomodulatory, anticancer, antidiabetic [131-146]
5-hydroxymethyl furfural (18)	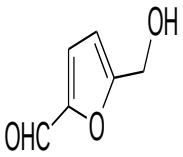	Inhibit sickling of red blood cells, relieve fatigue, improvement in learning and memory, antioxidative, anti-apoptotic activity anticarcinogenic action, antimicrobial, anti-hypoxic effect anti-inflammatory [147-164]

Santonin (19)	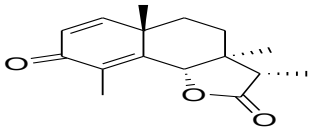	Anthelmintic [165-166]
α- Bulnesene (20)	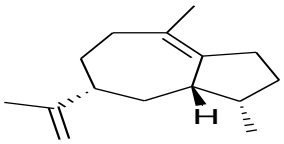	Inhibit platelet-activating factor, anti-inflammatory [167-168]
Quinine (21)	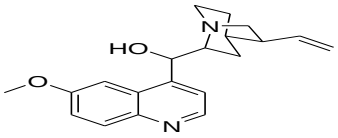	Antimalaria [169]
Kaempferol (22)	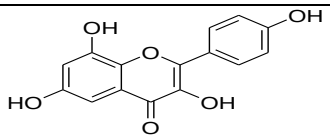	Antioxidant & antimicrobial [170-171]
Protocatechuic acid (23)	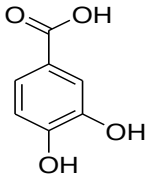	Anticancer, antidiabetic, anti-inflammatory, antioxidant & anti aging, cardioprotective , antimicrobial, antifibrotic activity, antihepatitic activity, neuroprotective, antihyperlipidemia, protection against reproductive toxicity [172-186]
Syringic acid (24)	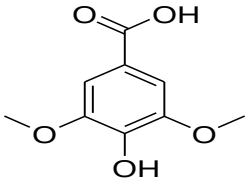	Reduce diabetic cataract by inhibiting aldose reductase antioxidant, antiproliferative, antiendotoxic, antimicrobial, anti-inflammatory, and anticancer, anti-angiogenic, anti-glycating, anti-hyperglyсaemic, neuroprotective, and memory-enhancing properties [187-189]
Peiminine (25)	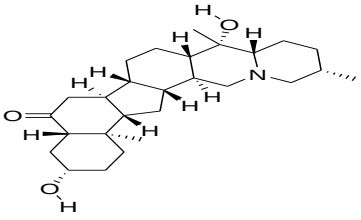	Anticancer anti-allergic & anti inflammatory [190-192]

Table 7: Chemical structure and biological activities of some of the compounds from Astavarga plants.

Riddhi (Habenaria edgeworthii syn. Platanthera edgeworthii (Hook.f. ex Collett) RK.Gupta: It belongs to the Family Orchidaceae. The botanical descriptions and habitat has been described in Tables 2 & 3. It is useful as nerve and cardiac tonic, blood related infections, fever, cough, asthma, muscular pain, sprains, arthritis, gout,

sciatica, leprosy, skin diseases, anorexia, emaciation, gout, helminthiasis, insanity, general debility and increase in sperm count [12,193].

Vriddhi (Habenaria intermedia D.Don syn. Habenaria arietina H.f.): It belongs to the Family Orchidaceae. The botanical descriptions and habitat has been described in Tables 2 & 3. It is useful as aphrodisiac, depurative, anthelmintic, nerve and cardiac tonic. It is also useful in treating respiratory and skin diseases. Habenaria intermedia is a significant constituent of a well acknowledged polyherbal formulation, Chyavanprasha [194,195].

Meda (Polygonatum verticillatum (L.) All syn. Convallaria verticillata L syn. Evallaria verticillata Necker): It belongs to the Family Liliaceae. The botanical descriptions and habitat has been described in Tables 2 & 3. It is useful as antipyretic, antimalarial, potential aphrodisiac, appetizer, galactagogue, antifungal and skin tonic [196-199].

Mahameda (Polygonatum cirrhifolium Wall Royle): It belongs to the Family Liliaceae. The botanical descriptions and habitat has been described in Tables 2 & 3. It is useful in the treatment of loss of vigor, accumulation of fluids in bone joints, skin diseases, tuberculosis, fever, bronchitis and general debility. It is also reported to have hypoglycemic, hypotensive, antibacterial and antifungal effects [200,201].

Jeevaka (Malaxis acuminta D. Don syn. Microstylis wallichii Lindl syn. Malaxis wallichii Deb): It belongs to the Family Orchidaceae. The botanical descriptions and habitat has been described in Tables 2 & 3. It is useful as therapeutics in bleeding diathesis, burning sensation, fever, phthisis, tonic, tuberculosis and increasing sperm count [201].

Rishbhaka (Microstylis Muscifera Ridley): It belongs to the Family Orchidaceae. The botanical descriptions and habitat has been described in Tables 2 & 3. It is useful for treatment of burning sensation, fever, phthisis, tuberculosis and increasing sperm count.

Kakoli (Roscoea procera Wall. formerly Roscoea purpurea or Fritillaria roylei Hook f.) Family: It belongs to the Family Zingiberaceae. The botanical descriptions and habitat has been described in Tables 2 & 3. It is useful as anti-rheumatic, antipyretic, galactagogue, expectorant, sexual stimulant, anti diabetic, anti hypertensive and diuretic. The fleshy roots are conventionally used to treat malaria and urinary infection [202-204]. Additionally, the ethanolic rhizome extract has immune-stimulatory potential in mice [205].

Kshirakakoli (Lilium polyphyllum D.Don): It belongs to the Family Liliaceae. The botanical descriptions and habitat has been described in Tables 2 & 3. It is useful as refrigerant, galactogogue, expectorant, aphrodisiac, diuretic and antipyretic. It is also used in cases of seminal weakness, hyperdipsia, intermittent fever, haematemesis, rheumatalgia and general disability [206].

Chemical and Biological activities

Habenaria Species

Both of the Habenaria species are of great therapeutic value in curing asthma, cough, facial paralysis, vaginal diseases and semen related disorders along with their application in rejuvenation [11]. These plants are the important ingredients of "Chyavanprasha' and are well acknowledged for having anti-ageing properties, helpful in providing protection against degenerative diseases [207].

Habenaria intermedia

The phytochemical studies on H. intermedia has substantiated that it is effective source of total phenols, thiamine, tannins, and calcium. Antioxidant activity of polyherbal formulation containing tubers of H. intermedia was examined for nitric oxide scavenging activity [208]. Also the content of hydroxybenzoic acid was almost double to that of some of the other species [209]. Presence of various phenolic compounds, such as catechin (1), gallic acid (2), ρ-coumaric acid (3), hydroxybenzoic acid (6), and scopoletin (7) supports them as the promising source of antioxidants [210-213]. In various fractions of H. intermedia, adaptogenic activity was also studied using immobilization induced acute stress (AS), chronic stress (CS) and swimming induced stress in experimental animals, which proved it as anti-stress agent [210].

Gallic acid (2) is a well known starting material for the synthesis of the psychedelic alkaloid mescaline (8) and has shown antioxidant and cytotoxic activities. Scopoletin (7) is a naturally occurring coumarin found in various medicinal plants with wide range of biological activities. Recent studies demonstrated that scopoletin (7) has anticonvulsant, antioxidant, antimicrobial, hypotensive, anticancer activities and prevents lipid peroxidation [214-223]. It also possesses antidepressant-like effect which is dependent on the serotonergic, noradrenergic and dopaminergic systems [224].

Habenaria egdeworthii

Very little information is available on the scientific work done on H. egdeworthii. However, it has been found to be a rich source of sodium and possesses antioxidant activity [208].

Malaxis Species

The plant species is used for the cure of tuberculosis and is a great aphrodisiac [225]. It is also known as febrifuge, tonic and useful in the conditions of sterility, seminal weakness, hemorrhages, dysentery, emaciation, burning sensation as well as general debility [12]. However, the investigation of its phyto-constituents is inadequate.

Malaxis acuminata

Bhatnagar, et al. reported β-sitosterol (17), cetyl alcohol (9), choline and two sugars namely glucose and rhamnose from Malaxis acuminate [226]. The thin layer chromatographic studies revealed the presence of constituents like limonene (10), eugenol (11), citronellal (12), 1,8-cineole (13), piperitone (14) and p-cymene (15) [227]. Atomic absorption spectroscopy indicated the presence of Cu, Zn, Mn, Fe, K, Ca, Mg, Al, Ba, B, Mo and Cl. The fatty acid analysis using GC-MS revealed the identification of common fatty acids including, linoleic acid, α-linolenic acid, oleic acid, palmitic acid, stearic acid, γ-linolenic acid, eicosanoic acid, eicosenoic acid and eicosadienoic acid [228]. The antioxidant activity in butanol extract of M. acuminata was observed using various available methods like, DPPH free radical scavenging activity, and hydrogen peroxide scavenging method [229].

Malaxis muscifera

(Syn. Dienia muscifera, Microstylis muscifera) is listed as a threatened species in IUCN Red List due to uncontrolled grazing unsustainable collection and unregulated trade [230]. There is an urgent need for developing sustainable cultivation, in situ and ex situ policies which can help to maintain the population.

Polygonatum Species

It is documented in "Abhinav niguntu" that “Meda” grows from the same place from where “Mahameda” originates, suggesting that both P. verticillatum and P. cirrhifolium grows together. The term “Meda” represents the mucilage present inside the rhizomes of these plant species [231]. Both species are perennial rhizomatous herbs with their habitation in the extensive range from Europe to the Himalayas to Siberia. They are used for treating pain, pyrexia, burning sensation, phthisis, appetizer, increase milk secretion, for gastric problems, improving sexual potency and improve general weakness [200,232].

Polygonatum verticillatum

It contains phyto-constituents such as lysine, serine, aspartic acid, threonine, diosgenin (16), β-sitosterol (17), sucrose, along with the micronutrients and macronutrients [12]. It is also rich in saponins, alkaloids, glycosides, flavonoids and phytohormones. Few compounds have been isolated from the rhizomes of P. verticillatum which include lectins, 5-hydroxymethyl-2-furaldehyde (18) diosgenin, santonin (19), β-sitosterol (17), 2-hydroxybenzoic acid, α-bulnesene (20) and quinine (21) [199,233-237].

The rhizome extract of P. verticillatum is used as tonic and energizer. It has also been studied for antimalarial and antioxidant, metal accumulating, insecticidal, antibacterial, antipyretic, tracheorelaxant and anti-inflammatory, antispasmodic and antidiarrheal, antinociceptive, aphrodisiac [199,235,238-242]. Lipoxygenase, urease inhibition, anti tyrosinase activity of the aerial parts of the P. verticillatum was also observed which were attributed to the presence of saponins, alkaloids, flavonoids, phenols, tannins and terpenoids in considerable amount [243-245].

Polygonatum cirrhifolium

It is reported to be used as a tonic in major Ayurvedic formulations like Asoka Ghrita, Sivagutika, Amrtaprasa Ghrita, Dasam, Ularista, Dhanvantara Taila, Brhatmasa Taila, Mahanarayana Taila and Vasacandanadi Taila [231]. A root infusion with milk is used as an aphrodisiac and blood purifier [200]. P. cirrhifolium is reported to have hypoglycemic, hypotensive, antibacterial, antifungal and antioxidant activities [22,201]. Its rhizomes are rich in starch, protein, pectin and asparagine [246].

Roscoea procera

Tubers of Kakoli are found to contain alkaloid, glycoside, flavonoid, tannin, saponins and active phenolic compounds and are reported to exhibit immuno-modulatory and anti-diabetic activities [205,247]. Quantification of metabolites suggested that the tubers are nutritionally rich having appreciable content of fiber (28.1%), protein (3.46%) and oil (3.5%). Quantification of secondary metabolites through HPTLC reveals that kaempferol (22) (0.30%) was the major metabolite

followed by vanillic acid (0.27%), protocatechuic acid (23) (0.14%), syringic acid (24) (0.08%) and ferulic acid (0.05%). In addition to this, there exists a positive, significant correlation between the phenolic and flavonoids content with the anti-oxidant activity of Roscoea extract [204]. HPTLC results of kakoli (ethanol and chloroform extracts) revealed the presence of alkaloids, glycosides and flavonoids [248]. Propeimin, peimine, peiminine (25), peimisine, kashmirine and sipeimine have also been reported [194,249-253].

Lilium Polyphyllum

Its bulbs have been used for diuretic, antipyretic, tonic in seminal weakness, in asthma, bronchitis and tuberculosis [8,254-257]. Phytoconstituents like alkaloids (peimine, peiminine, peimisine, peimiphine, peimidine and peimitidine), neutral constituents (propeimin, sterol) are reported to be present in Kshirkakoli [251]. Its HPTLC finger printing (ethyl acetate and chloroform extract) indicated the presence of saponins and steroids [248].

Conclusion

Astavarga is an important group of medicinal plants reported in old literature, however, the detailed information on the medicinal use was restricted as it was retained by the indigenous population and was transferred to the next generations through words of mouth [9,258,259]. As the scientific research conducted on Astavarga is limited, the information provided in the present review regarding the chemical constituents and biological activities along with their botanical aspects and Ayurvedic paradigm will be beneficial to the researchers to explore novel phytochemical and medicinal properties which were not investigated earlier. Further work on chemistry and biology of alkaloids needs to be strengthened to understand their active therapeutic roles in the Ayurvedic preparations. Additionally, the emphasis has been given to understand the Ayurvedic uses of these medicinal plants and the present review will generate fresh interest for their conservation and "reverse pharmacology" approach to validate the information that has been known for long time.

References

1. Pandeya G, Sashtri K (2011) Charaka Samhita (part I) (Sanskrit-Hindi) Chaukhambha Bharatee Academy, Varanasi, India, pp: 587.

2. Gupta A (2005) Astanga-samgraha. Varanasi, India: Chaukhambha Krishna Das Academy, pp: 2.

3. Sharma AR (2012) Sushruta Samhita (Part-1). Varanasi, India: Chaukhambha Sankrit Pratisthan, pp: 10.

4. Sharma I, Singh A (2017) Clinical Studies with Ayurvedic Formulations-A Practitioner's Preview. J Nat Ayurvedic Med 1(1): 1-5.

5. Farnsworth NR (1994) Ethnopharmacology and drug development. Ciba Found Symp 185: 42-59.

6. Mukherjee PK, Wahile A (2006) Integrated approaches towards drug development from Ayurveda and other Indian system of medicines. J Ethnopharmacol 103(1): 25-35.

7. Kala C, Dhyani P, Sajwan B (2006) Developing the medicinal plants sector in northern India: challenges and opportunities. J Ethnobiol Ethnomed 2(1): 32-36.

8. Dhyani A, Nautiyal B, Nautiyal M (2010) Importance of Astavarga plants in traditional systems of medicine in Garhwal, Indian Himalaya. Int J Biodiver Sci Ecosys Serv Manag 6(1-2): 13-19.

9. Mathur DR (2003) Yogtarangini. Chaukhamba Vidhyabhawan, Varanasi (India).

10. Pandey D (2005) Sarangadharasanhita. Chaukhamba Amarabharati Prakashan, Varanasi, India.

11. Sharma BD, Balkrishna A (2005) Vitality strengthening Astavargaplants (Jeevaniya & Vayasthapan Paudhe), Uttaranchal (India), Divya Publishers, Divya yog mandir Trust, Haridwar.

12. Balkrishna A (2012a) Secrets of Astavarga Plants (for vitality and anti-aging). Haridwar, Uttarakhand, India: Divya Prakashan, Patanjali Yogpeeth, pp: 1-104.

13. Siddique AA, Bhakuni RS, Misra LN, Gupta P, Darokar MP (2017) New triglyceride from antimicrobials extracts of Nepeta hindostana weed. In J Chem 56B(5): 542-550.

14. Tewari R, Rout PK, Misra LN (2016) Simultaneous RP-HPLC-PDA-RI separation and quantification of pinitol content in Sesbania bispinosa vis-à-vis harvesting age. Plant Biosyst 151(5): 924-930.

15. Gupta M, Rout PK, Misra LN, Gupta P, Singh, N, et al. (2016) Chemical composition and bioactivity of Boswellia serrata Roxb. Essential oil in relation to geographical variation. Plant Biosys 151(4): 623-629.

16. Ahmad F, Misra L, Tewari R, Gupta P, Gupta VK, et al. (2016a) Isolation and HPLC profiling of chemical constituents of Saraca asoca bark. Indian J Chem B 55B: 353-361.

17. Ahmad F, Misra L, Tewari R, Gupta P, Mishra P, et al. (2016b) Anti-inflammatory flavanol glycosides from Saraca asoca bark. Nat Prod Res 30: 489-492.

18. Ahmad F, Misra L, Gupta VK, Darokar MP, Prakash O, et al. (2015) Synergistic effect of (+)-pinitol from Saraca asoca with β-lactam antibiotics and studies on the in silico possible mechanism. J Asian Nat Prod Res 18(2): 172-183.

19. Balkrishna A, Misra LN (2017a) Ayurvedic plants in brain disorders: the herbal hope. J Tradit Med Clin Natur 6(2): 1-9.

20. Balkrishna A, Misra LN (2017b) Ayurvedic opportunities for restoration of skin health. J Tradit Med Clin. Natur 6(2): 221.

21. Balkrishna A, Misra LN (2018) Chemo-botanical and neurological accounts of some Ayurvedic plants useful in mental health. Nat Prod J 8(1): 14-31.

22. Giri L, Belwal T, Bahukhandi A, Suyal R, Bhatt ID, et al. (2017) Oxidative DNA damage, protective activity and antioxidant potential of Astavarga species growing in the Indian Himalayan region. Indust Crops Prod 102: 173-179.

23. Balkrishna A (2012a) Secrets of Astavarga Plants (for vitality and anti-aging). Haridwar, Divya Prakashan, Patanjali Yogpeeth, Uttarakhand, India, pp: 1-104.

24. Balkrishna A, Srivastava A, Mishra RK, Patel SP, Vashistha RK, et al. (2012b) Astavarga plants-threatened medicinal herbs of North -West Himalaya. Int J Med Arom Plants 6: 661-676.

25. Ghosh A, Damiki L, Singh NK (2013) Comparative estimation and chemical standardization of new and old sample of Chyawanprash. Int J Pharm Pharm Sci 5(3): 801-804.

26. Osmaston AE (1978) A Forest Flora for Kumaon. Bishen Singh Mahinder Pal Singh, Dehradun, India.

27. Naithani BD (1985) Flora of Chamoli II, Botanical Survey of India, Howrah, India.

28. Hooker JD (1978) The flora of British India. Bishen Singh Mahendra Pal Singh, Dehradun.

29. Gaur RD (1999) Flora of the district Garhwal North West Himalaya with ethnobotanical notes. Transmedia Publication, Srinagar, Garhwal, India.

30. Tripathi ID (2006) Raj Nighantu, Chowkhamba Krishanadass Academy, Varanasi, India.

31. Balwant ST, Chunekar KC (1972) Glossary of Vegetable Drugs in Brihattrayi, Chaukhamba Sanskrit Series office, Varanasi.

32. Pandit R (1998) Madanpal Nighantu, Khemraj Shri Krishanadass, Mumbai.

33. Tripathi B (2003) Asthangha Hridyam, Chaukhamba Sanskrit Pratishthan, Delhi.

34. Tripathi B (2004) Charaka-Samhita (I - II), Chaukhamba Surbharti Prakashan, Varanasi.

35. Rajashekhar I, Rathod H, Desai H (2015) A short review on astavarga plants-losing their existence. Int J Ayur Pharma Res 3(7): 32-38.

36. Chunekar KC, Pandey GS (2006) Bhavaprakasa Nighantu, Chaukhambha Bharti Academy, Varanasi, India.

37. Chunekar KC (1969) Vanaspatika Anusandhan Darshika, Vidya Bhavan, Varanasi, pp: 1.

38. Nayar MP, Sastry ARK (1987) Red data book of Indian plants, pp: 1.

39. Ved DK, Kinhal GA, Ravikumar K, Prabhakaran V, Ghate U, et al. (2003) Conservation assessment and management prioritization for the medicinal plants of Jammu & Kashmir. Himachal Pradesh & Uttaranchal. Foundation for revitalization of local health traditions, Bangalore, India.

40. Ali SI (2007) Flora of Pakistan. Missouri Botanical Garden Press. 215: 108.

41. Zhengyi W, Raven PH, Hong D (2013) Flora of China. Missouri Botanical Garden Press, St. Louis, USA.

42. Mandel SA (2012) The importance of the multiple target action of green tea polyphenols for neuroprotection. Front Biosci 4(1): 581-589.

43. Lambert JD, Yang CS (2003) Mechanisms of cancer prevention by tea constituents. J Nutr 133(10): 3262S-3267S.

44. Higdon JV, Frei B (2003) Tea Catechins and Polyphenols: Health Effects, Metabolism, and Antioxidant Functions. Criti Rev Food Sci Nutr 43(1): 89-143.

45. Kao Y, Hiipakka RA, Liao S (2000) Modulation of obesity by a green tea catechin. Am J Clin Nutr 72(5): 1232-1234.

46. Wu L, Juan C, Hwang LS, Hsu Y, Ho P, et al. (2004) Green tea supplementation ameliorates insulin resistance and increases glucose transporter IV content in a fructose-fed rat model. Eur J Nutr 43(2): 116-124.

47. Miura Y, Chiba T, Tomita I, Koizumi H, Miura S, et al. (2001) Tea catechins prevent the development of atherosclerosis in apoprotein e-deficient mice. J Nutr 131(1): 27-32.

48. Cao Y, Cao R (1999) Angiogenesis inhibited by drinking tea. Nature 398(6726): 381.

49. Chhillar R, Dhingra D (2012) Antidepressant-like activity of gallic acid in mice subjected to unpredictable chronic mild stress. Fundam Clin Pharm 27(4): 409-418.

50. Chen JJ (2004) Neuroprotection in Parkinson's disease. Medscape.

51. Prasad CN, Anjana T, Banerji A, Gopalakrishnapillai A (2010) Gallic acid induces GLUT4 translocation and glucose uptake activity in 3T3-L1 cells. FEBS Lett 584(3): 531-536.

52. Griffith R, Chanphen R, Leach SP, Keller PA (2002) New anti-malarial compounds from database searching. Bioorg Med Chem Lett 12(4): 539-542.

53. Ramya K, Mohandas SR, Ashok KJ (2014) Evaluation of diuretic activity of gallic acid in normal rats. J Sci Innov Res 3(2): 217-220.

54. Goyal R, Patel S (2011) Cardioprotective effects of gallic acid in diabetes-induced myocardial dysfunction in rats. Pharmacog Res 3(4): 239-245.

55. Kratz JM, Andrighetti-Fröhner CR, Kolling DJ, Leal PC, Cirne-Santos CC (2008) Anti-HSV-1 and anti-HIV-1 activity of gallic acid and pentyl gallate. Mem Inst Oswaldo Cruz 103(5): 437-442.

56. De Paula e Silva AC, Costa-Orlandi CB, Gullo FP, Sangalli-Leite F, De Oliveira HC, et al. (2014) Antifungal activity of decyl gallate against several species of pathogenic fungi. Evi Compl Alt Med 2014: 1-8.

57. Nayeem N, Karvekar MD (2011) Stability studies and evaluation of the semi-solid dosage form of the rutin, quercitin, ellagic acid, gallic acid and sitosterol isolated from the leaves of Tectona grandis for wound healing activity. Arch Appl Sci Res 3(1): 43-51.

58. Ndjonka D, Abladam ED, Djafsia B, Ajonina-Ekoti I, Achukwi MD (2014) Anthelmintic activity of phenolic acids from the axlewood tree Anogeissus leiocarpus on the filarial nematode Onchocerca ochengi and drug-resistant strains of the free-living nematode Caenorhabditis elegans. J Helminthol 88(4): 481-488.

59. Dhingra D, Chhillar R, Gupta A (2011) Anti anxiety-like activity of gallic acid in unstressed and stressed mice: possible involvement of nitriergic system. Neurochem Res 37(3): 487-494.

60. Saxena HO, Faridi U, Srivastava S, Kumar J, Darokar M, et al. (2008) Gallic acid-based indanone derivatives as anticancer agents. Bio Org Med Chem Lett 18(14): 3914-3918.

61. Locatelli C, Filippin-Monteiro FB, Creczynski-Pasa TB (2013) Alkyl esters of gallic acid as anticancer agents: A review. Eur J Med Chem 60: 233-239.

62. Zang L, Cosma G, Gardner H, Shi X, Castranova V, et al. (2000) Effect of antioxidant protection by p-coumaric acid on low-density lipoprotein cholesterol oxidation. Am J Physiol Cell Physiol 279(4): C954-C960.

63. Zhou Y, Wang H, Sui H, Li L, Zhou C, et al. (2016) Inhibitory effect of baicalin on allergic response in ovalbumin-induced allergic rhinitis guinea pigs and lipopolysaccharide-stimulated human mast cells. Inflamm Res. 65(8): 603-612.

64. Yoon BH, Choi JW, Jung JW, Shin JS, Hyeon SY, et al. (2005) Anxiolytic-like effects of phenylpropanoid compounds using the Elevated Plus-Maze in mice. Yakhak Hoeji 49(5): 437-442.

65. Lou Z, Wang H, Rao S, Sun J, Ma C, et al. (2012) p-Coumaric acid kills bacteria through dual damage mechanisms. Food Control 25(2): 550-554.

66. Stojković D, Petrović J, Soković M, Glamočlija J, Kukić-Marković J, et al. (2013) In situ anti oxidant and antimicrobial activities of naturally occurring caffeic acid, p-coumaric acid and rutin, using food systems. J Sci Food Agri 93(13): 3205-3208.

67. Amalan V, Vijayakumar N, Indumathi D, Ramakrishna A (2016) Antidiabetic and antihyperlipidemic activity of p-coumaric acid in diabetic rats, role of pancreatic GLUT 2: *In vivo* approach. Biomed Pharmacother 84: 230-236.

68. Yoon S, Kang S, Shin H, Kang S, Kim J, et al. (2013) p-Coumaric acid modulates glucose and lipid metabolism via AMP-activated protein kinase in L6 skeletal muscle cells. Biochem Biophy Res Comm 432(4): 553-557.

69. Jaganathan SK (2013) Events associated with apoptotic effect of p-Coumaric acid in HCT-15 colon cancer cells. World J Gastroenterol 19(43): 7726.

70. Janicke B, Önning G, Oredsson SM (2005) Differential Effects of Ferulic Acid andp-Coumaric Acid on S Phase Distribution and Length of S Phase in the Human Colonic Cell Line Caco-2. J Sci Food Agri 53(17): 6658-6665.

71. Kong C, Jeong C, Choi J, Kim K, Jeong J (2012) Antiangiogenic effects of p-coumaric acid in human endothelial cells. Phytother Res 27(3): 317-323.

72. Akihisa T, Yasukawa K, Yamaura M, Ukiya M, Kimura Y, et al. (2000) Triterpene alcohol and sterol ferulates from rice bran and their anti-inflammatory effects. J Sci Food Agri 48(6): 2313-2319.

73. Graf E (1992) Antioxidant potential of ferulic acid. Free Radical Biol Med 13(4): 435-448.

74. Ou S, Kwok KC (2004) Ferulic acid: pharmaceutical functions, preparation and applications in foods. J Sci Food Agric 84(11): 1261-1269.

75. Rukkumani R, Aruna K, Suresh VP, Padmanabhan MV (2004) Hepatoprotective role of ferulic acid: a dose-dependent study. J Med Food 7(4): 456-461.

76. Aragno M, Parola S, Tamagno E, Brignardello E, Manti R, et al. (2000) Oxidative derangement in rat synaptosomes induced by hyperglycaemia: restorative effect of dehydroepiandrosterone treatment. Biochem Pharmacol 60(3): 389-395.

77. Balasubashini MS, Rukkumani R, Viswanathan P, Menon VP (2004) Ferulic acid alleviates lipid peroxidation in diabetic rats. Phytother Res 18(4): 310-314.

78. Nomura E, Kashiwada A, Hosoda A, Nakamura K, Morishita H (2003) Synthesis of amide compounds of ferulic acid, and their stimulatory effects on insulin secretion *In vitro*. Bio org Med Chem 11(17): 3807-3813.

79. Barone E, Calabrese V, Mancuso C (2008) Ferulic acid and its therapeutic potential as a hormetin for age-related diseases. Biogerontol 10(2): 97-108.

80. Hirose M, Takahashi S, Ogawa K, Futakuchi M, Shirai T (1999) Phenolics: blocking agents for heterocyclic amine-induced carcinogenesis. Food Chem Toxicol 37(9-10): 985-992.

81. Mori H, Kawabata K, Yoshimi N, Tanaka T, Murakami T, et al. (1999) Chemopreventive effects of ferulic acid on oral and rice germ on large bowel carcinogenesis. Anticancer Res 19(5A): 3775-3778.

82. Hudson EA, Dinh PA, Kokubun T, Simmonds MS, Gescher AC (2000) Characterization of potentially chemopreventive phenols in extracts of brown rice that inhibit the growth of human breast and colon cancer cells. Cancer Epidemiol Biomark Prev 9(11): 1163-1170.

83. Wang B, Ouyang J, Liu Y, Yang J, Wei L, et al. (2004) Sodium ferulate inhibits atherosclerogenesis in hyperlipidemia rabbits. J Cardiovasc Pharmacol 43(4): 549-554.

84. Alam MA, Sernia C, Brown L (2013) Ferulic acid improves cardiovascular and kidney structure and function in hypertensive rats. J Cardiovas Pharmacol 61(3): 240-249.

85. Mori T, Koyama N, Guillot-Sestier M, Tan J, Town T (2013) Ferulic acid is a nutraceutical β-secretase modulator that improves behavioral impairment and Alzheimer-like pathology in transgenic mice. PLoS ONE 8(2): 1-16.

86. Singh JC, Kakalij RM, Kshirsagar RP, Kumar BH, Komakula SS, et al. (2014) Cognitive effects of vanillic

acid against streptozotocin-induced neurodegeneration in mice. Pharma Biol 53(5): 630-636.

87. Kim S, Kim M, Um J, Hong S (2010) The beneficial effect of vanillic acid on ulcerative colitis. Molecules 15(10): 7208-7217.

88. Cho J, Moon J, Seong K, Park K (1998) Antimicrobial activity of 4-hydroxybenzoic acid and trans-4-hydroxycinnamic acid isolated and identified from rice Hull. Biosci Biotech Biochem 62(11): 2273-2276.

89. Hornick A, Lieb A, Vo NP, Rollinger J, Stuppner H, et al. (2008) Effects of the coumarin scopoletin on learning and memory, on release of acetylcholine from brain synaptosomes and on long-term potentiation in hippocampus. BMC Pharmacol 8(1): A36.

90. Muschietti L, Gorzalczany S, Ferraro G, Acevedo C, Martino V (2001) Phenolic Compounds with Anti-Inflammatory Activity from Eupatorium buniifolium. Planta Med 67(8): 743-744.

91. Fujioka T, Furumi K, Fujii H, Okabe H, Mihashi K, et al. (1999) Antiproliferative constituents from umbellifereae plants. V. a new furanocoumarin and falcarindiol furanocoumarin ethers from the root of Angelica japonica. Chem Pharm Bull 47(1): 96-100.

92. Kim N, Pae H, Ko Y, Yoo J, Choi B, et al. (1999) *In vitro* inducible nitric oxide synthesis inhibitory active constituents from Fraxinus rhynchophylla. Planta Med 65(7): 656-658.

93. Kang T, Pae H, Jeong S, Yoo J, Choi B, et al. (1999) Scopoletin: an inducible nitric oxide synthesis inhibitory active constituent from Artemisia feddei. Planta Med 65(5): 400-403.

94. Farah M, Samuelsson G (1992) Pharmacologically active phenylpropanoids from Senra incana. Planta Med 58(01): 14-18.

95. Yun B, Lee I, Ryoo I, Yoo I (2001) Coumarins with monoamine oxidase inhibitory activity and antioxidative coumarino-lignans from Hibiscus syriacus. J Nat Prod 64(9): 1238-1240.

96. Shaw C, Chen C, Hsu C, Chen C, Tsai Y (2003) Antioxidant properties of scopoletin isolated from Sinomonium acutum. Phytoth Res 17(7): 823-825.

97. Toda S (2002) Inhibitory effects of phenylpropanoid metabolites on copper-induced protein oxidative modification of mice brain homogenate, *in vitro*. Biol Trace Elem Res 85(2): 183-188.

98. Mc Laughlin JL (1973) Peyote: an introduction. Lloydia 36(1): 1-8.

99. Fletcher RD, Gilbertson JR, Albers AC, White JD (1981) Inactivation of mycoplasmas by long-chain alcohols. Antimicrob Agent Chemother 19(5): 917-921.

100. Anonymous (1988) Final report on the safety assessment of cetearly alcohol, cetyl alcohol, isostearyl alcohol, myristyl alcohol and behenyl alcohol. J Am Coll Toxicol 7(3): 1-55.

101. Giri RK, Parija T, Das BR (1999) d-Limonene chemoprevention of hepatocarcinogenesis in AKR mice: inhibition of c-jun and c-myc. Oncolo Rep 6(5): 1123-1127.

102. Kaji I, Tatsuta M, Iishi H, Baba M, Inoue A, et al. (2001) Inhibition by D-limonene of experimental hepatocarcinogenesis in Sprague-Dawley rats does not involve p21ras plasma membrane association. Int J Cancer 93(3): 441-444.

103. Elegbede J, Elson C, Qureshi A, Tanner M, Gould M (1984) Inhibition of DMBA-induced mammary cancer by the monoterpene d-limonene. Carcinogenesis 5(5): 661-664.

104. Igimi H, Hisatsugu T, Nishimura M (1976) The use of d-limonene preparation as a dissolving agent of gallstones. Am J Dig Dis 21(11): 926-939.

105. Wilkins J (2002) Method for treating gastrointestinal disorder. US Patent 642045.

106. Lis-Balchin M, Ochocka RJ, Deans SG (1996) Bioactivity of the enantiomers of limonene. Med Sci Res 24: 309-310.

107. Gordon MH (1996) Dietary antioxidants in disease prevention. Nat Prod Rep 13(4): 265-273.

108. Wargovich MJ, Woods C, Hollis DM, Zander ME (2001) Herbals, cancer prevention and health. J Nutr 131: 3034S-3036S.

109. De M, Krishna De A, Banerjee AB (1999) Antimicrobial screening of some Indian spices. Phytother Res 13(7): 616-618.

110. Yonara MS, Morganna TA, Pedrita AS, Jullyana SS, Lucindo JQ, et al. (2014) Relaxant effect of carvacrol, citronellal and p-cymene, monoterpenes present in Thymus and Cymbopogon species, in guinea-pig trachea: A comparative study. J Med Plants Res 8(24): 881-888.

111. Juergens U (2014) Anti-inflammatory Properties of the Monoterpene 1,8-cineole: Current Evidence for Co-medication in Inflammatory Airway Diseases. Drug Res 64(12): 638-646.

112. Bastos VP, Gomes AS, Lima FJ, Brito TS, Soares PM, et al. (2010) Inhaled 1,8-cineole reduces inflammatory parameters in airways of ovalbumin-challenged guinea pigs. Basic Clin Pharm Toxicol 108(1): 34-39.

113. Kokate CK, Purohit AP (1999) Textbook of Pharmacognosy, Nirali Prakashan 12: 267-268.

114. Kumar HD, Sahoo L (2011) A Review on phytochemical and pharmacological of Eucalyptus globules: A multipurpose tree. Int J Res Ayur Pharm 2(5): 1527-1530.

115. Nagpal N, Shah G, Arora MN, Shri R, Arya Y (2010) Phytochemical and pharmacological aspects of Eucalyptus genus. Int J Pharma Sci Res 1(12): 28-36.

116. Mulyaningsih S, Sporer F, Zimmermann S, Reichling J, Wink M (2010) Synergistic properties of the terpenoids aromadendrene and 1,8-cineole from the essential oil of Eucalyptus globulus against antibiotic-susceptible and antibiotic-resistant pathogens. Phytomed 17(13): 1061-1066.

117. İşcan G, Kirimer N, Kürkcüoğlu M, Başer HC, Demirci F (2002) Antimicrobial screening of Mentha piperita essential oils. J Agri Food Chem 50(14): 3943-3946.

118. Kalemba D, Kunicka A (2003) Antibacterial and antifungal properties of essential oils. Curr Med Chem 10(10): 813-829.

119. De Oliveira TM, De Carvalho RB, Da Costa IH, De Oliveira GA, De Souza AA, et al. (2014) Evaluation of p-cymene, a natural antioxidant. Pharma Biol 53(3): 423-428.

120. Quintans-Júnior L, Moreira JC, Pasquali MA, Rabie SM, Pires AS (2013) Antinociceptive activity and redox profile of the monoterpenes (+)-camphene, p-cymene, and geranyl acetate in experimental models. ISRN Toxicol 2013: 1-11.

121. Zhong W, Chi G, Jiang L, Soromou L W, Chen N, et al. (2012) p-Cymene modulates in vitro and in vivo cytokine production by inhibiting MAPK and NF-κB activation. Inflamm 36(3): 529-537.

122. Bonjardim LR, Cunha ES, Guimarães AG, Santana MF, Oliveira MG, et al. (2012) Evaluation of the anti-inflammatory and antinociceptive properties of p-cymene in mice. Z Naturforsch C 67(1-2): 15-21.

123. De Santana MF, Guimarães AG, Chaves DO, Silva JC, Bonjardim LR (2015) The anti-hyperalgesic and anti-inflammatory profiles of p-cymene: Evidence for the involvement of opioid system and cytokines. Pharma Biol 53(11): 1583-1590.

124. Li J, Liu C, Sato T (2016) Novel antitumor invasive actions of p-cymene by decreasing MMP-9/TIMP-1 expression ratio in human fibrosarcoma HT-1080 cells. Biol Pharma Bull 39(8): 1247-1253.

125. Kaluđerović GN, Krajnović T, Momcilovic M, Stosic-Grujicic S, Mijatović S (2015) Ruthenium (II) p-cymene complex bearing 2,2-dipyridylamine targets caspase 3 deficient MCF-7 breast cancer cells without disruption of antitumor immune response. J Inorg Biochem153: 315-321.

126. Paunescu E, Nowak-Sliwinska P, Clavel CM, Scopelliti R, Griffioen AW, et al. (2015) Anticancer organometallic osmium (ii)- p-cymene complexes. Chem Med Chem 10(9): 1539-1547.

127. Joglekar MM, Panaskar SN, Arvindekar AU (2014) Inhibition of advanced glycation end product formation by cymene- A common food constituent. J Funct Food 6: 107-115.

128. Chen Y, Tang Y, Yu S, Han Y, Kou J, et al. (2015) Advances in the pharmacological activities and mechanisms of diosgenin. Chin J Nat Med 13(8): 578-587.

129. Raju J, Mehta R (2009) Cancer chemopreventive and therapeutic effects of diosgenin, a food saponin. Nutr Cancer 61(1): 27-35.

130. Raju J, Rao VC (2012) Diosgenin, a steroid saponin constituent of yams and fenugreek: emerging evidence for applications in medicine. Bioact Comp Phytomed pp: 125-142.

131. Prieto JM, Recio MC, Giner RM (2006) Anti-inflammatory activity of β-sitosterol in a model of oxazolone induced contact-delayed-type hypersensitivity. Bol Latin Caribe Plant Med Aromat 5(3): 57-62.

132. Loizou S, Lekakis I, Chrousos GP, Moutsatsou P (2010) β-Sitosterol exhibits anti-inflammatory activity in human aortic endothelial cells. Mol Nutr Food Res 54(4): 551-558.

133. Chai JW, Kuppusamy UR, Kanthimathi MS (2008) Beta-sitosterol induces apoptosis in MCF-7 cells. Malays. J Biochem Mol Bio 16(2): 28-30.

134. Park C, Moon D, Rhu C, Choi BT, Lee WH (2007) β-Sitosterol induces anti-proliferation and apoptosis in human leukemic u937 cells through activation of caspase-3 and induction of bax/bcl-2 ratio. Biol Pharma Bull 30(7): 1317-1323.

135. Ju YH, Clausen LM, Allred KF, Almada AL, Helferich WG (2004) β-Sitosterol, β-Sitosterol glucoside and a mixture of β-sitosterol and β-sitosterol glucoside modulate the growth of estrogen-responsive breast cancer cells in vitro and in ovariectomized athymic Mice. J Nutr 134(5): 1145-1151.

136. Awad AB, Downie AC, Fink CS (2000) Inhibition of growth and stimulation of apoptosis by beta-sitosterol treatment of MDA-MB-231 human breast cancer cells in culture. Int J Mol Med 5(5): 541-546.

137. Manayi A, Saeidnia S, Ostad SN, Hadjiakhoondi A, Ardekani MR, et al. (2013) Chemical constituents and cytotoxic effect of the main compounds of Lythrum salicaria L. Z Naturforsch C 68(9-10): 367-375.

138. Ovesna Z, Vachalkova A, Horvathova K (2004) Taraxasterol and beta-sitosterol: new naturally compounds with chemoprotective/chemopreventive effects. Neoplasma 51(6): 407-414.

139. Sugano M, Morioka H, Ikeda I (1977) A Comparison of hypocholesterolemic activity of β-sitosterol and β-sitostanol in rats. J Nutr 107(11): 2011-2019.

140. Moon EJ, Lee YM, Lee OH, Lee MJ, Lee SK, et al. (1999) A novel angiogenic factor derived from Aloe vera gel: beta - sitosterol, a plant sterol. Angiogen 3(2): 117-123.

141. Villaseñor IM, Angelada J, Canlas AP, Echegoyen D (2002) Bioactivity studies on β-sitosterol and its glucoside. Phytother Res 16(5): 417-421.

142. Bouic P, Etsebeth S, Liebenberg R, Albrecht C, Pegel K, et al. (1996) Beta-sitosterol and beta-sitosterol glucoside stimulate human peripheral blood lymphocyte proliferation: Implications for their use as an immunomodulatory vitamin combination. Int J Immunopharmacol 18(12): 693-700.

143. Wilt TJ, MacDonald R, Ishani A (1999) Beta-sitosterol for the treatment of benign prostatic hyperplasia: a systematic review. BJU Int 83(9): 976-983.

144. Jourdain C, Tenca G, Deguercy A, Troplin P, Poelman D (2006) *In-vitro* effects of polyphenols from cocoa and β-sitosterol on the growth of human prostate cancer and normal cells. Eur J Cancer Prev 15(4): 353-361.

145. Gupta R, Sharma AK, Dobhal M, Sharma M, Gupta R (2011) Antidiabetic and antioxidant potential of β-sitosterol in streptozotocin-induced experimental hyperglycemia. J Diabetes 3(1): 29-37.

146. Jamaluddin F, Mohamed S, Lajis M (1994) Hypoglycaemic effect of Parkia speciosa seeds due to the synergistic action of β-sitosterol and stigmasterol. Food Chem 49(4): 339-345.

147. Lin A, Qian K, Usami Y, Lin L, Itokawa H, et al. (2007) 5-Hydroxymethyl-2-furfural, a clinical trials agent for sickle cell anemia, and its mono/di-glucosides from classically processed steamed Rehmanniae Radix. J Nat Med 62(2): 164-167.

148. Abdulmalik O, Safo MK, Chen Q, Yang J, Brugnara C, et al. (2005) 5-hydroxymethyl-2-furfural modifies intracellular sickle haemoglobin and inhibits sickling of red blood cells. Br J Haematol 128(4): 552-561.

149. Mei-Ju Z, Tan NH, Xiong JY, Ji CJ, Zhu HZ (2012) Chemical constituents contained in ethanol extracts from Acorus tatarinowii and their anti-fatigue activity. Zhongguo Zhong Yao Za Zhi 37(19): 2898-2901.

150. Zhang L, Jin G, Zhang X, Gong Z, Gu C (2014) Effects of 5-hydroxymethyl furfural extracted from Rehmannia glutinosa Libosch on the expression of signaling

molecules relevant to learning and memory among hippocampal neurons exposed to high concentration of corticosterone. Chin J Integ Med 20(11): 844-849.

151. Song YR, Liu Y, Le GW, Zhang R, Shi YH (2010) Study on antioxidation capability of fructose - Oligosaccharide and 5 - hydroxymethylfurfural. Sci Technol Food Ind 31: 342- 345.

152. Ya BL, Zhang L, Zhang L, Li YL, Li L (2012) 5-Hydroxymethyl-2-furfural prolongs survival and inhibits oxidative stress in a mouse model of forebrain ischemia. Neur Regener Res 7(22): 1722-1728.

153. Ding X, Wang M, Yao Y, Li G, Cai B (2010) Protective effect of 5-hydroxymethylfurfural derived from processed Fructus Corni on human hepatocyte LO2 injured by hydrogen peroxide and its mechanism. J Ethnopharmacol 128(2): 373-376.

154. Cao G, Cai H, Cai B, Tu S (2013) Effect of 5-hydroxymethylfurfural derived from processed Cornus officinalis on the prevention of high glucose-induced oxidative stress in human umbilical vein endothelial cells and its mechanism. Food Chem 140(1-2): 273-279.

155. Groke K, Herwig R, Ferdinand P (2010) US Patent No. 7,855,191. US Patent and Trademark Office, Washington DC.

156. Michail K, Matzi V, Maier A, Herwig R, Greilberger J (2007) Hydroxymethylfurfural: an enemy or a friendly xenobiotic? A bioanalytical approach. Anal Bioana Chem 387(8): 2801-2814.

157. Rivero-Cruz JF, Zhu M, Kinghorn AD, Wu CD (2008) Antimicrobial constituents of Thompson seedless raisins (Vitis vinifera) against selected oral pathogens. Phytochem Lett 1(3): 151-154.

158. Yalcin O, Cabrales P (2012) Increased hemoglobin O2 affinity protects during acute hypoxia. Am J Physiol Heart Circ Physiol 303(3): H271-H281.

159. Li M, Wu L, Zhao T, Xiong L, Huang X, et al. (2010) The protective role of 5-HMF against hypoxic injury. Cell Stress Chaperones 16(3): 267-273.

160. Zhou Y, Wang H, Yang R, Huang H, Sun Y, et al. (2012) Effects of Litchi chinensis fruit isolates on prostaglandin E2 and nitric oxide production in J774 murine macrophage cells. BMC Complem Alt Med 12(1): 12.

161. Lin S, Wu J, Su C, Ferng S, Lo C, et al. (2012) Identification and mode of action of 5-hydroxymethyl-2-furfural (5-HMF) and 1-methyl-1,2,3,4-tetrahydro-β-carboline-3-carboxylic acid (MTCA) as potent xanthine oxidase inhibitors in vinegars. J Agri Food Chem 60(39): 9856-9862.

162. Kitts DD, Chen X, Jing H (2012) Demonstration of antioxidant and anti-inflammatory bioactivities from sugar-amino acid maillard reaction products. J Agri Food Chem 60(27): 6718-6727.

163. Lorne E, Zmijewski JW, Zhao X, Liu G, Tsuruta Y, et al. (2008) Role of extracellular superoxide in neutrophil activation: interactions between xanthine oxidase and TLR4 induce proinflammatory cytokine production. Am J Physiol Cell Physiol 294(4): 985-993.

164. Du Y, Hong J, Pan K, Yan X, Zhang W (2004) 5-(hydroxymethyl) furfural and derivatives as inhibitors of TNF alpha and IL - 1beta production: US Patent Application 10/930,887[P].

165. Evans W (2009) Trease and Evans Pharmacognosy, 16th (Edn.), WB Saunders Elsevier, Edinburgh, UK.

166. Anonymous (2016) CTI Reviews. Chemistry of natural products, a unified approach. Cram 101, Textbook Reviews, Heim/ Rafbekur.

167. Tsai Y, Hsu H, Yang W, Tsai W, Chen C, et al. (2007) α-Bulnesene, a PAF inhibitor isolated from the essential oil of Pogostemon cablin. Fitoter 78(1): 7-11.

168. Hsu HC, Yang WC, Tsai YC (2007) Alpha-bulnesene, its preparation and its use, Patent US.

169. Achan J, Talisuna AO, Erhart A, Yeka A, Tibenderana JK, et al. (2011) Quinine, an old anti-malarial drug in a modern world: role in the treatment of malaria. Malaria J 10: 144.

170. Tatsimo SJN, Tamokou JD, Havyarimana L, Csupor D, Peter F, et al. (2012) Antimicrobial and antioxidant activity of kaempferol rhamnoside derivatives from Bryophyllum pinnatum. BMC Res Note 5: 158.

171. Teffo LS, Aderogba M, Eloff JN (2010) Antibacterial and antioxidant activities of four kaempferol methyl ethers isolated from Dodonaea viscosa Jacq. var. angustifolia leaf extracts. S Afr J Bot 76(1): 25-29.

172. Tseng T, Kao T, Chu C, Chou F, Lin W, et al. (2000) Induction of apoptosis by Hibiscus protocatechuic acid in human leukemia cells via reduction of retinoblastoma (RB) phosphorylation and Bcl-2 expression. Biochem Pharmacol 60(3): 307-315.

173. Lin H, Chen J, Huang C, Wang C (2007) Apoptotic effect of 3,4-dihydroxybenzoic acid on human gastric carcinoma cells involving JNK/p38 MAPK signaling activation. Int J Cancer 120(11): 2306-2316.

174. Yip EC, Chan AS, Pang H, Tam YK, Wong YH (2006) Protocatechuic acid induces cell death in HepG2 hepatocellular carcinoma cells through a c-Jun N-terminal kinase-dependent mechanism. Cell Biol Toxicol 22(4): 293-302.

175. Yin M, Lin C, Wu H, Tsao S, Hsu C (2009) Apoptotic effects of protocatechuic acid in human breast, lung, liver, cervix, and prostate cancer cells: Potential mechanisms of action. J Food Chem 57(14): 6468-6473.

176. Harini R, Pugalendi K (2010) Antihyperglycemic effect of protocatechuic acid on streptozotocin-diabetic rats. J Basic Clin Physiol Pharmacol 21(1): 79-91.

177. Min S, Ryu, S, Kim D (2010) Anti-inflammatory effects of black rice, cyanidin-3-O-β-d-glycoside, and its metabolites, cyanidin and protocatechuic acid. Int Immunopharmacol 10(8): 959-966.

178. Tsai S, Yin M (2012) Anti-glycative and anti-inflammatory effects of protocatechuic acid in brain of mice treated by d-galactose. Food ChemToxicol 50(9): 3198-3205.

179. Zhang X, Shi G, Liu X, An L, Guan S (2011) Anti-ageing effects of protocatechuic acid from Alpinia on spleen and liver antioxidative system of senescent mice. Cell Biochem Funct 29(4): 342-347.

180. Semaming Y, Kumfu S, Pannangpetch P, Chattipakorn SC, Chattipakorn N (2014) Protocatechuic acid exerts a cardio protective effect in type 1 diabetic rats. J Endocrinol 223(1): 13-23.

181. Chao C, Yin M (2009) Antibacterial effects of roselle calyx extracts and protocatechuic acid in ground beef and apple juice. Foodborne Path Dis 6(2): 201-206.

182. Li C, Jiang W, Zhu H, Hou J (2011) Antifibrotic effects of protocatechuic aldehyde on experimental liver fibrosis. Pharma Biol 50(4): 413-419.

183. Zhou Z, Zhang Y, Ding X, Chen S, Yang J, et al. (2007) Protocatechuic aldehyde inhibits hepatitis B virus replication both *in vitro* and *in vivo*. Antiviral Res 74(1): 59-64.

184. Shui G, Bao Y, Bo J, An L (2006) Protective effect of protocatechuic acid from Alpinia oxyphylla on hydrogen peroxide-induced oxidative PC12 cell death. Eur J Pharmacol 538(1-3): 73-79.

185. Borate AR, Suralkar AA, Birje SS, Malusare PV, Bangale PA (2011) Antihyperlipidemic effect of protocatechuic acid in fructose induced hyperlipidemia in rats. Int J Pharma Bio Sci 2(4): 456-460.

186. Beytur CO, Aydin M, Cakir O, Timurkaan N, Yılmaz F (2002) Protocatechuic acid prevents reproductive damage caused by 2, 3, 7, 8-tetrachlorodibenzo-p-dioxin (TCDD) in male rats. Andrologia 44(1): 454-461.

187. Wei X, Chen D, Yi Y, Qi H, Gao X, et al. (2012) Syringic acid extracted from herba dendrobii prevents diabetic cataract pathogenesis by inhibiting aldose reductase activity. Evid Complem Alt Med 2012: 1-13.

188. Kumar S, Prahalathan P, Raja B (2012) Syringic acid ameliorates l-NAME-induced hypertension by reducing oxidative stress. Naunyn-Schmied. Arch Pharmacol 385(12): 1175-1184.

189. Thipparaboina R, Mittapalli S, Thatikonda S, Nangia A, Naidu VG, et al. (2016) Syringic acid: structural elucidation and co-crystallization. Cry Grow Des 16(8): 4679-4687.

190. Lyu Q, Tou F, Su H, Wu X, Chen X, et al. (2015). Biochem Biophys Res Comm 462(1): 38-45.

191. Zheng Z, Xu L, Zhang S, Li W, Tou F, et al. (2017) Peiminine inhibits colorectal cancer cell proliferation by inducing apoptosis and autophagy and modulating key metabolic pathways. Oncotarget 8(29): 47619-47631.

192. Zhao Y, Liu J, Liu C, Zeng X, Li X, et al. (2016) Anti-Inflammatory Effects of p-coumaric Acid in LPS-Stimulated RAW264.7 Cells: Involvement of NF-κB and MAPKs Pathways. Med Chem 6(5): 327-330.

193. Prajapati NS, Purohit SS, Sharma AK, Kumar T (2003) A Handbook of Medicinal Plants: A Complete Source Book, Agrobios, Jodhpur, India.

194. Warrier, Nambiar, VPK, Ramankutty, C (1997) Indian Medicinal Plants. In A compendium of 500 medicinal plants, Orient Longman, Hyderabad, India, pp: 176.

195. Kirtikar KR, Basu BD (1994) Indian Medicinal plants. Biogreen Books 2012, Delhi 4: 2413.

196. Alam G (2004) Database on medicinal plants. Calcutta: CUTS Centre for International Trade, Economics and Environment, pp: 45.

197. Chaumont JP (1979) Fungistatic activity of eight phanerogams against phyto pathogenic fungi. Acta Bot Gallica 126: 537-542.

198. Varier PS (1994) Indian medicinal plants: a compendium of 500 species. Orient Longman, New Delhi, 336-338.

199. Khan H, Saeed M, Khan MA, Khan I, Ahmad M, et al. (2011a) Antimalarial and free radical scavenging activities of rhizomes of Polygonatum verticillatum supported by isolated metabolites. Med Chem Res 21(7): 1278-1282.

200. Anonymous (2003) Medicinal Plants in India, Institute of Economic and Market Research Printways, New Delhi.

201. Singh AP (2006) Ashtavarga-Rare Medicinal Plants. Ethnobot Leaflets 10: 104-108.

202. Singh G, Rawat GS (2011) Ethnomedicinal survey of Kedarnath wildlife sanctuary in Western Himalaya, India. In J Fundamen App Life Sci 1(1): 35-36.

203. Subramoniam A, Madhavachandran V, Gangaprasad A (2013) Medicinal plants in the treatment of arthritis. Annal Phytomed 2: 3-36.

204. Misra A, Srivastava S, Verma, S, Rawat AK (2015) Nutritional evaluation, antioxidant studies and quantification of poly phenolics in Roscoea purpurea tubers. BMC Res Notes 8(1): 324.

205. Sahu M, Mali P, Waikar S, Rangari V (2010) Evaluation of immunomodulatory potential of ethanolic extract of Roscoea procera rhizomes in mice. J Pharm Bioallied Sci 2(4): 346-349.

206. Rana MS, Samant SS (2011) Population biology of Lilium polyphyllum D. Don ex Royle-A critically endangered medicinal plant in a protected area of Northwestern Himalaya. J Nat Conserv 19(3): 137-142.

207. Bhatt ID, Rawat S, Rawal RS (2012) Antioxidants in Medicinal Plants. Biotechnol Med Plant Springer Verlag Berlin Heidelberg pp: 295-326.

208. Jagetia GC, Rao SK, Baliga MS, Babu SK (2004) The evaluation of nitric oxide scavenging activity of certain herbal formulations *in vitro*: a preliminary study. Phytother Res 18(7): 561-565.

209. Rawat S, Jugran AK, Bahukhandi A, Bahuguna A, Bhatt ID, et al. (2016) Anti-oxidant and anti-microbial properties of some ethno-therapeutically important medicinal plants of Indian Himalayan region. Biotech 6(2): 154.

210. Habbu P, Smita D, Mahadevan K, Shastry R, Biradar S (2012) Protective effect of Habenaria intermedia tubers against acute and chronic physical and psychological stress paradigms in rats. Rev Bras Farmaco 22(3): 568-579.

211. Giri L, Jugran A, Rawat S, Dhyani P, Andola H, et al. (2011) *In vitro* propagation, genetic and phytochemical assessment of Habenaria edgeworthii: an important Astavarga plant. Acta Physiol Plant. 34(3): 869-875.

212. Rawat S, Andola H, Giri L, Dhyani P, Jugran A, et al. (2013) Assessment of nutritional and antioxidant potential of selected vitality strengthening Himalayan medicinal plants. Int J Food Proper 17(3): 703-712.

213. Goudar MA, Jayadevappa H, Mahadevan KM, Shastry RA, Habbu PV (2015) Isolation and characterization of secondary metabolite from Habenaria intermedia D. Don for screening of hepatoprotecitve potential against carbon tetrachloride induced toxicity in albino rat liver. Int J Curr Pharm Res 7(1): 57-61.

214. Tsao MU (1951) A new synthesis of Mescaline. J Am Chem Soc 73(11): 5495-5496.

215. Li L, Ng T, Gao W, Li W, Fu M, et al. (2005) Antioxidant activity of gallic acid from rose flowers in senescence accelerated mice. Life Sci 77(2): 230-240.

216. Sakaguchi N, Inoue M, Isuzugawa K, Ogihara Y, Hosaka K (1999) Cell death-inducing activity by gallic acid derivatives. Biol Pharma Bull 22(5): 471-475.

217. Mishra N, Oraon A, Dev A, Jayaprakash V, Basu A, et al. (2010) Anticonvulsant activity of Benkara malabarica (Linn.) root extract: In vitro and in vivo investigation. J Ethnopharmacol 128(2): 533-536.

218. Thuong PT, Hung TM, Ngoc TM, Ha DT, Min BS, et al. (2010) Antioxidant activities of coumarins from Korean medicinal plants and their structural activity relationships. Phytother Res 24(1): 101-106.

219. Yang B, Chen G, Song X, Chen Z, Song X, et al. (2010) Chemical constituents and antimicrobial activities of Canthium horridum. Nat Prod Commun 5(6): 913-914.

220. Ojewole JA, Adesina SK (1983) Mechanism of the hypotensive effect of scopoletin isolated from the fruit of Tetrapleura tetraptera. Planta Med 49(1): 46-50.

221. Liu XL, Zhang L, Fu XL, Chen K, Qian BC (2001) Effect of scopoletin on PC3 cell proliferation and apoptosis. Acta Pharmacol Sin 22(10): 929-933.

222. Manuele MG, Ferraro G, Barreiro AML, López, P, Cremaschi G, et al. (2006) Comparative immunomodulatory effect of scopoletin on tumoral and normal lymphocytes. Life Sci 79(21): 2043-2048.

223. Kang SY, Sung SH, Park JH, Kim YC (1998) Hepatoprotective activity of scopoletin, a constituent of Solanum lyratum. Arch Pharm Res 21(6): 718-722.

224. Capra JC, Cunha MP, Machado DG, Zomkowski AD, Mendes BG (2010) Antidepressant-like effect of scopoletin, a coumarin isolated from Polygala sabulosa (Polygalaceae) in mice: Evidence for the involvement of monoaminergic systems. Eur J Pharmacol 643(2-3): 232-238.

225. Chauhan NS (1990) Medicinal Orchids of Himachal Pradesh. J Orch Soc India 4(1-2): 99-105.

226. Bhatnagar JK, Handa SS, Duggal SC (1970) Chemical investigations on Microstylis wallichii. Planta Medica 20(4): 156-161.

227. Gupta R, Aggarwal M, Baslas RK (1978) Chromatographic separation and identification of various constituents of essential oil from bulb of Malaxis acuminate. Indian Perfum 22(4): 287-288.

228. Lohani N, Tewari LM, Kumar R, Joshi GC, Kishor K (2013) Chemical composition of Microstylis wallichii Lindl from Western Himalaya. J Med Plants Res 7(31): 2289-2292.

229. Garg P, Aggarwal P, Sharma P, Sharma S (2012) Antioxidant activity of the butanol extract of Malaxis acuminata (Jeevak). J Pharm Res 5(5): 2888-2889.

230. Saha D, Ved D, Ravikumar K, Haridasan K (2015) Malaxis muscifera. The IUCN Red List of Threatened Species.

231. Bisht P, Prasad P, Nautiyal BP (2011) Polygonatum Verticillatum (Linn.) All. and Polygonatum Cirrhifolium (Wall.) Royle: Two threatened vital healers from asthavarga nurtured by Garhwal Himalaya, India. J Plant Develop 18: 159-167.

232. Uniyal SK, Singh KN, Jamwal P, Lal B (2006) Traditional use of medicinal plants among the tribal communities of Chhota Bhangal, Western Himalaya. J Ethnobiol Ethnomed 2: 14.

233. Antoniuk VO (1993) Purification and properties of lectins of Polygonatum multiflorum [L.] All. and Polygonatum verticillatum [L.]. All]. Ukr Biokhim Zh 65(1): 41-48.

234. Khan H, Saeed M, Gilani AU, Khan MA, Khan I, et al. (2011b) Antinociceptive activity of aerial parts of Polygonatum verticillatum: attenuation of both peripheral and central pain mediators. Phytother Res 25(7): 1024-1030.

235. Khan H, Saeed M, Mehmood MH, Rehman N, Muhammad N, et al. (2013a) Studies on tracheorelaxant and anti-inflammatory activities of rhizomes of Polygonatum verticillatum. BMC Complt Alt Med 13(1): 197.

236. Khan H, Saeed M, Muhammad N, Gaffar R, Gul F, et al. (2013b) Lipoxygenase and urease inhibition of the aerial parts of the Polygonatum verticillatum. Toxicol Ind Health 31(8): 758-763.

237. Bansal P, Virk J, Kumar S, Singh R, Tripathi A, et al. (2016) Isolation and characterization of quinine from Polygonatum verticillatum: A new marker approach to identify substitution and adulteration. J Adv Pharma Technol Res 7(4): 153-158.

238. Saeed M, Khan H, Khan MA, Khan F, Khan SA, et al. (2010a) Quantification of various metals accumulation and cytotoxic profile of aerial parts of Polygonatum verticillatum. Pak J Bot 42(6): 3995-4002.

239. Muhammad S, Haroon K, Murad AK, Shabana US, Naveed M et al. (2010) Phytotoxic, insecticidal and leishmanicidal activities of aerial parts of Polygonatum verticillatum. Afr J Biotechnol 9(8): 1241-1244.

240. Khan H, Saeed M, Muhammad N, Ghaffar R, Khan SA, et al. (2012a) Antimicrobial activities of rhizomes of Polygonatum verticillatum: Attributed to its total flavonoidal and phenolic contents. Pak J Pharma Sci 25(2): 463-467.

241. Khan H, Saeed M, Gilani AH, Muhammad N, Haq IU, et al. (2012b) Antipyretic and anticonvulsant activity of Polygonatum verticillatum: comparison of rhizomes and aerial parts. Phytother Res 27(3): 468-471.

242. Kazmi I, Afzal M, Rahman M, Gupta G, Anwar F (2012) Aphrodisiac properties of Polygonatum verticillatum leaf extract. Asia Pac J Trop Dis 2: 841-845.

243. Khan H, Saeed M, Gilani A, Muhammad N, Ur Rehman N, et al. (2013b) Antispasmodic and antidiarrheal activities of rhizomes of Polygonatum verticillatum maneuvered predominately through activation of K+ channels. Components identification through TLC. Toxicol Ind Health 32(4): 677-685.

244. Khan H, Saeed M, Khan MA, Izhar-ul-Haq, Muhammad N, et al. (2012c) Isolation of long-chain esters from the rhizome of Polygonatum verticillatum by potent tyrosinase inhibition. Med Chem Res 22(5): 2088-2092.

245. Bisht S, Bisht NS, Bhandari S (2011b) In vitro micropropagation in Polygonatum verticillatum (L.) All. an important threatened medicinal herb of Northern India. Physiol Mol Biol Plant 18(1): 89-93.

246. Nautiyal MC, Nautiyal BP (2004) Agrotechniques for high altitude medicinal and aromatic plants. Bishen Singh Mahendra Pal Singh, Dehradun, 149-155.

247. Bairwa R, Basyal D, Srivastav B (2012) Study of antidiabetic and hypolipidemic activity of Roscoea purpurea (Zingiberaceae). Int J Institut Pharm Life Sci 2(4): 130-137.

248. Sahu R, Prakash I, Mishra R, Maliye A, Sonekar M (2016) Phytochemical screening and hptlc finger printing analysis of Roscea procera (Kakoli) and Lilium polyphyllum (Kshirkakoli). IJPPR 8(1): 53-69.

249. Chi Y, Kao Y, Chang K (1940) The Alkaloids of Fritilaria Roylei. II. Isolation of Peiminine[1]. J Am Chem Soc 62(11): 2896-2897.

250. Wu YH (1944) The constituents of Fritillaria roylei[1]. J Am.Chem Soc 66(10): 1778-1780.

251. Chatterjee A, Dhara K, Pascard C, Prange T (1976) Kashmirine, a new steroidal alkaloid from Frittilaria roylei, Hook (liliaceae). Tetrahedron Lett 17(33): 2903-2904.

252. Jiang R, Ma S, But PP, Dong H, Mak TC (2001) Sipeimine, a steroidal alkaloid from Fritillaria roylei Hooker. Acta Crystallograph Sec C Cryst St Commun 57(2): 170-171.

253. Khare CP (2007) Indian Medicinal Plants. An Illustrated Dictionary, Springer Verlag, Berlin.

254. Dhyani A, Bahuguna YM, Semwal DP, Nautiyal BP, Nautiyal MC (2009) Anatomical features of Lilium polyphyllum D. Don ex Royle (Liliaceae). J Am Sci 5(5): 85-90.

255. Chinmay R, Kumari S, Bishnupriya D, Mohanty RC, Renu D, et al. (2011) Retracted: Pharmacognostical & phytochemical studies of Roscea procera (Kakoli) and Lilium polyphyllum (Ksheerkakoli) in comparison with market samples. Pharmacognosy J 3(25): 32-38.

256. Trease GE, Evans WC (1989) Pharmacognosy. 11th (Edn.), Brailliar Tiridel Can: Macmillian publishers India, New Delhi.

257. Fursule R, Patil S (2010) Hepatoprotective and antioxidant activity of Phaseolus trilobus, Ait on bile duct ligation induced liver fibrosis in rats. J Ethnopharm 129(3): 416-419.

258. Pandeya G, Sashtri K (2011) Charaka Samhita (part I) (Sanskrit-Hindi Com). Chaukhambha Bharatee Academy. Varanasi, India, pp: 587.

259. Shastri V (2002) Bhavprakash nighantu. Motilaal Banarasidash, New Delhi, India.

Journal of Yoga and Physiotherapy
ISSN: 2476-1303

Juniper Publishers
key to the Researchers

Mini Review
Volume 6 Issue 4 - November 2018
DOI: 10.19080/JYP.2018.06.555694

J Yoga & Physio

Chakra Genesis, A Correlation Between Evolution of Chakras & Embryogenesis

Acharya Balkrishna[1,2], Vinay Kumar Sharma[1], Niti Sharma[1]*

[1]*Patanjali Research Institute, Haridwar, India*

[2]*University of Patanjali, Haridwar, India*

Submission: January 19, 2018; **Published:** November 06, 2018

***Corresponding author:** Nitti Sharma, Patanjali Research Institute, Haridwar, Uttarakhand, India

Abstract

The Chakras are energy hubs in the body which are important for physical, mental, and spiritual comfort. They are located on the spinal cord where flow of energy is intensified due to congregation of energies from various neuronal centers. Every Chakra is also related to a specific endocrine organ which is helpful in healing of a blocked energy center. Abundant literature is available on presence of Chakras but there is a little understanding how the Chakras are developed during embryogenesis in the human body. The spine is one of the first things to develop in the fetus and it is well known that the Chakra system is present in the spine, it make sense to study the Chakra system of fetus and see how it evolves and effects the development of the child. Hence in the present article we aim to gather knowledge on how Chakras evolve within the mother's womb.

Keywords: Chakra; Embryogenesis; Endocrine system; Yoga

Introduction

The Chakra (Sanskrit: "wheel") - a swirling wheel of energy which provide vital force of life which are important for physical, mental, and spiritual comfort. They are not made of nerves but are powerful and subtle centers of energy. They are located on the spinal cord where flow of energy is intensified due to congregation of energies from various neuronal centers. Chakras are an integral part of Yoga [1] and get activated through Yoga practices particularly Pranayama (Controlled breathing) which help in directing spinal cord energy upwards by producing spark in motor and sensory nerves. The power of consciousness of the brain is also controlled by this flow of energy. Therefore, by achieving a command over the Chakra all glandular secretions and mental function can be controlled [2]. Several research articles supports the physiological effects of Yoga on central nervous system [3-7], cardiovascular system [8-16], autonomic nervous system [17-21] and respiratory system [22-25].

The earliest known mention of Chakras is found around 1700-1100 BCE in the Brahma Upanishad, Yogatattva Upanishad and Vedas [26]. These Vedic models were adapted in Tibetan Buddhism as Vajrayana theory, and in the Tantric Shakti theory of Chakras [27]. The number of Chakras varies in different traditions of Yoga. Old Buddhist literature mentioned four Chakras which later got extended [28]. One hundred and twelve chakras were described [29] while others gave importance to seven Chakras [30-31]. The translation of two Indian texts, the Sat-Cakra-Nirupana, and the Padaka-Pancaka, by Arthur Avlon, in a book entitled The Serpent Power presented the idea of seven main Chakras in the West [32]. Vedas, the oldest scripture of world defined the eight chakras 'Astachakra navadvaradevanampurayodhya'. Out of the eight, five are situated on the spinal cord while the other three are related to brain [33]. Every Chakra is also related to a specific endocrine organ [34] which is helpful in healing of ablocked energy center. Abundant literature is available on presence of Chakras but there is a little understanding how the Chakras are developed during embryogenesis in the human body. The spine is one of the first things to develop in the fetus and it is well known that the Chakra system is present in the spine, it make sense to study the Chakra system of fetus and see how it evolves and effects the development of the child. Hence in the present review article we try to gather knowledge on how Chakras evolve within the womb (Figure 1) Table 1.

Table 1: Anatomical Location, Associated Gland and Diseases Related to Blocked Chakras.

SN	Chakra	Location	Derived from	Physiological system concerned	Diseases due to blocked Chakras	Associated Endocrine gland
1	Muladhara	Base of spine	Mesoderm	Excretory system, Uri-no-genital system	Urinary diseases, kidney disorders, genital disorders	Adrenal

2	Svadhisthana	Below the navel	Mesoderm	Reproductive system	Infertility, tissue disease, genital disorders	Adrenal
3	Manipura	Below the chest	Endoderm	Digestive system	Digestive system disorders, diabetes, low immunity	Pancreatic
4	Anahata	Center of the chest (Thoracic vertebra)	Mesoderm	Circulatory system, respiratory system, Auto-immune system	Heart diseases, hypertension	Thymus
5	Visuddha	Thyroid and para thyroid	Endoderm	Respiratory system	Bronchial asthma, lung disorders, thyroid, goiter	Thyroid
6	Ajna	Center of the forehead	Ectoderm	Nervous system	Epilepsy, fainting, paralysis	Pineal
7	Manas	Below the thalamus	Ectoderm	Sensory and motor system	Psycho-somatic and neurological disorders	Pituitary
8	Sahasrara	Top of the skull	Ectoderm	Central nervous System	Hormonal imbalances, metabolic syndromes	Pituitary

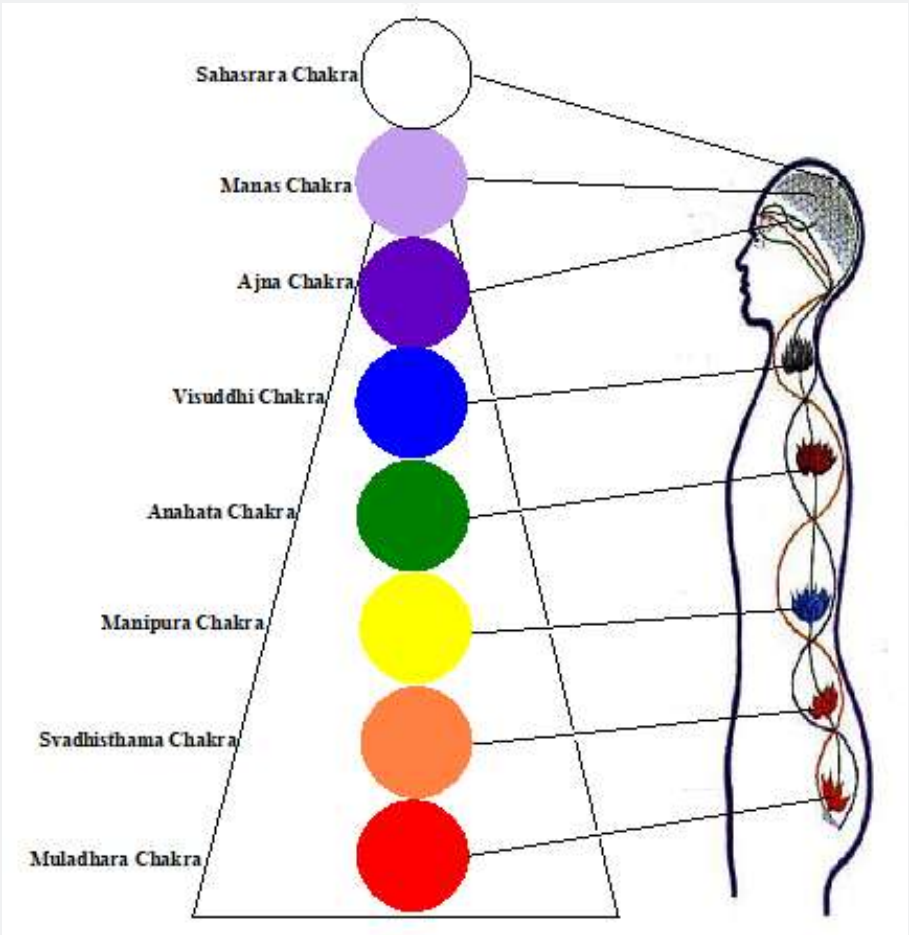

Figure 1: Position of Chakras in Human Body [54].

Discussion

During the initial stages of pregnancy, the embryo develops three germ layers. The innermost layer is called the endoderm which eventually forms digestive system, liver and lungs. The middle layer or mesoderm is the source of sex organs, bones, kidney and muscles. Ectoderm is the outer most layers, which forms the nervous system, skin and eyes [35].

Chakra system begins to develop during the first two months in the womb. The developing fetus at this stage is so attached with the life force energy that the Chakras are united together under one energy field i.e. at unanimity with the universe. As the embryo develops into afetus (after 8 weeks of fertilization), nervous tissue first develops as a flat sheet of cells called the neural plate. At an early point, the side edges of the neural plate begin to fold toward

How to cite this article: Acharya B, Vinay K S, Niti S. Chakra Genesis, A Correlation Between Evolution of Chakras & Embryogenesis. J Yoga & Physio. 2018; 6(4): 555694. DOI: 10.19080/JYP.2018.06.555694.

each other, ultimately forming a tube that mature into brain and spinal cord [36].

Thus the Sahasrara Chakra (Crown Chakra, the 8th Chakra) is the first to become active [37]. Meditation is the best way for the mother to support developing infant's Crown Chakra. During week 4, the forebrain, middle brain, hind brain, and the optical stalk begin to develop [38]. The differentiation of midbrain from forebrain would make the physical base of the Sahasrára Chakra [1]. The brain hemispheres start to form at week 6, and the brain waves begin. The hind brain develops during week 8, and controls the heart rate, breathing, and muscle movement. The nervous system is ready for functioning at 9th week and the brain develops approximately 25 million neurons per minute. During 15th week the spinal nerves emerge from the spinal cord and by week 19, the brain is able to form motor neurons, which allow the body to produce movement voluntarily. By the end of week 26, the brain's surface area increases due to folding.

After the formation of brain, motor and sensory neurons start functioning. The development of the fetus brings it closer to the material world even though they are engrossed in the spiritual world of the womb. The body organs began to differentiate, blood cells and hormones start forming and the fetus continues to grow. Along with that the Chakras also began to segregate. The heart is the first organ to be formed by day 22 or 23 after conception (week five of pregnancy), the heart begins to beat and can be noticed in vaginal ultrasound as a weak flicker. Initially heart is formed as a tube which later becomes fully functional by the end of week eight of embryonic development [39]. In four weeks after conception, the neural tube along fetus back is closing and heart is pumping blood. Embryo does not experience any kind of pain during first three months of pregnancy. It starts experiences consciousness after three weeks. It suggests that the soul (Atma) enters the body at this time [33] during the formation of Anahata Chakra (Heart Chakra, 4th Chakra). It lies at the center of the chest and includes the heart, cardiac plexus, thymus gland, lungs, and breasts besides ruling the lymphatic system.

Manas Chakra (7th Chakra) lies directly above Ajna Chakra and mostly considered as a minor Chakra. It consists of six petals, one for each of the five senses and one for sleep. These petals are normally white but adopt the color of the senses when stimulated by them, and turn black at the time of sleep. This Chakra is responsible for sending sense perceptions to the higher Chakras.

The Third Eye Chakra (Ajna Chakra, 6th Chakra) becomes active around 7 weeks after conception. It is a bridge that permits mind communication between two people. According to the Hindu belief the spiritual energy enters the body through this gateway and sometimes called 'seat of soul' [40]. Ajna has two petals, represent the pineal and pituitary glands, said to represent the psychic channels (nadis) Ida and Pingala, which meet the central Sushumna nadi before rising to the Crown Chakra. Pineal gland, which regulates the circadian rhythm, is light-sensitive gland that is why it is called the 'third eye'. It is also sometimes linked with the pituitary gland, the chief endocrine gland. This gland produces a melatonin and a powerful psychedelic chemical called DMT (N,N dimethyltryptamine). In normal human DMT is released in large amounts during two times in life: once at birth and at time of death [41]. From an embryological point of view, the most likely site of Ajna Chakra is the highly studied isthmus organizer that controls the differentiation of midbrain from hind brain structures [42]. Mother can develop this Chakra of her unborn baby by reading and speaking with her child on a mental level.

The Vishuddhi Chakra (5th Chakra) is located in the vicinity of the Larynx- and is therefore also known as the Throat Chakra. It regulates the functional regions of the thyroid, parathyroid, jaw, neck, mouth, tongue, and larynx. The thyroid is one of the initial endocrine organs to differentiate and has an important hormonal role in embryonic development. The thyroid gland is formed from two groups of embryonic cells by first dividing to form two lobes parted by a narrow connecting isthmus [43]. These two structures became obvious by 16 to 17 days of gestation. However, by 20 weeks only the fetus is able work through feedback mechanisms for thyroid hormones production [44]. Development of larynx starts during the 4th week and is closely connected with the development of trachea. The development starts in the form of laryngotracheal groove in the ventral wall of the pharynx. The groove steadily deepens and its edges fuse to form a septum which splits the laryngotracheal tube from the pharynx and oesophagus. This tube is lined with endoderm from which the epithelium of the airway develops. The cranial end of this laryngotracheal tube forms the larynx and the trachea while the other end of tube produces two branches from which the two main bronchi develop. This is also the place from which the two lung buds starts to develop.

The Pranayama has tremendous effect on the Vishuddhi Chakra, at both the physical and spiritual levels. The harmful materials are release from the body on a physical level, and spiritually the beliefs, sentiments, conscious and subconscious are cleansed and synchronized. To boost cognizance in the developing baby the mother can communicate with the baby by speaking or by playing music etc.

The third Chakra is called Manipura (Solar Plexus Chakra), which is located around the navel and extends up to the breastbone [45]. It is a source of personal power that governs self-esteem and also has the power of transformation. This Chakra has role in controlling metabolism and digestion too. Through this Chakra we absorbs solar energy with revitalize our etheric and physical body [46]. Manipura is "the center of etheric-psychic intuition" that is why listening to 'gut feeling' may help in making better decisions in life [47].

Initially, the digestive system is a series of tubes starting from mouth and terminating at anus. By about 8 weeks of gestation stomach starts forming and by 10th week start to produce gastric juices. The complete development of digestive system takes 32 weeks. The rudimentary structure of the eyes, ears, and smell develops early in gestation along with sensation for touch, position, and motion detection. Brain development includes sensory systems, motor systems, social/emotional systems, and

How to cite this article: Acharya B, Vinay K S, Niti S. Chakra Genesis, A Correlation Between Evolution of Chakras & Embryogenesis. J Yoga & Physio. 2018; 6(4): 555694. DOI: 10.19080/JYP.2018.06.555694

cognitive systems. The motor development occurs during six to ten weeks, in which the fetus starts to move its limbs and mouth. Sensory development begins at 8 weeks and progresses rapidly. The first sense to develop is touch followed by taste at 14 weeks. The ear is fully developed at 24 weeks, even though the fetus can react to sound by 16 weeks. The eyes open at 26 weeks but the ability to focus is developed toward the end of the pregnancy [48]. All of these systems are related and work together throughout late fetal and early neonatal life. All exogenous or outside sensory stimulation has an emotional component as well as the sensory component [49].

The pineal gland becomes visible at 49th day or 7th week after conception. During this time only sex differentiation takes place and gender is determined. The pineal gland influences the pituitary glands secretion of Follicle Stimulating Hormone and Luteinizing Hormone through some other transmitting molecule [50]. During this period the Sacral Chakra (Svadhisthana Chakra, 2nd Chakra) begins to develop and determine the sexuality during physical development. It is located above the pubic bone – below the navel, incorporating the genitals and the hypogastric plexus. The mother should engage in creative activities (writing, painting and paying music) to convey that verve to the baby.

The Muladhara Chakra (Root Chakra, 1st Chakra) is the foundation of the energy body. The root chakra is also associated with what is referred to as a psychic knot. Specifically, Muladhara Chakra is known as the Brahma granthi. This is like a knot of energy in the body. When this knot of energy is released, it allows us to enter Brahma Loka. It also purifies and balances energy in the urogenital region. The root Chakra becomes active when the baby changes its position and places the head in the birth canal. The child is ready to emerge from mother's womb and greet the material world. Thus in other words the Root Chakra relates to the survival needs, will to live, and sense of trust. Children with enough Root Chakra energy will be less prone to illness and have a stronger chance for survival. Mother's contentment and sense of security during this time will have a deep influence on the child's root Chakra.

The urogenital system starts developing during the fourth week from urogenital ridges in the intermediate mesoderm on each side of the primitive aorta. Both urinary and genital systems are interwoven and develop together. The nephrogenic ridge is the part of the urogenital ridge which forms the urinary system. Urine formation begins towards the end of the first trimester (weeks 11 to 12). Three sets of kidneys also develop consecutively in the embryo. The pronephros is nonfunctional and disappears very early; the structural elements of the mesonephros mostly degenerate, but the gonad is developed in their place, with which the Wolffian duct remains as the duct in males, and the Müllerian as that of the female.

Maxwell proposed a gap junction theory according to which physical systems related to a Chakra have three key features: (i) a physical base present in the dorsal CNS, (ii) a concentration point activating the physical base, (iii) and impact of that physical base on secretions from a particular gland which in turn affect the brain function. The gap junctions in the autonomic plexuses may become activate in the dorsal CNS, once energized. Moreover, gap junctions also modulate glandular functions, apparently by autonomic nerves linked with these dorsal CNS positions.

Conclusion

Previous efforts to correlate physical body and Chakra were inadequate. Additional information about stages of embryogenesis along with the formation of Chakras may be helpful in proposing a different aspect of Chakra theory. This is backed by the gap junction concept proposed by Maxwell according to which Chakras must have physical connection in addition to the apparent metaphysical features.Chakras have more than one dimension to them. One dimension is their spiritual while other is physical existence. The literaturehas described the Chakras as metaphysical equivalent of the endocrine glands, as noticeable similarity between the positions of the two has been observed [51]. Sturgess also linked the lower six chakras to specific nerve plexuses along the spinal cord as well as with the glands [52]. Likewise, the Ajna Chakra is linked with the pineal gland which is a part of the endocrine system [53]. These associations remain speculative, however, and have yet to be empirically validated. Initially, all Chakras are fused under one powerful energy source which gradually separates and develops along with the fetal development. The mother need to focus on meditation, creative activities, and positive thinking etc. all have tremendous role in strengthening the Chakras of growing fetus in the womb.

References

1. Maxwell R (2009) The physiological foundation of yoga chakra expression. Zygon 44(4): 807-824.
2. Sarkar SPR (1994) Yoga Psychology. (2nd edn), In: Ánanda M (Ed.), Glands Subglands, Calcutta, India, pp: 121.
3. Elson BE, Reter H, Cunis D (1977) Physiological changes in yoga meditation. Psychophysiol 14(1): 52-57.
4. Corby JC, Walton TR, Vincent PZ Jr, Bert SK (1978) Psychophysiological correlates of the practice of tantric yoga meditation. Arch Gen Psych 35(5): 571-577.
5. Lazar S, Bush G, Gollub RL, Fricchione GL, Khalsa G, et al. (2000) Functional brain mapping of the relaxation response and meditation. Neuro Report 11(7): 158-185.
6. Pete A, Peper E, Kawakami M, Gibney KH (2001) The physiological correlates of kundalini yoga meditation: A study of a yoga master. Appl Psychophysiol Biofeedback 26(2): 147-153.
7. Aftanas L, Semen G (2005) Impact of regular meditation practice on EEG activity at rest and during evoked negative emotions. Int J Neurosci 115: 893-909.
8. Patel C, Marmot MG, Terry DJ, Carruthers M, Hunt B, et al. (1985) Trial of relaxation in reducing the coronary risk: Four year follow up. Br Med J (Clin Res Ed) 290(6475): 1103-1106.
9. Bernardi L, Sleight P, Gabriele B, Simone C, Lamberto F, et al. (2001) Effect of rosary prayer and yoga mantras on autonomic cardiovascular rhythms: Comparative study. Br Med J 323(7327): 1446-1449.
10. Raub J (2002) Psychophysiologic effects of hatha yoga on musculoskeletal and cardiopulmonary function: A literature review. J Alt Compl Med 8(6): 797-812.

How to cite this article: Acharya B, Vinay K S, Niti S. Chakra Genesis, A Correlation Between Evolution of Chakras & Embryogenesis. J Yoga & Physio. 2018; 6(4): 555694. DOI: 10.19080/JYP.2018.06.555694.

11. Bharshankar G, Geeta B (2003) Effect of yoga on cardiovascular system in subjects above 40 years. In J Physiol Pharmacol 47 (2): 202-206.

12. Kasiganesan H, Malhotra AS, Pal K, Prasad R, Kumar R, et al. (2004) Effects of hatha yoga and Omkar meditation on cardiorespiratory performance, psychologic profile and melatonin secretion. J Alt Compl Med 10(2): 261-268.

13. Patil S, Telles S (2006) Effects of two yoga based relaxation techniques on heart rate variability (HRV). Int J Stress Manage 13 (4): 460-475.

14. Choudhary S, Choudhary R, Chawala VK, Soni ND, Kumar J, et al. (2013) Effects of Yoga and physical exercise on cardio-respiratory parameters. Natl J Integr Res Med 4(3): 50-55.

15. Maini S, Kaur H, Maini N (2011) Effect of Rajyoga meditation on the heart rate blood pressure and ECG. J Clin Diag Res 5(8): 1519-1522.

16. Chaturvedi DK, Arora, JK, Bhardwaj R (2015) Effect of meditation on Chakra energy and hemodynamic parameters. Int J Com Appl 126(12): 52-59.

17. Wenger MA, Bagchi BK (1961) Studies of autonomic functions in practitioners of Yoga in India. Behav Sci 6: 312-323.

18. Bujatti M, Riederer P (1976) Serotonin, noradrenaline dopamine metabolites in transcendental meditation-technique. J Neu Trans 39(3): 257-267.

19. Vempati RP, Telles S (2002) Yoga-based guided relaxation reduces sympathetic activity judged from baseline levels. Psychol Rep 90 (2): 487-494.

20. Streeter CC, Gerbarg PL, Saper RB, Ciraulo DA, Brown RP (2012) Effects of yoga on the autonomic nervous system, gamma-aminobutyric-acid, and allostasis in epilepsy, depression, and post-traumatic stress disorder. Med Hypotheses 78(5): 571-579.

21. Amihai I, Kozhevnikov M (2015) The influence of Buddhist meditation traditions on the autonomic system and attention. Biomed Res Int 731579.

22. Bhargava RM, Gogate G, Mascarenhas JF (1988) Autonomic responses to breath holding and its variations following Pranayama. In J Physiol Pharmacol 32(4): 257-264.

23. Telles S, Nagarathna R, Nagendra HR (1994) Breathing through a particular nostril can alter metabolism and autonomic activities. In J Physiol Pharmacol 38(2): 133–137.

24. Spicuzza L, Gabutti A, Porta C, Montano N, Bernardi L (2000) Yoga and chemoreflex response to hypoxia and hypercapnia. Lancet 356: 1495-1496.

25. Brown RP, Gerbarg PL (2005) Sudarshan Kriya yogic breathing in the treatment of stress, anxiety and depression: Part I-neurophysiological model. J Alt Compl Med 11(1): 189–201.

26. Fenton S (2009) Simply Chakras. Sterling Publishing Company Inc, New York, USA.

27. Gordon WD (2003) Kiss of the Yogini. University of Chicago Press, Chicago, USA.

28. Gordon WD (2011) Yoga in Practice. Princeton University Press, New Jersey, USA.

29. Sadhguru (2017) Adiyogi: The Source of Yoga. Harper Collins Publishers, India.

30. Grimes J (1996) A Concise Dictionary of Indian Philosophy: Sanskrit Terms Defined in English. State University of New York Press, USA, pp: 100–101.

31. Feuerstein G (1997) The Shambhala Encyclopedia of Yoga. Shambhala, Boston, USA.

32. Avalon A (1974) The Serpent Power: The Secrets of Tantric and Shaktic Yoga. Dover, New York, USA.

33. Balkrishna A (2017) Yog Vijnanam. Divya Publications, India.

34. Khalsa DS, Cameron S (2002) Meditation as Medicine: Activate the Power of Your Natural Healing Force. Fireside, New York, USA.

35. Kate MC (2013) The Embryo Project Encyclopedia. Arizona State University, Arizona, USA.

36. Gammill LS, Marianne BF (2003) Neural crest specification: Migrating into genomics. Nature Rev Neurosci 4(10): 795-805.

37. Kalashatra G (2004) A Handbook of Chakra Healing: Spiritual Practice for Health, Harmony and Inner Peace. (1st edn), CT: Konecky & Konecky Publishers, USA.

38. Rubenstein J, Shimamura K, Salvador M, Luis P (1998) Regionalization of the prosencephalic neural plate. Ann Rev Neurosci 21(1): 445–477.

39. Perkins S (2015) A description of the fetal heart development stages.

40. Lokhorst GJ (2016) Descartes and the Pineal Gland, (Summer edn), In: The Stanford Encyclopedia of Philosophy. Edward NZ (ed.), Stanford University, USA.

41. Strassman R (2001) DMT: The Spirit Molecule. A Doctor's Revolutionary Research into the Biology of Near-Death and Mystical Experiences, Rochester, USA.

42. Paula A, Wassef M (2003) The isthmic organizer links anteroposterior and dorsoventral patterning in the mid/hind brain by generating roof plate structures. Development 130(22): 5331–38.

43. Gardner D, Shoback D (2011) Greenspan's Basic & Clinical Endocrinology. (9th edn), McGraw Hill, New York, USA.

44. Balasubramanian T (2015) Anatomy of larynx. Otolaryngology Online Journal 5(1.5): 1-13.

45. Leadbeater CW (1994). The Chakras. The Theosophical Publishing House, Wheaton, USA.

46. Katzman M (2015) The Solar Plexus Chakra: The Third Chakra Manipura Guide. Kindle Edition.

47. Graven S, Browne J (2008) Sensory Development in the Fetus, Neonate, and Infant: Introduction and Overview. Newborn Infant Nur Rev 8(4): 169-172.

48. Purvis B (2005) Prenatal Sensory Development. The NICU Experience: Its Impact and Implications, Virginia Early Intervention Conference, Roanoke, USA.

49. Braverman L, Cooper D (2004) The Thyroid: A Fundamental and Clinical Text. (10th edn), Lippincott Williams and Wilkins, USA.

50. Motta M, Fraschini F, Martini L (1967) Endocrine effects of pineal gland and of melatonin. Exp Biol Med 126(2): 431–435.

51. Gardiner P, Osborn G (2006) The Shining Ones: The World's Most Powerful Secret Society Revealed. Watkins Publishing, London, UK.

52. Gyurme T (2013) 8-Alchemy: The Alchemy of the Soul. Lulu Press Inc, USA.

53. Sturgess S (2015) The Yoga Book: A Practical Guide to Self-Realization. Watkins Publishing, London, UK.

54. Balkrishna A (2013) A Practical Approach to the Science of Ayurveda. Divya Prakashan, India.

How to cite this article: Acharya B, Vinay K S, Niti S. Chakra Genesis, A Correlation Between Evolution of Chakras & Embryogenesis. J Yoga & Physio. 2018; 6(4): 555694. DOI: 10.19080/JYP.2018.06.555694

DOI: 10.19080/JYP.2018.06.555694

How to cite this article: Acharya B, Vinay K S, Niti S. Chakra Genesis, A Correlation Between Evolution of Chakras & Embryogenesis. J Yoga & Physio. 2018; 6(4): 555694. DOI: 10.19080/JYP.2018.06.555694.

CYTOCHROME P 450 INHIBITION STUDY OF PICRORHIZA KURROA: EVALUATION OF HERB–DRUG INTERACTION

Article · January 2017

DOI: 10.20959/wjpps20172-8581

5 authors, including:

Niti Sharma
Gachon University
65 PUBLICATIONS **1,365** CITATIONS

SEE PROFILE

Vinay Kumar Sharma
Patanjali Research Institute (PRI), Haridwar, India
58 PUBLICATIONS **1,757** CITATIONS

SEE PROFILE

Ashish Kumar Gupta
Patanjali Research Foundation Trust
24 PUBLICATIONS **209** CITATIONS

SEE PROFILE

WORLD JOURNAL OF PHARMACY AND PHARMACEUTICAL SCIENCES
SJIF Impact Factor 6.647
Volume 6, Issue 2, 1338-1343 Research Article ISSN 2278 – 4357

CYTOCHROME P_{450} INHIBITION STUDY OF *PICRORHIZA KURROA*: EVALUATION OF HERB-DRUG INTERACTION

Acharya Bal Krishna[1,2], Niti Sharma[2]*,Vinay K. Sharma[2] and Ashish Kumar Gupta[2]

[1]University of Patanjali, Haridwar, Uttarakhand - 249402, India.

[2]Patanjali Natural Coloroma Pvt. Ltd., Haridwar, Uttarakhand - 249404, India.

Article Received on
19 Dec. 2016,

Revised on 09 Jan. 2017,
Accepted on 29 Jan. 2017

DOI: 10.20959/wjpps20172-8581

***Corresponding Author**
Dr. Niti Sharma
Patanjali Natural Coloroma Pvt. Ltd., Haridwar, Uttarakhand – 249404, India.

Graphical Abstarct

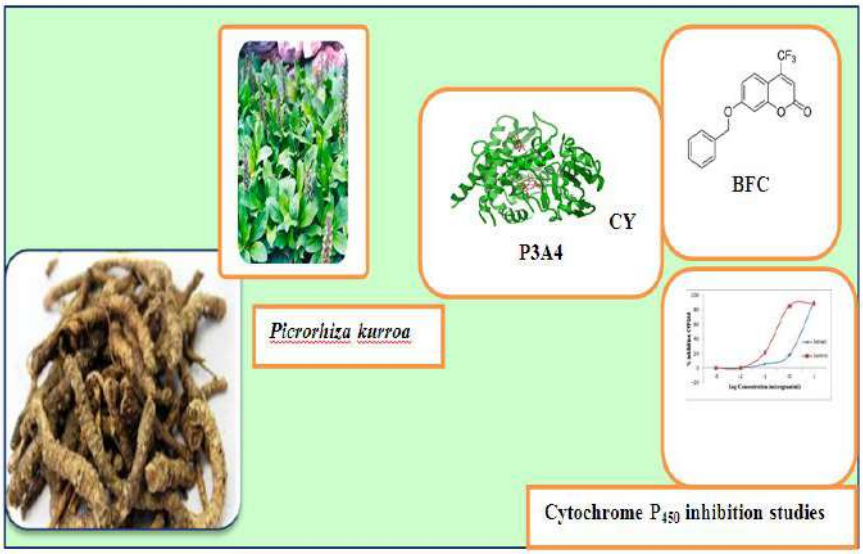

ABSTRACT

Background: *Picrorhiza kurroa* is an important medicinal plant in the traditional Chinese and Ayurvedic systems of medicine with wide therapeutic potential varing from anti-bacterial to immune-modulating properties. **Objective:** To establish the safety profile of *Picrorhiza kurroa* as a drug. **Material and Methods:** Cytochrome P_{450} mediated inhibitory potential is a useful tool to estimate the risk for drug interaction. To assess safety profile of *Picrorhiza kurroa*, CYP3A4 isoform was selected. Hydroalcoholic extract of *Picrorhiza kurroa* rhizome was prepared and assayed using a fluorescent substrate and recombinant CYP3A4 isoform. **Results:** It was observed that there is a very little possibility of herb-drug interaction of *Picrorhiza kurroa*, if it is administered along with other products that are metabolized by P_{450}. **Conclusion:** *Picrorhiza kurroa* is completely safe and can be used for therapeutic purposes. **Abbreviations used:** CYP, Cytochrome P_{450}; IC_{50}, Inhibitory concentration at 50%; BFC, 7-benzyloxy-4(trifluoromethyl)Coumarin.

KEYWORDS: *Picrorhiza kurroa*, Cytochrome P_{450} Inhibition, Herb-Drug interaction.

INTRODUCTION

Picrorhiza kurroa (Kutki, Kutka; Family Scrophulariaceae) is a perennial herb, abundantly found in the Himalayas. It is a significantly important plant in the traditional Chinese and Ayurvedic systems of medicine. It is reported to possess anti-bacterial, anti-periodic, hepatoprotective, anti-cholestatic[1],[2],[3],[4], anti-inflammatory, anti-oxidant[5],[6],[7], anti-allergy, anti-asthmatic[8],[9] and immune-modulating properties.[10] Due to immense therapeutic application of *Picrorhiza kurroa* in Ayurvedic medicine system it is necessary to evaluate its potential drug interaction with Cytochrome enzymes. The Cytochrome P_{450} isoenzymes (CYP) have an important role in xenobiotic metabolism and are involved in several types of interactions such as drugs, herbs, foods etc. Generally, the drug interactions involving CYP isoforms affects activation or inhibition of the enzyme.[11] The CYP mediated inhibitory activity is a useful tool to assess the risk for drug-drug interaction as it categories the compounds as high (IC_{50} <1 µM), moderate (1 µM<IC_{50}<10 µM) and low (IC_{50}>10 µM) potential for drug-drug interaction (DDI).

For the assessment of herb-drug interaction of *Picrorhiza kurroa*, CYP3A4 isoform (EC 1.14.13.97) was selected. Numerous other members of cytochrome P_{450} family are also involved in drug metabolism, but CYP3A4 is the most common and the most adaptable one. The use of CYP3A4 Inhibitor can decrease metabolism during the first pass and the elimination phases. Decreased drug elimination may enhance drugs therapeutic and also its toxicity. Thus, present research aims to develop the safety profile of *Picrorhiza kurroa* as a drug which will definitely be advantageous in endorsing traditional Ayurveda to the international level.

MATERIAL AND METHODS

Material

The rhizome of *Picrorhiza kurroa* was a generous gift from Patanjali Ayurveda Ltd., Haridwar. Recombinant CYP3A4 was purchased from XenoTech, LLC. Fluorescent substrate 7-benzyloxy-4(trifluoromethyl)Coumarin, CYP3A4 inhibitor Ketoconozole, solvents and chemicals were acquired from Sigma Aldrich, India.

Sample preparation

The *Picrorhiza kurroa* rhizomes were shade dried for nearly 3 weeks and coarse powder was prepared using a mixer grinder. The powdered, dried rhizome was extracted using petroleum ether (40-50^{o}C) for 18 h to remove the fat and other undesirable components. The resulted mixture was further treated with hydroalcoholic solution (60:40) for 18h and the extract was evaporated to dryness in a rotary flash evaporator at 60°C.

Assay Procedure

The CYP3A4 substrate (BFC) and the test compound were dissolved in 30% acetonitrile to prepare a stock solution of 10 mM. The assay was conducted using final volume of 200 µl, in a Microplate Fluorescence reader (BioTek FLx 800 T, U.S.A.). Cofactor (1.3 mM NADP, 3.3 mM glucose-6-phosphate, 3.3 mM $MgCl_2$ and 0.4 U/ml, glucose-6-phosphate dehydrogenase) was prepared using 100 mM of potassium phosphate buffer (pH 7.4). CYP3A4 enzyme was diluted to yield 1.5 pmole/well. The enzyme and cofactor were incubated in shaking incubator for 20 minutes at 37^{o}C. Substrate (50 µM final concentration), reference compound and test compound of each concentration were added in a 96 well black plate and incubated at 37^{o}C in a shaking incubator for 15 minutes. Incubation was continued for another 20 minutes with the addition of 100 µl of pre-warmed enzyme cofactor mix to the assay plate and the reaction was stopped by the addition of 50 µl of 50% acetonitrile and 20% Tris Base (0.5 M). Fluorescence per well was measured using an excitation wavelength of 410 nm and emission wavelength of 530 nm in the Fluorescence Reader. The data was analyzed using a Graph Pad Prism Software Version-5. The IC_{50} values were calculated using a Sigmoidal Dose Response.

Calculations and Statistical analysis

The obtained data was presented as mean ± S.E.M. The statistical significance was calculated by ANOVA using GraphPad InStat Version 5.0. In addition, the Dunnett's multiple comparison test was achieved by setting the significance level at $p<0.05$ and above.

Percent Inhibition calculated using below mentioned formula:

% Inhibition at x conc. = 100 -% Control

Where x denotes the inhibitor concentration, the IC_{50} value calculated using per cent inhibition data.

RESULTS AND DISCUSSION

Picrorhiza kurroa is metabolized by CYP3A4 as it has been shown to markedly reduce the clearance of fluorescence substrate of CYP3A4. A dose response study was conducted for *Picrorhiza kurroa*, using five concentrations (0.001, 0.01, 0.1, 1 and 10 µg/ml). Upto 0.01 µg/ml, the tests compound did not show any inhibition however, at higher concentrations the inhibition was prominent and showed a reduction in P_{450} concentration. Maximum inhibition of 90.6% was observed at 10 µg/ml of the test compound. The resulted inhibitory concentration at 50% (IC_{50}) of *Picrorhiza kurroa* was calculated to be 52.35µg/ml whereas for the inhibitor Ketoconozole, IC_{50} was 4.74 µg/ml. (**Figure 1**)

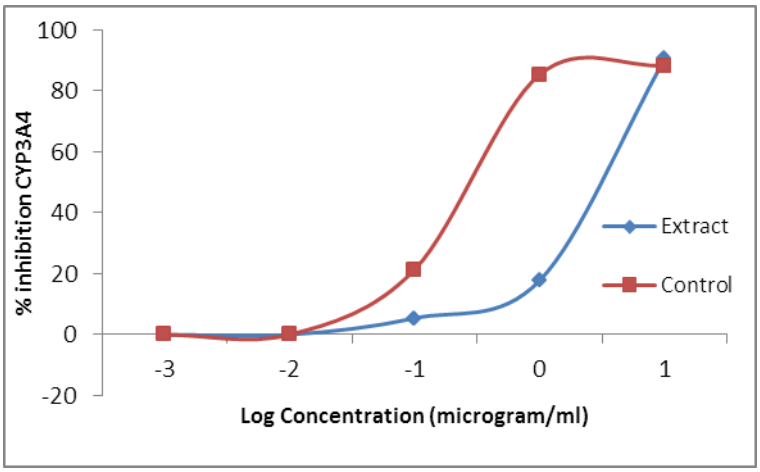

Figure 1. Percentage inhibitory effect of *Picrorhiza kurroa* extract and Ketoconazole on CYP3A4

The results indicate that the test extract has a higher IC_{50} value than respective positive inhibitor against CYP3A4. Higher IC_{50} value indicates that a high concentration of extract is required to reduce the total enzyme activity to its half (50%). The greater IC_{50} of the plant extract is desirable for the safety of the drug as it is less likely to display substantial drug interaction.

CONCLUSION

In the present study, we established the safety profile of *Picrorhiza kurroa* rhizome extract. It can be concluded that there is a very little possibility of herb-drug interaction of *Picrorhiza kurroa*, if it is administered along with other products that are metabolized by cytochrome P_{450}. The results confirmed that *Picrorhiza kurroa* can be used safely in the Ayurvedic formulations. However, advanced study is required to find out whether these inhibitory effects are clinically significant or not. Additionally, *in vivo* interactions must be taken into

account for better correlation between the potency and selectivity of cytochrome P_{450} inhibition.

Conflict of Interest

All authors declare that they have no conflict of interest.

ACKNOWLEDGEMENT

We are thankful to Patanjali Ayurveda Ltd., Haridwar, India for providing gift sample of *Picrorhiza kurroa* rhizomes.

REFERENCES

1. Kumar PV, Sivara A, Madhumitha G., Saral MA, Kumar BS. In vitro-antibacterial activities of *Picrorhiza kurroa* rhizome extract using agar well diffusion method. International Journal of Current Pharmaceutical Review and Research, 2010; 2(1): 30-33.
2. Shetty SN, Mengi S, Vaidya R, Vaidya ADB. A study of standardized extracts of *Picrorhiza kurroa* Royle ex Benth in experimental nonalcoholic fatty liver disease. Journal of Ayurveda and Integrative Medicine, 2010; 1(3): 203-210.
3. Zhang DK, Yu JJ, Li YM, Wei LN, Yu Y, Feng YH, Wang XA. *Picrorhiza kurroa* derivative, picroliv, attenuates the development of dextran-sulfate-sodium-induced colitis in mice. Mediators of Inflammation, 2012; 2012: 751629. doi: 10.1155/2012/751629.
4. Marín M, Giner RM, Ríos JL, Recio CM. Protective effect of apocynin in a mouse model of chemically-induced colitis. Planta Medica. 2013; 79(15): 1392-1400.
5. Rajkumar V, Guha G, Kumar RA. Antioxidant and anti-neoplastic activities of *Picrorhiza kurroa* extracts. Food and Chemical Toxicology, 2011; 49(2): 363-369.
6. Tiwari SS, Pandey MM, Srivastava S, Rawat AKS. TLC densitometric quantification of picrosides (picroside-I and picroside-II) in *Picrorhiza kurroa* and its substitute *Picrorhiza scrophulariiflora* and their antioxidant studies. Biomedical Chromatography, 2012; 26(1): 61-68.
7. Kant K, Walia M, Agnihotri VK, Pathania V, Singh B. Evaluation of antioxidant activity of *Picrorhiza kurroa* (leaves) extracts. Indian Journal of Pharmaceutical Sciences, 2013; 75(3): 324-329.
8. Dorsch W, Stuppner H, Wagner H, Gropp M, Demoulin S, Ring J. Antiasthmatic effects of *Picrorhiza kurroa*: Androsin prevents allergen- and PAF-induced bronchial obstruction in guinea pigs. International Archives of Allergy and Applied Immunology, 1991; 95(2): 128–133.

9. Baruah CC, Gupta PP, Nath A, Patnaik LG, Dhawan, BN. Anti-allergic and anti-anaphylactic activity of picroliv--a standardised iridoid glycoside fraction of *Picrorhiza kurroa*. Pharmacology Research, 1998; 38(6): 487-492.
10. Hussain A, Shadma W, Maksood A, Ansari SH. Protective effects of *Picrorhiza kurroa* on cyclophosphamide-induced immunosuppression in mice. Pharmacology Research, 2013; 5(1): 30–35.
11. Lin JH, Lu AY. Inter-individual variability in inhibition and induction of cytochrome P450 enzymes. Annual Review of Pharmacology and Toxicology, 2001; 41: 535–567.

Ergot Alkaloids: A Review on Therapeutic Applications

Research · May 2016

DOI: 10.13140/RG.2.1.4574.2960

1 author:

Vinay Kumar Sharma
Patanjali Research Institute (PRI), Haridwar, India
58 PUBLICATIONS **1,757** CITATIONS

SEE PROFILE

European Journal of Medicinal Plants
14(3): 1-17, 2016, Article no.EJMP.25975
ISSN: 2231-0894, NLM ID: 101583475

SCIENCEDOMAIN *international*
www.sciencedomain.org

Ergot Alkaloids: A Review on Therapeutic Applications

Niti Sharma[1*], Vinay K. Sharma[1], Hemanth Kumar Manikyam[1] and Acharya Bal Krishna[1,2]

[1]Patanjali Natural Coloroma Pvt. Ltd, Haridwar, Uttarakhand - 249404, India.
[2]University of Patanjali, Haridwar, Uttarakhand - 249402, India.

Authors' contributions

This work was carried out in collaboration between all authors. Authors NS and VKS designed the study, wrote the first draft of the manuscript. Authors ABK and HKM supervised the study. All authors read and approved the final manuscript.

Article Information

DOI: 10.9734/EJMP/2016/25975
Editor(s):
(1) Marcello Iriti, Professor of Plant Biology and Pathology, Department of Agricultural and Environmental Sciences, Milan State University, Italy.
Reviewers:
(1) Nyoman Kertia, Gadjah Mada University, Indonesia.
(2) Robert Perna, Texas Institute of Rehabilitation Research, Houston, TX, USA.
(3) Charu Gupta, AIHRS, Amity University, UP, India.
Complete Peer review History: http://sciencedomain.org/review-history/14283

Review Article

Received 28th March 2016
Accepted 12th April 2016
Published 21st April 2016

ABSTRACT

Ergot of Rye is a plant disease caused by the fungus *Claviceps purpurea* which infects the grains of cereals and grasses but it is being used for ages for its medicinal properties. All the naturally obtained ergot alkaloids contain tetracyclic ergoline ring system, which makes them structurally similar with other neurotransmitters such as noradrenaline, dopamine or serotonin. Due to this structure homology these alkaloids can be used for the treatment of neuro related conditions like migraine, Parkinson's disease etc. For hundreds of years, it has been used in *obsctrics and gynecology* as an uterotonics. Ergot drugs have important role in treating prolactinomas and type II Diabetes. Their role in cancer treatment has also been established. These drugs constitute an important group of compounds called "Smart drugs" used to improve cognitive function and memory and other age related brain disorders. Structural resemblance with various neurotransmitters allows them to interact with a number of receptors which makes them work on different target thus designing new ergot based drugs with receptor subtype selectivity will be more effective.

**Corresponding author: E-mail: nitivinay@yahoo.co.in;*

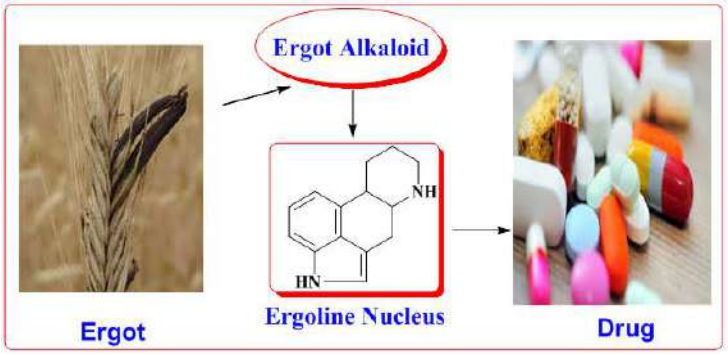

Keywords: Ergot alkaloids; smart drugs; ureotonic; type II diabetes; migraine; Parkinson's disease; cancer.

1. INTRODUCTION

Ergot of Rye is a plant disease caused by the fungus *Claviceps purpurea* which infects the grains of cereals and grasses. "Ergot" is the French word for "spur" named after the similarity between sclerotia of fungus and spurs on rooster legs. In Ayurveda it is known as "Annaamaya", or "Sraavikaa" and in Unnani it is called "Agrat". Briefly, the life cycle of *Claviceps purpurea* starts during spring season when the windborne ascospores infects the grain and initiates pathogenesis. The fungal sclerotia develop to produce mushroom-shaped stroma, which release spores. When a mature sclerotium drops to the ground, the fungus remains quiescent until next spring and the process continues [1]. The ergot symptoms are manifested during kernel formation, when ergot bodies are formed in place of kernels. Interestingly, the fungus does not infect any other plant part except the ovary, which is replaced by purplish-black sclerotium, commonly referred to as an ergot. The ergot sclerotium contains high concentrations of the alkaloid ergotamine and several other peptide alkaloids of the ergotamine group (including ergosine and ergocristine). It is possible that ergot infected grasses since farming began but it was first documented only around 600 BC. Chronic ergot poisoning (ergotism) was prevalent in Europe during the middle ages due to the consumption of bread made from contaminated rye. The disease was often referred to as *"Ignis sacer"*, meaning "Holy Fire", or "St. Anthony's Fire" [2-5]. The infection resulted in symptoms such as hallucinations, severe gastrointestinal upset with painful feelings of intense heat in the limbs due to severe restriction of blood flow with concomitant loss of limbs.

Regardless of serious safety concerns, ergot has been used in various systems of medicine (Ayurvedic, Unnani and Western) for hundreds of years. Ergot contains no lysergic acid diethylamide (LSD) but rather ergotamine, which is used to synthesize lysergic acid, the precursor for LSD. Ergot alkaloids are dopamine agonists which activate dopamine receptors (in the basal ganglia and other parts of the brain involved in motor function) and a prolactin inhibitor. Ergot is a strong vasoconstrictor and thus helps to reduce bleeding by narrowing of the blood vessels. In both Ayurvedic and Unnani system of medicine as in western herbal, ergot is employed to stimulate uterine contraction in the final stages of labor. It is also employed though rarely for arresting uterine hemorrhage. Ergot was perhaps first used in medicine as an oxytocic drug, to promote uterine contraction during child birth. They have been used for treating migraine headaches [6] since 1883 and also in treating Parkinson's disease, restless leg syndrome and other purposes. Ergot-derived drugs commonly used to treat Parkinson's disease include bromocriptine (Parlodel), pergolide (Permax), and lisuride (Revanil) [7]. Presently lysergic acid-derived drugs are used to treat Alzheimer's disease, dementia and hyperprolactinemia [8-10]. One of the most recent studies indicates role of ergots (bromocriptine) in treating Type II Diabetes [11]. In 2009, bromocriptine mesylate was approved by the FDA for treatment of type II diabetes.

Although ergotamine and ergometrine are the two naturally obtained ergot alkaloids of medical importance a number of new compounds have been synthesized by chemical modification of existing structures [12]. This article thus aims to

cover the role of different ergot alkaloids in the field of medicine.

2. BIOSYNTHESIS

The steps involved in biosynthesis of ergot ring formation are portrayed in Fig. 1 as described earlier [13-17]. Limited information is available on most of the enzymes involved in biosynthesis of ergot as they are instable in cell free extract, except for Dimethylallyltryptophan (DMAT) synthase. It catalyzes the condensation of L-tryptophan with dimethylallylpyrophosphate to yield dimethylallyltryptophan. All of the enzymatic steps after dimethylallyltryptophan formation ultimately lead to ring formation in ergoline. The DMAT-forming reaction is the committed step in biosynthetic pathway in ergot fungi and provides the carbon skeleton of the ergoline ring system [18]. The following steps are catalyzed by a methyltransferase, followed by decarboxylation and closure of ring C in Chanovlavine I by Chanoclavine-I cyclase. In the next step Agroclavine-17-monooxygenase converts Agroclavine to Elymoclavine [19] which in turn is converted to Paspalic acid by Elymoclavine-17-monooxygenase [20,21]. Both these enzymes are NADPH and dependent and molecular oxygen thus can be considered as Cytochrome P450-monooxygenase [22]. However, the presence of Elymoclavine-17-monooxygenase was not detected in a *Claviceps* strain that produces Agroclavine and Elymoclavine but in a strain that produces D-lysergic acid amides and peptides [20,21]. This shows that the clavine-producing *Claviceps* strain is deficient in the enzyme that converts Elymoclavine to Paspalic acid which isomerizes to form D-lysergic acid in the next step.

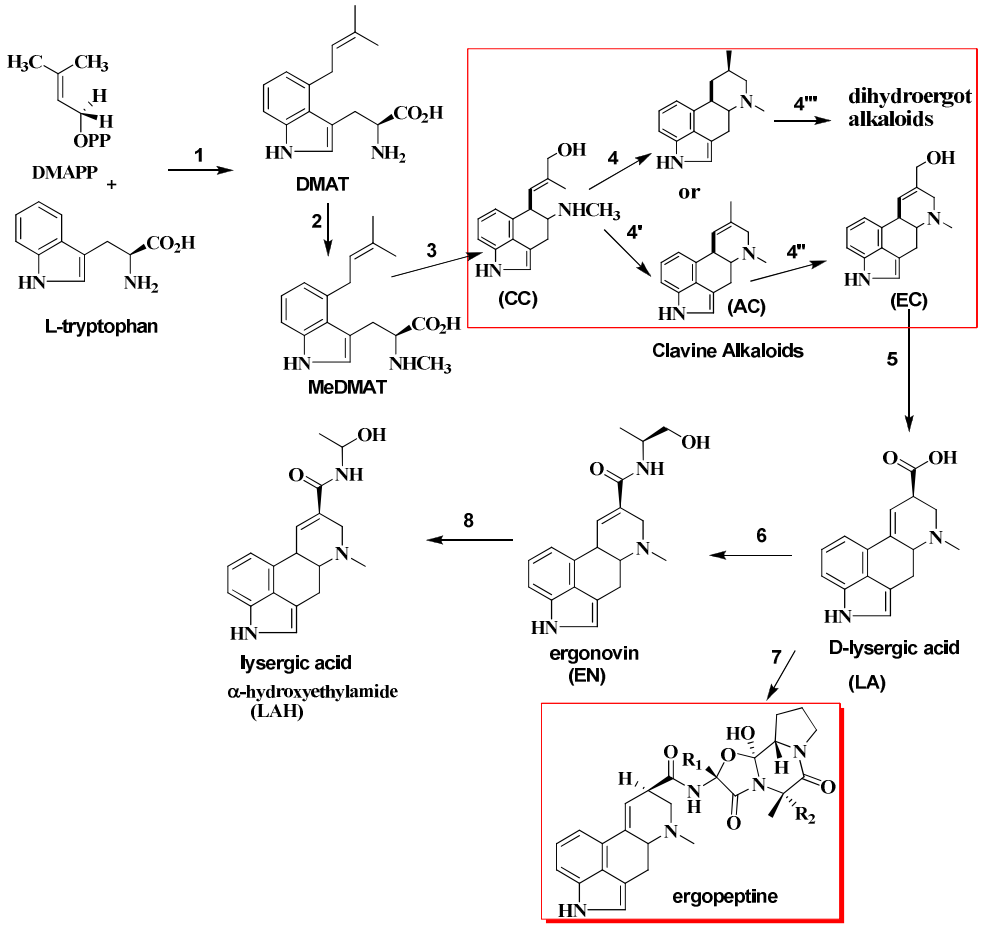

Fig. 1. Biosynthetic pathway of ergot alkaloids

3. CHEMISTRY OF ERGOT ALKALOIDS

The nucleus common to all ergot alkaloids (lysergic acid) was isolated and characterized in 1934 by Jacobs and Craig of the Rockefeller Institute of New York [23]. All the naturally obtained ergot alkaloids contain tetracyclic ergoline ring system, which makes them structurally similar with other neurotransmitters such as noradrenaline, dopamine or serotonin (Fig. 2). This structure homology of ergot alkaloids with these neurotransmitters implies that these alkaloids can be used for the treatment of neuro related conditions like migraine, Parkinson's disease etc.

Structurally the most common features of these alkaloids are methylation at 6th position of nitrogen and substitution at 8th position of carbon in the tetracyclic ring system. Interestingly, due to asymmetric carbon atom at 8th position, the 10-ergolens produce two epimers; ergolenes and isoergolenes [24-27]. Based on the substitution at 8th position these alkaloids can be categorized into four groups as (i) **Clavine alkaloids**: the hydroxy and dehydro derivatives of 6,8-dimethylergolenes and the corresponding ergolines. They also include the chanoclavines with an open D-ring between N-6 and C-7. (ii) **Lysergic acid derivatives**: These derivatives of lysergic acid are amides in which the amidic moiety is formed by a small peptide or an alkylamide. Nonpeptide amides of lysergic acids isolated from ergot fungi are ergometrine, lysergic acid 2-hydroxyethylamide, lysergic acid amide, and paspalic acid [24-26] (iii) **Ergopeptine alkaloids**: the unique feature of these alkaloids is the cyclic part which is formed by the reaction of an *a*-hydroxy-amino acid adjacent to lysergic acid with a carboxyl group of proline. In addition these ergot alkaloids are composed of lysergic acid and a tripeptide moiety. This tripeptide moiety of ergopeptines contains various amino acids such as L-alanine, L-phenylalanine, L-valine, L-leucine, and L-isoleucine, as well as 2-aminobutyric acid. The compounds usually formed by these amino acids are ergotamine, ergotoxine, ergoxine, and ergoannines [24,26] (iv) **Ergopeptam alkaloids**: have structure similar to ergopeptines however the major difference between them is the proline moiety i.e. D-proline (ergopeptam) than L-proline (ergopeptines) and the tripeptide chain is a noncyclol lactam. The examples are ergotamams, ergoxams, ergotoxams, and ergoannams [24,26,27] (Fig. 3)

4. PHARMACOLOGY

4.1 Mode of Action of Ergot Alkaloids

The ergot alkaloids can modulate several receptors of neurotransmitters, such as, dopamine, serotonin and noradrenalin due to the structural similarity of their ergoline ring with biogenic amine receptors [28] (Fig. 2). Till now at least 14 different subtypes of 5-HT receptors [29], 5 subtypes of dopamine receptors [30-32] and at least 10 subtypes of adreno receptors [33-35] could be identified on the basis of information based on different biochemical studies. As they target different receptors their pharmacological action is quite broad. The pharmacologic relevance of ergots is determined by the relative affinity and efficacy of the individual agents for these receptor systems. Many ergot alkaloids

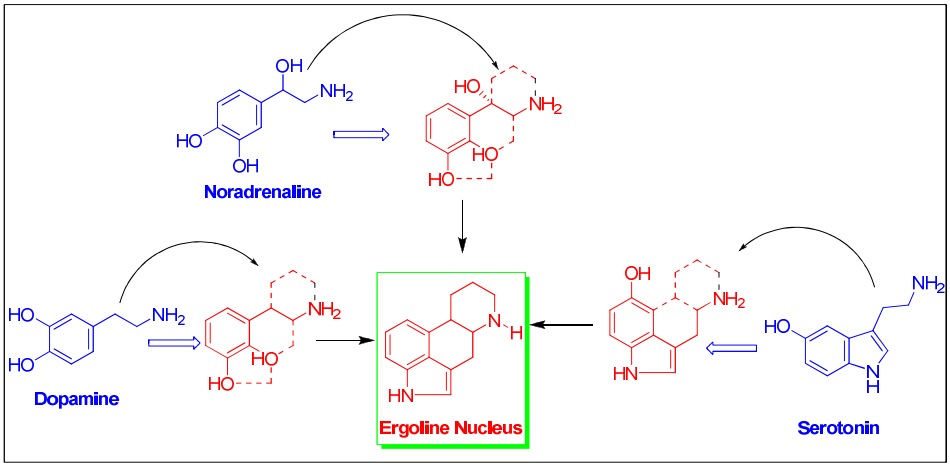

Fig. 2. Structural similarity of ergoline ring with biogenic amine receptors [22]

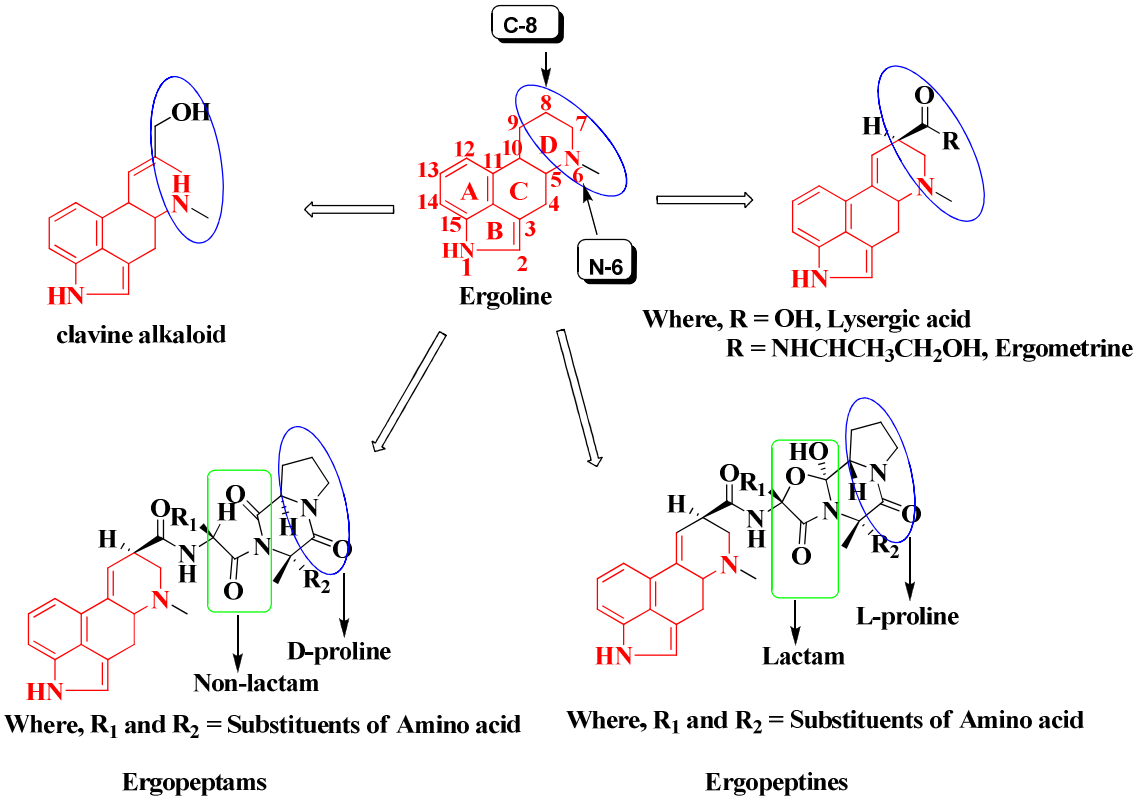

Fig. 3. Chemistry of ergot alkaloids

exhibit partial agonist activities and thus can display either stimulatory or inhibitory effect (Table 1). These receptors and their related neurotransmitters control cardiovascular function, endocrine activity, gastrointestinal tract motility, smooth muscle contraction, temperature regulation, and appetite. Owing to these properties a number of ergot based drugs have been approved by FDA (Table 2).

The important pharmaceutical actions of ergot alkaloid are vasoconstriction and hypoprolactinaemia. Vasoconstriction is linked with inhibition of D1-dopamine receptor and partial activation of the α1-adrenergic and serotonin receptors. Binding of ergot alkaloids to D2-dopamine receptors stimulates the release of dopamine which inhibits prolactin secretion from anterior pituitary [36-40]. Additionally, the binding affinities of ergopeptide and ergoline alkaloids as D2 receptors agonists resemble dopamine itself [41,42].

4.2 Effect on Organ Systems

Central Nervous System: some naturally occurring alkaloids are powerful hallucinogens such as lysergic acid diethylamide. Hofmann [43] (U.S. Patent, 1948) discovered the psychedelic properties of LSD in 1943. It was introduced commercially in 1947 by Sandoz Laboratories as a drug with various psychiatric uses. LSD mimics the effects of serotonin and acts on the human nervous system by rapidly crossing the blood-brain barrier and binding to most serotonin (5-HT) and all dopamine receptors subtypes, with the serotonin agonism (especially the activation of the 5-HT_{2A} receptor) [44-46]. Compounds like bromocriptine acts as D2 dopamine receptors agonist [47] and both agonist and antagonist at D1 receptor, at the level of the hypothalamus and corpus striatum. It directly stimulates ovarian dopamine receptors leading to menses in amenorrhiec women and directly activates lactotrope dopamine receptors, leading to inhibition of prolactin release [48].

Cardiovascular system: The effect of ergot alkaloids on vascular smooth muscles varies with individual agent and type of blood vessel. The natural amino acid alkaloid like ergotamine constricts most human blood vessels including both veins and arteries whereas

dihydroergotamine is more effective in capacitance rather than on resistance vesicles. Ergotamine also acts as α1-receptor antagonist and causes reversal of pressor effects of adrenaline [49]. Ergotamine, ergonovine and methysergide, all are non specific partial agonist of 5-HT2 vascular receptors [50]. These drugs stimulate serotonin, decrease inflammation, and reverse blood vessel dilation around the brain, thereby relieving the migraine or cluster headache symptoms [51].

Uterine smooth muscle: The stimulatory effect of ergot alkaloids on uterus which varies with hormonal status (pregnancy). In small doses, ergot preparations can bring about rhythmic contractions and relaxation of the uterus while at higher doses; it results in a strong and prolonged contraction [52]. As compared to other ergot alkaloids, Ergonovine is more selective and the agent of choice in obstetrics [53]. It directly stimulates uterine smooth muscle contraction resulting in increased muscular tone and enhanced contraction.

4.3 Ergot Derived Smart Drugs

Smart Drugs are nootropics drugs i.e. chemical substance that improves cognitive function and memory or facilitate learning. Three famous ergot derived smart drugs are Bromocriptine, Hydergine and Nicergoline. Few others are Ergoloid mesylates, co-dergocrine and dihydroergotoxine, all with a common ancestry.

4.4 Bromocriptine

Bromocriptine is an agonist of dopamine D2 [47,54] and various serotonin receptors. By reversing the glutamate GLT1 transporter it also inhibits the release of glutamate thus protecting the brain against ischaemia [55]. As bromocriptine has role in dopamine enrichment, it is also referred to as an aphrodisiac and thus a potential drug for the treatment of ‘weak orgasm syndrome’ as it helps to reinstate normal sexual function in cases where the possible cause is prolactin over secretion [56,57].

4.5 Hydergine

Hydergine (Ergoloid Mesylates) was synthesized for the first time in 1940’s by Albert Hofman, the father of LSD. Since then it is being used for memory loss associated with ageing and also as an effective anti-oxidant [58]. Hydergine thought to work by mimicking the effect of nerve growth factor (NGF) therefore, enhancing memory and cognition. NGF has role in stimulating protein synthesis, resulting in the growth of dendrites. These dendrites are communication links between nerve and brain cells and are crucial to memory and learning. Thus an increase in dendrites will ultimately enhance cognitive functions, mental alertness, clarity and mood [59].

Hydergine is regarded as the first effective drug in treatment of Alzheimer's disease [60,61] approved by FDA. It is also used in dementias and for treating psychiatric disorders [62,63]. Even though it is only approved for treating senility and cerebro-vascular insufficiency, it is being used in various European countries to maintain brain oxygen levels after emergencies and accidents that involve shock, hemorrhage, strokes, heart attacks, drowning, electrocution and drug over-dose [64]. An optimum oxygen supply in brain, keeps a check on free radicals production. Hydergine also reduces the accumulation of the age-related toxin, lipofuscin [65-67]. Therefore, it can be regarded as an all-purpose brain booster and also an incredible anti-aging medicine.

4.6 Nicergoline

Nicergoline (trade name Sermion) is another ergot derivative used to treat senility and other disorders with vascular origins. It is used worldwide for the treatment of cognitive, affective, and behavioral disorders in elderly [68,69]. Apart from having neurotrophic and antioxidant properties it is reported to have a vast therapeutic potential as an α1-adrenoceptor antagonist [70] boost cholinergic and catecholaminergic neurotransmitter action; restrain platelet aggregation [71,72] and accelerates metabolism [73]. As it works on wide variety of targets it is used for the treatment of vascular disorders such as cerebral thrombosis and atherosclerosis, arterial blockages in the limbs, increases serum substance P levels, in patients with an ischaemic stroke, which cause reduction in the risk of aspiration pneumonia and with improvement in dysphagia [74,75], Raynaud's disease, vascular migraines, and retinopathy, peripheral arterial occlusive disease [76-78]. The safety profile of nicergoline is better than any other ergot derivatives like ergotamine and ergotoxine as no incidence of fibrosis or ergotism are reported till date, with Nicergoline [79].

Table 1. Receptor mediated actions of ergot alkaloids [49]

Ergot alkaloids	α adrenoreceptor	D2 receptor	5 HT_2 receptor	Uterine smooth muscle
Ergotamine	Agonist/antagonist	agonist(+)	partial agonist	+++
Dihydroergotamine	Agonist/antagonist	agonist(+)	partial agonist	++
Ergonovine	partial agonist	0	partial agonist	+++
Bromocryptin	_	+++	_	0
Methylsergide	+/0	+/0	partial agonist	+/0
LSD	+/0	+/0	partial agonist	+/0

Table 2. FDA approved ergot drugs [160]

Drug	FDA application	Active ingredient	Company address	Current market status
Bromocriptine Mesylate (Tablet; oral)	ANDA (074631)	Bromocriptine Mesylate	LEK PHARMS	Prescription
Bromocriptine Mesylate (Capsule; Oral)	ANDA (075100)	Bromocriptine Mesylate	LEK PHARM	Discontinued
Bromocriptine Mesylate (Tablet; oral)	ANDA (076962)	Bromocriptine Mesylate	MYLAN	Prescription
Bromocriptine Mesylate (Capsule; Oral)	ANDA (077226)	Bromocriptine Mesylate	MYLAN	Prescription
Bromocriptine Mesylate (Tablet; oral)	ANDA (077646)	Bromocriptine Mesylate	PADDOCK LLC	Prescription
Bromocriptine Mesylate (Capsule; Oral)	ANDA (078899)	Bromocriptine Mesylate	ZYDUS PHARMS USA INC	Prescription
Cycloset (Tablet; oral)	NDA (020866)	Bromocriptine Mesylate	VEROSCIENCE	Prescription
Parlodel (Tablet; oral)	NDA (017962)	Bromocriptine Mesylate	US PHARMS HOLDINGS	Prescription
Parlode (Capsule; Oral)	NDA (017962)	Bromocriptine Mesylate	US PHARMS HOLDINGS	Prescription
Digoxin	ANDA (077002)	Digoxin	HIKMA INTL PHARMS	Prescription
Digoxin	ANDA (078556)	Digoxin	IMPAX LABS	Prescription
Digoxin	ANDA (083217)	Digoxin	ABRAXIS PHARM	Discontinued
Digoxin	ANDA (083391)	Digoxin	HIKMA MAPLE	Prescription
Digoxin	ANDA (084386)	Digoxin	WYETH AYERST	Discontinued
Digoxin Pediatric	ANDA (040092)	Digoxin	HOSPIRA	Discontinued
Lanoxicaps	NDA (018118)	Digoxin	GLAXOSMITHKLINE LLC	Discontinued
Lanoxin	NDA (009330)	Digoxin	COVIS INJECTABLES	Prescription
Lanoxin	NDA (020405)	Digoxin	COVIS PHARMA	Prescription
Lanoxin pediatric	NDA (009330)	Digoxin	COVIS INJECTABLES	Prescription

4.7 Other Therapeutic Applications of Ergot Derived Drugs

4.7.1 Role in migraine treatment

Dihydroergotamine is being used to treat migraine headaches for a long time. They were the first 'migraine-specific' drugs [80] as they relieve only severe headaches and symptoms associated with migraines. Because these medicines have serious side effects like ergotism and gangrene [81] they are generally prescribed for patients whose headaches are not relieved by any other pain reliever. The two drugs used for treating migraine, ergotamine (ET) and dihydro-ergotamine (DHE), differ in pharmacokinetic and pharmacodynamic profile. The caffeine present in many ergotamine-containing combinations (e.g. Cafergot) helps ergotamine work better and faster by causing more of it to be quickly absorbed into the body. More recently, orally inhaled DHE (Semprana, Allergan Inc.; formarly known as Levedex by MAP Pharmaceuticals) is currently under process of FDA approval for treatment of migraine and the company expect it to get FDA approval by second quarter of 2015 [82].

The oral assimilation of ergotamine is around 60%, which is improved by the simultaneous administration of caffeine. Ergotamine has a very low bioavailability [83,84] through oral route. As compared to intravenous bioavailability (100%), the oral bioavailability of ergotamine is <1%, owing to high first-pass metabolism. Ergotamine is metabolized in the liver by indeterminate pathways and approximately 90% of the metabolites are excreted in the bile [85]. Ergotamines are well known vasoconstrictors [50,86]. Various *in vivo* experiments show that this vasoconstrictor effect is exerted within the coronary [87], cerebral [86], pulmonary [88] and temporal [89] arteries, selectivity extending to the arteriovenous anastomotic parts. The large arteries (conducting vessels) are affected more compared to the arterioles (resistance vessels). Thus the arterial blood pressure is reasonably increased by these drugs [90,91]. The mechanism of action of ergot alkaloids is quite complex and involves interaction with a range of receptors. Both ergotamine and DHE have affinity for 5-HT (5-hydroxytryptamine), dopamine and noradrenaline receptors [50,86,92-94]. In addition, there is evidence that both ergotamine and DHE can activate novel, as yet uncharacterized receptors [93].

4.7.2 Role as uterotonics

Uterotonics work by directly affecting uterine smooth muscle contraction and used to induce or augment labor by increasing the quality, rate, and force of periodic contractions.

The role of ergot in pregnancy has been known for over 2000 years, and it was used by physicians to stimulate abortion 400 years ago. The first authentic information of use of ergot in obstetrics appeared in Chinese writings in 1100 BC. Adam Lonicer in his *Kreuterbuch* described the use of ergot preparation by midwives to produce strong uterine contractions [95]. The ergot also became popular in France, Germany, and the United States as an oxytocic in childbirth. It was in 1808 when ergot was first used as an official medicine by American physician John for uterine to quicken childbirth [96]. Ergometrine was first isolated by the chemists Dudley and Moir [97-99] and its prophylactic use for treating haemorrhaging lead to a decline in the maternal mortality rate during the early 20th century [100].

Presently, Methylergonovine maleate (Methergine) and Ergonovine (Ergometrine) are the two main ergot based drugs used in Obstetrics as a uterine stimulant to control Postpartum Hemorrhage [101-106].

Ergot alkaloids have a stimulatory effect on the motor activity of the uterus. In small doses, ergot can induce rhythmic contractions and relaxation of the uterus while at higher doses; ergot a powerful and prolonged contraction is observed [107,108]. Ergonovine is more selective thus a preferred drug in obstetric applicants compared to other alkaloids and is on the World Health Organization's List of Essential Medicines [109]. It is generally combined with oxytocin (Syntocinon) as syntometrine which makes it superior to syntocinon alone in lessening occurrence of postpartum haemorrhage in caesarean section and associated maternal morbidity and mortality [110]. The most prominent effect of ergonovine is uterine smooth muscle contraction, increasing both muscular tone and the rate of rhythmic contractions. This stimulatory effect seems to be most closely associated with agonist or partial agonist effects at 5-HT2 receptors [49,111]. Both drugs stimulate alpha-adrenergic and serotonin receptors and inhibition of endothelial-derived relaxation factor release [112,113]. They are less potent vasoconstrictor than ergotamine and

have minor actions on the central nervous system.

4.8 Effect on Prolactin Secretion

Prolactin is also known as "mothering hormone" as one of its primary functions is to promote lactation and weight gain in pregnancy. Bromocriptine, an ergot derivative, suppresses hormone prolactin, leading to their use as fertility drugs by women but it also helps to reduce serum prolactin levels in men although the precise role of prolactin in men is unclear.

Bromocriptine mesylate (also known by its brand name Parlodel) is a non-hormonal, non-estrogenic agent that inhibits the secretion of prolactin in humans, with little or no effect on other pituitary hormones [114]. It works by increasing the levels of dopamine in brain. The drug acts on the pituitary gland, reducing the production of prolactin.

The *in vivo* and *in vitro* effects of ergot derivatives on prolactin and growth hormone biosynthesis in the rat have been studied [115] and it was observed that ergot alkaloids suppress prolactin synthesis and release by the pituitary gland as well as pituitary tumors. The results supported the prior finding [116-120] that ergocornine and ergocryptine inhibit release and synthesis of prolactin. As the ergot derivatives reduce serum prolactin and leutinizing hormone levels [120] it can be proposed that the drugs have a general repressive effect on pituitary function rather than a specific effect on selected pituitary cell receptors. Additionally, the drugs apparently decrease ACTH secretion by the pituitary tumors in view of the fact that the ergots cause degeneration of the adrenal glands [115].

These days another ergot derivative, Cabergoline [121] (brand names Caberlin, Dostinex and Cabaser), is being frequently used as a first-line agent in the treating prolactinomas due to higher affinity for D2- receptor sites and lesser side effects compared to bromocriptine [122].

4.8.1 Role in type II diabetes

The effects of ergot alkaloid on glycaemic variables have been known [123] since 1980 but it was only in 2009, when bromocriptine mesylate was approved by the FDA for treatment of Type II diabetes under the trade name Cycloset (VeroScience). Bromocriptine is a semi-synthetic derivative of a natural ergot alkaloid, Ergocriptin (a derivative of lysergic acid), which is synthesized by bromination of ergocriptin using *N*-bromosuccinimide [124]. It is an ergot alkaloid dopamine-D2-receptor agonist [125]. It is currently unknown how this drug improves glycemic control but somehow it may help resetting the circadian dopamine signal [126-128]. The possible explanation is that it produces its effects by varying the activity of hypothalamic neurons, through a vagal route, to reduce hepatic gluconeogenesis, without increasing insulin concentrations [123,129-132]. In an experiment conducted on a large group of patients with Type II diabetes, Bromocriptine-quick release (as single or in combination with two blood-glucose-lowering drugs) reduced the risk of cardiovascular disease compared with control [133-136]. Even though the mechanism of action is not clear, Bromocriptine-QR's action indicates a vital target in the hypothalamus which may help to reset abnormally elevated hypothalamic drive for metabolic parameter like increased plasma glucose, triglyceride, and free fatty acid levels in fasting and postprandial states in insulin-resistant patients [137,138]. The encouraging cardiovascular risk profile of Bromocriptine-QR proposes its usefulness in the treating patients with Type II diabetes with a history of cardiovascular disease [139].

4.8.2 Role in Parkinson's disease

Ergot alkaloids work as dopamine agonists to trigger dopamine receptors in the basal ganglia and other parts of the brain implicated in motor function. However, the precise mechanism through which this process occurs is not yet clear. Ergot-derived medications commonly used to treat Parkinson's disease include Bromocriptine (Parlodel), Cabergoline (Caberlin), Pergolide (Permax), and Lisuride (Revanil). Bromocriptine has been in normal use as adjunct therapy with levodopa to treat patients with Parkinson's disease [140]. Also in new patients, bromocriptine monotherapy has delayed the need for levodopa treatment [141].

Cabergoline is a potent dopamine receptor agonist on D_2 receptors with a long (~65 hours) plasma half-life [142]. It is also effective as an addition therapy to levodopa in patients with advanced Parkinson's disease [143]. Reports have also established the efficacy of cabergoline in delaying motor complication [144,145]. Pergolide is more beneficial than bromocriptine as it act on both D1 and D2-like receptors, in

comparison with bromocriptine, which stimulates D2-like receptors and is a weak antagonist at D1 sites [146]. A high dose of pergolide has shown to improve motor function without simultaneous levodopa treatment, in some patients with complicated Parkinson's disease [147]. Lisuride, resembles bromocriptine in target and mode of action and has beneficial effect when used in combination with levodopa in patients with advanced Parkinson's disease [148]. It permits reduction of levodopa dose when used as monotherapy and/or in combination with levodopa [149,150]. In a study conducted on a large number of Parkinson's disease patients revealed that two ergot-derived drugs, Pergolide and Cabergoline may increase the risk of cardiac valve regurgitation (CVR) but not in hyperprolactinaemia patients [151-153]. Whereas, results of another study indicate that ergot dopamine agonist use in Parkinson's disease patients are unrelated with an increased risk of newly diagnosed heart failure [154].

Even though agonism of 5-HT (2B) receptors in the heart is apprehended to play an important role, the accurate pathway leading to valvulopathy is still unidentified, as these unfavorable result is not observed in all patients and also it is unclear whether the fibrotic changes are reversible or not. Thus it can be speculated that dopamine agonists devoid of 5-HT(2B) agonistic activity, such as Lisuride (ergolinic dopamine agonists) and non-ergot dopamine, might not induce fibrotic changes in heart valves, but it need more experimental validation [155].

4.8.3 Role in cancer

A vast literature is available on receptor effects of ergot alkaloids but their cytotoxic effect has not been studied much. A low dose of bromocriptine is usually recommended along with the classical antitumor therapies in treatment of metastatic breast cancer and prostate carcinoma patients showing cancer-related hyperprolactinemia [156]. However, for the first time a new role of ergot alkaloid was unveiled by Mulac and Humf [157]. They studied the six main ergot alkaloids (ergotamine, ergocornine, ergocryptine, ergocristine, ergosine and ergometrine, and their isomeric forms) in order to evaluate their toxic effect on human primary cells. The toxic properties changes with the structure of ergot alkaloids; the ergometrine (lysergic acid amide) did not show any effect, while peptide ergot alkaloids showed activity, ergocristine being most effective in human kidney cells. An exciting connection between the alkaloid concentration (in the cell lysate of the receptor-inactive isomers) and cytotoxicity was observed in ergot alkaloids. They displayed strong apoptotic effects in two cancer cell lines (HepG2 and HT-29). Also, by exploiting the natural fluorescence properties of ergot alkaloids, strong accumulative effects were first visualized by fluorescence microscopy [158]. Unfortunately, the mechanism or cytotoxicity is not yet clear and need in depth research in this field. Very recently, six ergot alkaloids (agroclavine, ergosterol, ergocornin E, ergotamine, dihydroergocristine, and 1-propylagroclavine tartrate) were investigated for their cytotoxicity towards tumor cell lines and 1-Propylagroclavine tartrate (1-PAT) found to be most potent. As the cytotoxicity profile of ergot alkaloids does not follow classical mechanisms of drug resistance, it can be used to deal with drug-resistant tumors [159]. The cytotoxicity of ergot alkaloids is not involved in classical mechanisms of drug resistance opening the possibility to bypass resistance and to treat otherwise drug-resistant and refractory tumors.

5. CONCLUDING REMARKS

Ergot alkaloids have had medicinal importance for a long time varying from helping in child birth to headaches to psychological problems. Structural resemblance with various neurotransmitters allows them to interact with a number of receptors which makes them work on different target. However, it becomes very difficult to explain pharmacological profile without identifying receptor homogeneity. As a result of the progress in alkaloid chemistry it is possible to designing new ergot based drugs with receptor subtype selectivity, by different modifications on the ergoline ring, which will resolve the problem of side effects associated with these drugs.

CONSENT

It is not applicable.

ETHICAL APPROVAL

It is not applicable.

COMPETING INTERESTS

Authors have declared that no competing interests exist.

REFERENCES

1. Schardl CL, Panaccione DG, Tudzynski P. Ergot alkaloids – Biology and molecular biology. Alkaloids Chem Biol. 2006;45-86.
2. Bove FJ. The story of ergot. S. Karger: NY. 1970;97.
3. Tanner JR. St. Anthony's fire, then and now: a case report and a historical review. Can J Surg. 1987;30:291-293.
4. Heritage J, Evans G, Killington RA. What is the role of fungal toxins in food poisoning? In Microbiology in Action, Cambridge University Press. 1999;115.
5. Battin J. Saint Anthony's fire or gangrenous ergotism and its medieval iconography. Hist Sci Med. 2010;44:373-382.
6. Friedman AP, von Storch TJC, Araki S. Ergotamine tartrate: Its history, action, and proven use in the treatment of migraine. N Y State J Med. 1959;59:2359-2366.
7. Samii MD, Mosley AD, Romaine DS, Samii A. the encyclopedia of parkinson's disease. Facts on File; 2009.
8. Baskys A, Hou AC. Vascular dementia: Pharmacological treatment approaches and perspectives. Clin Interv Aging. 2007;2:327–335.
9. Morren JA, Galvez-Jimenez N. Where is dihydroergotamine mesylate in the changing landscape of migraine therapy? Expert Opin Pharmacother. 2010;11:3085–3093.
10. Perez-Lloret S, Rascol O. Dopamine receptor agonists for the treatment of early or advanced Parkinson’s disease. CNS Drugs. 2010;24:941–968.
11. Kerr JL, Timpe EM, Petkewicz KA. Bromocriptine mesylate for glycemic management in type 2 diabetes mellitus. Ann Pharmacother. 2010;44:1777–1785.
12. Carlile MJ, Watkinson SC, Gooday GW. The Fungi (2nd edn). Academic Press: London; 2001.
13. Floss HG, Tcheng-Lin M, Kobel H, Stadler P. On the biosynthesis of peptide ergot alkaloids. Experientia. 1974;30:1369-1370.
14. Floss HG. Biosynthesis of ergot alkaloids and related compounds. Tetrahedron. 1976;32:873–912.
15. Floss HG, Anderson JA. Biosynthesis of ergot toxins. In the biosynthesis of mycotoxins. A study in secondary metabolism, Steyn PS (ed). Academic: New York. 1980;17–67.
16. Keller U. Biosynthesis of ergot alkaloids. In Ergot, the genus *Claviceps*. Kr˘en V, Cvak L (eds). Harwood Academic: Chur. 1999;95–163.
17. Jakubczyk D, Cheng JZ, O'Connor SE. Biosynthesis of the ergot alkaloids. Nat Prod Rep. 2014;31:1328-1338.
18. Heinstein PF, Lee SL, Floss HG. Isolation of dimethylallylpyrophosphate: tryptophan dimethylallyltransferase from the ergot fungus (*Claviceps* spec.). Biochem Biophys Res Commun. 1971;44:1244–1251.
19. Kim IS, Kim SU, Anderson JA. Microsomal agroclavine hydroxylase of *Claviceps* species. Phytochem. 1981;20:2311–2314.
20. Kim SU, Cho YJ, Floss HG, Anderson JA. Conversion of elymoclavine to paspalic acid by a particulate fraction from an ergotamine-producing strain of *Claviceps* sp. Planta Med. 1983;48:145–148.
21. Maier W, Schumann B, Gröger D. Microsomal oxygenases involved in ergoline alkloid biosynthesis of various *Claviceps* strains. J Basic Microbiol. 1988;28:83–93.
22. Tudzynski P, Correia T, Keller U. Biotechnology and genetics of ergot alkaloids. Appl Microbiol Biotechnol. 2001;57:593–605.
23. Jacobs WC, Craig LC. The ergot alkaloids: ii. The degradation of ergotinine with alkali. Lysergic acid. J Biol Chem. 1934;104:547-551.
24. Kobel H, Sanglier JJ. Ergot alkaloids. In Biotechnology, Rehm HJ, Reed G, (eds). VCH: Weinheim. 1986;569-609.
25. Rehácek Z, Sajdl P. Ergot alkaloids. Elsevier: New York, NY. 1990;28–86.
26. Flieger M, Wurst M, Shelby R. Ergot alkaloids—sources, structures, and analytical methods. Folia Microbiol. 1997;42:3–29.
27. Gröger D, Floss HG. Biochemistry of ergot alkaloids – Achievements and challenges. In the alkaloids: Chemistry and biology, Cordell GA. (ed). Academic: London. 1988;171–218.
28. Pertz H, Eich E. Ergot alkaloids and their derivatives as ligands for serotoninergic, dopaminergic and adrenergic receptors. In: Křen V, Cvak L, editors. Ergot: The Genus *Claviceps*. Amsterdam, The Netherland: Harwood Academic Publishers. 1999;411-440.
29. Malenka RC, Nestler EJ, Hyman SE. Chapter 10: Neural and Neuroendocrine

Control of the Internal Milieu. In: Sydor A, Brown RY, editors. Molecular Neuropharmacology: A Foundation for Clinical Neuroscience. New York: McGraw-Hill Medical. 2009;249.
30. Sibley DR, Monsma FJ Jr. Molecular biology of dopamine receptors. Trends Pharmacol Sci. 1992;13:61–69.
31. Strange PG. New insights into dopamine receptors in the central nervous system. Neurochem Int. 1993;22:223–236.
32. Seeman P, Van Tol HHM. Dopamine receptor pharmacology. Trends Pharmacol Sci. 1994;15:264–270.
33. Bylund DB, Eikenberg DC, Hieble JP, Langer SZ, Lefkowitz RJ, Minneman KP, Molinoff P B, Ruffolo RR Jr, Trendelenburg U. Nomenclature of adrenoceptors. Pharmacol Rev. 1994;46:121–136.
34. Hieble JP, Bylund DB, Clarke DE, Eikenburg DC, Langer SZ, Lefkowitz RJ, Minneman KP, Ruffolo RR Jr. Recommendation for nomenclature eof α1-adrenoceptors: Consensus update. Pharmacol Rev. 1995a;47:267–270.
35. Hieble JP, Bondinell WE, Ruffolo RR Jr. α- and ß-Adrenoceptors: from the gene to the clinic. 1. Molecular biology and adrenoceptor subclassification. J Med Chem. 1995b;38:3415–3444.
36. Berde B, Stürmer E. Introduction to the pharmacology of ergot alkaloids and related compounds as a basis of their therapeutic action. In: Berde B, Schild HO, editors. Handbook of Experimental Pharmacology: Ergot Alkaloids and Related Compounds. Berlin: Springer-Verlag. 1978;1-29.
37. Denef C, Manet D, Dewals R. Dopaminergic stimulation of prolactin release. Nat. 1980;285:243-246.
38. Goldstein M, Lieberman A, Lew JY, Asano T, Rosenfeld MR, Makman MH. Interaction of pergolide with central dopaminergic receptors. Proc Natl Acad Sci U.S.A. 1980;77:3725–3728.
39. Sibley DR, Creese I. Interactions of ergot alkaloids with anterior pituitary D2 dopamine receptors. Mol Pharmacol. 1983;23:585–593.
40. Schillo KK, Leshin LS, Boling JA, Gay N. Effects of endophyte-infected fescue on concentrations of prolactin in blood sera and the anterior pituitary and concentrations of dopamine and dopamine metabolites in brains of steers. J Anim Sci. 1988;66:713–718.
41. Larson BT, Samford MD, Camden JM, Piper EL, Kerley MS, Paterson JA, Turner JT. Ergovaline binding and activation of D2 dopamine receptors in GH4ZR7 cells. J Anim Sci. 1995;73:1396–1400.
42. Larson BT, Harmon DL, Piper EL, Griffis LM, Bush LP. Alkaloid binding and activation of D2dopamine receptors in cell culture. J Anim Sci. 1999;77:942-947.
43. U.S. Patent 2. 1948;438:259.
44. Aghajanian GK. LSD and CNS Transmission. Ann Rev Pharmacol. 1972;12: 157-168.
45. Hintzen A, Passie T. The pharmacology of LSD: A Critical Review, Annelie editor. Oxford, UK: Oxford University Press; 2010.
46. Hanson ND, Owens MJ, Nemeroff CB. Depression, antidepressants, and neurogenesis: A Critical Reappraisal. Neuropsychopharmacol. 2011;36:2589–2602.
47. DeFronzo RA. Bromocriptine: A sympatholytic, D2-dopamine agonist for the treatment of type 2 diabetes. Diabetes Care. 2011;34:789–794.
48. Borgelt LM. Women's health across the lifespan: A pharmacotherapeutic approach. ASHP. 2010;834.
49. Prasad JP. Conceptual Pharmacology (Ist edn). India: Universities Press. 2010;700.
50. Müller-Schweinitzer E, Weidmann H. Basic pharmacological properties. In: Berde B, Schild HO, editors. Ergot alkaloids and related compounds. Handbook of experimental pharmacology. Berlin: Springer-Verlag. 1978;87–232.
51. Olesen J. The headaches. US: Lippincott Williams & Wilkins. 2006;1169.
52. Williams DA, Foye WO, Lemke TL. Foye's Principles of Medicinal Chemistry. US: Lippincott Williams & Wilkins. 2002;1114.
53. Seth SD. Textbook of pharmacology. India: Elsevier. 2008;1000.
54. De Leeuw Van Weenen JE, Parlevliet ET, Maechler P, Havekes LM, Romijn JA, Ouwens DM, Pijl H, Guigas B. The dopamine receptor D2 agonist bromocriptine inhibits glucose-stimulated insulin secretion by direct activation of the α2-adrenergic receptors in beta cells. Biochem Pharmacol. 2010;79:1827–1836.
55. Shirasaki Y, Sugimura M, Sato T. Bromocriptine, an ergot alkaloid, inhibits excitatory amino acid release mediated by glutamate transporter reversal. Eur J Pharmacol. 2010;643:48–57.

56. Emsley J. Vanity, vitality, and virility: the science behind the products you love to buy. Oxford University Press: US. 2006;272.
57. Taberne PV. Aphrodisiacs: The Science and the Myth. Germany: Springer. 2012; 288.
58. Pearson D, Shaw S. Life extension: A practical scientific approach. New York: Warner Books. 1982;858.
59. Turkington C, Harris JR. The encyclopedia of the brain and brain disorders (3rd edn). Facts on File. 2009;434.
60. Branconnier R. The efficacy of the cerebral metabolic enhancers in the treatment of senile dementia. Psychopharmacol Bull. 1983;19:212-220.
61. Thompson TL II, Filley CM, Mitchell WD, Culing KM, LoVerde M, Byyny RI. Lack of efficacy of hydergine in patients with alzheimer's disease. New Engl J Medicine. 1990;323:445-448.
62. Yoshikawa M, Hirai S, Aizawa T, Kuroiwa Y, Goto F, Sofue I, Toyokura Y, Yamamura H, Iwasaki Y. A dose response study with dihydroergotoxine mesylate in cerebrovascular disturbances. J Am Geriatrics Soc. 1983;31:1-7.
63. Hollister LE. Ergoloid mesylates and the treatment of senile dementias. Perspectives. In: Alan R, editor. Psychopharmacology: A Collection of Papers in Honor of Earl Usdin. New York: Liss, Inc. 1988;613-620.
64. Dean W, Morgenthaler J. How to improve your memory and increase your intelligence using the latest discoveries. In Neuroscience in the Smart Drugs Series, B and J Publications: US. 1991;192.
65. Amenta D, Ferrante F, Franch F, Amenta F. Effects of long-term Hydergine® administration on lipofuscin accumulation in senescent rat brain. Gerontol. 1988;34: 250–256.
66. Weil C. Hydergine ®: Pharmacologic and clinical facts. Berlin: Springer-Verlag. 1988;111.
67. Smart drugs.
Available:http://nutritionreview.org/smart-drugs
(Date accessed March, 2015)
68. Voronina TA, Nerobkova LN, Garibova TL, Dikova M, Nikolov RE, Nikolova M, Markina NV. Effect of nicergoline on learning and memory. Meth Find Exp Clin Pharmacol. 1998;10:431–435.
69. Fioravanti M, Flicker L. Efficacy of nicergoline in dementia and other age associated forms of cognitive impairment. Cochrane Database Syst Rev. 2001;4: CD003159.
70. Alvarez-Guerra M, Bertholom N, Garay R. Selective blockade by nicergoline of vascular responses elicited by stimulation of alpha 1A-adrenoceptor subtype in the rat. Fund Clin Pharmacol. 1999;13:50–58.
71. Pogliani E, Volpe AD, Ferrari R, Recalcati P, Praga C. Inhibition of human platelet aggregation by oral administration of nicergoline. A double blind study. Il Farmaco Edizione Pratica. 1975;30:630–640.
72. Bolli R, Ware JA, Brandon TA, Weilbaecher DG, Mace ML Jr. Platelet-mediated thrombosis in stenosed canine coronary arteries: Inhibition by nicergoline, a platelet-active alpha-adrenergic antagonist. J Am Coll Cardiol. 1984;3:1417–1426.
73. Winblad B, Fioravanti M, Dolezal T, Logina I, Milanov IG, Popescu DC, Solomon A. Therapeutic use of nicergoline. Clin Drug Investig. 2008;28:533-552.
74. Nishiyama Y, Abe A, Ueda M, Katsura KI, Katayama Y. Nicergoline increases serum substance P levels in patients with an ischaemic stroke. Cerebrovas Dis. 2010; 29:194-198.
75. Nakashima T, Hattori N, Okimoto M, Yanagida J, Kohno N. Nicergoline improves dysphagia by upregulating substance p in the elderly. Medicine. 2011;90:279–283.
76. Borgioli M, Merendino E, Ricci B. Therapeutic efficacy of nicergoline in ophthalmology fluorescence retinographic study. Arzneimittel-Forschung. 1979;29: 1311–1316.
77. Article 116 of Directive 2001/83/EC. Ergot derivatives Article-31 referral - Nicergoline - AnnexII.
Available:http://www.ema.europa.eu/docs/en_GB/document_library/Referrals_document/Ergot_derivatives-containing_products/WC500161724.pdf
(Date accessed April, 2015)
78. European Medicines Agency.
Available:http://www.ema.europa.eu/docs/en_GB/document_library/Referrals_document/Ergot_derivatives-containing_products/WC500161305.pdf
(Date accessed April, 2015)

79. Fioravanti M, Nakashima T, Xu J, Garg A. A systematic review and meta-analysis assessing adverse event profile and tolerability of nicergoline. BMJ Open. 2014;4:e005090.
80. Tfelt-Hansen PC, Koehler PJ. History of the use of ergotamine and dihydro-ergotamine in migraine from 1906 and onward. Cephalalgia. 2008;28:877-886.
81. Schiff PL. Ergot and its alkaloids. Am J Pharm. Educ. 2006;70:98-107.
82. Biospace. Available:www.biospace.com/news/allergan-inc-gets-fda-approval-for-orzurdex third/338536 (Date accessed April, 2015)
83. Ibraheem JJ, Paalzow L, Tfelt-Hansen P. Low bioavailability of ergotamine tartrate after oral and rectal administration in migraine sufferers. Br J Clin Pharmacol. 1983;16:695–699.
84. Sanders SW, Haering N, Mosberg H, Jaeger H. Pharmacokinetics of ergotamine in healthy volunteers following oral and rectal dosing. Eur J Clin Pharmacol. 1983;30:331–334.
85. Tfelt-Hansen P, Johnson ES. Ergotamine. In The headaches, Olesen J, Tfelt-Hansen P, Welch KM, (eds). Raven Press: New York. 1993;313–322.
86. Müller-Schweinitzer E. Ergot alkaloids in migraine: is the effect via 5-HT receptors? In 5-Hydroxytryptamine mechanisms in primary headaches, Olesen J, Saxena PR (eds). Raven Press: New York. 1992;297–304.
87. MaassenVanDenBrink A, Reekers M, Bax WA, Ferrari MD, Saxena, PR. Coronary side-effect potential of current and prospective antimigraine drugs. Circulation 1998;98:25–30.
88. Cortijo J, Martí-Cabrera M, Bernabeu E, Domenech T, Bou J, Fernández AG, Beleta J, Palacios JM, Morcillo EJ. Characterization of 5-HT receptors on human pulmonary artery and vein: Functional and binding studies. Br J Pharmacol. 1997;122:1455–1463.
89. Østergaard JR, Mikkelsen E, Voldby B. Effects of 5-hydroxytryptamine and ergotamine on human superficial temporal artery. Cephalalgia. 1981;1:223–228.
90. Bulow PM, Ibraheem JJ, Paalzow G, Tfelt-Hansen P. Comparison of pharma-codynamic effects and plasma levels of oral and rectal ergotamine. Cephalalgia. 1986;6:107–111.
91. Dixon RM, Meire HB, Evans DH, Watt H, On N, Posner J, Rolan PE. Peripheral vascular effects and pharmacokinetics of the antimigraine compound, zolmitriptan, in combination with oral ergotamine in healthy volunteers. Cephalalgia. 1997;17: 639–646.
92. Saxena PR, Cairo-Rawlins WI. Presynaptic inhibition by ergotamine of the responses to cardioaccelerator nerve stimulations in the cat. Eur J Pharmacol. 1979;58:305–312.
93. De Vries P, Villalon CM, Heiligers JP, Saxena PR. Characterization of 5-HT receptors mediating constriction of porcine carotid arteriovenous anastomoses; involvement of 5-HT1B/1D and novel receptors. Br J Pharmacol. 1998;123: 1561–1570.
94. Villalón CM, De Vries P, Rabelo G, Centurión D, Sánchez-López A, Saxena PR. Canine external carotid vaso-constriction to methysergide, ergotamine and dihydroergotamine: role of 5-HT1B/1D receptors and α2-adrenoceptors. Br J Pharmacol. 1999;126:585–594.
95. Lonicer A. Kreuterbuch (Frankfurt-am-Main: Christian Egenolff, 1557) [Christ's College, Rouse 15.16] Frankfurt; 1557.
96. Aronson SM. The tapestery of medicine. Manisses Communications Group, Inc: Providence, RI. 1999;189–92.
97. Dudley HW, Moir JC. The substance responsible for the traditional clinical effect of ergot. BMJ. 1935a;1:520–523.
98. Dudley HW, Moir JC. The new active principle of ergot. Sci. 1935b;81:559-560.
99. Dudley HW. Ergometrine. Proc Roy Soc London B. 1935;118:478-484.
100. De Costa C. St Anthony's fire and living ligatures: A short history of ergometrine. Lancet. 2002;359:1768–1770.
101. McEvoy GK. Ergonovine Maleate and Methylergonovine Maleate, In AHFS drug information 2004. American Society of Health-System Pharmacists: Bethesda, MD. 2007;3269-3270.
102. Novartis. Methergine (methylergonovine maleate) tablets and injection prescribing information. East Hanover, NJ; 2007. Available:http://www.drugs.com/monograph/methylergonovine-maleate.html (Date accessed April, 2015)
103. Pharmacist Pharmaceutical. Ergotrate (ergonovine maleate) tablets prescribing information. Salem, V; 2007a.

Available:http://www.drugs.com/monograph/ergonovine-maleate.html
(Date accessed April, 2015)
104. Pharmacist Pharmaceutical. Ergotrate (ergonovine maleate) injection prescribing information. Salem, VA; 2007b.
Available:http://www.drugs.com/monograph/ergonovine-maleate.html
(Date accessed April, 2015)
105. Silvestri LA. Saunders Comprehensive Review for the NCLEX-RN Examination. (6th edn). Saunders: US, 1184; 2013.
106. MCHN.
Available:http://www.path.org/publications/files/MCHN_popphi_amtsl_ref_man_2of3.pdf
(Date accessed April, 2015)
107. Graves CR. Agents that cause contraction or relaxation of the uterus. In Goodman & Gilman's the pharmacological basis of therapeutics. (9th edn). Hardman JG, Limbird LE, Molinoff PB, Ruddon RW, Gilman AG (eds). McGraw-Hill: New York. 1996;939–949.
108. Liabsuetrakul T, Choobun T, Peeyananjarassri K, Islam QM. Prophylactic use of ergot alkaloids in the third stage of labour. Cochrane Database Syst Rev. 2007;2:CD005456.
109. WHO Model List of essential medicines; 2013.
Available:http://apps.who.int/iris/bitstream/10665/93142/1/EML_18_eng.pdf
(Date accessed March, 2015)
110. Mahmud G, Javaid K, Tasnim N, Tabassum A, Bangash KT. Where does ergometrine stand in prevention of postpartum haemorrhage in caesarean section? J Pak Med Assoc. 2014;64:911-914.
111. Prasad JP. Conceptual Pharmacology (Ist edn). Universities Press: India. 2010;700.
112. Michaluk LA. Dopaminergic and serotonergic effects of ergometrine. Pol J Pharmacol Pharm. 1977;29:273-279.
113. Medsafe.
Available:http://www.medsafe.govt.nz/profs/datasheet/d/DBLErgometrineinj.pdf
(Date accessed March, 2015)
114. Drugs.
Available:http://www.drugs.com/pro/bromocriptine.html
(Date accessed March, 2015)
115. MacLeod RM, Lehmeyer JE. Suppression of pituitary tumor growth and function by ergot. Cancer Res. 1973;33:849-855.
116. MacLeod RM, Abad A, Eidson LL. *in vivo* effect of sex hormones on the *in vitro* synthesis of prolactin and growth hormone in normal and pituitary tumor-bearing rats. Endocrinol. 1969;84:1475-1483.
117. Nagasawa H, Meites J. Suppression by ergocornine and iproniazid of carcinogen-induced mammary tumors in rats; effects on serum and pituitary prolactin levels. Proc Soc Exptl Biol Med. 1970;135:469-472.
118. Yanai R, Nagasawa H. Suppression of mammary hyperplastic nodule formation and pituitary prolactin secretion in mice induced by ergocornine or 2-Bromo-a-Ergocryptine. J Natl Cancer Inst. 1970;45: 1105-1112.
119. Lu KH, Koch Y, Meites J. Direct inhibition by ergocornine of pituitary prolactin release. Endocrinol. 1971;89:229-233.
120. Wuttke W, Cassell E, Meites J. Effects of ergocornine on serum prolactin and LH, and on hypothalamic content of PIP and LRF. Endrocrinol. 1971;88:737-741.
121. US patent 4526892 A; 1985.
122. Colao A, di Sarno A, Pivonello R, di Somma C, Lombardi G. Dopamine receptor agonists for treating prolactinomas. Expert Opin Investig Drugs. 2002;11:787-800.
123. Barnett AH, Chapman C, Gailer K, Hayter, CJ. Effect of bromocriptine on maturity onset diabetes. Postgrad Med J. 1980;56: 11–14.
124. US patent 3,752,814; 1973.
125. Cincotta AH, Meier AH, Cincotta M Jr. Bromocriptine improves glycaemic control and serum lipid profile in obese type 2 diabetic subjects: a new approach in the treatment of diabetes. Expert Opin Investig Drugs. 1999;8:1683–1707.
126. Holt RI, Barnett AH, Bailey CJ. Bromocriptine: Old drug, new formulation and new indication. Diabetes Obe. Metab. 2010;12:1048-1057.
127. Mikhail N. Quick-release bromocriptine for treatment of type 2 diabetes. Curr Drug Deliv. 2011;8:511-516.
128. Shivaprasad C, Kalra S. Bromocriptine in type 2 diabetes mellitus. In. J Endocrinol Metab. 2011;15:S17-24.
129. Pijl H, Ohashi S, Matsuda M, Miyazaki Y, Mahankali A, Kumar V, Pipek R, Iozzo P, Lancaster JL, Cincotta AH, DeFronzo RA. Bromocriptine: A novel approach to the treatment of type 2 diabetes. Diabetes Care. 2000;23:1154–1161.

130. Baggio LL, Drucker DJ. Biology of incretins: GLP-1 and GIP. Gastroenterol 2007;132:2131–2157.
131. Lam CK, Chari M, Lam TK. CNS regulation of glucose homeostasis. Physiol (Bethesda). 2009;24:159–170.
132. Tahrani AA, Bailey CJ, Prato SD, Barnett AH. Management of type 2 diabetes: New and future developments in treatment. Lancet. 2011;378:182–197.
133. Gaziano JM, Cincotta AH, O'Connor CM, Ezrokhi M, Rutty D, Ma ZJ, Scranton RE. Randomized clinical trial of quick-release bromocriptine among patients with type 2 diabetes on overall safety and cardiovascular outcomes. Diabetes Care. 2010;33:1503–1508.
134. Ramteke KB, Ramanand SJ, Ramanand JB, Jain SS, Raparti GT, Patwardhan MH, Murthy M, Ghanghas RG. Evaluation of the efficacy and safety of bromocriptine QR in type 2 diabetes. In J Endocrinol Metab. 2011;15:S33-S39.
135. Bell DS. Focusing on cardiovascular disease in type 2 diabetes mellitus: An introduction to bromocriptine QR. Postgrad Med. 2012;124:121-135.
136. Weiland CM, Hilaire ML. Bromocriptine Mesylate (Cycloset) for type 2 diabetes mellitus. Am Fam Physician. 2013;87:718-720.
137. Keche Y. Bromocriptine mesylate: Food and drug administration approved new approach in therapy of non-insulin dependent diabetes mellitus with poor glycemic control. J Pharm Bioallied Sci. 2010;2:148-150.
138. Scranton R, Cincotta A. Bromocriptine--unique formulation of a dopamine agonist for the treatment of type 2 diabetes. Expert Opin Pharmacother. 2010;11:269-279.
139. Garber AJ, Blonde L, Bloomgarden ZT, Handelsman Y, Dagogo-Jack S. The role of bromocriptine-QR in the management of type 2 diabetes expert panel recommendations. Endocr Pract. 2013;19: 100-106.
140. Agid Y, Destée A, Durif F, Montastruc JL, Pollak P. Tolcapone, bromocriptine, and Parkinson's disease. Lancet. 1998;350:2–5.
141. Montastruc JL, Rascol O, Senard JM, Rascol A. A randomised controlled study comparing bromocriptine to which levodopa was later added, with levodopa alone in previously untreated patients with Parkinson's disease: a five year follow up. J Neurol Neurosurg Psychiatry. 1994;57: 1034–1038.
142. Rinne UK, Bracco F, Chouza C, Dupont E, Gershanik O, Marti Masso JF, Montastruc JL, Marsden CD, Dubini A, Orlando N, Grimaldi R. Cabergoline in the treatment of early Parkinson's disease: Results of the first year of treatment in a double-blind comparison of cabergoline and levodopa. The PKDS009 Collaborative Study Group. Neurol. 1997;48:363–368.
143. Del Dotto P, Colzi A, Musatti E, Benedetti MS, Persiani S, Fariello R, Bonuccelli U. Clinical and pharmacokinetic evaluation of L-dopa and cabergoline cotreatment in Parkinson's disease. Clinical Neuropharmacol. 1997;20:455-465.
144. Rinne UK, Bracco F, Chouza C, Dupont E, Gershanik O, Marti Masso JF, Montastruc, JL, Marsden CD. Early treatment of Parkinson's disease with cabergoline delays the onset of motor complications. Results of a double-blind levodopa controlled trial. The PKDS009 Study Group. Drugs. 1998;55:23–30.
145. Marsden CD. Clinical experience with cabergoline in patients with advanced Parkinson's disease treated with levodopa. Drugs. 1998;55:17–22.
146. Boas J, Worm-Petersen J, Dupont E, Mikkelsen B, Wermuth L. The levodopa dose-sparing capacity of pergolide compared with that of bromocriptine in an open-label, crossover study. Eur J Neurol. 1996;3:44–49.
147. Schwarz J, Scheidtmann K, Trenkwalder C. Improvement of motor fluctuations in patients with Parkinson's disease following treatment with high doses of pergolide and cessation of levodopa. Eur Neurol. 1997;37:236–238.
148. Laihinen A, Rinne UK, Suchy I. Comparison of lisuride and bromocriptine in the treatment of advanced Parkinson's disease. Acta Neurol Scand. 1992;86:593–595.
149. Bayulkem K, Erisir K, Tuncel A, Bayulkem B. A study on the effect and tolerance of lisuride on Parkinson's disease. Adv Neurol. 1996;69:519–530.
150. Rinne UK. Combination therapy with lisuride and L-dopa in the early stages of Parkinson's disease decreases and delays the development of motor fluctuatuations. Long-term study over 10 years in comparison with L-dopa monotherapy. Nervenarzt. 1999;70:S19–S25.

151. Schade R, Andersohn F, Suissa S, Haverkamp W, Garbe E. Dopamine agonists and the risk of cardiac-valve regurgitation. N Engl J Med. 1997;356:29–38.
152. Zanettini R, Antonini A, Gatto G, Gentile R, Tesei S, Pezzoli G. Valvular heart disease and the use of dopamine agonists for Parkinson's disease. N Engl J Med. 2007;356:39-46.
153. Trifirò G, Mokhles MM, Dieleman JP, van Soest EM, Verhamme K, Mazzaglia G, Herings R, de Luise C, Ross D, Brusselle G, Colao A, Haverkamp W, Schade R, van Camp G, Zanettini R, Sturkenboom MC. Risk of cardiac valve regurgitation with dopamine agonist use in Parkinson's disease and hyperprolactinaemia: A multi-country, nested case-control study. Drug Saf. 2012;35:159-171.
154. Mokhles MM, Trifirò G, Dieleman JP, Haag MD, van Soest EM, Verhamme KM, Mazzaglia G, Herings R, Luise C, Ross D, Brusselle G, Colao A, Haverkamp W, Schade R, Camp GV, Zanettini R, Sturkenboom MC. The risk of new onset heart failure associated with dopamine agonist use in Parkinson's disease. Pharmacol Res. 2012;65:358-364.
155. Antonini A, Poewe W. Fibrotic heart-valve reactions to dopamine-agonist treatment in Parkinson's disease. Lancet Neurol. 2007;6:826-829.
156. Lissoni P, Mandalà M, Giani L, Malugani F, Secondino S, Zonato S, Rocco F, Gardani G. Efficacy of bromocriptine in the treatment of metastatic breast cancer- and prostate cancer-related hyperpro-lactinemia. Neuro Endocrinol Lett. 2000; 21:405-408.
157. Mulac D, Humpf HU. Cytotoxicity and accumulation of ergot alkaloids in human primary cells. Toxicol. 2011;282:112-121.
158. Mulac D, Lepski S, Ebert F, Schwerdtle T, Humpf HU. Cytotoxicity and fluorescence visualization of ergot alkaloids in human cell lines. J Agric Food Chem. 2013;61: 462-471.
159. Mrusek M, Seo EJ, Greten HJ, Simon M, Efferth T. Identification of cellular and molecular factors determining the response of cancer cells to six ergot alkaloids. Invest. N Drugs. 2015;33:32-44.
160. FDA.
Available:http://www.accessdta.fda.gov/scripts/cder/drugstfda/index.cfm
(Date accessed March, 2015)

Peer-review history:
The peer review history for this paper can be accessed here:
http://sciencedomain.org/review-history/14283

Biocatalysis and Agricultural Biotechnology 29 (2020) 101804

Contents lists available at ScienceDirect

Biocatalysis and Agricultural Biotechnology

journal homepage: http://www.elsevier.com/locate/bab

Polyphenolic rich extract of *Oroxylum indicum* alleviate β-glucuronidase activity via down-regulate oxidative stress: Experimental and computational studies

Prateek Pathak [a, *], Jurica Novak [a], Vladislav Naumovich [a], Maria Grishina [a], Acharya Balkrishna [b, c], Niti Sharma [b], Vinay Sharma [b], Vladimir Potemkin [a], Amita Verma [d]

[a] Laboratory of Computational Modeling of Drugs, Higher Medical and Biological School, South Ural State University, Chelyabinsk, Russia, 454080
[b] Drug Discovery and Development Division, Patanjali Research Institute, Haridwar, 249405, India
[c] Department of Allied and Applied Sciences, University of Patanjali, Patanjali Yogpeeth, Haridwar, 249 405, India
[d] Bioorganic and Medicinal Chemistry Research Laboratory, Department of Pharmaceutical Sciences, Sam Higginbottom University of Agriculture, Technology & Sciences, Allahabad, 211007, India

ARTICLE INFO

Keywords:
Oroxylum indicum stem Bark
Antioxidant activity
β-glucuronidase activity
ADME study
Docking study

ABSTRACT

Oroxilum indicum has an extensive history in the Indian traditional medicine system. The root and stem bark of this plant is well accepted for the treatment, prevention, and cure of various types of diseases. The bark of the plant has a high content of flavonoids and other phenolics, which are known to be responsible for exhibiting various therapeutic effects. The role of *O. indicum* in liver disease is well known, but until now, the mechanism has not been well studied. In the present study, the stem bark of *O. indicum* was extracted with ethanol using a hot extraction method and their phyto-chemical analysis was performed. Further, the plant extract was also used to evaluate their role in reducing oxidative stress and β-glucuronidase enzyme activity. The antioxidant study showed that extract has the capability to down-regulate oxidative stress, while β-glucuronidase assay displayed IC_{50} at 174.36 μg/mL. Additionally, we selected the major polyphenolic phyto-compounds derived from the bark of *O. indicum* for *in silico* ADME and docking studies. The ADME study reflected the optimal pharmacokinetic profile of the compounds. However, the docking experiments confirmed that all the selected phyto-compounds have tendency to interact with β-glucuronidase receptor.

1. Introduction

The liver is an imperative organ involved in maintaining a variety of metabolic functions and its related diseases have become one of important health concern worldwide (Byass, 2014). Liver act in the detoxification process via countering various exogenous and endogenous challenges (Kshirsagar et al., 2011). Exogenous compounds (xenobiotics such as alcohol, nicotine and drugs) (Benković et al., 2019) are mainly metabolized in the liver by biotransformation phase I and II. Briefly, the biotransformation phase I reactions are majorly involved in the exposure of functional groups on the drug through oxidation, reduction, and hydrolysis (Tripathi, 2013). However, the biotransformation phase-II reactions are majorly controlled and coordinated by glucuronidation (Graaf et al., 2002). It was observed that during the process of metabolism various toxins conjugate with glucuronic acid and are converted into inactive forms (converting conju-

Abbreviations: O. indicum, *Oroxylum indicum*, ADME, Absorption, distribution, metabolism, excretion, IP, Indian Pharmacopoeia, API, Indian Ayurvedic Pharmacopoeia, PDB, Protein data Bank, LGA, Local grid analysis, TS, Transverse section, μg/QE, μg/ quercetin equivalent in mg, μg/DE, μg/ diosgenin equivalent in mg, IC_{50}, 50% inhibition, DPPH, 2,2-diphenyl-1-picrylhydrazyl, ABTS, 2,2′-azino-bis(3-ethylbenzothiazoline-6-sulfonic acid, ANOVA, Analysis of variance, EDTA, Ethylene diamine tetra acetic acid, logP, The logarithm of the octanol–water partition coefficient, Lip, Vio, Total number of violation of Lipinski rule of five, H don, Number of H donors, H Acc, Number of H acceptors, GI abs, Gastrointestinal absorption, BBB, Blood brain barrier, P450-3A4, The probability of metabolism at CYP450 3A4, P450-2D6, The probability of metabolism at CYP450 2D6, TPSA, Total polar surface area, Tox, Probability of maximum toxicity of the compounds, Ph Score, Predicted glucosidase activity score calculated by the Cinderella shoe

* Corresponding author. .
E-mail address: patkhakp@susu.ru (P. Pathak).

https://doi.org/10.1016/j.bcab.2020.101804
Received 20 July 2020; Received in revised form 14 August 2020; Accepted 28 September 2020
Available online 28 September 2020
1878-8181/

gated bilirubin to the unconjugated promotes its re-absorption). These inactive forms of toxins are eliminated from the organ without arising any harm. The rate of deglucuronidation is controlled by β-glucuronidase enzyme. These β-glucuronidase enzymes are present in endocrine, reproductive organs, and other tissue surfaces, which play an important role in the hydrolysis of glucuronide moiety (Dutton, 1980). It is also noticed that liver damage and other related complications increase blood β-glucuronidase level (Pineda et al., 1959). Therefore, β-glucuronidase inhibitors can play a vital role in reducing this toxic stimulants and act as potential hepatoprotective agents (Walaszek et al., 1984). Silymarin is a well-recognized phytopharmaceutical used as β-glucuronidase inhibitor and widely used for the treatment of various liver disorders such as liver cancer and jaundice (Kim et al., 1994). Nevertheless, silymarin also contains some major drawback like poor bioavailability (Dixit et al., 2007), GI bloating, dyspepsia, nausea, irregular stool, diarrhea, pruritus, headache, exanthema, malaise, asthenia, and vertigo (Pradhan and Girish, 2006). Thus, search towards identification of new hepatoprotective formulation from the traditional plants is worthful. There are vast varieties of medicinal herbs known for β-glucuronidase enzyme inhibition (Joshi and Sanmuga Priya, 2007). *Oroxylum indicum* (Shyonaka) (Family: Bignoniaceae) is one of the well-recognized species mentioned in ancient traditional Indian medication system Ayurveda (API, 2016). Ayurvedic medication system considers this plant in single or as a poly-herbal formulation for the treatment of various ailments like fever, jaundice, measles, bronchitis, intestinal worms, leucoderma, asthma, inflammation, anal troubles, snakebite, rheumatism, diarrhea, and dysentery (Atara et al., 2014; Di Bisceglie, 2009). The plant bark consist of enrich amount of flavonoids and other phenolics (mainly baicalein, oroxyline-A, chrysin, baicalin, naphthoquinone-lapachol, and phenolic ellagic acid) (Dinda et al., 2015; Teshima et al., 1996; Yadav et al., 2013; Yan et al., 2011). Some studies reported that one of the major components of this plant, baicalein shows hepatoprotective characteristics through free radicals scavenging and lipid peroxidation inhibition (Kim et al., 1994; Tenpe et al., 2009). Even though, the hepatoprotective activity of *O. indicum* is well acknowledged but the mechanism of action still has not been well studied. Studies shows that polyphenols (especially flavonoids) participates as antioxidants through lowering the oxidative stress (Benković et al., 2019; Hussain et al., 2016; Singh et al., 2018). Therefore, in this study, we evaluated the β-glucuronidase inhibitory potency of polyphenolic rich extract of *O. indicum* stem bark, followed by its role in reduction of oxidative stress. Additionally, we selected previously identified polyphenolic compounds of the stem bark (Yadav et al., 2013) (Fig. 1) for docking study to establish the possible ligand-amino acid residue necessary for β-glucuronidase inhibition.

2. Material and methods

2.1. Plant material

The stem bark of *O. indicum* was purchased from Patanjali Ayurveda Ltd, India. Further, the sample was authenticated by regional office of Botanical Survey of India, Allahabad, Uttar Pradesh, India and a voucher specimen (TR No-197,054) was deposited for future reference.

2.1.1. Extract preparation

300 mL of ethanol was added into a round bottom flask with 20 g of powdered material. Then the sample was refluxed for 3 h. Further, the solution was filtered using Whatman filter (paper # 41) to remove the particulate matter and concentrated at 30 °C under reduced pressure.

2.2. Chemicals

The chemicals and reagents used for the study were β-glucuronidase (from bovine liver; Sigma, India), *p*.-nitrophenyl-β-glucuronide (Merck, India), silymarin (Sigma, India), sodium dihydrogen orthophosphate (Merck, India), di-sodium hydrogen phosphate (Merck, India).

2.3. Macroscopy

Macroscopy consist the methodology of evaluation of the plant for the confirmation of its originality and purity. For this purpose, detection of adulteration was based on visual appearance by the naked eyes and other sensory characteristics such as odor, taste, and touch.

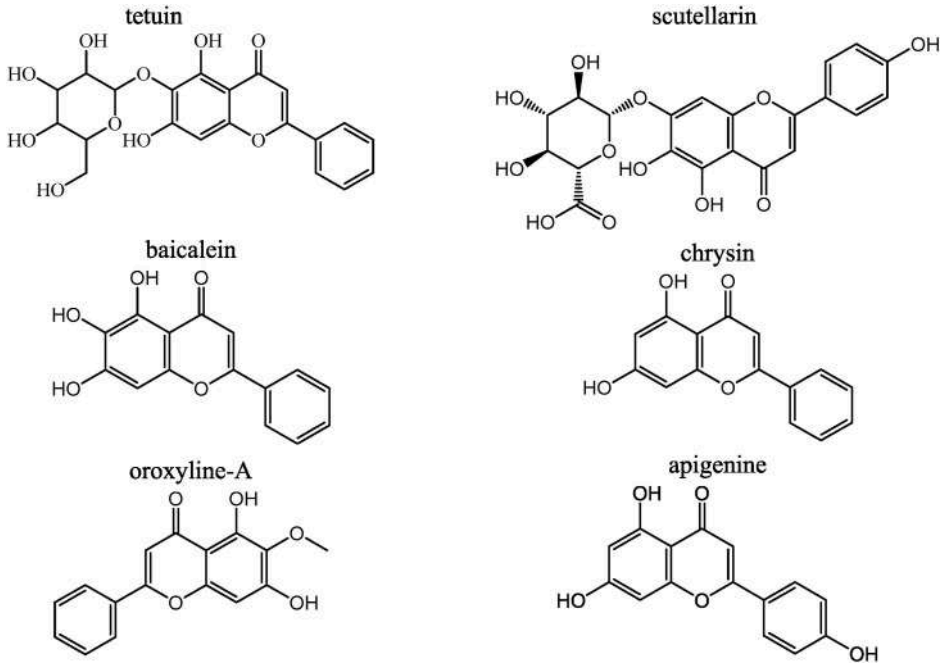

Fig. 1. Structure of selected polyphenolic compounds.

2.4. Microscopic features

The plant material was fixed in the solution mixture of formaldehyde (45 mL of 70% ethanol + 4.5 mL of glacial acetic acid + 4.5 mL of formaldehyde). The section was cut transversely and stained with safranin and mounted following the usual plants micro techniques (Creighton, 1965).

2.5. Pharmacognostical analysis

Different pharmacognostical parameters (moisture, ash value, extractive value, etc.) were analyzed according to the standard methods mentioned in official Pharmacopoeias (API, 2016; IP, 1996).

2.5.1. Preliminary phytochemical screening

The extract was screened for the presence of phyto-constituents (terpenoids, saponins, tannins, alkaloids, flavonoids, steroids, carbohydrates, glycosides, fats and oils) (Evans, 1997; Khandelwal, 2004; Mohapatra et al., 2018).

2.5.2. Quantative phyto-chemical analysis

The estimation of total phenolics, flavonoids and saponins content was done according to the methods described by Siddhuraju et al., (2007) (Siddhuraju and Becker, 2007), Zhishen et al., 1999 (Zhishen et al., 1999) and Makkar et al., (2007) (Makkar et al., 2007), respectevly.

2.6. Antioxidant activity

The antioxidant activity of extract was determined by DPPH free radical scavenging assay, ABTS radical cation decolorization assay, hydroxyl and superoxide radical scavenging assay, nitric oxide scavenging assay, iron chelating activity, and total antioxidant capacity. All the set of experiments were carried out in triplicates. However, the measurements of IC_{50} values were calculated by probit analysis.

The scavenging activity was calculated using the formula

$$\%\ scavenging = \frac{A_0 - A_t}{A_0} \times 100 \quad (1)$$

where A_0 and A_t are the absorbance of the control and sample, respectively.

2.6.1. DPPH radical scavenging activity

The free radical scavenging potential was calculated by DPPH free radical assay as described in the literature (Bansal et al., 2011; Chaudhary et al., 2015). Briefly, 1.0 mL methanolic solution of DPPH (c = 0.1 mM) was added to 1.0 mL of extract and ascorbic acid at different concentrations. Further, the reaction mixture was kept 20 min for incubation and the absorbance was observed at 517 nm with ascorbic acid as positive control. Stronger DPPH radical-scavenging activity is indicated by a decrease in absorbance of the reaction mixture. Percentage scavenging was calculated by formula (1).

2.6.2. ABTS radical cation decolorization assay

The ABTS free radical scavenging assay was conducted as per previously described methods (Liu et al., 2015; Stanković et al., 2016; Tachakittirungrod et al., 2007). Briefly, ABTS solution (c = 7.0 mM, 1 mL) was mixed with potassium persulfate (c = 2.45 mM, 1 mL) and incubated for 12–16 h in the dark. This incubation allows to generate ABTS radical cation. The $ABTS^+$ solution mixtures were diluted with ethanol until the absorbance appeared as 0.70 ± 0.05 at 734 nm. Then, 50 μL of the diluted sample (different concentration) were mixed with diluted $ABTS^+$ solution mixture (1.9 mL). The final test mixtures were kept for 6 min at room temperature, followed by measurements of absorbance at 734 nm (Stanković et al., 2016). Ascorbic acid was used as reference standard. Percentage scavenging was calculated by formula (1).

2.6.3. Superoxide radical scavenging activity

Superoxide radical scavenging activity was measured on the basis of a reduction in the nitro blue tetrazolium (NBT), according to a previously reported method (Fontana et al., 2001). Superoxide radicals produced through the non-enzymatic PMS/NADH (phenazine methosulfate-nicotinamide adenine dinucleotide) system, reduced the NBT to purple formazan (Fontana et al., 2001). 1.0 mL of the reaction mixture (contains 100 μL of NADH, c = 73 μM; 200 μL of NBT, c = 20 mM; 200 μL of PMS, c = 15 μM; 400 μL phosphate buffer at pH 7.4, and 100 μL of the sample solution with different concentrations) was prepared. Allow the reaction mixture at room temperature for 5 min. The absorbance was measured at 562 nm against a blank. Curcumin was used as standard positive control. Formula (1) was used to calculate the percentage scavenging activity.

2.6.4. Hydroxyl radical scavenging

Hydroxyl radical scavenging assay was performed as described by Elizabeth and Rao (Kunchandy and Rao, 1990) with a minor modification. 1 mL of reaction mixture in phosphate buffer (pH 7.4, c = 20 mM), containing ferric chloride (c = 100 μM, 200 μL), EDTA (c = 100 μM, 200 μL), ascorbic acid (c = 100 μM, 100 μL), H_2O_2 (c = 200 μM, 200 μL) and 2-deoxy-2-ribose (c = 2.8 mM, 300 μL) was prepared. Further, 1 mL of test sample with different concentration or reference compounds were added into the reaction mixture to make up the final volume up to 3 mL using DMSO. The mixture was incubated at 37 °C for 1 h. Then, 1.0 mL of 2.8% TCA was added in 0.5 mL of the reaction mixture followed by the addition of 1.0 mL of 1% aqueous TBA. Again, the mixture was incubated for 15 min at 90 °C. The sample was cooled to the room temperature and absorbance of blank, test, and reference (catechin) were measured at 532 nm. The scavenging percentage was calculated by formula (1).

2.6.5. Nitric oxide scavenging activity

Nitric oxide scavenging activity was examined by Griess reagent assay (Garratt, 1976). Shortly, 2.0 mL of 10 mM sodium nitroprusside was mixed with 0.5 mL of phosphate buffered saline (PBS) (pH 7.4), and 0.5 mL of different concentrations containing standard/extract solutions. Then, the reaction mixture was incubated for 150 min at 25 °C. After that, 1.0 mL sulphanilic acid reagent was added and allowed to incubate for next 5 min. Then, 1.0 mL of 0.1% naphthyl ethylene diamine dihydrochloride was added and re-incubated for another 30 min. Finally, the absorbance of test and standard were measure at 540 nm. There was curcumin as a positive control. Formula (1) was used to calculate the scavenging activity.

2.6.6. Iron chelating activity

The measurement of iron chelating activity was based on chelation property. In this experiment, 1,10-phenanthroline monohydrate (0.198 g), hydrochloric acid (2.0 mL, concentration = 1 M), and ferric ammonium sulphate (0.16 g) were dissolved in 100 mL of water for preparing 1,10-phenanthroline-iron (III) reagent. Briefly, standard/extracts (0.2 mL), 1,10-phenanthroline-iron (III) reagent (0.2 mL), methanol (0.6 mL), and water (4.0 mL) were mixed together. Further, the solutions were allowed to incubate at 50 °C for 30 min. The absorbance was measured at 510 nm against ascorbic acid as positive control (Besada, 1987; Chaudhary et al., 2015). Percentage of scavenging was calculated by formula (1).

2.6.7. Total antioxidant capacity

The measurement of total antioxidant capacity were calculated through phosphomolybdenum method (Chaudhary et al., 2015; Prieto

et al., 1999). Concisely, a mixture of standard/extract solution (0.1 mL) and reagent solution (0.3 mL) (contains 28 mM sodium phosphate, 0.6 M sulfuric acid, and 4 mM ammonium molybdate, 100 μL each) were prepared. Further, the reaction mixture was incubated at 95 °C for 90 min. After reaction mixture was cooled down to the room temperature, the absorbance of the test sample was recorded at 695 nm against blank solution (Chaudhary et al., 2015), and expressed as ascorbic acid equivalents.

2.7. β-glucuronidase activity

β-glucuronidase inhibition activity was carried out according to the method described by Kim et al. (1994) with minor modification. Concisely, β-glucuronidase (2 mg/mL of 0.1 M phosphate buffer at pH 7.0) was incubated for 15 min (at 37 °C). Then, *p*-nitrophenyl β-glucuronide (15 mL, contains 3.15 mg/mL in 0.1 M phosphate buffer, pH 7.0) was added and allowed to incubate for 50 min at 37 °C (Hazra et al., 2008; Joshi and Sanmuga Priya, 2007). The absorbance of test sample, blank solution and silymarin were measured at 405 nm using microplate reader (Molecular Devices, Sunnyvale, USA). . The percent inhibition was calculated according to equation (1).

2.8. Computational physicochemical and β-glucuronidase activity prediction

The ADME computations (logP, toxicity, metabolism at CYP450: 3A4, CYP450: 2D6) and the prediction of the β-glucuronidase activity was carried out using Chemosophia software developed by our laboratory team (Potemkin and Grishina, 2018) (www.chemosophia.com). The program works on the basis of CoMIn algorithm (Potemkin et al., 2017; Potemkin and Grishina, 2018) and alteQ approach (Potemkin and Grishina, 2018, 2008). However, TPSA, Lipinski violation (Lipinski, 2004), numbers of H donor and H acceptor, water solubility score, GI absorption score, and possibility of metabolism at CYP1A2, CYP2C19, and CYP2C9 were calculated at Swissadme. ch (Daina et al., 2017).

2.9. Computational methodology

The computational simulation were carried out on a 4 CPUs (Intel Core 2 Quad CPU Q9550 @ 2.83 GHz) ACPI x64 workstation with windows 8.1 operating system. The protein and ligands were prepared and docked using Auto dock 4.2 software (Morris et al., 2009).

2.9.1. Receptor preparation

The crystal structure of β-glucuronidase with an activity-based probe (PDB code: 5G0Q) was retrieved from Protein Data Bank (Berman, 2000) and analyzed with Chimera 1.5.3 software (Pettersen et al., 2004) for missing atoms and unphysically close contacts. Further, the water molecule, cofactor, and ligand (IF6) were removed. Gasteiger charges were added to each atom, nonpolar hydrogens were merged, atom types were determined and the structure of the prepared receptor was saved as pdbqt file.

2.9.2. Ligand setup

The structures of known major chemical components of the plant extract e.g. apigenin, baicalein, chrysin, oroxyline-A, scutellarin, and tetuin (Fig. 1) were prepared using Marvin Sketch 5.5.0.1 software (Chemaxon Group, 2011) and built-and-edit module in Open Babel 2.2.3 tool (O'Boyle et al., 2011). MMFF94s force field parameters were assigned to ligands' atoms and then the energy has been minimized. Gasteiger partial charges were added to the each ligand atoms. However, non-polar hydrogen atoms were merged and rotatable bonds defined. The structure of the ligands was saved in pdbqt format and used as input file for Autodock 4 in the next step.

2.9.3. Docking methodology

Molecular docking simulations were performed to find optimal position of the ligand inside catalytic pocket. To achieve realistic results, flexibility of ligand has to be accounted. For the ligand's conformational search, LGA was applied with the mutation rate of 0.02, the crossover rate of 0.80 and the starting population of 150 individuals. Initial position, their orientation, and torsions were set randomly. The docking simulations were performed by ligand Fit protocol of Auto dock 4.2 software (Trott and Olson, 2009). Grid box size of 60 Å × 60 Å × 60 Å with 0.375 Å spacing was generated using the Autogrid module and was centered at the center of the mass of the IF6 inhibitor bounded to the hydrolase (complex 5G0Q). Each of the docking experiment was derived from 100 different runs and set to terminate after a maximum of 250,000 energy evaluations. The ligand-receptor complexes of the lowest free energy of binding are saved and the interaction patterns between ligand and receptor are analyzed.

3. Results and discussion

3.1. Macroscopic features

The stem bark is 0.3–1.0 cm thick, curved, with outer surface being rough, warty owing lenticels, black or buff-whitish in color. The black or dark green in color filaments attached on the outer surface. Inner surface is light yellow, longitudinally striated, odorless. The taste is mild sweet and astringent. However, the fracture is coarse and medium.

3.2. Microscopic features

The TS of the stem bark consists 12–15 layered cork cells with 170–185 μm thickness. The corks cells are radially arranged with lignified stone cells. Just below the cork, 3–4 layered cambiums are showed, with thickness between 20 and 25 μm. The bark contains 285–380 μm thickened narrow phelloderm, fiber region and stone cells. The size of stone cells appears smaller and is connected to phloem region. However, the remaining bark section is composed of secondary phloem. The phloem is alienated into outer and inner region. In outer phloem, groups of stone cells and few fibers are present. Inner phloem has more fibers and less stones cells, opposite to outer phloem. The inner phloem region also contains ceratenchyma. The majority of the parenchymatous tissues are encapsulated with brownish-black matter. The stem bark consists multiseriate heterogenous much smaller medullary rays (up to 5 μm in diameter) in the secondary phloem region. Some acicular crystals are surrounded in parenchymatous tissues of phloem and medullary rays.

3.3. Pharmacognostical analysis

Moisture, ash value, extractive value and other pharmacognostical parameters are presented in Table 1. The values were found within the mentioned limits of Ayurvedic Pharmacopoeia of India and Indian Pharmacopoeia (API, 2016; IP, 1996).

3.3.1. Phytochemical screening

Phytochemical screening results demonstrated the presence of carbohydrates, coumarin, flavonoids, fixed oil, glycoside, saponins and tannins in the stem bark of *O. indicum* (Table 2). In brief, the ferric chloride test showed a strong presence of phenols. The lead acetate test proved the presence of tannins in the ethanolic extract of stem bark of *O. indicum*. Further, the Shinoda test and foam test were positive, which confirms the presence of flavonoids and saponins. Chaudhary and his coworkers (Chaudhary et al., 2015) illustrated that phenols and its derivatives consists prominent antioxidant activity due to

Table 1
The pharmacognostical analysis results of stem bark of *Oroxylum indicum*.

Parameter	Value[a] (%)
Ash Values	
Total ash	17.15 ± 3.80
Acid–insoluble ash	2.25 ± 0.75
Water–soluble ash	3.62 ± 1.25
Sulphated ash	17.25 ± 2.60
Extractive Values	
Alcohol soluble	19.15 ± 0.65
Water soluble	28.32 ± 1.50
Loss on drying	14.62 ± 0.82
Crude fiber content	24.95 ± 0.40

[a] Average of three readings.

Table 2
The results of qualitative phytochemical screening of stem bark of Oroxylum indicum.

Test	Result
Alkaloid	–
Amino acid	–
Carbohydrate	+
Coumarin	+
Flavonoid	+
Fixed oil	+
Glycoside	+
Gum/Mucilage	–
Saponin	+
Sterol	–
Tannin	+
Terpenoid	–
Phenols	+

their ideal structural chemistry for free-radical scavenging activity. They can also serve as reducing agents and free radical quenchers because of their participation as electron or hydrogen donor to free radicals. The quantative assay displayed that the plant extract contains enriched phenolic content (182.5 μg/GAE of plant extract). The total flavonoids content was calculated using a standard linear calibration curve of quercetin (R^2 = 0.999) applying the aluminum chloride method. It turned out that flavonoids dominate over other natural phenolics compounds. The ethanolic extract showed the highest quantity of flavonoids (155.2 μg/QE in mg of plant extract). As a part of comparative study with other research work (Chaudhary et al., 2015), we found that methanolic extract of *Nardostachys jatamansi* root showed 1.11 ± 0.04 mg QE/g of total flavonoids and also holds excellent antioxidant properties. Therefore, it can concluded that our selected plant *O. indicum* ethanolic stem bark extract certainly contains excellent free radical scavenging and antioxidant properties. The quantitative estimation of saponins is done by vanillin-sulfuric acid reagent and the total saponins were determined using a linear calibration curve of diosgenin (R^2 = 0.999). The extract has enrich amount of saponins (110 μg/DE in mg of plant extract) (Lim et al., 2020). The quantative estimation is summarized in Table 3.

Table 3
The results of quantative phytochemical screening of stem bark of Oroxylum indicum.

Test	Concentration [a]
Flavonoid	155.2 μg/QE
Phenol	182.5 μg/GAE
Saponin	110 μg/DE

[a] μg/QE (μg/quercetin equivalent); μg/GAE (μg/gallic acid equivalent); μg/DE (μg/diosgenin equivalent).

3.3.2. Antioxidant activity

Several studies suggested (Seitz and Stickel, 2006; Troll, 1985; Vanden Berghe, 2012) that reactive oxygen (ROS) or nitrogen species mediated pathways have a well-documented function in many ailments including hepatic system inflammation. In the initial phase of liver or other cancer, ROS and free radical interact directly with DNA and stimulate the process of cell growth and differentiation (Seitz and Stickel, 2006; Troll, 1985; Vanden Berghe, 2012). It is already proven that in the liver inflammation, significant amount of free radicals were produced and increase the oxidative stress (Seitz and Stickel, 2006; Troll, 1985; Vanden Berghe, 2012). Therefore, free radical scavenging potential of any drug or formulation can be considered as effective and adjuvant in the treatment of liver related disease (Seitz and Stickel, 2006; Troll, 1985; Vanden Berghe, 2012). We evaluated the free radical scavenging activity of the plant extract because this would further act as adjuvant in the hepatoprotective activity. The results are illustrated in Table 4 and Fig. 2.

3.3.2.1. In vitro free radical scavenging activity. The stem bark extract of *O. indicum* showed dose-dependent scavenging activity against DPPH free radical, ABTS radical cation decolorization, superoxide radical, and hydroxyl radical.

In the present study, the ethanolic extract of stem bark of *O. indicum* showed 50% DPPH inhibitory scavenging at 149.97 ± 1.10 μg/mL. However, the standard drug, L-ascorbic acid displayed IC_{50} at 20 times lower concentration, 7.12 ± 0.31 μg/mL. The previous studies (Fernando and Soysa, 2014; Mishra et al., 2009) related to hepatoprotective activity through oxidative stress of *Atalantia ceylanica* and *Murraya koenigii,* showed the 50% DPPH scavenging at 187 μg/mL and 131.2 μg/mL, respectively. The comparison analysis illustrated that hot ethanolic extraction of *O. indicum* stem bark has stronger DPPH scavenger potency than methanolic leaf extract of *Atalantia ceylanica* and slightly lower DPPH antioxidant property than *Murraya koenigii* alcoholic leaf extract. Thus, we can consider that *O. indicum* have comparable DPPH scavenging potency as compare to other traditionally used hepatoprotective plants, such as *A. ceylanica.*

Table 4
Antioxidant activity of stem bark of Oroxylum indicum.

Name	DPPH scavenging IC_{50} value (μg/mL)	ABTS scavenging IC_{50} value (μg/mL)	Superoxide radical scavenging IC_{50} value (μg/mL)	Hydroxyl radical scavenging IC_{50} value (μg/mL)	Nitric oxide scavenging IC_{50} value (μg/mL)	Iron chelating activity IC_{50} value (μg/mL)	Total antioxidant capacity (μg ascorbic acid eq/mg extract)
Oroxylum indicum	149.97 ± 1.10[b]	80.10 ± 0.90[b]	139.10 ± 1.80[b]	34.20 ± 1.75[b]	136.80 ± 4.20[b]	44.10 ± 0.25[b]	170.70 ± 1.50[b]
Ascorbic acid	7.82 ± 0.36	2.62 ± 0.50	–	–	–	1.19 ± 0.01	–
Curcumin	–	–	17.60 ± 0.80	–	23.10 ± 1.10	–	–
Catechin	–	–		25.85 ± 1.05	–	–	–

All the values are expressed as mean ± SEM (n = 3).
[b] *Significant difference ($P < 0.05$)* (Dunnet's *t*-test) *as compare to standards.*

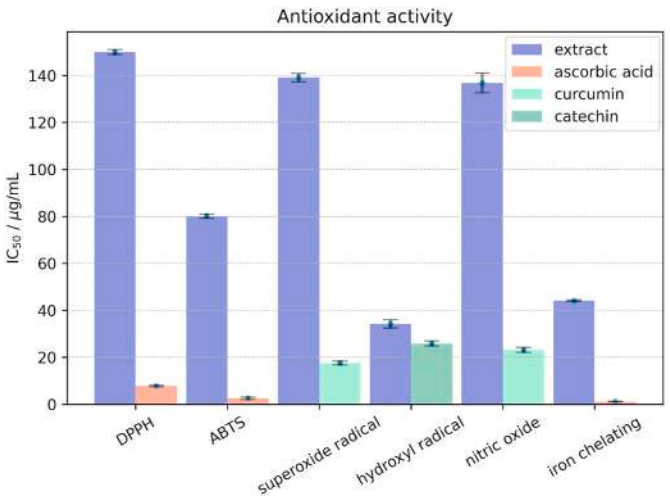

Fig. 2. The antioxidant activity of ethanol extracts stem bark of *Oroxylum indicum*.

Furthermore, the ethanolic extract of *O. indicum* stem bark and ascorbic acid displayed IC_{50} at 80.10 ± 0.90 µg/mL and 2.62 ± 0.50 µg/mL, respectively in $ABTS^+$ scavenging assay. Vikas and his team (Vikas et al., 2017) highlighted that the seed of *Annona squamosa* showed half of inhibitory potential at 94.2 ± 0.9 µg/mL against $ABTS^+$ scavenging assay and was used in several disease. $ABTS^+$ scavenging potential assessment of *O. indicum* bark was found more significant as compare to seed extract of *Annona squamosa,* which also shows the good sign for prominent role in reducing oxidative stress.

The next analysis was focused on the measurement superoxide radical scavenging. The extract and standard curcumin showed IC_{50} at 139.10 ± 1.80 µg/mL and 17.60 ± 0.80 µg/mL, respectively. For the evaluation superoxide radical scavenging capacity of tested extract, we compare the result with study related to hepatoprotective plants (Vikas et al., 2017). We found that the tested bark extract possess lower superoxide radical scavenging ability than methanolic extract of *Annona squamosa.*

The subsequent step towards antioxidant capacity measurement was based on hydroxyl radical scavenging assay. The ethanolic extract of *O. indicum* bark and catechin showed hydroxyl radical scavenging activity at IC_{50} = 34.20 ± 1.75 µg/mL and 25.85 ± 1.05 µg/mL, respectively. We compared the hydroxyl radical scavenging activity of ethanolic extract of *O. indicum* stem bark with methanolic leaves extract *Citrus aurantium* (Suzuki et al., 2005) and *Ruta graveolens* (Freire et al., 2010). Both plants, *Citrus aurantium* and *Ruta graveolens* are reported as hepatoprotective, with IC_{50} values 160.1 µg/mL and 96.8 µg/mL, respectively. The results significantly designate that the *O. indicum* is capable of protecting deoxyribose in the presence of hydroxyl radicals (Fernando and Soysa, 2014). Therefore, based on the presented results and comparison with similar studies, we can conclude that ethanolic extract of *O. indicum* has a greater potential for scavenging DPPH, hydroxyl, and $ABTS^+$ free radicals.

3.3.2.2. Nitric oxide scavenging activity. Nitric oxide acts as a significant player in numerous inflammatory diseases. The elevation of NO concentration level is noticed in inflammation and other related disease (Malinski, 2007). Biochemically, in aerobic condition nitric oxide reacts with oxygen and produce peroxy-nitrite anion, which act as strong oxidant. The studies showed that nitric oxide does not involve directly in to any interaction with macromolecules of biological system but peroxy-nitrite anion participates in rising some adverse effects like DNA impairment, cell damage and neuronal cell death. Furthermore, the biochemical studies revealed that at physiological pH, sodium nitroprusside interacts with oxygen atom and produces nitrite ions (Malinski, 2007). Recently, these nitrite ions showed diazotization of sulphanilamide, followed by azo-dye formation (Fernando and Soysa, 2014; Malinski, 2007). In our present research, we tested the nitric oxide scavenging activity of ethanolic extract of *O. indicum*. The experiment was based on the production of nitric oxide using Griess reagent. The result was found very promising and showed that the plant extract have tendency to lower the production of NO in a dose-dependent manner. The IC_{50} of extract and standard curcumin were estimated at 136.80 ± 4.20 µg/mL and 23.10 ± 1.10 µg/mL respectively. It was demonstrated that *Atalantia ceylanica* leaves extract have potent activity against liver disease, with IC_{50} = 263.5 ± 28.3 µg/mL against NO radicals production (Fernando and Soysa, 2014). Our stem bark extract of *O. indicum* has greater NO radicals scavenging potential compared to *Atalantia ceylanica* leaves extract.

3.3.2.3. Iron chelation activity. Iron ions are acknowledged for the interchange of less reactive class like lipid peroxides or H_2O_2 to more reactive ones such as peroxyl, alkoxyl, or hydroxyl radicals. The discharge of iron ion via the cellular deterioration can speed up oxidative damage. Therefore, in the FRP assay, the electron-donating potential of any sample is measured and the compounds with higher iron chelating capacity are considered as potent antioxidants (Halliwell, 2009). The measurement of potency is expressed in term of IC_{50} (µg/mL). The tested extract displayed 50% inhibition (IC_{50}) at 44.10 ± 0.25 µg/mL. The reference compound ascorbic acid showed the 50% inhibition (IC_{50}) at 1.19 ± 0.01 µg/mL. The study related to another hepato-protective plant *Atalantia ceylanica* leaves extract reported IC_{50} at 87.70 ± 6.06 µg/mL (Fernando and Soysa, 2014). The comparative analysis showed that ethanolic extract of stem bark of *O. indicum* have higher chelate formation property.

3.3.2.4. Total antioxidant activity. The measurement of total antioxidant capacity of extract/fractions were analyzed by the phosphomolybdenum complex formation. The stem bark extract of *O. indicum* showed the antioxidant capacity equal to 170.70 ± 1.50 AAE/mg extract (Table 4). The result confirmed that the ethanolic stem bark extract of *O. indicum* have significant antioxidant capacity. Therefore, it can act as a key factor in the reduction of oxidative stress and promote the repairing of liver cells.

3.4. β-glucuronidase activity

The plant ethanolic extract was evaluated for β-glucuronidase activity. The assay showed that the tested plant extract have mild to moderate β-glucuronidase enzyme inhibition potency. All the data related with % inhibition and IC_{50} are collected in Table 5 and Fig. 3 Succinctly, at 50 µg/mL concentration the plant extract shows 42.05 ± 1.15% enzyme inhibition. However, increasing the extract

Table 5
β-glucuronidase activity of stem bark of Oroxylum indicum.

Name	Concentration (µg/mL)	% Inhibition [a]	IC_{50} (µg/mL)
Oroxylum indicum	50	42.05 ± 1.15 [b]	174.36
	100	47.01 ± 1.49 [b]	
	200	52.13 ± 4.42	
	400	62.20 ± 1.72 [b]	
	600	71.14 ± 3.06	
silymarin	50	8.18 ± 5.20	222.57
	100	21.93 ± 2.00	
	200	48.24 ± 4.24	
	300	66.26 ± 1.38	
	400	88.12 ± 1.70	

[a] All the values are expressed as mean ± SEM (n = 3).
[b] $p > 0.05$ (significant), with silymarin (Dunnet's *t*-test).

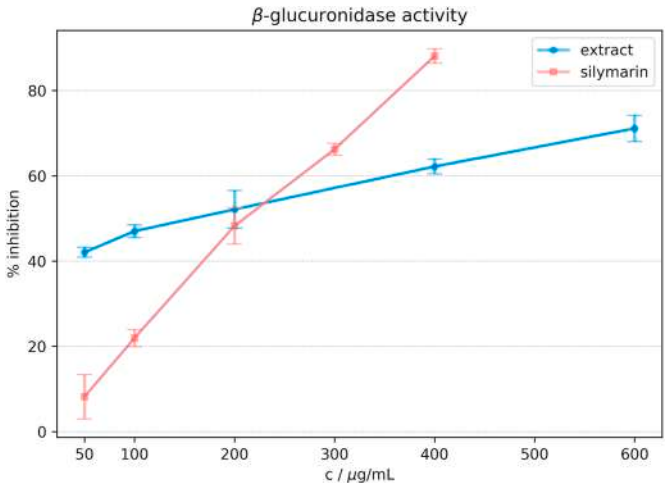

Fig. 3. The β-glucuronidase activity of stem bark of Oroxylum indicum and standard drug silymarin.

dose to 100 µg/mL showed only a slight improvement of the inhibitory response (47.01 ± 1.49%). Further, at 200 µg/mL and 400 µg/mL concentration the percentage inhibition increased from 52.13 ± 4.42 to 62.20 ± 1.72%, respectively. The comparison with the standard drug silymarin revealed that stem bark extract of *O. indicum* exhibits higher activity up to 200 µg/mL concentration. However, at 400 µg/mL concentration, the inhibition potency of the plant extract is found slightly lower as compared to silymarin. Ethanolic extract of *O. indicum* stem bark and silymarin showed IC_{50} at 174.36 µg/mL and 222.57 µg/mL, respectively. In other study, Joshi and Priya in 2007 (Joshi and Sanmuga Priya, 2007), evaluated the β-glucuronidase inhibitor potency of different fractional extracts of *Phyllanthus amarus* leaves. We compared β-glucuronidase inhibition potential of *O. indicum* with the result of *Phyllanthus amarus*. It was found that H_2O and 50% MeOH extracts of leaves of *Phyllanthus amarus* displayed IC_{50} at 139.15 and 218.85 µg/mL, respectively. Results for *O. indium* extract show slightly lower β-glucuronidase inhibitor potency as compared to 50% MeOH extract of leaves of *Phyllanthus amarus*, but are found comparable active as aqueous extract. Individually, *O. indicum* extract does not shows significant β-glucuronidase inhibition potency, but it acts as potent antioxidant. This additional feature makes the plant extract more valuable and can promote in synergizing the liver protective nature. To conclude experimental part, the stem bark of *O. indicum* may be welcomed alternative in the treatment of various liver alignments and complications.

3.5. Computational ADME prognosis and β-glucuronidase activity prediction

The ADME profile has an immense role in drug discovery and development. Whenever any study or selection of drugs is performed, scientists always try to minimize adverse effects of the drugs by optimizing ADME profile. The current part of our work explored ADME profile of major phyto-constituents identified from *O. indicum*. The physicochemical and ADME prognosis results are presented in Table 6. They show that all of the identified phyto-compounds have optimal logP value (less than 5) and low to ideal TPSA value (in the range between 70.67 and 207.35). These two characteristics make all the selected compounds very interesting. Baicalein, chrysin, oroxyline-A, and apigenin completely followed the Lipinski's rule of five. However, the phyto-compounds tetuin and scutellarin shown deviation from Lipinski's rule of five in term of the number of the H donor and acceptor and need to be optimized, if synthetic modifications will be performed in future. All the tested herbo-compounds, except tetuin and scutellarin, show higher rate of GI absorption. However, only chrysin have tendency to cross blood brain barrier and it can produce some adverse psychological response. Therefore, the use of chrysin as single medicament needs great attention or precaution. The combined summary based on GI absorption and BBB permeability study concise that baicalein, oroxyline-A and apigenin are the best choice for provoking the biological response. The metabolism study revealed that compounds have moderate to higher metabolic possibility (score of 0.8412–0.9974) on the site of cytochrome P450-3A4. Whereas, tetuin (score of 0.2170), scutellarin (score of 0.0508), apigenin (score of 0.6838) have minimal metabolic ability on the site of cytochrome P450-2D6. The toxicity predication stated that all the compounds are non- or moderately toxic, with scores within 0.00–0.69 range. Thus, this can propound that the compounds (except than chrysin) are safer and permissible for further study. The computational activity predication for glucosidase inhibition expressed that selected phyto-compounds have mild to moderate potency. It may be that individually these compounds have not any prominent effect, but an extract of whole bark can demonstrate synergistic effect.

3.6. Molecular docking study

Molecular docking simulations were performed with two main goals in mind. First, we wanted to explore the possibility of binding of series of isolated phyto-compounds (Yadav et al., 2013) to the catalytic pocket of the β-glucuronidase. In the case of positive outcome, we are interested in the intermolecular nonbonding interaction network, responsible for successful binding. Results (Table 4 and Fig. 4) are compared relative to the docked structure of the IF6 inhibitor, for which experimentally determined structure is known (PDB code 5G0Q). Although the molecular docking is not the method of choice for the precise evaluation of binding energies, we compare binding energies relative to the IF6 inhibitor, so errors introduced for all complexes are similar. In the crystal structure, IF6 inhibitor is covalently bound via C1 to the enzyme's GLU287 residue in a $^4C_1$ conformation (Wu et al., 2017). In the docked pose, 3, 4, 5, 6 – tetrakis (oxidanyl) cyclohexane – 1 – carboxylic acid moiety occupies the same space in the catalytic pocket and can form the same hydrogen bond pattern (Gln 293, Gly 294, Tyr334) as in the crystal structure. Since it is favorably oriented as in covalently bound complex, we can conclude that the docking identified correct pose. The difference is more pronounced for the 8-azidooctyl tail, which is flexible and has higher conformational space to explore within the pocket.

All studied phyto-compounds have similar binding potential as IF6. Due to a standard error of the docking experiments of

Table 6
Physiochemical properties (ADME) and predicted glucosidase activity score of selected phyto-compounds identified from the stem bark of O. indicum.*

compound	logP	Lip. vio	H don.	H acc.	GI Abs	BBP	P450-3A4	P450-2D6	TPSA	Tox	Ph Score
tetuin	2.52	1	6	10	Low	No	0.8412	0.2170	170.05	0.00	0.1928
scutellarin	3.17	2	7	12	Low	No	0.9846	0.0508	207.35	0.00	0.4005
baicalein	2.60	0	3	5	High	No	0.9974	0.8561	90.90	0.43	0.5230
chrysin	1.80	0	2	4	High	Yes	0.9875	0.7504	70.67	0.69	0.2606
oroxyline-A	1.66	0	2	5	High	No	0.9974	0.7494	79.90	0.42	0.4791
apigenin	1.62	0	3	5	High	No	0.9967	0.6838	90.90	0.47	0.1098

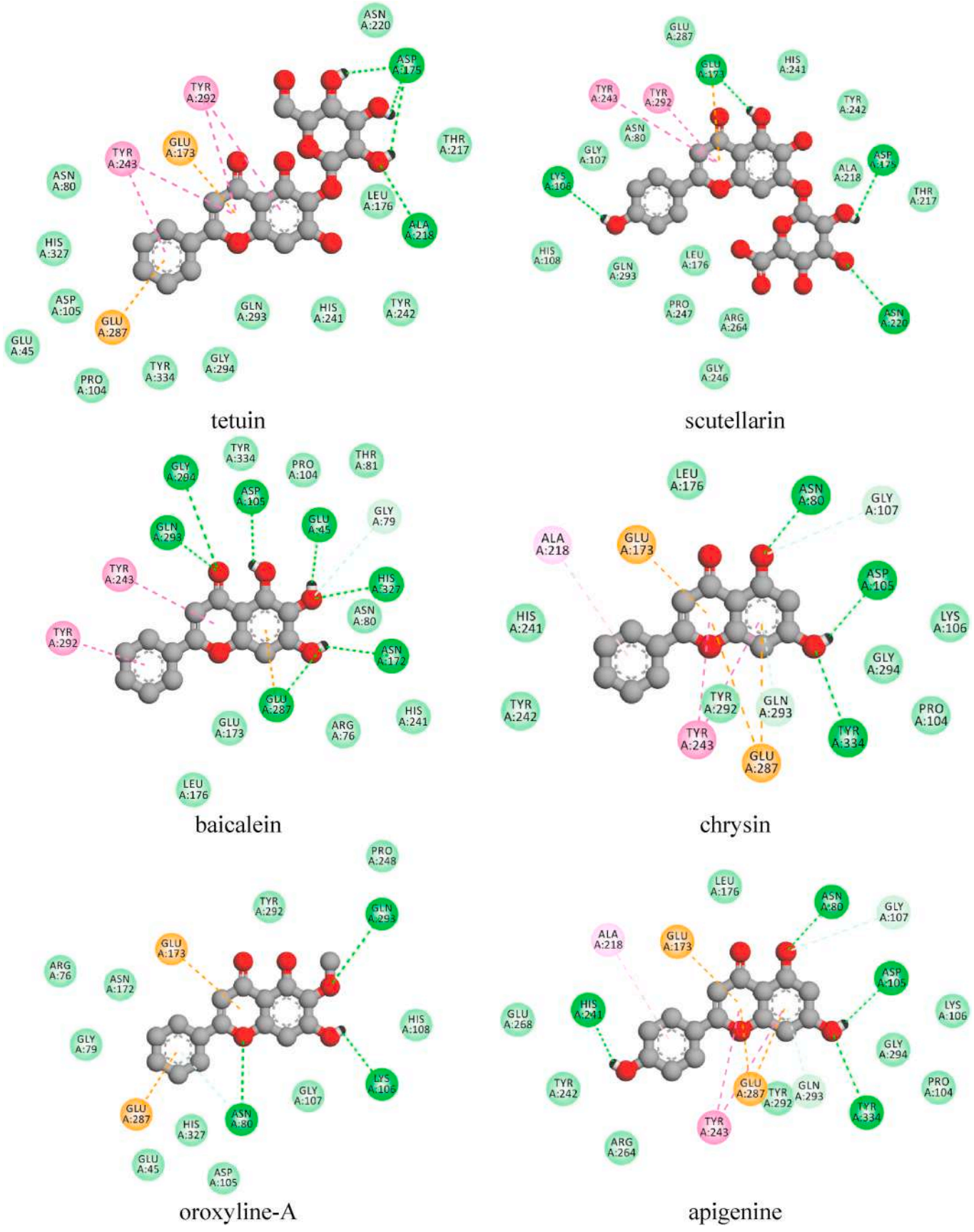

Fig. 4. The interactions patterns between selected phyto-compounds and active site of the β-glucuronidase receptor (PDB: 5G0Q).

2.85 kcal mol^{-1}, (Trott and Olson, 2009). It is hard to pinpoint to a single molecule as a potential hit when docking scores are similar. Nevertheless, scutellarin has the highest potential to bind to the active site of the β-glucuronidase better then reference inhibitor IF6. Tetuin forms four hydrogen bonds with the receptor and the binding energy of tetuin is practically the same as of the IF6 inhibitor that establishes six H-bonds. Three hydroxyl functional groups attached to the pyran ring form strong H-bond, according to the classification made by Rozas (2007). Two out of three OH groups are at the same time H-bond acceptors, with side chain of ASP175 and nitrogen (ALA218) from the peptide bond being the hydrogen donors. On the other hand, scutellarin, a phyto-compound showing the highest potential for binding to the β-glucuronidase, forms only three strong hydrogen bridges and the ligand is in the role of hydrogen donor. It is interesting that its proposed mechanism of action, based on the docked position, would be different from the one of IF6. Since scutellarin is positioned in the narrow groove of the catalytic pocket, completely blocking the access to the enzyme nucleophile GLU287, we expect it will disable the binding of the substrate to the active place. Hopefully, our work will motivate scientific community to investigate the proposed mechanism.

The careful analysis of the non-bonded interaction showed that the common feature of the entire set is the prominent tendency towards formation of the aromatic interactions. The chromene, phenyl ring and its substituent's form a variety of aromatic interaction in different geometrical arrangements. Two kinds of H-aromatic interactions, H-heteroatom and/or H-alkyl, contribute to the overall stability of the complexes of apigenin, chrysin, oroxyline-A, scutellarin and tetuin with the receptor. Additional positive contribution are introduced by parallel offset and perpendicular T-shaped aromatic interactions of the side chains of the residues TYR243 and TYR292 with chromene based moiety of the ligand. From Table 7 it is obvious that the number of the hydrogen bonds and aromatic interaction itself cannot be correlated with the binding energies, but the hydrophobic interactions and the strength of the interactions has to be accounted. This kind of investigation exceeds the scope of the present work.

4. Conclusion

Our results suggest that *Oroxylum indicum* may serve as an exceptional lead for the development of hepatoprotective medicaments. The plant attributed a potent radical scavenging capacity, which provide an additional scope to the study. Furthermore, the ADME study revealed that all the major phyto-constituents of the plant have optimal logP value, GI absorption, blood brain barer permeability, toxicity score, metabolic profile, and total polar surface area (except fewer deviations). The overall ADME study presents that the plant extract can transport through physiological barriers. *In-vitro* activity assay confirms that the plant extract have prominent dose dependent inhibitory response against β-glucuronidase. The docking studies confirmed that selected set of major phyto-compounds have capability to interact with β-glucuronidase proteins. Combining results of this interdisciplinary study, it is justified to suggest the formulation of *Oroxylum indicum* bark to be utilized as natural medicine in the treatment of various liver diseases. In addition, our research elucidates mechanisms of action against hepatic inflammation and is currently being studied in our laboratory to identify active components.

Statistical analysis

The data are expressed as mean ± standard error of mean (SEM) for each group. Statistical analysis was done using GraphPad Prism version 8.0 software.(GraphPad software, 2019).

Table 7
The analysis of the interactions patterns inside the active site of the β-glucuronidase receptor (PDB: 5G0Q) for docked phyto-compounds. See text for the computational details.

compound	H-bond (bond length in Å)	aromatic interactions (bond length in Å)	relative binding energy (kcal/mol)
tetuin	tetrahydro-2H-pyran ring OH···ASP175 (1.72, 1.93, 2.04) tetrahydro-2H-pyran ring OH···ALA218 (2.68*)	chromene···GLU173 (3.62) chromene···TYR234 (4.81) chromene···TYR292 (5.07, 5.63) phenyl···GLU287 (3.51) phenyl···TYR243 (5.51)	−0.01
scutellarin	phenol···LYS106 (1.97) chromene OH···GLU173 (2.10) 1 ring OH···ASP175(2.20) 1 ring OH···ASN220(2.81*)	chromene···TYR292 (5.11) chromene···TYR243 (5.22)	−2.23
baicalein	chromene C═O···GLY294 (3.15*) chromene C═O···GLN293 (3.08*) chromene OH···ASP105 (2.07) chromene OH···HIS327 (3.03*) chromene OH···ASN172 (2.20) chromene OH···GLU45 (1.70) chromene OH···GLU287 (2.28)	phenyl···TYR292 (3.74) chromene···TYR243 (4.90)	−0.03
chrysin	chromene OH···TYR334 (2.97* chromene OH···ASP105 (2.29) chromene OH···ASN80 (2.92*)	chromene···GLN293 (3.68) chromene···GLU173 (3.46) chromene···GLU287 (4.73, 4.91) chromene···TYR243 (4.89, 5.35) phenyl···ALA218 (5.26)	−0.47
oroxyline-A	chromene O···ASN80 (3.10*) chromene OH···LYS106 (2.15) chromene -*O*-···GLN293 (3.10*)	phenyl···GLU287 (2.85) chromene···GLU173 (3.76)	+0.03
apigenine	phenyl OH···TYR243 (2.24) phenyl OH···HIS241 (2.43) 2ring OH···ASN80 (2.93*) 2ring OH···TYR334 (2.99*) 2ring OH···ASP105 (2.31)	chromene···GLU173 (3.45) chromene···GLU287 (4.74, 4.93) chromene···TYR243 (4.91, 5.38) phenyl···ALA218 (5.28)	−0.74
IF6	OH···ASN80 (1.95, 2.96*) OH···GLU45 (1.87) C = O···ASP105 (1.94) C = O(OH)···GLN293 (2.56) (C═O)OH···ASP8105 (1.94) C = O··· TYR334 (2.14) C = O···GLY294 (2.73*)	–	0.00

Credit author contribution statement

Prateek Pathak: performed the extraction. **Jurica Novak:** performed computational study. **Vladislav Naumovich:** performed literature search and structural geometry optimization for ADME studies. **Maria Grishina:** Resources, Supervision, Funding acquisition. **Acharya Balkrishna:** Supervision. **Niti Sharma:** Supervision. **Vinay Sharma:** Supervision. **Vladimir Potemkin:** Supervision. **Amita Verma:** Supervision.

Declaration of competing interest

The authors have no conflict of interest.

Acknowledgments

The work was supported by Act 211 Government of the Russian Federation, contract 02. A03.21.0011 and Ministry of Science and Higher Education of Russia (Grant FENU-2020-0019). The authors NS and VS also acknowledged Dr. Nirupama Trehanpati, Institute of Liver and Biliary Sciences, New Delhi for her valuable help and support.

Appendix A. Supplementary data

Supplementary data to this article can be found online at https://doi.org/10.1016/j.bcab.2020.101804.

References

API, 2016. The Ayurvedic Pharmacopoeia of India. 1st, third ed ed. Controller of Publications, Ministry of Health and Family Welfare, Government of India, New Delhi.

Atara, A., R, M., Cr, H., Pandya, P., Shukla, V., 2014. Pharmacognostical and physicochemical evaluation of Chitraka haritaki avaleha: A compound ayurvedic formulation. Int. J. Res. Ayurveda Pharm. 5, 274–279. https://doi.org/10.7897/2277-4343.05356.

Bansal, P., Paul, P., Nayak, P.G., Pannakal, S.T., Zou, J., Laatsch, H., Priyadarsini, K.I., Unnikrishnan, M.K., 2011. Phenolic compounds isolated from Pilea microphylla prevent radiation-induced cellular DNA damage. Acta Pharm. Sin. B 1, 226–235. https://doi.org/10.1016/j.apsb.2011.10.006.

Benković, G., Rimac, H., Maleš, Ž., Tomić, S., Lončar, Z., Bojić, M., 2019. Characterization of O-demethylations and aromatic hydroxylations mediated by cytochromes P450 in the metabolism of flavonoid aglycons. Croat. Chem. Acta 92, 115–123. https://doi.org/10.5562/cca3528.

Berman, H.M., 2000. The protein Data Bank. Nucleic Acids Res. 28, 235–242. https://doi.org/10.1093/nar/28.1.235.

Besada, A., 1987. A facile and sensitive spectrophotometric determination of ascorbic acid. Talanta 34, 731–732. https://doi.org/10.1016/0039-9140(87)80229-1.

Byass, P., 2014. The global burden of liver disease: A challenge for methods and for public health. BMC Med. 12, 159. https://doi.org/10.1186/s12916-014-0159-5.

Chaudhary, S., Chandrashekar, K.S., Pai, K.S.R., Setty, M.M., Devkar, R.A., Reddy, N.D., Shoja, M.H., 2015. Evaluation of antioxidant and anticancer activity of extract and fractions of Nardostachys jatamansi DC in breast carcinoma. BMC Compl. Alternative Med. 15, 50. https://doi.org/10.1186/s12906-015-0563-1.

Chemaxon Group, 2011. Marvin Sketch 5.5.0.1.

Creighton, H.B., Purvis, M.J., Collier, D.C., Walls, D., 1965. Laboratory techniques in botany. In: The Quarterly Review of Biology. https://doi.org/10.1086/404580.

Daina, A., Michielin, O., Zoete, V., 2017. SwissADME: A free web tool to evaluate pharmacokinetics, drug-likeness and medicinal chemistry friendliness of small molecules. Sci. Rep. 7, 1–17. https://doi.org/10.1038/srep42717.

Di Bisceglie, A.M., 2009. Hepatitis B and hepatocellular carcinoma. Hepatology 49, S56–S60. https://doi.org/10.1002/hep.22962.

Dinda, B., SilSarma, I., Dinda, M., Rudrapaul, P., 2015. Oroxylum indicum (L.) Kurz, an important Asian traditional medicine: from traditional uses to scientific data for its commercial exploitation. J. Ethnopharmacol. 161, 255–278. https://doi.org/10.1016/j.jep.2014.12.027.

Dixit, N., Baboota, S., Kohli, K., Ahmad, S., Ali, J., 2007. Silymarin: a review of pharmacological aspects and bioavailability enhancement approaches. Indian J. Pharmacol. 39, 172. https://doi.org/10.4103/0253-7613.36534.

Dutton, G.J., 1980. Glucuronidation of Drugs and Other Compounds. first ed. CRC Press, BocaRaton, FL.

Evans, W.C., 1997. Trease and Evan's Pharmacognosy. fourteenth ed. WB Suunders Company, A division of Harcourt brace and company, London, UK.

Fernando, C.D., Soysa, P., 2014. Total phenolic, flavonoid contents, in-vitro antioxidant activities and hepatoprotective effect of aqueous leaf extract of Atalantia ceylanica. BMC Compl. Alternative Med. 14, 2–8 395. https://doi.org/10.1186/1472-6882-14-395.

Fontana, M., Mosca, L., Rosei, M.A., 2001. Interaction of enkephalins with oxyradicals11Abbreviations: ABAP, 2,2′-azobis(2-amidinopropane); dopa, dihydroxyphenyl-alanine; H2O2, hydrogen peroxide; leu-enk, leu-enkephalin; met-enk, met-enkephalin; LOOH, linoleic acid 13-hydroperoxide; NBT, nitro blu. Biochem. Pharmacol. 61, 1253–1257. https://doi.org/10.1016/S0006-2952(01)00565-2.

Freire, R., Borba, H., Coelho, C., 2010. Ruta graveolens L. toxicity in Vampirolepis nana infected mice. Indian J. Pharmacol. 42, 345. https://doi.org/10.4103/0253-7613.71898.

Garratt, D.C., 1976. The Quantitative Analysis of Drugs. first ed. Springer US, Boston, MA. https://doi.org/10.1007/978-1-4613-3380-7.

Graaf, M., Boven, E., Scheeren, H., Haisma, H., Pinedo, H., 2002. Beta-glucuronidase-mediated drug release. Curr. Pharmaceut. Des. 8, 1391–1403. https://doi.org/10.2174/1381612023394485.

GraphPad software, 2019. GraphPad Prism Version 8.00 for Windows.

Halliwell, B., 2009. The wanderings of a free radical. Free Radic. Biol. Med. 46, 531–542. https://doi.org/10.1016/j.freeradbiomed.2008.11.008.

Hazra, B., Biswas, S., Mandal, N., 2008. Antioxidant and free radical scavenging activity of Spondias pinnata. BMC Compl. Alternative Med. 8, 63. https://doi.org/10.1186/1472-6882-8-63.

Hussain, T., Tan, B., Yin, Y., Blachier, F., Tossou, M.C.B., Rahu, N., 2016. Oxidative stress and inflammation: What polyphenols can do for us?. Oxid. Med. Cell. Longev. 1–9. https://doi.org/10.1155/2016/7432797.

IP, 1996. Indian Pharmacopoeia, fourth ed. The Controller of Publications, Ministry of Health and Family Welfare, Government of India, New Delhi, India.

Joshi, C.S., Sanmuga Priya, E., 2007. β-Glucuronidase inhibitory effect of phenolic constituents from Phyllanthus amarus. Pharm. Biol. 45, 363–365. https://doi.org/10.1080/13880200701214706.

Khandelwal, K.R., 2004. Practical Pharmacognosy Techniques and Experiments. twelfth ed. Nirali Prakashan, Pune, India.

Kim, D.H., Jin, Y.H., Park, J.B., Kobashi, K., 1994. Silymarin and its components are inhibitors of beta-glucuronidase. Biol. Pharm. Bull. 17, 443–445. https://doi.org/10.1248/bpb.17.443.

Kshirsagar, A.D., Mohite, R., Aggrawal, A.S., Suralkar, U.R., 2011. Hepatoprotective medicinal plants of Ayurveda – a review. Asian J. Pharmaceut. Clin. Res. 4, 1–8.

Kunchandy, E., Rao, M.N.A., 1990. Oxygen radical scavenging activity of curcumin. Int. J. Pharm. 58, 237–240. https://doi.org/10.1016/0378-5173(90)90201-E.

Lim, J.G., Park, H., Yoon, K.S., 2020. Analysis of saponin composition and comparison of the antioxidant activity of various parts of the quinoa plant (Chenopodium quinoa Willd.). Food Sci. Nutr. 8, 694–702. https://doi.org/10.1002/fsn3.1358.

Lipinski, C.A., 2004. Lead- and drug-like compounds: the rule-of-five revolution. Drug Discov. Today Technol. 1, 337–341. https://doi.org/10.1016/j.ddtec.2004.11.007.

Liu, J., Lu, J., Wen, X., Kan, J., Jin, C., 2015. Antioxidant and protective effect of inulin and catechin grafted inulin against CCl4-induced liver injury. Int. J. Biol. Macromol. 72, 1479–1484. https://doi.org/10.1016/j.ijbiomac.2014.09.066.

Makkar, H.P.S., Siddhuraju, P., Becker, K., 2007. Plant secondary metabolites. In: Methods in Molecular Biology™. Humana Press, Totowa, NJ. https://doi.org/10.1007/978-1-59745-425-4.

Malinski, T., 2007. Nitric oxide and nitroxidative stress in alzheimer's disease. J. Alzheim. Dis. 11, 207–218. https://doi.org/10.3233/JAD-2007-11208.

Mishra, J., Yousuf, A., Singh, R.D., 2009. Phytochemical investigation and in-vitro antioxidant potential of leaves of Murraya koenigii Plant material Evaluation of phytochemical constituents it is the presence of a wide variety of phytochemicals. Int. J. Integr. Biol. 7, 171–174.

Mohapatra, S.S., Roy, R.K., Mohan, P., Upadhyaya, T.N., Sarma, J., 2018. Phytochemical analysis and hepatoprotective effect of hydroethanolic extract of stem bark of Oroxylum indicum. Int. J. Curr. Microbiol. Appl. Sci. 7, 1000–1006. https://doi.org/10.20546/ijcmas.2018.701.120.

Morris, G.M., Huey, R., Lindstrom, W., Sanner, M.F., Belew, R.K., Goodsell, D.S., Olson, A.J., 2009. AutoDock4 and AutoDockTools 4: Automated docking with selective receptor flexibility. J. Comput. Chem. 30, 2785–2791. https://doi.org/10.1002/jcc.21256.

O'Boyle, N.M., Banck, M., James, C.A., Morley, C., Vandermeersch, T., Hutchison, G.R., 2011. Open Babel: An open chemical toolbox. J. Cheminf. 3. https://doi.org/10.1186/1758-2946-3-33.

Pettersen, E.F., Goddard, T.D., Huang, C.C., Couch, G.S., Greenblatt, D.M., Meng, E.C., Ferrin, T.E., 2004. UCSF Chimera--a visualization system for exploratory research and analysis. J. Comput. Chem. 25, 1605–1612. https://doi.org/10.1002/jcc.20084.

Pineda, E.P., Goldbarg, J.A., Banks, B.M., Rutenburg, A.M., 1959. The significance of serum β-glucuronidase activity in patients with liver disease. Gastroenterology 36, 202–213. https://doi.org/10.1016/S0016-5085(59)80004-4.

Potemkin, A.V., Grishina, M.A., Potemkin, V.A., 2017. Grid-based continual analysis of molecular interior for drug discovery, QSAR and QSPR. Curr. Drug Discov. Technol. 14, 181–205. https://doi.org/10.2174/1570163814666170207144018.

Potemkin, V., Grishina, M., 2018. Grid-based technologies for in silico screening and drug design. Curr. Med. Chem. 25, 3526–3537. https://doi.org/10.2174/0929867325666180309112454.

Potemkin, V., Grishina, M., 2008. Principles for 3D/4D QSAR classification of drugs. Drug Discov. Today 13, 952–959. https://doi.org/10.1016/j.drudis.2008.07.006.

Pradhan, S.C., Girish, C., 2006. Hepatoprotective herbal drug, silymarin from experimental pharmacology to clinical medicine. Indian J. Med. Res. 124, 491–504.

Prieto, P., Pineda, M., Aguilar, M., 1999. Spectrophotometric quantitation of antioxidant capacity through the formation of a phosphomolybdenum complex: specific application to the determination of vitamin E. Anal. Biochem. 269, 337–341. https://doi.org/10.1006/abio.1999.4019.

Rozas, I., 2007. On the nature of hydrogen bonds: An overview on computational studies and a word about patterns. Phys. Chem. Chem. Phys. 9, 2782. https://doi.org/10.1039/b618225a.

Seitz, H.K., Stickel, F., 2006. Risk factors and mechanisms of hepatocarcinogenesis with special emphasis on alcohol and oxidative stress. Biol. Chem. 387, 349–360. https://doi.org/10.1515/BC.2006.047.

Siddhuraju, P., Becker, K., 2007. The antioxidant and free radical scavenging activities of processed cowpea (Vigna unguiculata (L.) Walp.) seed extracts. Food Chem. 101, 10–19. https://doi.org/10.1016/j.foodchem.2006.01.004.

Singh, D., Singh, M., Yadav, E., Falls, N., Komal, U., Dangi, D.S., Kumar, V., Verma, A., 2018. Amelioration of diethylnitrosamine (DEN)-induced hepatocellular carcinogenesis in animal models via knockdown oxidative stress and proinflammatory markers by Madhuca longifolia embedded silver nanoparticles. RSC Adv. 8, 6940–6953. https://doi.org/10.1039/C7RA12775H.

Stanković, N., Mihajilov-Krstev, T., Zlatković, B., Stankov-Jovanović, V., Mitić, V., Jović, J., Čomić, L., Kocić, B., Bernstein, N., 2016. Antibacterial and antioxidant activity of traditional medicinal plants from the balkan peninsula. NJAS - Wageningen J. Life Sci. 78, 21–28. https://doi.org/10.1016/j.njas.2015.12.006.

Suzuki, M., Sasaki, K., Yoshizaki, F., Fujisawa, M., Oguchi, K., Cyong, J.-C., 2005. Anti-hepatitis C virus effect of Citrus unshiu peel and its active ingredient nobiletin. Am. J. Chin. Med. 33, 87–94. https://doi.org/10.1142/S0192415X05002680.

Tachakittirungrod, S., Okonogi, S., Chowwanapoonpohn, S., 2007. Study on antioxidant activity of certain plants in Thailand: mechanism of antioxidant action of guava leaf extract. Food Chem. 103, 381–388. https://doi.org/10.1016/j.foodchem.2006.07.034.

Tenpe, C.R., Aman, U., Sushil, B., Yeole, P.G., 2009. In vitro antioxidant and preliminary hepatoprotective activity of Oroxylum indicum vent leaf extracts. Pharmacologyonline 1, 35–43.

Teshima, K.I., Kaneko, T., Ohtani, K., Kasai, R., Lhieochaiphant, S., Yamasaki, K., 1996. Phenylethanoids and cyclohexylethanoids from Oroxylum indicum. Nat. Med. 50, 307–308.

Tripathi, K.D., 2013. Essentials of Medical Pharmacology. seventh ed. Jaypee Brothers Medical Publishes (P) Ltd, New Delhi, India.

Troll, W., 1985. The role of oxygen radicals as a possible mechanism of tumor promotion. Annu. Rev. Pharmacol. Toxicol. 25, 509–528. https://doi.org/10.1146/annurev.pharmtox.25.1.509.

Trott, O., Olson, A.J., 2009. AutoDock Vina: improving the speed and accuracy of docking with a new scoring function, efficient optimization, and multithreading. J. Comput Chem. 31 (2), 455–461. https://doi.org/10.1002/jcc.21334.

Vanden Berghe, W., 2012. Epigenetic impact of dietary polyphenols in cancer chemoprevention: Lifelong remodeling of our epigenomes. Pharmacol. Res. 65, 565–576. https://doi.org/10.1016/j.phrs.2012.03.007.

Vikas, B., Akhil, B.S., Remani, P., Sujathan, K., 2017. Free radical scavenging properties of Annona squamosa. Asian Pac. J. Cancer Prev. APJCP 18, 2725–2731. https://doi.org/10.22034/APJCP.2017.18.10.2725.

Walaszek, Z., Hanausek-walaszek, M., Webb, T.E., 1984. Inhibition of 7,12-dimethylbenzanthracene-induced rat mammary tumorigenesis by 2,5-di-o-acetyl-d-glucaro-1, 4:6,3-dilactone, an in vivo β-glucuronidase inhibitor. Carcinogenesis 5, 767–772. https://doi.org/10.1093/carcin/5.6.767.

Wu, L., Jiang, J., Jin, Y., Kallemeijn, W.W., Kuo, C.-L., Artola, M., Dai, W., van Elk, C., van Eijk, M., van der Marel, G.A., Codée, J.D.C., Florea, B.I., Aerts, J.M.F.G., Overkleeft, H.S., Davies, G.J., 2017. Activity-based probes for functional interrogation of retaining β-glucuronidases. Nat. Chem. Biol. 13, 867–873. https://doi.org/10.1038/nchembio.2395.

Yadav, A.K., Manika, N., Bagchi, G.D., Gupta, M.M., 2013. Simultaneous determination of flavonoids in Oroxylum indicum by RP-HPLC. Med. Chem. Res. 22, 2222–2227. https://doi.org/10.1007/s00044-012-0214-8.

Yan, R.Y., Cao, Y.Y., Chen, C.Y., Dai, H.Q., Yu, S.X., Wei, J.L., Li, H., Yang, B., 2011. Antioxidant flavonoids from the seed of Oroxylum indicum. Fitoterapia 82, 841–848. https://doi.org/10.1016/j.fitote.2011.04.006.

Zhishen, J., Mengcheng, T., Jianming, W., 1999. The determination of flavonoid contents in mulberry and their scavenging effects on superoxide radicals. Food Chem. 64, 555–559. https://doi.org/10.1016/S0308-8146(98)00102-2.

Journal of Ethnopharmacology 235 (2019) 361–374

Contents lists available at ScienceDirect

Journal of Ethnopharmacology

journal homepage: www.elsevier.com/locate/jethpharm

Evaluation of polyherbal ayurvedic formulation 'Peedantak Vati' for anti-inflammatory and analgesic properties

Acharya Balkrishna, Ravikant Ranjan*, Sachin S. Sakat, Vinay K. Sharma, Ravikant Shukla, Khemraj Joshi, Raviraj Devkar, Niti Sharma, Sonia Saklani, Prateek Pathak, Pratima Kumari, Veena R. Agarwal

Drug Discovery and Development Division, Patanjali Research Institute, Haridwar, India

ARTICLE INFO

Keywords:
Peedantak Vati
Inflammation
Analgesic
Edema
Nitric oxide
RAW264.7
THP-1
HPLC
HPTLC
LC-MS/MS

ABSTRACT

Ethnopharmacological relevance: Peedantak Vati (PV) is a polyherbal ayurvedic formulation, which is regularly prescribed by the ayurvedic practitioner for the inflammatory disorders and joints pain in India. It is composed of 23 different herbs and minerals, described in ayurvedic text for their anti-inflammatory and analgesic properties.

Aim of the study: To investigate anti-inflammatory and anti-nociceptive potential of 'Peedantak Vati' using in *vitro* and *in vivo* methods.

Materials and methods: In-vitro anti-inflammatory activity of PV was studied by estimating nitric oxide (NO) and LPS-induced pro-inflammatory cytokines IL-6 and TNF-α, using murine macrophage RAW264.7 and human monocyte THP-1 cell lines. PV's anti-inflammatory potential was studied *in vivo* using carrageenan-induced rat paw edema model. Similarly, anti-nociceptive property of PV was evaluated using hot plate, tail flick, formalin and writhing tests on CD-1 mice. Phytochemical profiling of hydro-alcoholic extract of PV was done using HPLC and HPTLC techniques to identify different marker compounds. These identified marker compounds were confirmed using LC-MS/MS analysis.

Results: In vitro results strongly suggest that, PV significantly ($p < 0.001$) inhibited NO release and LPS-stimulated pro-inflammatory cytokines IL-6 and TNF-α, in murine RAW264.7 and human THP-1 cells. Further, PV demonstrated significant ($p < 0.05$) anti-inflammatory activity at different time points after carrageenan injection with maximum effect at 2 h (40.4 ± 5.2% at 400 mg/kg). Similarly, PV significantly ($p < 0.05$) decreased nociceptive pain, studied using hot plate, tail flick, formalin and writhing tests. Moreover, HPLC and HPTLC methods were developed for the standardization of PV. Five marker phytocompounds viz. rutin, caffeic acid, colchicine, withaferin A and curcumin were identified and quantified by HPLC and HPTLC methods. The presence of these phytoconstituents was confirmed by LC-MS/MS analysis.

Conclusion: The findings of the study strongly suggest that, the polyherbal ayurvedic formulation 'Peedantak Vati' possesses remarkable anti-inflammatory and analgesic property, providing potent alternative for currently available allopathic medicines such as non steroidal anti-inflammatory drugs (NSAIDs).

Abbreviations: NO, Nitric oxide; TNF-α, Tumor necrosis factor-α; IL-6, Interleukins-6; IL-1β, Interleukins-1beta; PGs, Prostaglandins; COX, Cyclooxygenase; LPS, lipopolysaccharides; ELISA, Enzyme-linked immunosorbent assay; MTT, (3-(4,5-Dimethylthiazol-2-yl)-2,5-Diphenyltetrazolium Bromide); DMEM, Dulbecco's Modified Eagle Medium; RPMI, Roswell Park Memorial Institute 1640 Medium; FBS, Fetal Bovine Serum; PMA, Phorbol 12-myristate 13-acetate; NSAIDs, Non steroidal anti-inflammatory drugs; PV, Peedantak Vati; CPCSEA, Committee for the Purpose of Control And Supervision of Experiments on Animals; IAEC, Institutional Animal Ethical Committee; AYUSH, Ministry of Ayurveda, Yoga & Naturopathy, Unani, Siddha and Homoeopathy; ANOVA, A one-way analysis of variance; TED, Therapeutic equivalent dose; HD, High dose; MPE, maximum possible effect; LT, Latency time; INDO, Indomethacin; NC, normal control; HPLC, High Performance Liquid Chromatography; LOD, Limit of detections; LOQ, Limit of quantification; HPTLC, High-Performance Thin-Layer Chromatography, Liquid chromatography–mass spectrometry; API, The Ayurvedic Pharmacopoeia of India; AFI, Ayurvedic Formulary of India; LC-MS/MS, Liquid chromatography-tandem mass spectrometry; ICP-MS, Inductively coupled plasma mass spectrometry

* Correspondence to: Patanjali Research Institute, Patanjali Research Foundation, Delhi-Haridwar National Highway, Haridwar 249405, India.
E-mail address: ravikant.ranjan@prft.co.in (R. Ranjan).

https://doi.org/10.1016/j.jep.2019.01.028
Received 27 September 2017; Received in revised form 19 August 2018; Accepted 26 January 2019
Available online 28 January 2019
0378-8741/

1. Introduction

Inflammation is one of the first protective responses of immune system to infection or cellular damages. This response can be against foreign pathogens, irritation as well as disorder or diseases like autoimmune or neurodegenerative diseases. It is a self-defense mechanism, characterized by redness, pain, swelling and a sensation of heat. The inflammatory responses play an important role in host survival although it can also lead to pathogenesis of many diseases such as cancer, rheumatoid arthritis, cardiovascular dysfunction (Grivennikov et al., 2010; Skeoch and Bruce, 2015; Libby, 2006) etc.

Inflammation is the complex biological response of vascular tissue to harmful stimuli including pathogens, irritants, or damage cells, which leads to influx of neutrophils resulting in activation of macrophages (Schett et al., 2013; MacMicking et al., 1997). This causes release of various inflammatory mediators such as NO, pro-inflammatory cytokines including TNF-α, interleukins (IL-6, IL-1β), prostaglandins (PGs) (MacMicking et al., 1997; Zelová and Hošek, 2013; Tanaka et al., 2014) etc. NO is a central inflammatory mediator which is produced by nitric oxide synthetase from L-arginine in response to inflammatory stimuli. Increased NO level is one of the well known causative agent of inflammatory disorders such as rheumatoid arthritis (RA) and ulcerative colitis (Wright et al., 2014). NO and PGs are widely known to act as secondary mediators of pro-inflammatory cytokines TNF-α and IL-6 (Skelly et al., 2013).

In most cases pain is associated with inflammation, regardless of cause behind inflammation. Now it is well understood and defined mechanism supported by scientific evidences that relief from pain is caused by alleviation of inflammation (Cooper et al., 2017). Most of anti-inflammatory drugs, particularly NSAIDs primarily act by inhibiting the production of PGs, thus interfering with inflammatory cascade (Ricciotti and FitzGerald, 2011). However, regular use of these medicine causes severe side effects including inflammation of gastrointestinal tract, renal failure and liver toxicity (Harirforoosh et al., 2013).

Due to these severe side effects, in recent times interest in traditional medicine is rising. In this scenario, use of plant derived products to treat inflammation and related condition becomes viable and valid approach. It has been observed that, isolated molecule(s) from the plant fail to illicit desired therapeutic effect in comparison to whole plant extract (Kunnumakkara et al., 2017). Moreover, according to the Indian traditional medicine system, a combination of substances such as polyherbal formulations is used to enhance the desired activity and eliminate unwanted side effects (Kono et al., 2015; Rasoanaivo et al., 2011; Zhou et al., 2016).

Peedantak Vati is one of the polyherbal ayurvedic formulation used by Indian population to treat pain and inflammatory disorders. The traditional name 'Peedantak' is composed of two words; 'peeda' (pain) and 'antak' (ending), altogether 'pain ending'. The formulation is composed of 23 different plants and minerals as shown in Table 1. All of its components have detailed individually in the literature of Indian Traditional Medicine such as Charak Samhita (Trikamji, 2007), The Ayurvedic Pharmacopoeia of India et al. (2008), The Unani Pharmacopoeia of India (2007) and The Ayurvedic Formulary of India (2003) about its anti-inflammatory and pain relieving effects. Furthermore, all these plants viz. *Commiphora wightii* (Arn.) Bhand (Shishodia et al., 2008), *Colchicum luteum* Baker (Nair et al., 2012), *Withania* somnifera (L.) Dunal (Gupta and Singh, 2014; Orrù et al., 2016), *Strychnos nux vomica* L. (Chen et al., 2012), *Cyperus rotundus* L. (Dang et al., 2011), *Pluchea lanceolata* (DC.) C.B. Clarke (Srivastava et al., 2014), *Vitex negundo* L. (Dharmasiri et al., 2003), *Boerhavia diffusa* L. (Bairwa and Jachak, 2015; Hiruma-Lima et al., 2000), *Trigonella foenum-graecum* L. (Bae et al., 2012), *Operculina turpethum* (L.) Silva Manso (Aggarwal et al., 2011), *Asparagus racemosus* Willd. (Tiwari et al., 2017), *Cissus quadrangularis* L. (Bhujade et al., 2012), *Curcuma longa* L. (Lee et al., 2013), *Zingiber officinale* Roscoe (Ojewole, 2006), *Picrorhiza kurroa* Royle ex Benth (Kumar et al., 2016), *Trachyspermum ammi* (L.) Sprague (Bairwa et al., 2012), *Tinospora cordifolia* (Willd) Miers (Patgiri et al., 2014), Dashmool (Grampurohit et al., 1992; Gupta et al., 1089) have been reported for the anti-inflammatory and/or analgesic potential and/or their beneficial effects on inflammatory disorders in peer reviewed journals.

Though PV formulation has been prescribed by ayurvedic practitioner for the treatment of inflammatory disorders, its scientific validation for anti-inflammatory and anti-nociceptive effect has never been explored so far. Keeping this in view, present study was designed to explore PV's anti-inflammatory and anti-nociceptive effects using *in vitro* and *in vivo* methods. In addition, chemical fingerprinting of PV was done using different chromatographic techniques viz. HPLC, HPTLC and LC-MS/MS.

2. Materials and methods

2.1. Chemicals and reagents

Cell culture reagents viz. DMEM, RPMI, FBS, antibiotic/antimycotic and their supplements were purchased from Gibco, USA. Bacterial origin endotoxin LPS (O111:B4) Griess reagent, MTT, PMA, λ-carrageenan, Indomethacin and standard compounds (> 95% by HPLC) such as berberine, rutin, caffeic acid, colchicine, cinnamic acid, quercetin, withaferin A, withanolide A and as curcumin were purchased from Sigma-Aldrich (St. Louis, MO, USA). ELISA reagents and kits (TNF-α, IL-6) were purchased from BD Biosciences. Tramadol hydrochloride (Tramacad, Cadila Pharmaceuticals) injection and sodium chloride injection I.P. 0.9% w/v (Infutec Healthcare Ltd) were procured from the local market. Analytical grade toluene, ethyl acetate, formic acid, chloroform, ethanol, diethyl ether, HPLC grade acetonitrile, methanol, and concentrated sulphuric acid, concentrated nitric acid were purchased from Merck India Ltd. Precoated TLC aluminum sheets silica gel $60F_{254}$ (10 × 10 cm, 0.2 mm thick) were obtained from E. Merck Ltd, India. All other chemicals and reagents were of the highest commercial grade.

2.2. Preparation of extract

About 20 g of PV formulation (Batch no. PTV203) was powdered and refluxed for 6 h at 88 °C in 300 mL of 70% ethanol. The solution was filtered through Whatman filter paper no 41 to remove the particulate matter and filtrate was evaporated dry at 45 °C under reduced pressure in rotary film evaporator. The final dried sample was weighed (3.12 g; extraction yield: 15.60% w/w) and stored under vacuum in the desiccators for further *in vitro* experiments and chromatographic method development.

The powdered form of PV was suspended as in 0.25% Na-CMC, triturated to form uniform suspension and used for the *in vivo* experiments.

2.3. Cell culture for in vitro experiments

RAW264.7 and THP-1 cell lines were obtained from the National Centre For Cell Science (NCCS), India and cultured in Dulbecco's Modified Eagle's Medium (DMEM) and RPMI1640. Media was supplemented with 10% heat-inactivated fetal bovine serum (FBS), in presence of 100 U/mL concentrations of penicillin-streptomycin, 1 mM sodium pyruvate and 4 mM L-glutamine. Cells were grown at 37 °C in a 5% CO_2/air environment, following standard protocol.

2.3.1. MTT assay

MTT assay was performed according to protocol described earlier (Mosmann, 1983) with minor modifications. Briefly, cells were seeded in 96 well culture plates at density of 1×10^6/mL and treated with different concentrations of PV. After overnight treatment, 10 µL of MTT

Table 1
Ingredients of Peedantak Vati.

S. no.	Common name	English name	Scientific name	Part(s) used	Quantity (mg)	Voucher specimen number	Reference(s)* for traditional use (anti-inflammatory &/or pain relief)
1	Mukul Guggulu	Gum guggul	*Commiphora wightii* (Arn.) Bhand.	Exudates	75	NISCAIR/RHMD/CONSULT/2017/3082–31–31	API, P-I, Vol-I, p43
2	Suranjan meethi	Colchicicum	*Colchicum luteum* Baker	Rhizomes	36	QCD1/RM/12–17/3182	UPI, P-II, Vol-III
3	Ashwagandha	Winter cherry	*Withania somnifera* (L.) Dunal	Roots	35	NISCAIR/RHMD/CONSULT/2017/3034–61–5	API, P-I, Vol-I, p15
4	Kuchla shudh	Poison nut	*Strychnos nux vomica* L.	Seeds	20	NISCAIR/RHMD/CONSULT/2017/3034–61–35	API, P-I, Vol-IV, p140
5	Nagarmotha	Nutgrass	*Cyperus rotundus* L.	Roots	20	NISCAIR/RHMD/CONSULT/2017/3034–61–43	API, P-I, Vol-III, p129
6	Rasana	Rasana	*Pluchea lanceolata* (DC.) C.B.Clarke	Leaves	20	NISCAIR/RHMD/CONSULT/2017/3034–61–50	API, P-I, Vol-III, p162
7	Nirgundi	Five leaved Chaste Tree	*Vitex negundo* L.	Leaves & roots	20 & 71.6	NISCAIR/RHMD/CONSULT/2017/3034–61–45	API, P-I, Vol-IV, p76
8	Punarnava	Hog weed	*Boerhavia diffusa* L.	Roots	20	NISCAIR/RHMD/CONSULT/2017/3034–61–48	API, P-I, Vol-I, p95
9	Methi	Fenugreek	*Trigonella foenum-graecum* L.	Seeds	20	NISCAIR/RHMD/CONSULT/2017/3034–61–42	API, P-I, Vol-II, p107
10	Nishodh	Indian jalap	*Operculina turpethum* (L.) Silva Manso	Roots	20	QCD1/RM/11–17/3038	API, P-I, Vol-III, p213
11	Shatavar	Wild Asparagus	*Asparagus racemosus* Willd.	Roots	20	NISCAIR/RHMD/CONSULT/2017/3034–61–54	API, P-I, Vol-VIII, p143
12	Hajrod	Bone settler	*Cissus quadrangularis* L.	Stems	20	NISCAIR/RHMD/CONSULT/2017/3082–31–33	API, P-I, Vol-III, p21
13	Haldi Turmeric	Turmeric	*Curcuma longa* L.	Rhizomes	20	NISCAIR/RHMD/CONSULT/2017/3034–61–23	API, P-I, Vol-I, p45
14	Sonth	Ginger	*Zingiber officinale* Roscoe	Rhizomes	20	NISCAIR/RHMD/CONSULT/2017/3082–31–88	API, P-I, Vol-II, p12
15	Kutki	Hellebore	*Picrorhiza Kurroa* Royle ex Benth	Roots	20	NISCAIR/RHMD/CONSULT/2017/3034–61–37	API, P-I, Vol-II, p85
16	Ajvayan	Thyme	*Trachyspermum ammi* (L.) Sprague	Fruits	3.5	NISCAIR/RHMD/CONSULT/2017/3082–31–5	API, P-I, Vol-I, p129
17	Giloy	Indian Tinospora	*Tinospora cordifolia* (Willd) Miers.	Stems	1.8	NISCAIR/RHMD/CONSULT/2017/3034–61–19	API, P-I, Vol-I. p41
18	Dashmool	(Composition of 10 different roots)		Roots	35.7	QCD1/FP/10–17/1719	AFI, Vol-1, p10, 47, 73,74
19	Shilajeet	Mineral Pitch	Mineral Pitch	Exudates	35	QCD1/SF/06–17/853	Charak Samhita
20	Godanti Bhasma	–	Processed gypsum	–	20	QCD/FP/02–16/393	API, P-I, Vol-VII, p11
21	Mukta shukti Bh.	–	Processed pearl oyster	–	20	QCD/FP/02–16/032	Charak Samhita
22	Yograj Guggulu	–	AFI, Part-I, 5:7	–	20	QCD1/FP/12–17/2202	API, P-II, Vol-II, p141
23	Praval Pishti	–	Processed red coral powder	–	3.5	QCD/FP/10–15/073	AFI, Vol-I, p119

(Ingredients 1–16 in the form of fine powders; Ingredients 17–19 in the form of aqueous extracts).

* **API**- The Ayurvedic Pharmacopeia of India, **UPI**- The Unani Pharmacopeia of India, **AFI**- The Ayurvedic Formulary of India.

stock solution (5 mg/mL) was added to 100 µL media in each well and incubated in CO_2 incubator for 3–4 h until formazan crystals were observed. Water insoluble formazan crystals were solubilized in acidic isopropanol (0.1 N HCl) and absorbance was taken using Envision microplate reader (Perkin Elmer) at 590 nm.

2.3.2. Nitric oxide assay

RAW264.7 cells were seeded in 24 well culture plates at the density of 2×10^5 cells/well. Cells were treated with vehicle or PV (15.62, 31.25, 62.5, 125 and 250 µg/mL) and incubated for 1 h. Cells were stimulated with LPS (500 ng/mL) and incubated for an additional 24 h at 37 °C in a CO_2 incubator. NO release in the culture media was determined using modified Griess reagent, following manufacturer's protocol. Equal volume of modified Griess reagent solution was added to cell supernatant and absorbance was recorded at 540 nm using Envision Microplate reader (Perkin Elmer). Modulation of NO production was measured (nitrite content) using the standard curve of sodium nitrite.

Similarly, THP-1 monocytes were seeded at the density 1×10^6 cells/mL in 24 well culture plates and treated with phorbol 12-myristate 13- acetate (PMA; 25 ng/mL; 48 h incubation). Experiments were performed according to the protocol mentioned earlier using PV (50, 100, 150, 200 and 250 µg/mL).

2.3.3. Cytokines level measurement

For cytokines level modulation studies, human monocyte THP-1 cells (5×10^5cells/well) were seeded in 24 well culture plates and treated with 25 ng/mL PMA. For experiment, PV was added to the wells at final conc. of 50, 100, 150, 200 and 250 µg/mL. After treating cells for an hour, LPS was added at final concentration 500 ng/mL except in control wells. Cell supernatants were collected after 4 and 24 h to measure different cytokines such as TNF-α and IL-6 using ELISA kits. ELISA assay was performed according to manufacturer's protocol and absorbance was recorded at 450 nm using Envision microplate reader (Perkin Elmer).

2.4. Experimental animals

Male Wistar rats (160–180 g) and CD-1 mice (20–22 g) were procured from Liveon Biolabs Pvt. Ltd (India) and Hylasco Biotechnology Pvt. Ltd, India respectively. All the animals were placed in optimal controlled environment with relative humidity of 60–70% with 12:12 h light and dark cycle in a registered animal house (1964/PO/Rc/S/17/CPCSEA). The animals were maintained on standard pellet diet (Golden Feed, India) and sterile filtered water *ad libitum*. All the animal experiments were approved by the Institutional Animal Ethical Committee and were performed in accordance with the guidelines of the Committee.

2.4.1. Dose selection for in-vivo experiments

The animal equivalent doses of PV powder for rat and mouse studies were calculated based on body surface area. The recommended dose of the PV for the human is 1–2 tablets twice a day. The weight of each tablet is 500 mg. According to this, total humane dose is 1500 mg/60 kg/day (25 mg/kg/day). Animal equivalent doses (mg/kg) for rat and mouse were calculated by multiplying human equivalent dose (mg/kg) by factor 6.2 and 12.3 respectively (Nair and Jacob, 2016). According to this, therapeutic equivalent doses (TEDs) for rat and mouse were found to be approx. 200 and 400 mg/kg respectively. However, two different doses for rat and mouse studies were selected i.e. TED and HD (High dose), 200 and 400 mg/kg for rat and 400 and 600 mg/kg for mouse.

2.5. Evaluation of in-vivo anti-inflammatory and anti-nociceptive activities

2.5.1. Carrageenan induced paw edema

Carrageenan induced paw edema test was performed according to the modified methods described earlier (Winter et al., 1962; Sakat et al., 2014). Wistar rats were divided into different groups (eight animals per group) based on basal paw volume (0 h) measured using 37140 plethysmometer (Ugo Basile, Italy). Inflammation was induced by the subcutaneous injection of λ-carrageenan (0.1 mL of 1% solution in normal saline) into the plantar side of the left hind paw. The paw was marked with ink at the level of lateral malleolus and volume was measured up to the mark at 1, 2, 3, 4 and 5 h after injection of carrageenan for all the animals. Further, animals were treated orally with vehicle or PV at 200 and 400 mg/kg or Indomethacin at 10 mg/kg, 1 h before carrageenan challenge. Paw edema was calculated by subtracting 0 h (basal) paw volume from the respective paw volumes at 1, 2, 3, 4, and 5 h. The anti-inflammatory activity (%) was calculated for each animal using the following formula: Mean paw edema of control animals (mL) − paw edema of each test animals (mL)/Mean paw edema of control animals (mL) × 100.

2.5.2. Hot plate test

The hot plate test was performed to measure response latencies according to previously described method (Arrau et al., 2011; Eddy and Leimbach, 1953) with minor modifications. Albino mice were initially screened for basal latency time into different groups (eight animals each). Test groups were treated orally with PV 400 and 600 mg/kg, while the control group received 0.25% Na-CMC. TMD (Tramadol hydrochloride Inj.) was used as a standard drug and administered intraperitoneally at the dose of 40 mg/kg. After 1 h of drug treatment, all the animals were placed into the perspex cylinder of the hot plate (Ugo Saile, Italy) maintained at 55.0 ± 0.5 °C and time to discomfort reaction (licking paws or jumping) was recorded as response latency. The latency time was recorded at 30, 60, 90, 120 and 180 min after the administration of test and standard drugs. A cut-off point of 20 s was considered to avoid any possible accidental paw damage. The percentage of maximum possible effect (% MPE) was calculated as $[(LT_1 - LT_0)/(LT_2 - LT_0)] \times 100$. LT_0 and LT_1 were the latencies time before and after drug administration, and LT_2 was the cut off time.

2.5.3. Tail flick test

Tail flick test as an acute model of pain was used to assess anti-nociceptive effect of the drugs by measuring the latency of response. Tail flick test was performed as described earlier (Keyhanfar et al., 2013; Meymandi et al., 2006) with minor modifications using a plantar test device (7370 plantar test; Ugo Basile, Italy) at high-intensity infrared radiation (infrared intensity of 99) with cut off time of 5 s. The animals were divided into four different groups containing eight animals each with mean basal latency time 2.0 ± 0.2 s. All the groups of animals were treated orally with vehicle or PV 400 and 600 mg/kg or TMD at 40 mg/kg (i.p.). The latency time was recorded at 30, 60, 90 and 120 min after the administration of test and standard drugs. The percentage of maximum possible effect (% MPE) was calculated by the formula mentioned above.

2.5.4. Formalin test

To assess chemical-induced acute and tonic pain, method of Hunskaar and Hole (1987) was followed with minor modifications. Eight animals in each group were treated with vehicle or PV (400 and 600 mg/kg, p.o.) or INDO (10 mg/kg, p.o.) 1 h before 1% formalin injection (20 µL) in normal saline (v/v). Immediately after the formalin injection in dorsal hind paw, the time of pain reactions were recorded that the animals remained licking or biting the paw during the first phase (0–5 min) and the second phase (20–30 min) of the test. Percent anti-nociceptive pain activity in each phase was calculated by the formula: (Mean Control-Test) X100/Mean Control

2.5.5. Acetic induced writhing test

The modified method (Torri et al., 2007) of writhing test was used to assess visceral pain. Animals were devided into four groups with 8

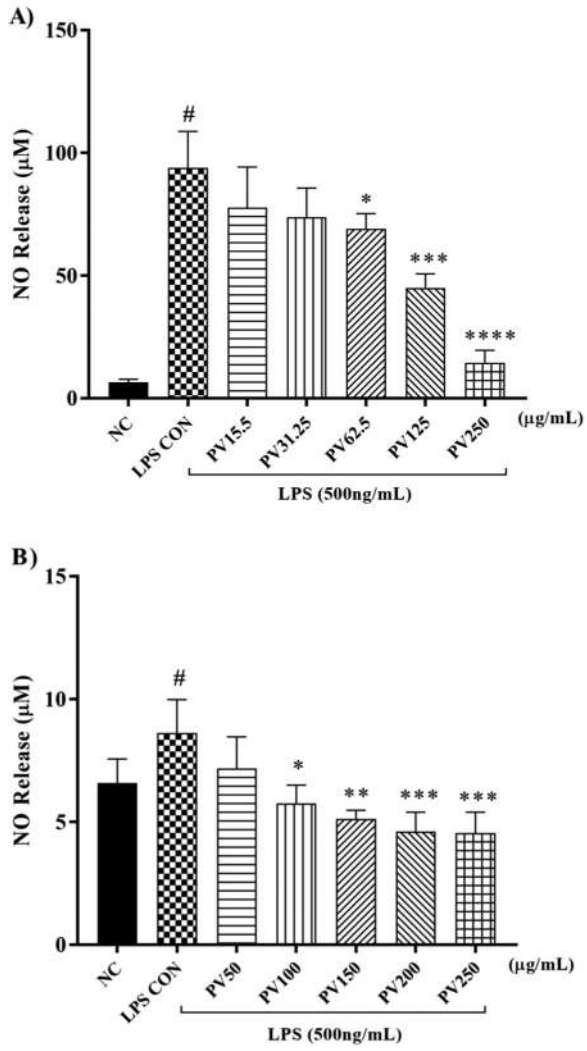

Fig. 1. Effect of vehicle, Peedantak Vati on nitric oxide release using A) Murine RAW264.7 (PV conc. 15.5, 31.25, 62.5, 125 and 250 μg/mL) and B) Human THP-1 (PV conc. 50, 100, 150, 200 and 250 μg/mL) cells. Values in the results are expressed as mean ± SEM, (n = 3). *p < 0.05, **p < 0.01, ***p < 0.001 considered significantly different in comparison to LPS control; #p < 0.001 considered significantly different in comparison to normal control. **Abbreviations**: NC: Normal control; LPS CON: LPS control; LPS- Lipopolysaccharides; PV: Peedantak Vati.

animals in each. One hour after the treatment of 0.25% Na-CMC or PV (400 and 600 mg/kg; p.o.) or INDO (10 mg/kg; p.o.), all the animals were received intra-peritoneal injections of 0.6% acetic acid (0.1 mL/10 g), for induction of writhing. A writhe is indicated by abdominal constriction and full extension of the hind limbs. After 10 min of the acetic acid injection, the numbers of writhing were registered for 20 min for each session. Percent anti-nociceptive pain activity was calculated by the formula mentioned in Section 2.5.4.

2.6. Statistical analysis

The data are expressed as mean ± standard error of mean (SEM) for each group. Statistical analysis was done using GraphPad Prism version 7.0 software. A one-way analysis of variance (ANOVA) followed by Dunnett's multiple comparison *t*-test was used to calculate statistical difference for *in-vitro* and *in-vivo* tests. Two-way ANOVA followed by Newman-Keuls multiple comparison test was used to calculate statistical difference for carrageenan induced paw edema test. A value of $p < 0.05$ was considered as significant.

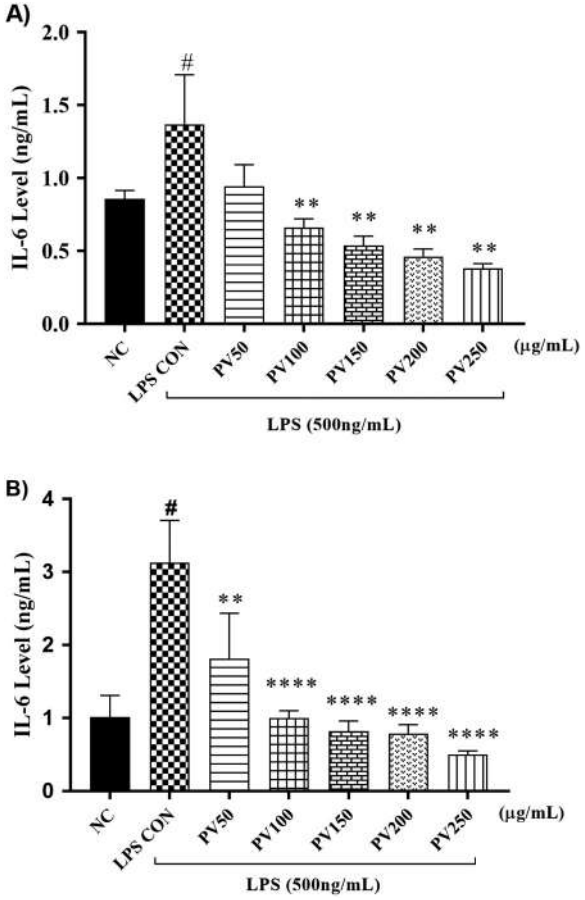

Fig. 2. Effect of vehicle, Peedantak Vati (PV conc. 50, 100, 150, 200 and 250 μg/mL) on pro-inflammatory cytokine IL-6 release by THP-1 cells at A) 4 h and B) 24 h. Values in the results are expressed as mean ± SEM, (n = 3). *p < 0.05, **p < 0.01, ***p < 0.001, ****p < 0.0001 considered significantly different in comparison to LPS control; #p < 0.001 considered significantly different in comparison to normal control. **Abbreviations**: NC: Normal control, LPS CON: LPS control, LPS- Lipopolysaccharides; PV: Peedantak Vati.

2.7. Phytochemical analysis

Physiochemical analysis of PV was performed qualitatively and quantitatively using colorimetric analyses. The phytoconstituents present in the formulation were analyzed quantitatively based on their class of molecules. Alkaloids were determined using 1,10-phenantroline in ethanol and the results were expressed as colchicine equivalents (Singh et al., 2004). Folin–Ciocalteau reagent in an alkaline medium was used to assess phenols and the results were expressed as the gallic acid equivalents (Singh et al., 2002). Flavonoid content was measured and expressed as the quercetin equivalent (Zhishen et al., 1999). Total saponin content was determined using Vanillin-Sulphuric acid colorimetric reaction with some modifications (Makkar et al., 2007) and the values were expressed as diosgenin equivalents.

2.8. HPLC analysis

The hydro-alcoholic extract of PV (HA-PV) was diluted in 50% methanol (1 mg/mL) and subjected to high performance liquid chromatography (HPLC) analysis. Waters binary HPLC system (Waters Corporation, Milford, MA, USA), equipped with, column oven, autosampler (Waters 2707) and photo diode array (PDA) detector (Waters 2998) was used for analyses. A reversed phase C18 analytical column of 4.60 × 250 mm and 5 μm particle size (Sunfire, Waters, USA) was

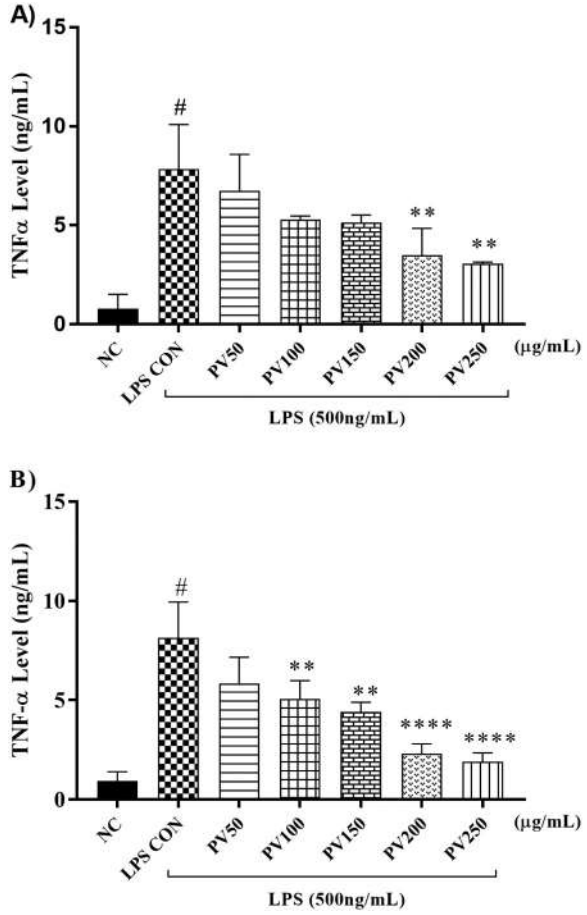

Fig. 3. Effect of vehicle, Peedantak Vati (PV conc. 50, 100, 150, 200 and 250 μg/mL) on pro-inflammatory cytokine TNF-α level release by THP-1 cells at A) 4 h and B) 24 h. Values in the results are expressed as mean ± SEM, (n = 3). *p < 0.05, **p < 0.01, ***p < 0.001, ****p < 0.0001 considered significantly different in comparison to LPS control; #p < 0.001 considered significantly different in comparison to normal control. **Abbreviations**: NC: Normal control, LPS CON: LPS control, LPS- Lipopolysaccharides PV: Peedantak Vati.

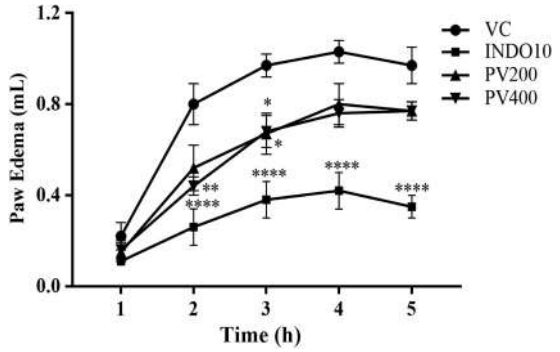

Fig. 4. Effect of vehicle, Peedantak Vati (PV, 200 and 400mpk) and Indomethacin (INDO 10mpk) on carrageenan induced paw edema. Values in the results are expressed as mean ± SEM, (n = 7), *p < 0.05, **p < 0.01, ***p < 0.001, ****p < 0.0001 significantly different in comparison to vehicle control at respective time points.

utilized and its temperature maintained at 30 °C.

A clear separation was achieved by using a mobile phase consisting of 0.1% formic acid (A) and acetonitrile (B). The following gradient program was used: 5% B (0 min, flow rate 1 mL/min), 10% B (4 min, flow rate 0.9 mL/min), 23% B (5 min, flow rate 1.1 mL/min), 28% B

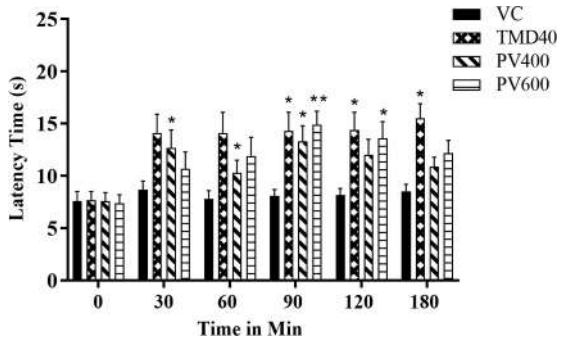

Fig. 5. Effect of vehicle, Peedantak Vati (PV, 400 and 600mpk) and Tramadol (TMD, 40 mpk) for anti-nociceptive activity using hot plate test. Values in the results are expressed as mean ± SEM, (n = 7), *p < 0.05, **p < 0.01, ***p < 0.001, ****p < 0.0001 significantly different in comparison to basal control (0 min).

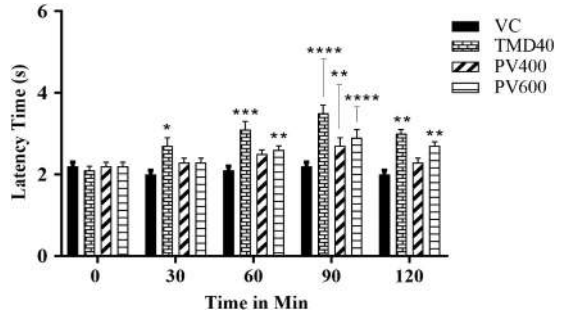

Fig. 6. Effect of vehicle, Peedantak Vati (PV, 400 and 600mpk) and Tramadol (TMD, 40 mpk) for anti-nociceptive activity using tail flick test. Values in the results are expressed as mean ± SEM, (n = 7), *p < 0.05, **p < 0.01, ***p < 0.001, ****p < 0.0001 significantly different in comparison to basal control (0 min).

(14 min, flow rate 1 mL/min), 35% B (20 min, flow rate 1 mL/min), 43% B (25 min, flow rate 0.9 mL/min), 45% B (35 min, flow rate 0.9 mL/min) 5% B (39 min, flow rate 1 mL/min) and 5% B (40 min, flow rate 1 mL/min). After filtration through 0.45 μm PTFE membrane filters, 20 μL of HA-PV was injected. Different concentrations of standard solution were prepared to make standard curve. Analysis of standard mixture and test sample solution was done in six sets to ensure repeatability of the method. An analytical methodology of marker compound quantification in HA extracts of PV was validated in accordance with ICH guidelines. The limits of detection (LOD) and quantitation (LOQ) were estimated as the minimum concentration of marker compound is able to produce signal-to-noise ratios (S/N) of 3 and 10, respectively. To assess the linearity of the method, marker solutions (1.0 mg/mL, triplicate) was added in extract solution (1.0 mg/mL) at concentrations of zero, 20.0, 40.0, 60.0, 80.0, 100.0 μg/mL. Analytical curves were obtained by ratio of marker peak areas at 270 nm. The precision and accuracy experiments were performed triplicate. The precision were expressed as residual standard deviation (RSD %) and accuracy was measured as percent deviation from nominal concentration.

2.9. LC-MS/MS analysis

LC-MS/MS analysis was performed to confirm the phytoconstituents, which were identified and quantified by HPLC. The HA-PV was diluted with 50% methanol (1 mg/mL) and subjected to LC-MS/MS analysis using Waters Xevo TQS micro with UPLC H class instrument. A reversed phase C18 analytical column of 2.1 × 100 mm and 1.8 μm particle size (HSS T3, C18 Column from Waters, USA) was used at 30 °C. HPLC method was used as guidance point for LCMS/MS analysis. Binary

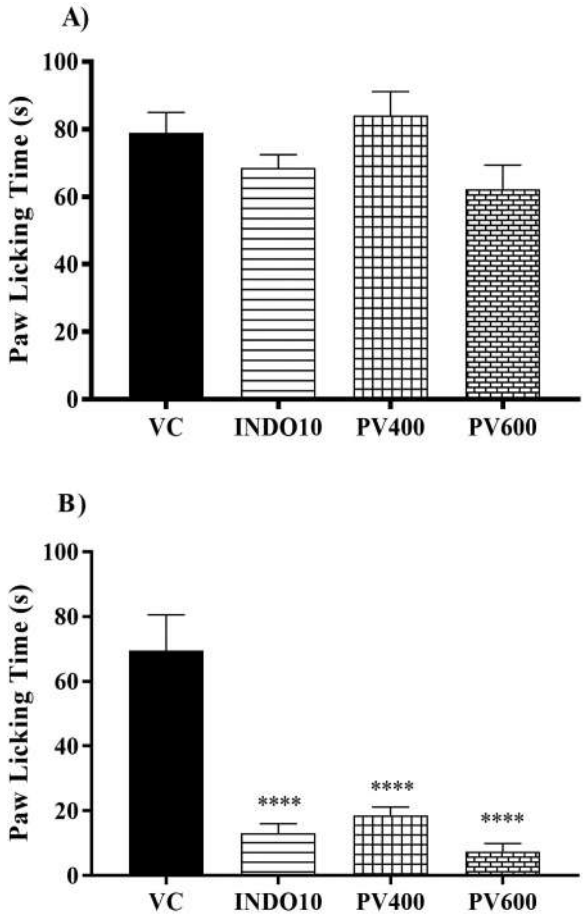

Fig. 7. Effect of vehicle, Peedantak Vati (PV, 400 and 600mpk) and Indomethacin (INDO, 10mpk) for anti-nociceptive effect using formalin test are represented as A: Early phase and B: Late phase. Values in the results are expressed as mean ± SEM, (n = 7), *p < 0.05, **p < 0.01, ***p < 0.001, **** *p < 0.0001 significantly different in comparison to vehicle control.

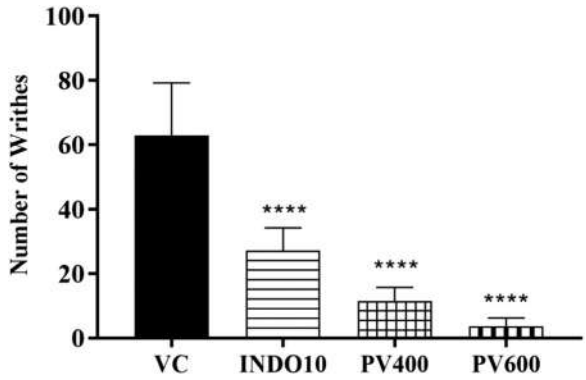

Fig. 8. Effect of vehicle, Peedantak Vati (PV, 400 and 600mpk) and Indomethacin (INDO, 10mpk) for anti-nociceptive effect using writhing test. Values in the results are expressed as mean ± SEM, (n = 7), *p < 0.05, **p < 0.01, ***p < 0.001, ****p < 0.0001 significantly different in comparison to vehicle control.

gradient of water and acetonitrile were used as mobile phase with constant flow rate of 0.4 mL/min. Gradient elution was programmed as follows: 5% B (0 min), 10% B (1 min), 23% B (1.5 min), 28% B (3.8 min), 35% B (6.5 min), 43% B (8 min), 45% B (9.5 min), 95% B (12 min), 5% B (20 min).

2.10. HPTLC analysis

Standardization of HA-PV (2 mg/mL) was performed using HPTLC system (CAMAG, Switzerland) equipped with a sample applicator (ATS4), development chamber (ADC2). Simple and precise HPTLC methods were developed, optimized and validated using a precoated TLC plate (60 F254,Merck, Germany) with mobile phase as chloroform: methanol: water: formic acid in the ratio of 7.0:0.65:0.1:0.2 (v/v). The TLC chamber was saturated with mobile phase for 20 min at room temperature. Detection and quantification was achieved at 218 nm using integrated TLC scanner and analyzed by WinCats software. Analytical performance of the proposed HPTLC method was validated according to the ICH guidelines with respect to the linearity, detection and quantitation limits.

2.11. ICP-MS analysis

Presence of heavy metals was determined following standard protocol (citation). Briefly, 2 gm of PV was digested in 10 mL of concentrated nitric acid and placed in hot oven at 60 °C. After complete digestion ultrapure elemental water was added to make complete 50 mL solution. Internal standard of known concentrations were added to the sample and the solution was subjected to heavy metal analysis by direct injection using instrument in helium gas mode (Agilent Technology model 7800). For data processing software provided with the instrument Mass hunter was used and results were calculated in PPM and experiments were performed in triplicates and RSD% values were calculated.

3. Results

3.1. Effect of PV on NO release

Cytotoxic level of PV was determined by standard MTT assay. The study results demonstrated that, PV was found to be safe for cells at ≤ 250 μg/mL concentration (data not shown). Hence, all the *in vitro* assays were performed below cyto-toxic concentration of PV. The effect of PV on NO release was studied using RAW264.7 cells (Fig. 1**A**) and THP-1 (Fig. 1**B**) cells. Cells treated with LPS (500 ng/mL) led to significant increase ($p < 0.001$) in NO production in LPS control of RAW264.7 and THP-1 cells as compared to respective normal control (NC). However cells treated with PV at 62.5 ($p < 0.05$), 125 ($P < 0.001$) and 250 ($p < 0.0001$) μg/mL showed significant decrease NO production by RAW264.7 cells. However, THP-1 cells treated with PV at 100 ($p < 0.05$), 150 ($p < 0.01$), 200 ($p < 0.001$) and 250 ($p < 0.001$) μg/mL showed significant decrease NO production.

3.2. Effect of PV on IL-6 and TNF-α level

To determine the effect of PV on pro-inflammatory cytokine production, differentiated THP-1 macrophage cells were pretreated with PV extracts at different concentrations (50, 100, 150, 200, 250 μg/mL) and challenged with LPS after 1 h. Fig. 2 displays significant rise ($p < 0.001$) in IL-6 level as compared to NC. Treatment of PV at 200 and 250 μg/mL led to significant ($p < 0.01$) decrease in IL-6 level measured at 4 h. However, PV showed remarkable decrease in IL-6 production at 50 ($p < 0.01$) and 100–250 μg/mL ($p < 0.0001$) estimated at 24 h time point. The anti-inflammatory effect of PV was displayed in a conc.-dependent manner.

Similarly, cytokine TNF-α level in LPS treated cells was prominently ($p < 0.001$) increased in LPS control as compared to NC (Fig. 3). THP-1 cells treated with PV exhibited substantial decrease in TNF-α level at 4 h (200 and 250 μg/mL; $p < 0.01$). Similarly, treatment of PV at 100 ($p < 0.01$), 150 ($p < 0.01$), 200 ($p < 0.0001$) and 250 μg/mL ($p < 0.0001$) showed remarkable decrease in TNF-α level measured at 24 h and the effect observed was conc.-dependent.

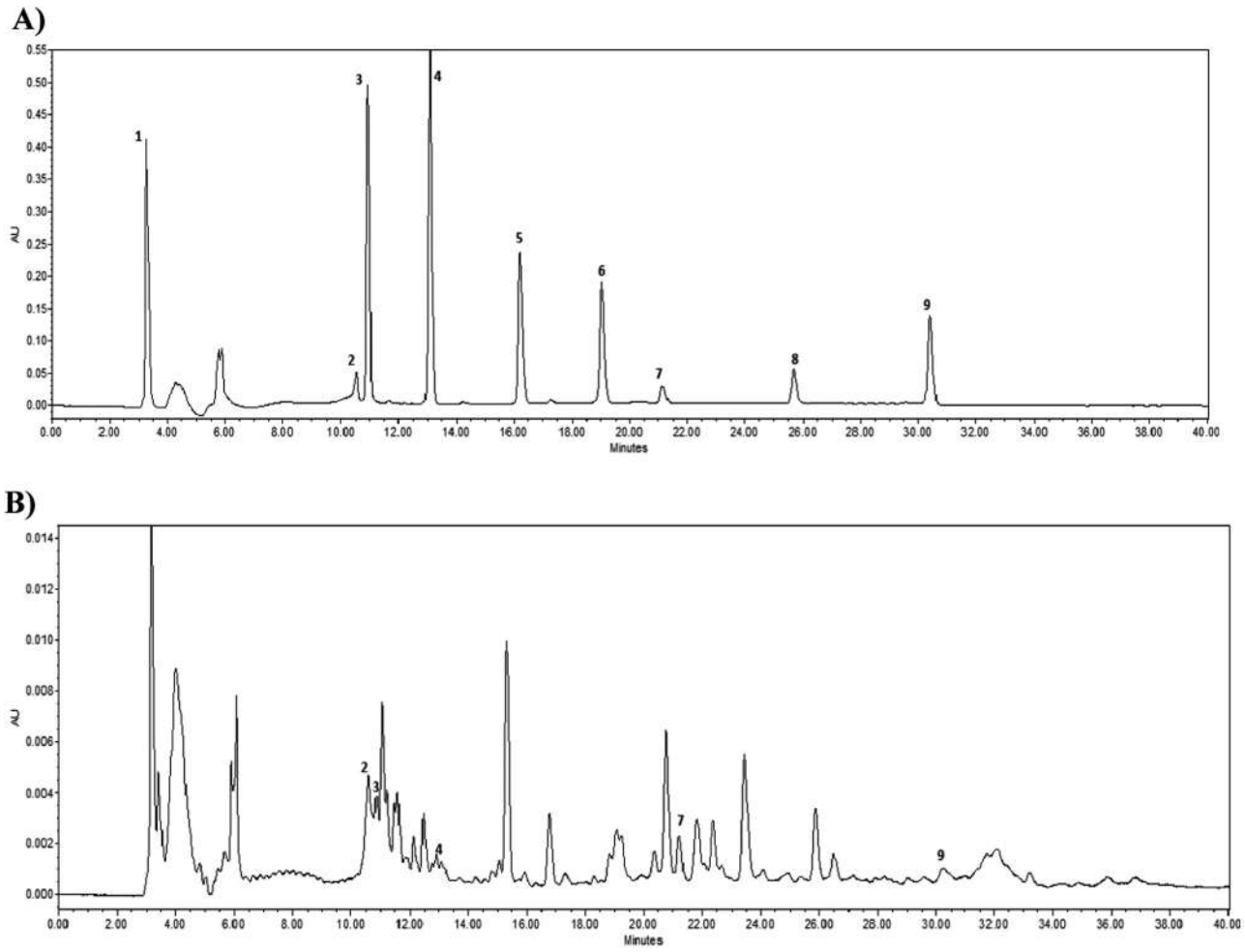

Fig. 9. A) HPLC Chromatogram of reference marker compounds. **Peak details:** 1: Berberine; 2: Rutin; 3: Caffeic acid; 4: Colchicine; 5: Quercetin; 6: trans-Cinnamic acid; 7: Withaferin A; 8: Withanolide A; 9: Curcumin **B)** HPLC Chromatogram of marker compounds in hydro-alcoholic extract of Peedantak Vati (HA-PV). **Peak details:** 2: Rutin; 3: Caffeic acid; 4: Colchicine; 7: Withaferin A; 9: Curcumin.

Table 2
Quantification of marker compounds in HA-PV by HPLC.

S. no	Peak no.	Name	Quantity (ppm)	% content
1	2	Rutin	1.204	0.120
2	3	Caffeic acid	0.154	0.015
3	4	Colchicine	0.251	0.025
4	7	Withaferin A	39.188	3.919
5	9	Curcumin	0.363	0.036

Table 3
HPLC method validation.

S. no.	Name of compound	LOD (ppm)	LOQ (ppm)
1	Rutin	0.5 ppm	1.0 ppm
2	Caffeic Acid	0.5 ppm	1.0 ppm
3	Withaferine A	0.5 ppm	1.0 ppm
4	Colchicine	0.5 ppm	1.0 ppm
5	Curcumin	0.2 ppm	0.5 ppm

3.3. In vivo anti-inflammatory effect of PV

The anti-inflammatory effect of PV was assessed by the carrageenan induced paw edema model (Fig. 4). The intraplantar injection of carrageenan in vehicle control rats led to a time dependent increase in paw volume that was maximal at 4 h followed by marginal decrease at 5 h. Animals treated orally with PV at 200 mg/kg displayed significant ($p < 0.05$) decrease in paw edema at 3 h, whereas high dose 400 mg/kg showed significant decrease in paw volume at 2 ($p < 0.01$) and 3 h ($p < 0.05$). The effect of 200 mg/kg dose was not significantly ($p > 0.05$) different as compared to high dose 400 mg/kg. Further, high dose of PV demonstrated maximum anti-inflammatory activity (data not shown) as 40.4 ± 5.2% at 2 h, followed by gradual decrease up to 5 h. The standard drug INDO at 10 mg/kg exhibited prominent ($p < 0.0001$) anti-inflammatory activity (> 50%) at all time points except 1 h (44.9 ± 6.5%).

3.4. Anti-nociceptive activity

3.4.1. Hot plate test

The PV was evaluated for anti-nociceptive pain effect using hot plate test is shown in Fig. 5. Control animals showed no significant difference ($p > 0.05$) in the latency time at different time points as compared to basal readouts (0 min). PV at 400 mg/kg exhibited significant ($p < 0.05$) increase in latency time at 30 and 90 min as compared to basal latency and high dose 600 mg/kg showed considerable increase in latency time at 90 ($p < 0.01$) and 120 min ($p < 0.05$) as compared to basal latency. The % MPE (data not shown) shown by the high dose of PV was found to be maximal (> 50%) at 90 and 120 min. The standard opoid analgesic TMD at 40 mg/kg; treated intra-peritoneally displayed noticeable ($p < 0.05$) increase in latency at 90, 120 and 180 min. The anti-nociceptive pain activity shown by the

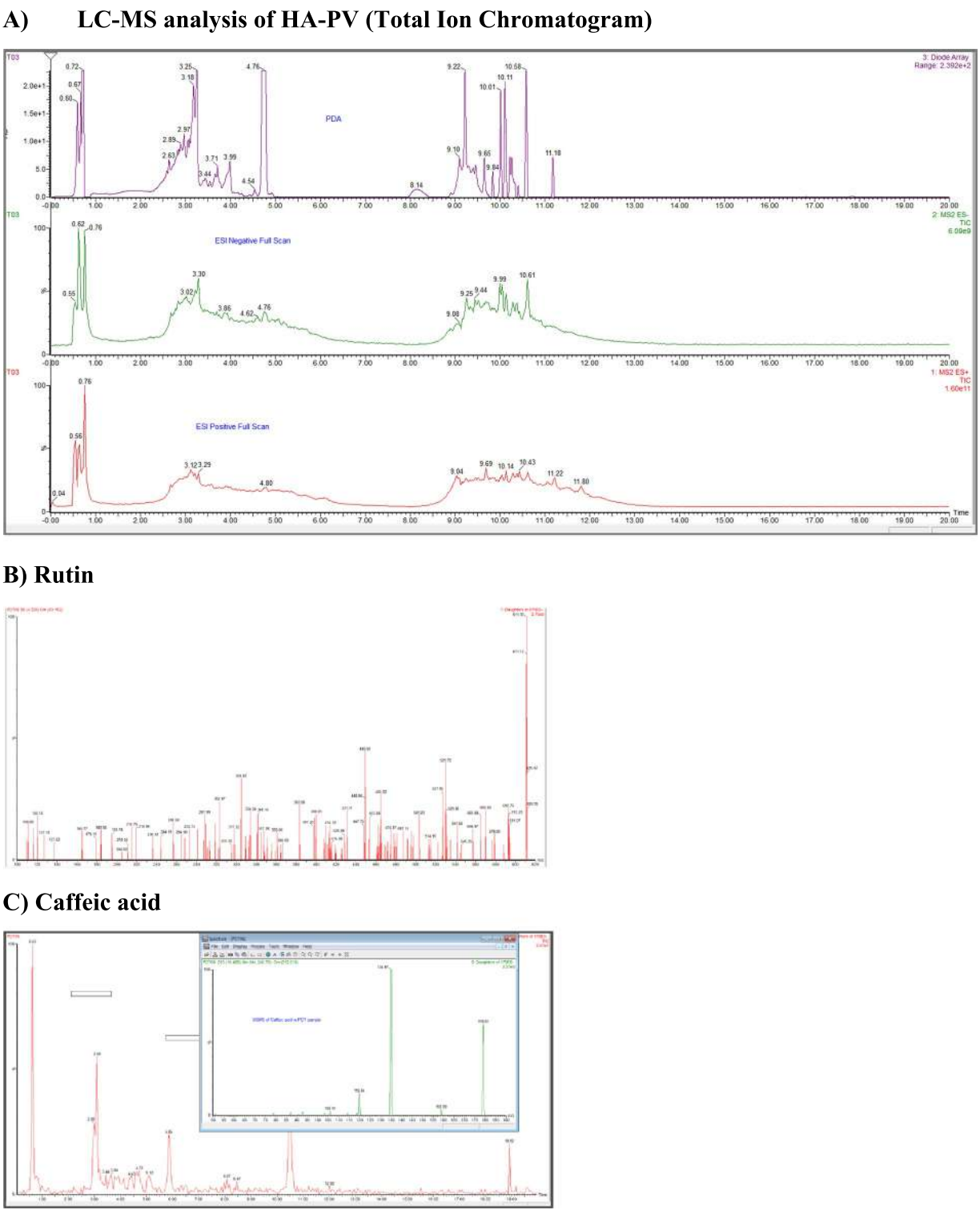

Fig. 10. : A) LC-MS/MS chromatogram of marker compounds in HA-PV (Full scan) **B)** LC-MS/MS chromatogram of Rutin **C)** LC-MS/MS chromatogram of Caffeic acid **D)** LC-MS/MS chromatogram of Colchicines **E)** LC-MS/MS chromatogram of Withaferrin A **F)** LC-MS/MS chromatogram of Curcumin.

TMD was found to be > 50% at all time points. Importantly, the % MPE of PV of high dose was found to be similar to that of TMD at 90 min (data not shown).

3.4.2. Tail flick test

Anti-nociceptive pain effect of PV was studied using the predominantly spinally mediated tail flick latency test (Fig. 6). The data suggest, PV at 400 mg/kg exhibited noticeable ($p < 0.01$) increase in latency only at 90 min as compared to basal latency. However, PV at 600 mg/kg showed significant anti-nociceptive property by increase in latency time at 60 ($p < 0.01$), 90 ($p < 0.0001$) and 180 min ($p < 0.01$) with MPE (data not shown) as 30 ± 3.8% at 90 min. However, TMD displayed gradual increase in % MPE of anti-nociceptive pain potential till 90 min. The results of the study clearly indicate the PV's considerable anti-nociceptive pain activity possibly mediated by spinal mechanism.

D) Colchicines

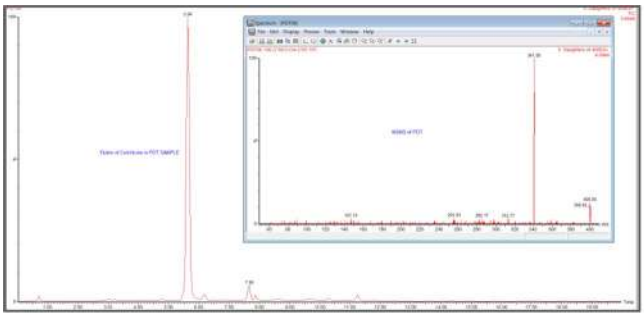

E) Withaferrin A

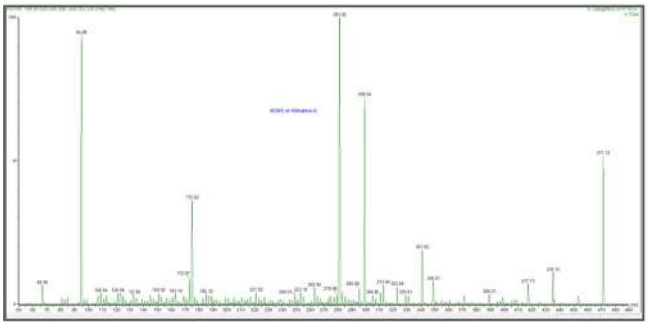

F) Curcumin

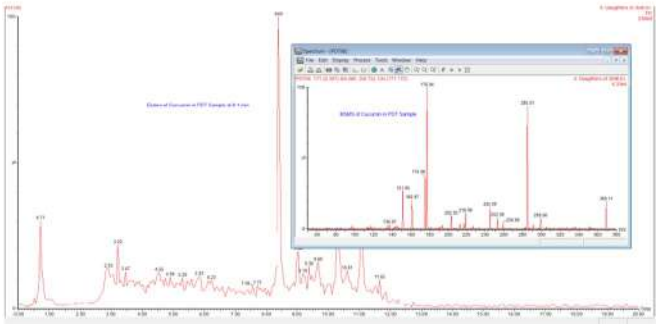

Fig. 10. (*continued*)

Table 4
Compounds identified by LCMS.

S. no.	R.T.	*m/z*	Compound identified
1	4.320	608.92	Rutin
2	7.661	399.15	Colchicine
3	8.397	368.05	Curcumin
4	9.243	470.63	Withaferine A
5	10.456	178.03	Caffeic Acid

3.4.3. Formalin test

This method elucidates central and peripheral nervous system activities. Formalin-induced pain is biphasic in which first phase involves direct stimulation of sensory nerve fibers representing neuropathic pain and second phase involves inflammatory pain mediated by prostaglandin, serotonin, histamine, bradykinin, and cytokines such as IL-1β, IL-6, TNF-α, eicosanoids and NO. In the present study, PV tested at 400 and 600 mg/kg showed no significant ($p > 0.05$) activity in the early phase (Fig. 7**A**), similar to that of INDO. However, in late phase PV showed remarkable ($p < 0.0001$) anti-nociceptive pain activity at 400 (76.4 ± 3.3%) and 600 mg/kg (90.6 ± 3.1%) (data not shown) by decreasing paw licking time (Fig. 7**B**). The standard drug INDO at 10 mg/kg displayed significant ($p < 0.0001$) anti-nociceptive pain activity (81.1 ± 4.2%) by lowering paw licking time.

3.4.4. Writhing test

The anti-nociceptive pain effect of PV against visceral pain was assessed by the acetic acid induced writhing test. Normal control animals showed maximum writhing response 72.5 ± 11.8 induced by intraperitoneal injection of 0.6% acetic acid in normal saline (Fig. 8). Orally administered PV at 400 and 600 mg/kg showed remarkable ($p < 0.0001$) and dose-related anti-nociceptive activity as 81.0 ± 4.0 (writhes: 13.8 ± 2.9) and 90.7 ± 4.6% (writhes: 6.8 ± 3.4) respectively. The standard NSAID drug, INDO also produced considerable ($p < 0.0001$) decrease in number of writhes (23.8 ± 4.4) with 67.2 ± 6.2% anti-nociceptive pain activity (data not shown).

3.5. Chemical analyses

HA-PV was prepared for all the downstream analyses. HPLC and HPTLC analytical techniques were utilized for chemical profiling, identification and quantification of marker compounds in PV. Identified compounds were confirmed by LC-MS/MS analysis.

3.5.1. Phytochemical analysis

The colorimetric analyses of PV indicated the presence of phenols, saponins, flavonoids and alkaloids. Quantitative analyses revealed the presence of alkaloids (560 ± 4.51 µg of colchicine equivalent/mg of extract), phenolic (2.73 ± 0.28 µg of gallic acid equivalent/mg of extract), flavonoids (0.20 ± 0.05 µg of quercetin equivalent/mg of extract) and saponins (268 ± 5.78 µg of diosgenin equivalent/mg of extract).

3.5.2. Identification and quantification of marker compounds by HPLC

Phytochemical profiling of HA-PV was performed using HPLC technique. A binary gradient method for HPLC was developed and optimized. HA-PV was analyzed along with mixture of standard marker compounds. Altogether five different compounds viz. rutin, caffeic acid, colchicine, withaferin A and curcumin were identified using newly developed method. Each compound was identified and confirmed using its retention time and UV profile in photodiode array (PDA) detector under similar conditions (Fig. 9**A-B**). These marker compounds were quantified in HA-PV and represented in Table 2. The HPLC method validation ensures reliability of results and reducing batch to batch variations. The retention time for different markers was validated with slope, linearity and accuracy (S1, Table A). The method was considered linear between concentrations of 20–100 µg/mL for Colchicine, Withaferin A, Curcumin, caffeic acid. The mean regression equation was curcumin was $y = 16{,}364 \times -86{,}483$, whereas for rutin it was $y = 29{,}039 \times -879{,}282$. The LOD and LOQ for identified marker compounds were obtained (Table 3).

3.5.3. Confirmation of marker compounds by LC-MS/MS

LC-MS/MS analysis was carried out to confirm marker compounds, which were identified and quantified by HPLC. Total ion chromatogram (TIC) both in +ve and -ve mode were obtained (Fig. 10A) Ionization pattern of major peaks were compared to the library and prediction was subjected to validation. Fragmentation pattern of predicted standards and HA-PV peaks were compared with standards to confirm the identity. Different marker compounds (Table 4) including caffeic acid, colchicine and curcumin were confirmed for their presence in HA-PV by LC-MS/MS (Fig. 10**A-F**).

3.5.4. Chromatographic profiling by HPTLC

HPTLC profile with optimized mobile phase chloroform: methanol: water: formic acid in the ration of 7.0:0.65:0.1:0.2 gave sharp peaks of different components present in HA-PV (Fig. 11A). Comparing with reference standards, two well defined peaks with R_f value of 23 and 28

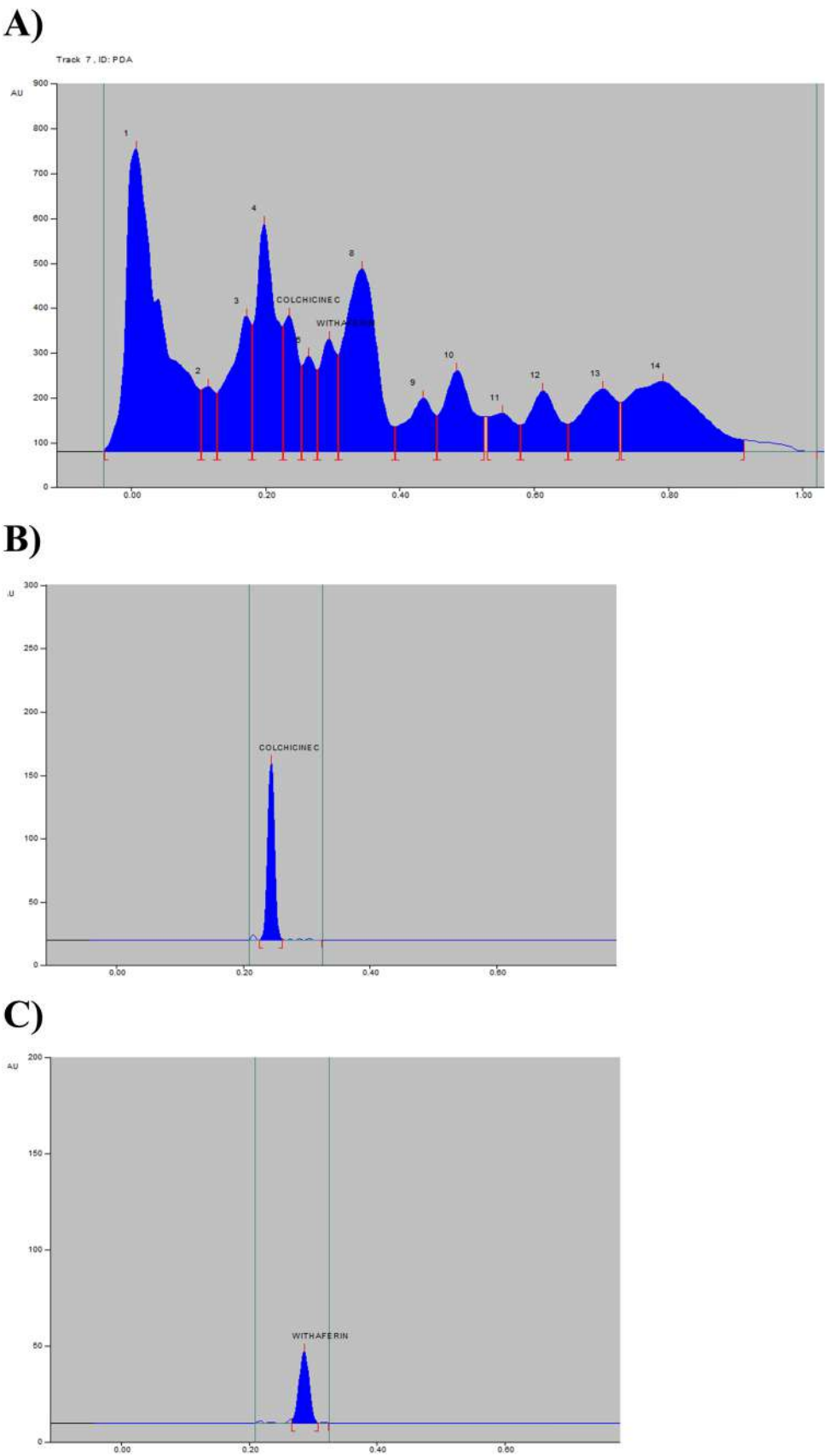

Fig. 11. A) Profile of hydro-alcoholic extract of Peedantak Vati (HA-PV) by HPTLC at λ = 210 nm. **B)** Densitogram of reference marker Colchicine by HPTLC at λ = 210 nm. **C)** Densitogram of reference marker Withaferin A by HPTLC at λ = 210 nm.

Table 5
HPTLC peaks for HA-PV.

Peak	R_f	Height	Area	Area %	Assigned substance	Quantity %
1	0.15	310.6	8652.6	6.97		
2	0.19	501.5	12,442.7	10.02		
3	0.23	308.2	5923.6	4.77	Colchicine	0.0295
4	0.26	222.3	3354.8	2.70		
5	0.28	261.7	5170.6	4.16	Withaferin A	0.049
6	0.32	420.2	16,330.6	13.15		
7	0.41	127.9	4264.6	3.43		
8	0.47	190.3	7113.6	5.73		
9	0.59	142.1	5155.3	4.15		

were identified as colchicines and withaferin A, respectively. The identity of the Colchicine and withaferin A band in sample chromatogram was confirmed by comparing chromatogram (Fig. 11: B, C) and R_f values of reference standards (Table 5). The percent area was represented by area normalization. The calibration plots were linear within the concentration range of 40–200 and 80–240 ng/spot for colchicine and withaferin, respectively (S1, Fig. A). The correlation coefficient intercept and slope were 0.990835, + 8638, 206.010 and 0.9984, + 5.099, 91.044 for colchicines and withafern A, respectively. Quantitative evaluation of identified standards colchicine and withaferin were found 0.0295% and 0.049% per 100 µg PV respectively (Table 5). The LOD for colchicine and withaferin A was 40 and 80 ng/spot and LOQ was 120 and 240 ng/spot, respectively (Table 6).

3.5.5. Heavy metal analysis by ICP-MS

Plants are known for heavy metal absorbance and accumulation. Therefore, AYUSH (Anonymous, 2003) had set standard limits (citation) for different heavy metal in herbal origin products. Important heavy metal content was measured in PV and found to be below safe standard limit (Table 7). PPM content of Arsenic (As), cadmium (Cd), mercury (Hg) and lead (Pb) were 0.788, 0.186, 0.687 and 0.476 respectively with low RSD% value in experiments performed in triplicates.

4. Discussion

The aim of the present study was to establish scientific evidences of the polyherbal ayurvedic formulation Peedantak Vati's biological activities. Keeping this in view, present study was designed to evaluate PV's anti-inflammatory and anti-nociceptive pain potential using different *in-vitro* and *in-vivo* models.

NO level was examined using LPS-stimulated murine macrophage cells RAW264.7 and human THP-1. Macrophages produce inflammatory mediators such as NO and other free radicals, in addition to numerous cytokines such as TNF-α, IL-1β, and IL-6 (Yang et al., 2012) during inflammation. Significant inhibition of NO production was observed in a concentration-dependent manner, which suggests remarkable anti-inflammatory activity.

Pro-inflammatory cytokines TNF-α and IL-6 are biomarkers of the inflammation, and their role in diseases such as RA, inflammatory bowel disease, sarcoidosis, psoriasis (Glaudemans et al., 2010; Sanchez-Munoz and Dominguez-Lopez, 2008), systemic lupus erythematosus and Crohn's disease (Gabay, 2006) has been reported. The level of IL-6 and TNF-α in LPS-stimulated human THP-1 cells was measured using ELISA at different time points. The results clearly demonstrate that, the

Table 7
Heavy metal analysis by ICP-MS.

S. no.	Name of heavy metal	Concentration (ppm)	RSD %	Permissible limit* (ppm)
1	Pb (Lead)	0.476 ppm	0.4	10
2	As (Arsenic)	0.788 ppm	0.9	3
3	Hg (Mercury)	0.687 ppm	4.1	1
4	Cd (Cadmium)	0.186 ppm	2.7	0.3

* AYUSH guidelines.

treatment of PV causes significant decrease in IL-6 and TNF-α level in a conc. dependent manner. Also, it was observed that, IL-6 level was robustly inhibited by PV in comparison to TNF-α, which could be due to modulation of NF-κB signaling pathways.

Further *in vivo* studies were performed to confirm the anti-inflammatory effects of PV in rat inflammation models. Paw edema model is widely used as a simple and reliable model to assess anti-inflammatory activity of various agents (Ashok et al., 2010; Fernandes et al., 2010). It is a biphasic event, During the early phase of inflammation (0–2 h) mediators like histamine, 5-hydroxytryptamine and bradykinin play important role, while during the late accelerating phase (post 2 h) there is elevated production of PGs, and production of COX-2 (Di Rosa et al., 1971; Sakat et al., 2014). PV treatement at low dose was found to be active only in the late phase. However, at the high dose of PV displayed considerable inhibition in both early and late phase of inflammation induced by carrageenan by inhibiting the release of different inflammatory mediators disturbing cyclooxygenase pathway.

PV was evaluated by hot plate and tail flick tests to assess its anti-nociceptive effect via supraspinal and spinal mechanisms respectively (South and Smith, 1998). The oral treatment of PV demonstrated a dose dependent, significant anti-nociceptive pain activity in hot plate test, suggesting its activity is mediated by supraspinal mechanism. With tail flick test, PV displayed remarkable anti-nociceptive potential via spinal mechanism particularly at high dose. Similar to reference drug TMD showed considerable reduction in tail flick latency time and confirm its analgesic potential. The results suggest that the anti-nociceptive activity of PV Altogether involves both supraspinal and spinal mechanism.

The acetic acid induced writhing reflex is a model of visceral pain, which is simple and commonly used method for the screening of peripherally acting analgesic drugs (Abdollahi et al., 2003; Ezeja et al., 2011; Golshani et al., 2004). The data of the writhing test emphasized the significant peripheral anti-nociceptive activity of PV by reducing writhing response. As standard NSAID drug INDO at 10 mg/kg also exhibited prominent anti-nociceptive activity, known to relieve the pain response peripherally by inhibiting production of prostaglandins, thromboxane by acting on cyclooxygenase enzymes.

The formalin test discriminates pain into early and late phases. It is useful not only for assessing the analgesic substances but also for elucidating the mechanism of analgesia (Shibata et al., 1989). The first phase involves neuropathic pain and second phase involves inflammatory pain mediated by prostaglandin and cytokines such as IL-1β, IL-6, TNF-α, eicosanoids, and NO (Chichorro et al., 2004; Hunskaar and Hole, 1987). Although, PV displayed marginal activity in the first phase at high dose, it displayed prominent activity in the second phase at both dose levels.

Table 6
HPTLC method validation.

Compound	Retention factor (RF)	Correlation coefficient (r2)	Slope	Intercept	% RSD of slope	LOD (ng/spot)	LOQ (ng/spot)
Colchicine	0.22 ±	0.998	8.638	206.01	0.0214	40	120
Withaferin A	0.28 ±	0.999	5.099	91.044	0.0074	80	240

Standardization of herbal formulations is essential in order to assess the quality of drugs, based on the concentration of their active principles (Chawla et al., 2013). We developed HPLC, HPTLC and LC-MS/MS methods for standardization of PV. The different markers compounds were identified and quantified by chromatographic techniques. Method was validated for HPLC and HPLC. This will help in maintaining consistency of the product. LC-MS/MS analysis confirmed presence of standard marker compounds, identified by HPLC and HPTLC, which substantiate the robustness of newly developed method and analysis. This method of analysis was found suitable for simultaneous identification and quantification of these five phytoconstituents from different class of phyto-compounds such as flavonoids (rutin), phenols (curcumin) and phenolic acids (caffeic acid), alkaloids (colchicine) and terpenoids (withaferin A) in a single run. Furthermore, these identified compounds can be used for quality control, consistency and accuracy of the PV formulation.

5. Conclusion

Based on the results shown in the present study, it can be concluded that polyherbal ayurvedic formulation 'Peedantak Vati' possesses significant anti-inflammatory and analgesic properties, providing potent and promising herbal alternative to currently available NSAIDs. Our studies also show that PV's anti-inflammatory activities could be targeting arachidonic acid cascade and modulating pro-inflammatory cytokines.

Conflict of interest

The authors declare that they have no conflicts of interest.

Acknowledgments

The authors are thankful to Patanjali Research Foundation Trust and Dr. Sumitro Nag, Divya Pharmacy, Patanjali Ayurved Ltd., Haridwar, India for providing the Peedantak Vati formulation to carry out the project.

Appendix A. Supporting information

Supplementary data associated with this article can be found in the online version at doi:10.1016/j.jep.2019.01.028

References

Abdollahi, M., Karimpour, H., Monsef-Esfehani, H.R., 2003. Antinociceptive effects of *Teucrium polium* L. total extract and essential oil in mouse writhing test. Pharmacol. Res. 48, 31–35. https://doi.org/10.1016/S1043-6618(03)00059-8.

Aggarwal, B.B., Prasad, S., Reuter, S., Kannappan, R., Yadev, V.R., Park, B., Kim, J.H., Gupta, S.C., Phromnoi, K., Sundaram, C., Prasad, S., Chaturvedi, M.M., Sung, B., 2011. Identification of novel anti-inflammatory agents from ayurvedic medicine for prevention of chronic diseases: "reverse pharmacology" and "bedside to bench" approach. Curr. Drug Targets 12 (11), 1595–1653.

Anonymous, 2003. The Ayurvedic Formulary of India, Part 1, 2nd ed. The Controller of Publications, Delhi.

Arrau, S., Delporte, C., Cartagena, C., Rodríguez-Díaz, M., González, P., Silva, X., Cassels, B.K., Miranda, H.F., 2011. Antinociceptive activity of *Quillaja saponaria* Mol. saponin extract, quillaic acid and derivatives in mice. J. Ethnopharmacol. 133, 164–167. https://doi.org/10.1016/j.jep.2010.09.016.

Ashok, P., Koti, B.C., Thippeswamy, A.H.M., Tikare, V.P., Dabadi, P., Viswanathaswamy, A.H.M., 2010. Evaluation of anti-inflammatory activity of *Centratherum anthelminticum* (L) Kuntze seed. Indian J. Pharm. Sci. 72, 697–703. https://doi.org/10.4103/0250-474X.84577.

The Ayurvedic formulary of India, 2003. Ayurvedic Pharmacopoeia Committee. Govt of India, Ministry of Health and Family Welfare. Controller of Publications, New Delhi.

Bae, M.J., Shin, H.S., Choi, D.W., Shon, D.H., 2012. Antiallergic effect of *Trigonella foenum-graecum* L. extracts on allergic skin inflammation induced by trimellitic anhydride in BALB/c mice. J. Ethnopharmacol. 144, 514–522. https://doi.org/10.1016/j.jep.2012.09.030.

Bairwa, K., Jachak, S.M., 2015. Anti-inflammatory potential of a lipid-based formulation of a rotenoid-rich fraction prepared from *Boerhavia diffusa*. Pharm. Biol. 53 (8), 1231–1238. https://doi.org/10.3109/13880209.2014.971382.

Bairwa, R., Sodha, R.S., Rajawat, B.S., 2012. Trachyspermum ammi. Pharmacogn. Rev. 6 (11), 56–60. https://doi.org/10.4103/0973-7847.95871.

Bhujade, A.M., Talmale, S., Kumar, N., Gupta, G., Reddanna, P., Das, S.K., Patil, M.B., 2012. Evaluation of *Cissus quadrangularis* extracts as an inhibitor of COX, 5-LOX, and proinflammatory mediators. J. Ethnopharmacol. 141, 989–996. https://doi.org/10.1016/j.jep.2012.03.044.

Chawla, R., Thakur, P., Chowdhry, A., Jaiswal, S., Sharma, A., Goel, R., Sharma, J., Priyadarshi, S.S., Kumar, V., Sharma, R.K., Arora, R., 2013. Evidence based herbal drug standardization approach in coping with challenges of holistic management of diabetes: a dreadful lifestyle disorder of 21st century. J. Diabetes Metab. Disord. 12, 35.

Chen, J., Wang, X., Qu, Y.G., Chen, Z.P., Cai, H., Liu, X., Xu, F., Lu, T.L., Cai, B.C., 2012. Analgesic and anti-inflammatory activity and pharmacokinetics of alkaloids from seeds of *Strychnos nux-vomica* after transdermal administration: effect of changes in alkaloid composition. J. Ethnopharmacol. 139 (1), 181–188. https://doi.org/10.1016/j.jep.2011.10.038.

Chichorro, J.G., Lorenzetti, B.B., Zampronio, A.R., 2004. Involvement of bradykinin, cytokines, sympathetic amines and prostaglandins in formalin-induced orofacial nociception in rats. Br. J. Pharmacol. https://doi.org/10.1038/sj.bjp.0705724.

Cooper, T.E., Heathcote, L.C., Anderson, B., Grégoire, M.-C., Ljungman, G., Eccleston, C., 2017. Non-steroidal anti-inflammatory drugs (NSAIDs) for cancer-related pain in children and adolescents. Cochrane Database Syst. Rev. 7, CD012563. https://doi.org/10.1002/14651858.CD012563.pub2.

Dang, G.K., Parekar, R.R., Kamat, S.K., Scindia, A.M., Rege, N.N., 2011. Antiinflammatory activity of *Phyllanthus emblica*, *Plumbago zeylanica* and *Cyperus rotundus* in acute models of inflammation. Phytother. Res. 25 (6), 904–908. https://doi.org/10.1002/ptr.3345.

Dharmasiri, M.G., Jayakody, J.R., Galhena, G., Liyanage, S.S., Ratnasooriya, W.D., 2003. Anti-inflammatory and analgesic activities of mature fresh leaves of *Vitex negundo*. J. Ethnopharmacol. 87 (2–3), 199–206.

Di Rosa, M., Giroud, J.P., Willoughby, D.A., 1971. Studies of the mediators of the acute inflammatory response induced in rats in different sites by carrageenan and turpentine. J. Pathol. 104, 15–29. https://doi.org/10.1002/path.1711040103.

Eddy, N.B., Leimbach, D., 1953. Synthetic analgesics. II. Dithienylbutenyl- and dithienylbutylamines. J. Pharmacol. Exp. Ther. 107.

Ezeja, M., Omeh, Y., Ezeigbo, I., Ekechukwu, A., 2011. Evaluation of the analgesic activity of the methanolic stem bark extract of *dialium guineense* (wild). Ann. Med. Health Sci. Res. 1, 55–62.

Fernandes, J.C., Spindola, H., De Sousa, V., Santos-Silva, A., Pintado, M.E., Malcata, F.X., Carvalho, J.E., 2010. Anti-inflammatory activity of chitooligosaccharides in vivo. Mar. Drugs 8, 1763–1768. https://doi.org/10.3390/md8061763.

Gabay, C., 2006. Interleukin-6 and chronic inflammation. Arthritis Res. Ther. 8 (Suppl. 2), S3.

Glaudemans, A.W., Dierckx, R.A., Kallenberg, C.G., Fuentes, K.L., 2010. The role of radiolabelled anti- TNFa monoclonal antibodies for diagnostic purposes and therapy evaluation. J. Nucl. Med. Mol. Imagin. 54 (6), 639–653.

Golshani, S., Karamkhani, F., Monsef-Esfehani, H.R., Abdollahi, M., 2004. Antinociceptive effects of the essential oil of *Dracocephalum kotschyi* in the mouse writhing test. J. Pharm. Pharm. Sci. 7, 76–79.

Gupta, A., Singh, S., 2014. Evaluation of anti-inflammatory effect of *Withania somnifera* root on collagen-induced arthritis in rats. Pharm. Biol. 52 (3), 308–320. https://doi.org/10.3109/13880209.2013.835325.

Gupta, R.A., Singh, B.N., Singh, R.N., 1089. Pharmacological Studies on Dashumulakwatha, J. Res. Ayur. Sid. IV, 74, pp. 1–4.

Grampurohit, N.D., Baichwal, M.R., Jolly, C.I., 1992. Estimation of sterols from dashmula. Anc. Sci. Life 12 (1–2), 245–247.

Grivennikov, S.I., Greten, F.R., Karin, M., 2010. Immunity, inflammation, and cancer. Cell 140, 883–899. https://doi.org/10.1016/j.cell.2010.01.025.

Harirforoosh, S., Asghar, W., Jamali, F., 2013. Adverse effects of nonsteroidal antiinflammatory drugs: an update of gastrointestinal, cardiovascular and renal complications. J. Pharm. Pharm. Sci. 16, 821–847.

Hiruma-Lima, C.A., Gracioso, J.S., Bighetti, E.J., Germonsén Robineou, L., Souza Brito, A.R., 2000. The juice of fresh leaves of *Boerhaavia diffusa* L. (Nyctaginaceae) markedly reduces pain in mice. J. Ethnopharmacol. 71 (1–2), 267–274.

Hunskaar, S., Hole, K., 1987. The formalin test in mice: dissociation between inflammatory and non-inflammatory pain. Pain 30, 103–114.

Keyhanfar, F., Shamsi Meymandi, M., Sepehri, G., Rastegaryanzadeh, R., Heravi, G., 2013. Evaluation of antinociceptive effect of pregabalin in mice and its combination with tramadol using tail flick test. Iran. J. Pharm. Res. IJPR 12, 483–493.

Kono, T., Shimada, M., Yamamoto, M., Kaneko, A., Oomiya, Y., Kubota, K., Kase, Y., Lee, K., Uezono, Y., 2015. Complementary and synergistic therapeutic effects of compounds found in Kampo medicine: analysis of daikenchuto. Front. Pharmacol. 6, 159. https://doi.org/10.3389/fphar.2015.00159.

Kumar, R., Gupta, Y.K., Singh, S., Raj, A., 2016. Anti-inflammatory effect of *Picrorhiza kurroa* in experimental models of inflammation. Planta Med. 82 (16), 1403–1409.

Kunnumakkara, A.B., Bordoloi, D., Padmavathi, G., Monisha, J., Roy, N.K., Prasad, S., Aggarwal, B.B., 2017. Curcumin, the golden nutraceutical: multitargeting for multiple chronic diseases. Br. J. Pharmacol. 174, 1325–1348. https://doi.org/10.1111/bph.13621.

Lee, J.Y., Shin, T.J., Choi, J.M., Seo, K.S., Kim, H.J., Yoon, T.G., Lee, Y.S., Han, H., Chung, H.J., Oh, Y., Jung, S.J., Shin, K.J., 2013. Antinociceptive curcuminoid, KMS4034, effects on inflammatory and neuropathic pain likely via modulating TRPV1 in mice. Br. J. Anaesth. 111 (4), 667–672. https://doi.org/10.1093/bja/aet176.

Libby, P., 2006. Inflammation and cardiovascular disease mechanisms. Am. J. Clin. Nutr. 83, 456S–460SS.

MacMicking, J., Xie, Q.W., Nathan, C., 1997. Nitric oxide and macrophage function. Ann.

Rev. Immunol. 15, 323–350. https://doi.org/10.1146/annurev.immunol.15.1.323.
Makkar, H.P., Siddhuraju, P., Becker, K., 2007. Methods in molecular biology: plant secondary. In: Metabolites. Human Press, Totowa, pp. 93–100. https://doi.org/10.1007/978-1-59745-425-4.
Meymandi, M.S., Sepehri, G.R., Mobasher, M., 2006. Gabapentin enhances the analgesic response to morphine in acute model of pain in male rats. Pharmacol. Biochem. Behav. 85, 185–189. https://doi.org/10.1016/j.pbb.2006.07.037.
Mosmann, T., 1983. Rapid colorimetric assay for cellular growth and survival: application to proliferation and cytotoxicity assays. J. Immunol. Methods 65, 55–63.
Nair, A., Jacob, S., 2016. A simple practice guide for dose conversion between animals and human. J. Basic Clin. Pharm. 7, 27. https://doi.org/10.4103/0976-0105.177703.
Nair, V., Kumar, R., Singh, S., Gupta, Y.K., 2012. Investigation into the anti-inflammatory and antigranuloma activity of *Colchicum luteum* Baker in experimental models. Inflammation 35 (3), 881–888. https://doi.org/10.1007/s10753-011-9389-9392.
Ojewole, J.A., 2006. Analgesic, antiinflammatory and hypoglycaemic effects of ethanol extract of *Zingiber officinale* (Roscoe) rhizomes (Zingiberaceae) in mice and rats. Phytother. Res. 20 (9), 764–772. https://doi.org/10.1002/ptr.1952.
Orrù, A., Casu, M.A., Tambaro, S., Marchese, G., Casu, G., Ruiu, S., 2016. *Withania somnifera* (L.) Dunal root extract alleviates formalin-induced nociception in mice: involvement of the opioidergic system. Behav. Pharmacol. 27 (1), 57–68. https://doi.org/10.1097/FBP.0000000000000195.
Patgiri, B., Umretia, B.L., Vaishnav, P.U., Prajapati, P.K., Shukla, V.J., Ravishankar, B., 2014. Anti-inflammatory activity of Guduchi Ghana (aqueous extract of *Tinospora Cordifolia* Miers.). Ayu 35 (1), 108–110. https://doi.org/10.4103/0974-8520.141958.
Rasoanaivo, P., Wright, C.W., Willcox, M.L., Gilbert, B., 2011. Whole plant extracts versus single compounds for the treatment of malaria: synergy and positive interactions. Malar. J. 10 (Suppl. 1), S4. https://doi.org/10.1186/1475-2875-10-S1-S4.
Ricciotti, E., FitzGerald, G.A., 2011. Prostaglandins and inflammation. Arterioscler. Thromb. Vasc. Biol. 31, 986–1000. https://doi.org/10.1161/ATVBAHA.110.207449.
Sakat, S.S., Mani, K., Demidchenko, Y.O., Gorbunov, E.A., Tarasov, S.A., Mathur, A., Epstein, O.I., 2014. Release-active dilutions of diclofenac enhance anti-inflammatory effect of diclofenac in carrageenan-induced rat paw edema model. Inflammation 37, 1–9. https://doi.org/10.1007/s10753-013-9705-0.
Sanchez-Munoz, F., Dominguez-Lopez, A., Yamamoto-Furusho, J.K., 2008. Role of cytokines in inflammatory bowel disease. World J. Gastroenterol. 14 (27), 4280–4288.
Schett, G., Elewaut, D., McInnes, I.B., Dayer, J.-M., Neurath, M.F., 2013. How cytokine networks fuel inflammation: toward a cytokine-based disease taxonomy. Nat. Med. 19, 822–824. https://doi.org/10.1038/nm.3260.
Shibata, M., Ohkubo, T., Takahashi, H., Inoki, R., 1989. Modified formalin test: characteristic biphasic pain response. Pain 38, 347–352. https://doi.org/10.1016/0304-3959(89)90222-4.
Shishodia, S., Harikumar, K.B., Dass, S., Ramawat, K.G., Aggarwal, B.B., 2008. The guggul for chronic diseases: ancient medicine, modern targets. Anticancer Res. 28 (6A), 3647–3664.
Singh, D.K., Srivastava, B., Sahu, A., 2004. Spectrophotometric determination of Rauwolfia alkaloids: estimation of reserpine in pharmaceuticals. Anal. Sci. 20, 571–573.
Singh, R.P., Chidambara Murthy, K.N., Jayaprakasha, G.K., 2002. Studies on the antioxidant activity of pomegranate (*Punica granatum*) peel and seed extracts using in vitro models. J. Agric. Food Chem. 50, 81–86.
Skelly, D.T., Hennessy, E., Dansereau, M.-A., Cunningham, C., 2013. A systematic analysis of the peripheral and CNS effects of systemic LPS, IL-1β, [corrected] TNF-α and IL-6 challenges in C57BL/6 mice. PLoS One 8, e69123. https://doi.org/10.1371/journal.pone.0069123.
Skeoch, S., Bruce, I.N., 2015. Atherosclerosis in rheumatoid arthritis: is it all about inflammation? Nat. Rev. Rheumatol. 11, 390–400. https://doi.org/10.1038/nrrheum.2015.40.
South, S.M., Smith, M.T., 1998. Apparent insensitivity of the hot plate latency test for detection of antinociception following intraperitoneal, intravenous or intracerebroventricular M6G administration to rats. J. Pharmacol. Exp. Ther. 286, 1326–1332.
Srivastava, P., Mohanti, S., Bawankule, D.U., Khan, F., Shanker, K., 2014. Effect of *Pluchea lanceolata* bioactives in LPS-induced neuroinflammation in C6 rat glial cells. Naunyn. Schmiede. Arch. Pharmacol. 387, 119–127. https://doi.org/10.1007/s00210-013-0924-6.
Tanaka, T., Narazaki, M., Kishimoto, T., 2014. Il-6 in inflammation, Immunity, and disease. Cold Spring Harb. Perspect. Biol. 6. https://doi.org/10.1101/cshperspect.a016295.
The Unani Pharmacopoeia of India, Ministry for Health and Family Welfare, Govt. of India, 2007. First ed.
The Ayurvedic Pharmacopoeia of India, Ministry for Health and Family Welfare, Govt. of India, 2008. 171. ⟨http://dx.doi.org/10.1017/CBO9781107415324.004⟩.
Tiwari, N., Gupta, V.K., Pandey, P., Patel, D.K., Banerjee, S., Darokar, M.P., Pal, A., 2017. Adjuvant effect of *Asparagus racemosus* Willd. derived saponins in antibody production, allergic response and pro-inflammatory cytokine modulation. Biomed. Pharmacother. 86, 555–561. https://doi.org/10.1016/j.biopha.2016.11.087.
Torri, E., Lemos, M., Caliari, V., Kassuya, C.A.L., Bastos, J.K., Andrade, S.F. de, 2007. Anti-inflammatory and antinociceptive properties of blueberry extract (*Vaccinium corymbosum*). J. Pharm. Pharmacol. 59, 591–596. https://doi.org/10.1211/jpp.59.4.0015.
Trikamji, J. (Ed.), 2007. Charaka Samhita of Agnivesha, Chikitsa Sthana; Abhaya Amalaki Rasayana Pada, 1st ed. Chowkhambha Prakashan, Varanasi, pp. 378–379 (Chap. 1, Verse 41-57).
Winter, C.A., Risley, E.A., Nuss, G.W., 1962. Carrageenan induced oedema in hind paw of rat as assay for anti-inflammatory drugs. Proc. Soc. Exp. Biol. Med. 111, 544–547.
Wright, H.L., Moots, R.J., Edwards, S.W., 2014. The multifactorial role of neutrophils in rheumatoid arthritis. Nat. Rev. Rheumatol. 10, 593–601. https://doi.org/10.1038/nrrheum.2014.80.
Yang, G., Lee, K., Lee, M., Ham, I., Choi, H.Y., 2012. Inhibition of lipopolysaccharide-induced nitric oxide and prostaglandin E2 production by chloroform fraction of Cudrania tricuspidata in RAW 264.7 macrophages. BMC Complement. Altern. Med. 10 (12), 250. https://doi.org/10.1186/1472-6882-12-250.
Zelová, H., Hošek, J., 2013. TNF-α signalling and inflammation: interactions between old acquaintances. Inflamm. Res. https://doi.org/10.1007/s00011-013-0633-0.
Zhishen, J., Mengcheng, T., Jianming, W., 1999. The determination of flavonoid contents in mulberry and their scavenging effects on superoxide radicals. Food Chem. 64, 555–559. https://doi.org/10.1016/S0308-8146(98)00102-2.
Zhou, X., Seto, S.W., Chang, D., Kiat, H., Razmovski-Naumovski, V., Chan, K., Bensoussan, A., 2016. Synergistic effects of Chinese herbal medicine: a comprehensive review of methodology and current research. Front. Pharmacol. 7, 201. https://doi.org/10.3389/fphar.2016.00201.

International Journal of Nanomedicine

Dovepress
open access to scientific and medical research

Open Access Full Text Article

ORIGINAL RESEARCH

Characterization and Anti-Cancerous Effect of *Putranjiva roxburghii* Seed Extract Mediated Silver Nanoparticles on Human Colon (HCT-116), Pancreatic (PANC-1) and Breast (MDA-MB 231) Cancer Cell Lines: A Comparative Study

This article was published in the following Dove Press journal:
International Journal of Nanomedicine

Acharya Balkrishna[1,2]
Vinay Kumar Sharma[1,2]
Subrata K Das[1]
Nayan Mishra[1]
Laxmi Bisht[1]
Alpana Joshi[1]
Niti Sharma[1]

[1]Drug Discovery and Development Division, Patanjali Research Foundation Trust, Haridwar, Uttarakhand 249405, India; [2]University of Patanjali, Haridwar, Uttarakhand 249405, India

Introduction: A comparative study of *Putranjiva roxburghii Wall*. seed extract and developed silver nanoparticles (PJSNPs) for improving bioavailability that enhance their anti-cancer activity against HCT-116 (colon carcinoma), PANC-1 (pancreatic carcinoma), MDA-MB 231 (breast carcinoma) cell lines was performed.

Materials and Methods: The green synthesis of PJSNPs (*Putranjiva* silver nanoparticles) was performed using PJ (*Putranjiva*) extract, and characterization of synthesized nanoparticles was accomplished through UV-Vis spectrum, X-ray diffraction (XRD), transmission electron microscopy, energy-dispersive X-ray spectroscopy (TEM-EDAX), scanning electron microscopy (SEM), Fourier transform infrared spectroscopy (FTIR), atomic force microscopy (AFM), and Raman spectroscopy.

Results: The results revealed that PJSNPs are homogeneous, spherical in shape, ~8±2 nm in size, and negatively charged with a zeta potential of about −26.71 mV. The cytotoxicity pattern observed was $AgNO_3$ > PJSNPs > PJ extract. The morphological changes of the cells were observed by flow cytometry and also by the DNA ladder pattern on gel electrophoresis, which indicated that the process of cell death occurred via the apoptosis mechanism and PJSNPs were exerting late-stage apoptosis in all the tested cell lines. The small size and negative value of zeta potential could be the factors responsible for greater bioavailability and thus increased uptake by the tumor cells.

Conclusion: The MTT assay and morphological changes observed by various methods indicate that the novel PJSNPs are a better anticancer agent than PJ extract. All the above properties make biologically synthesized PJSNPs an important target in the field of anti-cancer drug discovery.

Keywords: green synthesis, *Putranjiva*, silver nanoparticles, anti-cancer, apoptosis

Background

Nanotechnology has gained tremendous popularity in recent years and has become a vital part of the drug discovery and development particularly, the drug delivery system. Due to their distinctive properties, metal nanoparticles have proved their worth in electronics, photonics, as well as biomedicine.[1–3] Amongst all the metals used, silver is the most desirable one as pure silver has the maximum electrical and

Correspondence: Niti Sharma
Tel +91-1334-242418
Email nitivinay@yahoo.co.in

Vinay Kumar Sharma
Email vinay_sharma_2000@yahoo.com

submit your manuscript | www.dovepress.com
DovePress
http://doi.org/10.2147/IJN.S230244

thermal conductivity and minimum contact resistance.[4] Silver nanoparticles are being used in industries[5] and also have shown to improve antimicrobial and anti-cancer activity besides having a significant role in the drug delivery system.[6,7]

Various chemical[8–10] and physical[11–13] methods have been used for the synthesis of nanoparticles. However, these methods are losing reputation due to low yield, high energy supplies and generation of toxic by-products.[14] The concept of green synthesis has evolved to overcome the above limitations for the synthesis of nanoparticles as it is cost-effective, bio-compatible and eco-friendly in nature. Various green methods such as using the microwave, electrochemical reduction, sono-chemical preparation, or supercritical technology[15–17] have been deployed for the synthesis of SNPs. Other than that, the use of micro- or marine organisms and plant extracts for the synthesis of SNPs are well accepted due to their biocompatibility or biomimetic approach.[18,19]

Moreover, the plant extracts not only act as reducing agents but also stabilize the preparation of nanoparticles.[20,21] They are rich in biomolecules that act as bio-reductants for the formation of metallic nanoparticles in the solution resulting in color change of the solution due to the surface plasmon resonance phenomenon.[22]

In the present study, a facile green method for the synthesis of silver nanoparticles (SNPs) using silver nitrate solution and *Putranjiva roxburghii* Wall. extract as the reducing agent has been reported.

Putranjiva roxburghii Wall. (Family Putranjivaceae) is an evergreen tree found growing in wild as well as cultivated in the Indian subcontinent. It is regarded as one of the best herbs for rejuvenation and restoration of the female reproductive system in the Indian traditional system of medicine. Apart from having analgesic, antipyretic, and anti-inflammatory activities[23,24] it is also used for treating azoospermia,[25] elephantiasis, eye infection, habitual abortion, sterility, constipation, cough, cold and fever.[26,27] In spite of tremendous ethnobiological importance, its anti-cancer properties have not been fully explored yet and also there is no report on green synthesis of AgNPs (Silver nanoparticles) from *Putranjiva roxburghii* Wall. seed extract till now; hence, in the present article, we have prepared a novel nano-composite named '*Putranjiva roxburghii* Wall. seed extract mediated SNPs' (abbreviated as PJSNPs) to target tumor cells for the development of new anti-cancer agents, and characterized them using UV-Vis absorption spectrum, X-ray Diffraction (XRD), Transmission Electron Microscopy Energy-Dispersive X-ray Spectroscopy (TEM-EDAX), Scanning Electron Microscopy (SEM), Fourier Transform Infrared Spectroscopy (FTIR), Atomic Force Microscopy (AFM), Zeta potential and Raman spectroscopy. Additionally, the cytotoxic properties of PJSNPs and their anti-cancerous effects were investigated against HCT-116 (colon carcinoma), PANC-1 (pancreatic carcinoma), MDA-MB 231 (breast carcinoma) cell lines.

Materials and Methods

Materials

The seeds of *Putranjiva roxburghii* Wall. were a generous gift by Patanjali Ayurveda Ltd., Haridwar, India. The specimen was deposited at PHD, Patanjali Yogpeeth, Haridwar (Voucher no. PRIA/06/05/2017/002). The solvents, chemicals and kits were purchased from Merck, Sigma-Aldrich, and Invitrogen. The cell lines HCT-116 (colon carcinoma), PANC-1 (pancreatic carcinoma), MDA-MB 231 (breast carcinoma) were purchased from NCCS, Pune, India. The microorganism for antimicrobial study were procured from NCL, Pune, India. The blinded blood sample of a healthy volunteer was taken after obtaining his written consent by a registered clinician at Pathology lab, Patanjali Ayurvedic Hospital, Haridwar, India and was generously gifted to us. The study was approved by the Bioethical Committee for Scientific Research at the Patanjali Ayurvedic Hospital, Haridwar, India.

Preparation of Extract

About 10 g of seeds were milled into a fine powder and boiled for 2 hrs in 100 mL of deionized water. The extract was filtered to remove the particulate matter to get the clear solutions which were then refrigerated (4°C) for further experiments. At each and every step of the experiment, sterility conditions were maintained for the accuracy of the results.

Synthesis of PJSNPs

During the initial optimization procedure, different concentrations of silver nitrate solutions (1–10 mM) were prepared and treated with different amount of the seed extract (1–5 mL). The mixture was heated at 80°C for 1 hr. The best results were obtained with 1 mM $AgNO_3$ and 5 mL extract. So we proceeded with the best conditions for further experiments.[28]

On reduction of Ag^{+} to Ag^{o} in $AgNO_3$ solution, through the *Putranjiva* seed extract, the color of the solution changes. The formation of SNPs (Silver Nano Particles) was furthermore confirmed by spectrophotometric investigation (Absorbance scan 200–800 nm). The precipitate was collected by filtration, washed with deionized water several times, and finally dried in air at 60°C for 6 hrs.

Characterization of Nanoparticles

The prepared silver nanoparticles were analyzed and characterized using UV-Vis spectrophotometer (Shimadzu UV-1800), crystalline metallic silver was examined by X-ray diffractometer (Bruker D8), AFM (Shimadzu SPM9500J2), TEM (TEM-TECNAI-20-G2), FTIR (Cary 630), Raman spectrometer (Nuspec 2.0), Zeta-Sizer (Anton Paar MCP 300), and EDAX (JEOL, JSM-2100F).

Cell Lines & Culture Conditions

The human cancer cell lines, namely, HCT-116 (colon carcinoma), PANC-1 (pancreatic carcinoma) and MDA-MB 231 (breast carcinoma) were cultured in DMEM medium supplemented with 10% FBS (Invitrogen) and 1% antibiotic (Invitrogen) and grown overnight at 37ºC in a humidified atmosphere with 5% CO_2.

Peripheral Blood Mononuclear Cell (PBMC) Preparation and Cell Culture

The PBMCs were isolated from 5 mL of whole blood consisting of anti-coagulant EDTA (Sigma, MO, USA) from a healthy adult donor on a Ficoll-Hypaque (Hornby, Ontario, Canada) density gradient according to the method described earlier.[29] The cells were cultured within T25 culture flask (Corning Incorporated, NY, USA) for overnight in the supplemented RPMI (Sigma, MO, USA) with fetal bovine serum (FBS), 100 U/mL penicillin, 100 µg/mL streptomycin (Sigma, MO, USA) and 2 mM L-glutamine (Gibco, NY, USA) at 37°C for 24 h before any treatments. Before performing the experiment, the medium was discarded and the separated cells were washed and counted.

Cytotoxicity Assay

The MTT (3-(4,5-dimethylthiazol-2-yl)-2,5-diphenyltetrazolium bromide) assay is a colorimetric assay for determining cell viability. The NAD(P)H oxidoreductase enzymes may possibly reveal the number of viable cells as these enzymes can reduce the tetrazolium dye MTT to purple insoluble formazan. Cytotoxicity evaluation of $AgNO_3$, PJ & PJSNPs was performed in cancer cells (HCT-116, PANC-1 and MDA-MB 231) using MTT assay as described by Mosmann.[30] The cytotoxic effect of $AgNO_3$ & PJSNPs was also evaluated in PBMC cells. The cells were harvested and seeded at a density of 1×10^5 cells/mL in a 96-well plate and were incubated for 24 h in an incubator (37°C, 5% CO_2). A series of dilution (10 to 0.0097 mg/mL) of nanoparticles in the medium was added to the cells. After 24 h of incubation, 12 mM MTT stock solution was added to each well and was further incubated at 37°C for 4 hrs. Formazan crystals formed after 4 hrs in each well were dissolved in 100 µL of SDS-HCl solution and kept for incubation in a humidified chamber at 37°C for 4 hrs. The plate was read on a multi-mode plate reader (EnVision, Perkin Elmer) at 570 nm.

$$\%\ \text{Cell viability} = A_{570}\ \text{of treated cells}/A_{570}\ \text{of control cells} \times 100$$

Cell Apoptosis Assay

The number of apoptotic cells induced by PJSNPs with different concentrations was measured by flow cytometry using Annexin V-FITC-PI kit (Sigma-Aldrich, Germany). The Annexin V-PI assay evaluates phosphatidylserine translocation from the inner to the outer layer of the plasma membrane which is an event typically associated with apoptosis. HCT-116, PANC-1 and MDA-MB 231 cells (2×10^5 per well) were seeded into 6-well plates and treated with IC_{50} concentrations of PJSNPs. Both control and treated cells were incubated for 24 hrs in an incubator (37°C, 5% CO_2). Following the incubation, the cells were washed twice with PBS. Later, the cells (1×10^6 cells/mL) were resuspended in 1X binding buffer. Subsequently, 5 µL each of AnnexinV-FITC and propidium iodide were added to control and treated cell lines. The tubes were incubated at room temperature for exactly 15 min and protected from light. Finally, the cells were analyzed by flow cytometry (FC500, Beckman-Coulter, Hialeah, FL, USA). The controls used to set up compensation and quadrants were unstained cells, cell stained with FITC and Annexin V and cell stained with PI. Flow cytometric analysis was performed using Partec FloMax software.

DNA Fragmentation Assay

The suspension of HCT-116, MDA-MB 231, PANC-1 (10^6 cells/mL) were seeded in 6-well microplates and

treated with IC_{50} concentration of PJSNPs. The DNA extraction was done using a salting-out method. Extracted DNA was run on a 1% agarose gel for 20 min by applying 100 V, which was then stained with ethidium bromide, and the bands were detected using an ultraviolet transilluminator.

Statistical Analysis

The results are presented as mean ± standard deviation of three experiments. Analysis of the dose–response curve was done using the Software GraphPad Prism 7. IC_{50} values were determined by plotting triplicate data points over a concentration range and calculating values using regression analysis of Prism software using a 95% confidence level.

Results and Discussion

Characterization of Silver Nanoparticles

UV-Vis Spectra Analysis

The synthesis of the SNPs in aqueous solution was monitored by recording the absorption spectra at a wavelength range of 200–800 nm (Figure 1A). As the plant extract was mixed with $AgNO_3$, the color of the reaction mixture changed from brown to reddish brown (Figure 1A inset) due to excitation of surface plasmon resonance (SPR) vibration of silver nanoparticles,[22] while no color change was observed in the absence of plant extract in $AgNO_3$. The complete color change took after about 30 mins; thereafter, no further color of the reaction mixture changed, indicating that the silver salt present in the reaction mixture has been reduced completely. Nanoparticles absorb light at a different wavelength and get excited due to charge density at the interface between conductor and insulator, the mechanism known as surface plasmon resonance. The absorbance peak between 400 and 450 nm by UV-Vis analysis is the characteristic of SNPs[31] and the results obtained are in complete correlation with the earlier studies.[21,32] The change in color and λ_{max} with a prominent peak around 420 nm correspond to SNPs formation. SPR peak located between 410 and 450 nm has been observed for SNPs and might be attributed to spherical nanoparticles.[31,33,34]

Raman Spectroscopic Analysis

Raman spectroscopy (Deitanu Rock Hound Nuspec 2.0) can be used to study chemical identification, characterization of molecular structures, effects of bonding, environment and the stress of the compounds. The *Putranjiva roxburghii* Wall. capped silver nanoparticles are fine black powder, highly photosensitive towards a wide range of light wavelength similar to the majority of silver compounds.

The most representative Ag_2O spectrum shows a very intense band with a peak at 146 cm^{-1} attributing to Ag lattice vibrational modes, ie, phonons (Figure 1B). The range 200–580 cm^{-1} is characterized by a broadband in which it is possible to define Raman shifts at 288 and 537 cm^{-1}. The bands at 537 cm^{-1} can be ascribed to the n(Ag–O) vibrations for sub-surface species and n(O–O) mode for adsorbed molecular oxygen. The peak observed at 1030 cm^{-1} is probably due to chemosorbed atomic/molecular oxygen species.[35] Although sub-surface species might promote adsorption of molecular oxygen, it could also be a probable consequence of surface restructuring in silver nanoparticles.[36]

Atomic Force Microscopy

The surface topology of the PJSNPs was studied by atomic force microscopy analysis (Figure 1C). This method is used as a primary method to monitor SNPs dissolution and agglomeration pattern. The biologically synthesized silver nanoparticle size was measured using line profile determination of individual particles in the range of 32.85 x 32.85 nm.[37] The silver nanoparticles were imaged by AFM to understand the accurate configuration and to confirm that the silver nanoparticles were more or less homogeneous in size and shape. The topography of AFM micrograph clearly indicates that PJSNPs possess spherical shape with ~8 ±2 nm size measured using line profile determination of individual spherical-shaped particles.

X-Ray Diffraction Analysis

The XRD spectrum was recorded to confirm the crystalline structure of synthesized AgNP. The crystallographic structure of biologically synthesized silver nanoparticles (Table 1; Figure 1D) depicted four distinct peaks at 37.96°, 45.95°, 64.36° and 77.10° which were the corresponding values of (1 1 1), (2 0 0), (2 2 0) and (311) lattice planes of the face-centered cubic (FCC) silver, closely matching with the reported reference values.[38] All diffraction peaks could be well indexed with the cubic structure of silver (Ag) [JCPDS No. 087–0720]. The absence of any other chemical phase indicated the purity and crystallinity of the synthesized PJSNPs. A systematic increase in the broadening of the diffraction peaks with increasing 2θ indicated a concomitant reduction in particle size. The obtained diffraction spectrum strongly suggested the presence of silver nanoparticles in accordance with AFM and Raman spectrum analysis. The 2θ positions of lattice planes were

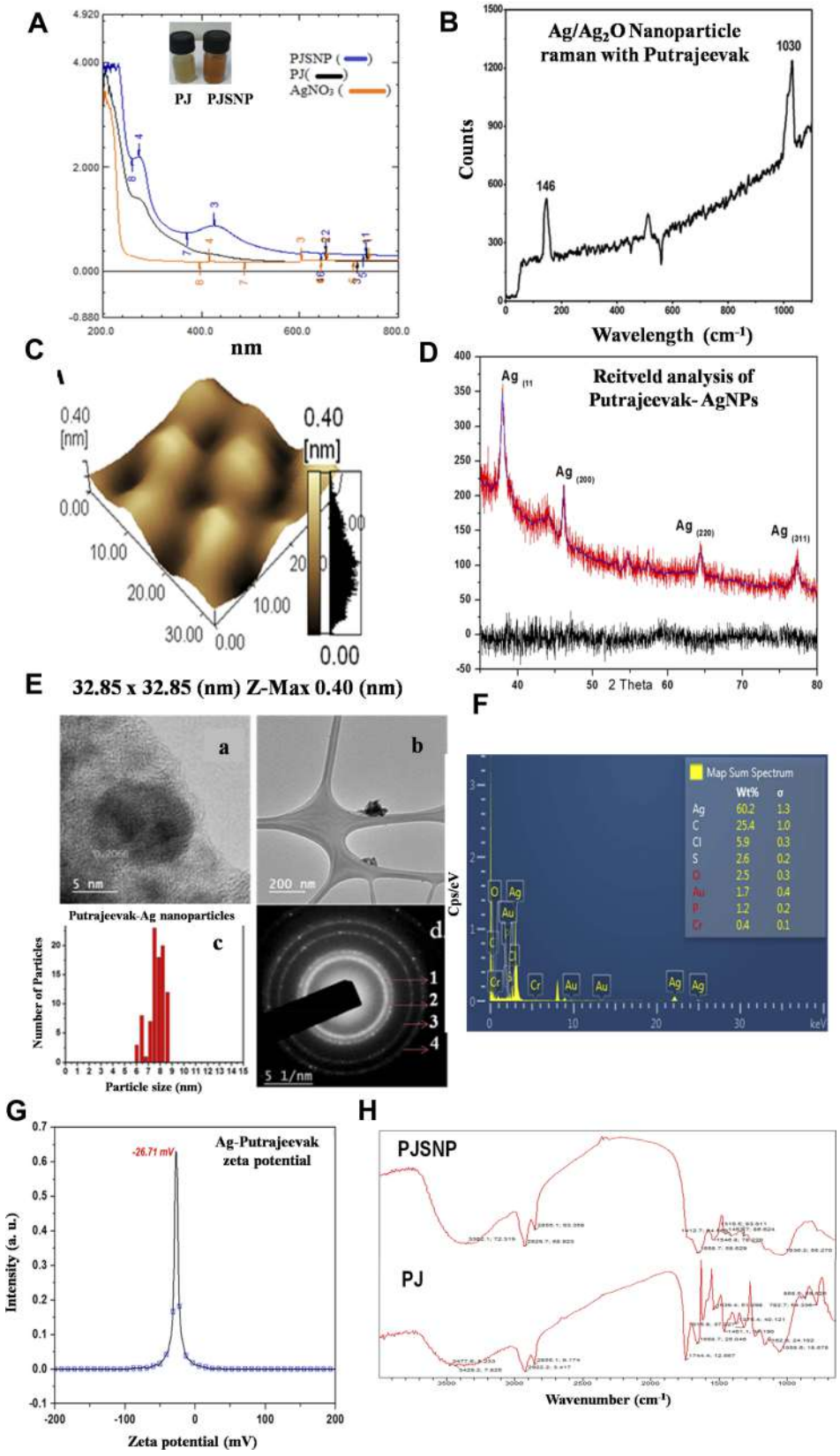

Figure 1 Characterization of silver nanoparticles synthesized using *P. roxburghii* seed extract. (**A**) UV–Vis spectra of PJ and PJSNPs (**B**) Raman spectra of PJSNPs (**C**) Atomic force microscopic image of PJSNPs (**D**) Calculated (Blue line) Rietveld refinement and Observed (Red line) plot of the powder XRD patterns for the Putrajeevak-Ag NPs (PJSNPs). The difference plot is at the bottom of the figure (blue line) and tick marks represent allowed reflections for each sample (**E**) Transmission electron microscopy of PJSNPs. HTEM micrograph (a and b) particle size distribution histogram (c) selected area diffraction pattern (d) (**F**) EDAX of PJSNPs (**G**) Zeta potential of PJSNPs (**H**) Fourier transformation infrared spectra PJSNPs and PJ extract.

Table 1 A Summary of Observed d-Spacings, hkl and Lattice Constant for the Biologically Synthesized PJSNPs

Sample Name	2θ (Degree)	FWHM (Degree)	Lattice Constant (A)	(hkl)	Standard d-Value	Observed d-Value
PJSNP	37.96	0.63	4.092	(111)	2.36	2.36
	45.95	1.16		(200)	2.04	2.01
	64.36	0.77		(220)	1.44	1.44
	77.10	0.67		(311)	1.23	1.23

slightly shifted towards the lower angle because of strain generation in silver nano-crystals due to the presence of *Putranjiva roxburghii* Wall. The resulting PJSNPs are highly uniform in phase & composition. The crystalline phase purity was confirmed by Rietveld refinement of XRD and the uniformity in composition was deduced from the Vegard's law because the occupancy refinement of PJSNPs cannot give a satisfactory measurement of the stoichiometry. The obtained results were consistent with the sizes of SNPs obtained from TEM analysis.

Apart from the characteristic peaks FCC Ag, the diffractogram also showed small hump-like peaks at 44.05° and 54.61° which may be due to the crystallization of the bio-organic phase on the surface of the SNPs. In the Rietveld analysis, the d-value at 44.05° and 54.61° were also under consideration limit but not matched with the SNPs lattice plane. Some other studies reported similar results with various additional peaks[39,40] and bio-organic compound/protein (s) might be responsible for such pattern. The authors have suggested that magnesium ions present in the chlorophyll might act as strong X-ray scattering centers in the bio-organic crystalline phase.[41]

Transmission Electron Microscopy and EDAX

The Transmission electron microscopy (TEM) provided further insight into the morphology and size details of the synthesized SNPs. Transmission electron micrograph reveals that PJSNPs are spherical, as can be observed in Figure 1E, HTEM micrograph (Figure 1E-a and b) and particle size distribution histogram (Figure 1E-c) correspond to silver nanoparticles formed after 24 h of reaction. PJSNPs sizes are ~8 ±2 nm. A typical selected area diffraction pattern is shown in the inset of (Figure 1E-d). Main Diffraction rings can be indexed as (111), (200), (220) and (311) reflections (indicated by numbers 1, 2, 3 and 4, respectively), corresponding to a face-centered cubic (FCC) crystalline structure of PJSNPs. In Figure (1E-a), few particles appeared with contrast difference, while the inorganic core Ag nanoparticles can be seen as darker contrast and polymer shell can be seen as lighter contrast.[42] The results are being in good agreement with XRD data. The SAED pattern of nanoparticles sample has also been shown in Figure (1E-d), which revealed a characteristic circular diffraction pattern corresponding to (111), (200), (220) and (311) planes of the face-centered cubic silver nanoparticles.

EDAX analysis shows the presence of eight elements (Ag, C, Cl, S, O, Au, P and Cr) in the PJSNPs powder (Figure 1F), where the silver (60.2 weight%) is present as major element followed by carbon (25.4 weight%), chlorine (5.9 weight%), sulfur (2.6 weight%), oxygen (2.5 weight%) and gold (1.7 weight%). However, some other unidentified peaks were also seen (contributing 1.7 weight%). Thus, this study indicates that pure crystalline nature is solely composed of silver. Similar studies exhibiting weak signals from Cl in synthesized SNPs colloid have also been reported which may be due to the presence of impurities in bacterial supernatant.[43]

As TEM coupled Oxford EDAX, microprobe analysis is a quantitative analysis of several spots was carried out, and finally, an average value of elements is considered. TEM and EDAX studies revealed the spherical nature of particles synthesized from silver metal.

Zeta Potential

Zeta potential experiments were carried out to investigate the electrostatic stability of the synthesized PJSNPs. The magnitude of the zeta potential is a measure of electrostatic repulsion between adjoining and similarly charged particles in a dispersion. Molecules or colloids with high zeta potential values are electrostatically stable in comparison to colloids with low zeta potential as in the later case attractive forces are greater than the repulsive forces resulting in coagulation.[44] In the present study, PJSNPs owned a zeta potential of −26.71 mV (Figure 1G) which suggests that the surface of the nanoparticles is negatively charged and dispersed in the medium. The negative value confirms the repulsion between the particles and proves that they are very stable. Also, the negatively charged particles are less cytotoxic compared to positively charged and the later ones are rapidly cleared from the bloodstream.[45]

Fourier Transform Infrared Spectroscopy

The FTIR measurement was studied to identify the possible biomolecules responsible as capping and reducing agent for the SNPs synthesized by the extract (Figure 1H). The intense broadbands at 3600 and 3200 cm^{-1} are probably due to the O–H and C–H stretching modes, respectively. The PJSNPs did not show any band at 1744 cm^{-1}, whereas the prominent band of the same frequency was observed in the PJ extract, indicating that the SNPs are stabilized through the C=O bond. Carbonyl groups of the amino acid residues and peptides of proteins have a strong affinity for metal binding, signifying the importance of protein as an encapsulating agent.[46] Similarly, the absence of a peak at 1461 cm^{-1} (C=C group) in PJSNPs is probably due to the reduction of $AgNO_3$ to Ag.[47] Comparison of the FTIR spectra of PJSNPs with PJ extract discloses the occurrence of functional groups such as amines, carboxylic acids, aldehydes and alcohols which are most likely to be accountable for reducing and capping the silver ions.[48]

Anticancer Potential of PJ Extract and PJSNPs

Brine Shrimp Lethality Assay

It is an important tool for the preliminary cytotoxicity screening of plant extracts based on the ability to kill laboratory-cultured brine shrimp. Criteria of toxicity followed were LC_{50} values >1000 µg/mL (non-toxic), 500 to 1000 µg/mL (weak toxicity) and <500 µg/mL (toxic).[49,50]

In the present study, four different concentrations (2, 20, 200 and 2000 µg/mL) of PJ extract, as well as PJSNPs, were used to access their cytotoxicity using the brine shrimp lethality assay. LC_{50} values for PJ (2000 µg/mL) were three times higher than the PJSNPs (632.45 µg/mL). As already reported LC_{50} values > 1000 µg/mL are non-toxic; consequently, PJ is non-cytotoxic in nature; however, PJSNPs exhibited weak toxicity in the brine shrimp lethality assay. The toxicity of silver nanoparticles against brine shrimp has also been reported in the literature.[51,52] Collectively, the cytotoxic effects of PJSNPs to brine shrimp can be associated with anti-cancer properties and could be developed further as an unconventional source of anti-cancer drugs. Therefore, we further studied the cytotoxic effect of the PJ extract and PJSNPs in the different cell lines using the MTT assay.

MTT Assay

The MTT reduction assay is used for the determination of the cytotoxic effect of a substance in the liver cells. The $AgNO_3$, PJ extract and PJSNPs were tested against PANC-1, MDA-MB 231 and HCT-116 cell lines. The results (Table 2; Figure 2) show the cytotoxicity at different concentrations (10 to 0.0097 mg/mL) in a dose-dependent manner which is supported by a previous study in which silver nanoparticles have affected the cell viability in a dose-dependent manner in a variety of mammalian cell lines.[53]

Table 2 IC_{50} Values of PJ, PJSNPs and $AgNO_3$ Against PANC-1, MDA-MB 231 and HCT-116

Compound	Cell Line	Cell Type	IC_{50} (mg/mL)
PJ	PANC-1	Pancreatic cancer cell line	8.6
PJ	MDA-MB 231	Breast cancer cell line	7.7
PJ	HCT-116	Colon cancer cell line	6.0
PJSNP	PANC-1	Pancreatic cancer cell line	0.36
PJSNP	MDA-MB 231	Breast cancer cell line	0.26
PJSNP	HCT-116	Colon cancer cell line	0.54
$AgNO_3$	PANC-1	Pancreatic cancer cell line	0.00025
$AgNO_3$	MDA-MB 231	Breast cancer cell line	0.00029
$AgNO_3$	HCT-116	Colon cancer cell line	0.00025

As compared to control, the percentage of cell growth inhibition was found to be very high with different concentrations of $AgNO_3$ followed by PJSNPs and PJ. The cytotoxic effect of $AgNO_3$ and PJSNPs were also tested in isolated PBMC cells where $AgNO_3$ caused cytotoxicity (55% cell viability) even at the lowest concentration (0.0097 mg/mL) whereas PJSNPs showed no toxic effect of the same concentration (Figure 3). The IC_{50} values of PJ extract (8.6, 6.0 and 7.7 mg/mL) were higher compared to PJSNPs (0.36, 0.54 and 0.26 mg/mL) and $AgNO_3$ (0.00025, 0.0025 and 0.0029 mg/mL) against PANC-1, HCT-116 and MDA-MB 231 cell lines after 24 hrs of incubation (Table 2). From the results, the cytotoxicity of $AgNO_3$ > PJSNPs > PJ which signifies the importance of nanonization of $AgNO_3$ to PJSNP as the former is showing toxicity in normal cells also at the lowest tested concentration. The reason for higher toxicity of PJSNPs may be due to the stimulation of reactive oxygen species (ROS) activity leading to various cellular events like cytotoxicity, unregulated cell signaling, DNA damage, apoptosis, and cancer.[54,55] In the previous studies, silver nanoparticles are reported to interfere with the electron-transport chain by activation of NADPH-related enzymes and depolarizing the mitochondrial membrane resulting in increased cellular levels of ROS.[56–58] In another study when human gliob lastoma and fibroblast cells were treated with silver

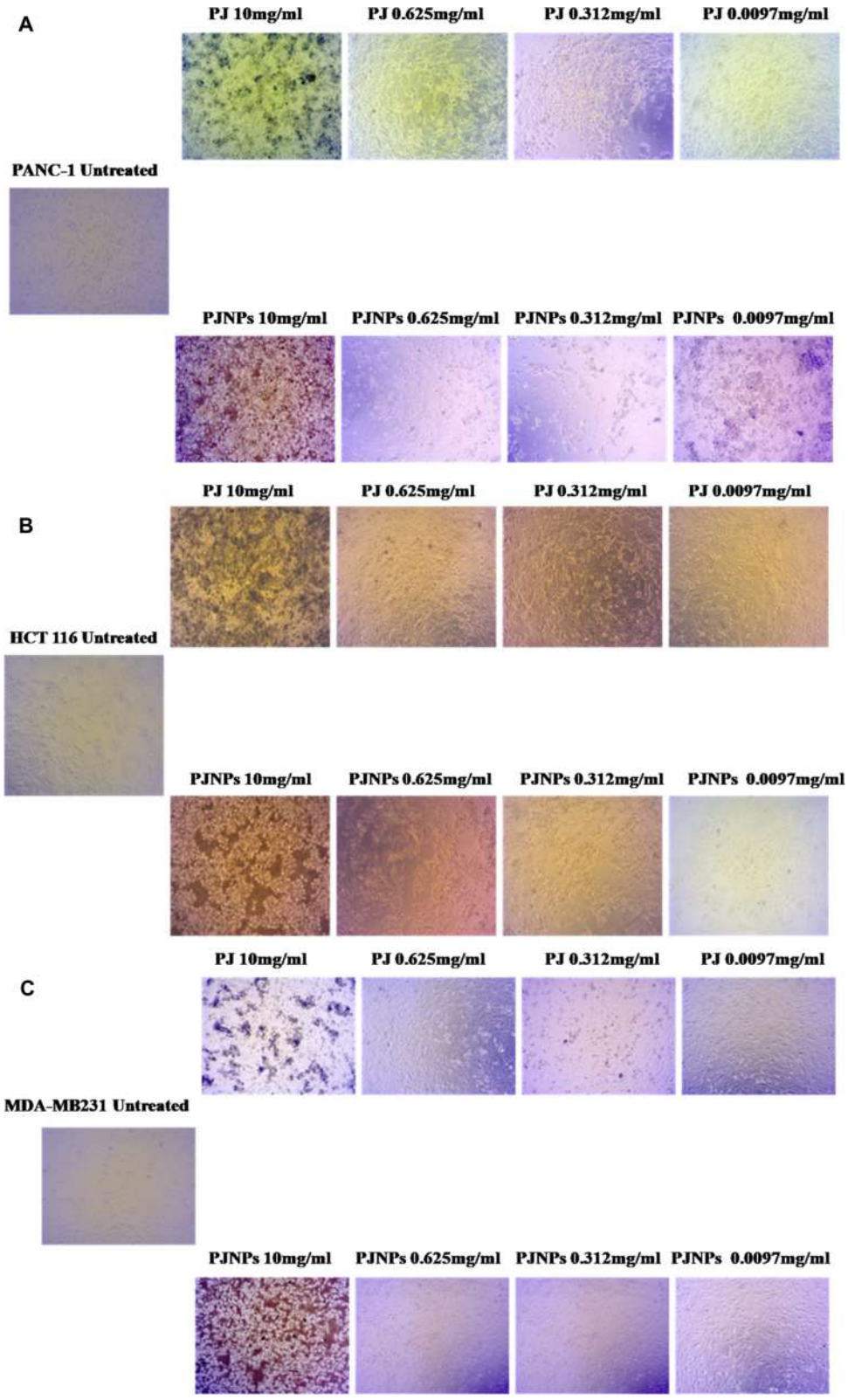

Figure 2 Effects of PJ extract and PJSNPs on cell viability against human cell lines based on MTT assay after 24 h of incubation. Cell lines treated with various concentrations of PJ and PJSNPs ranging from 0.0097 mg/mL to 10 mg/mL. Phase-contrast microscopy showing cytotoxic effect on (**A**) Pancreatic Carcinoma PANC-1; (**B**) Colon carcinoma HCT-116 and (**C**) Breast cancer MDA-MB 231 cells.

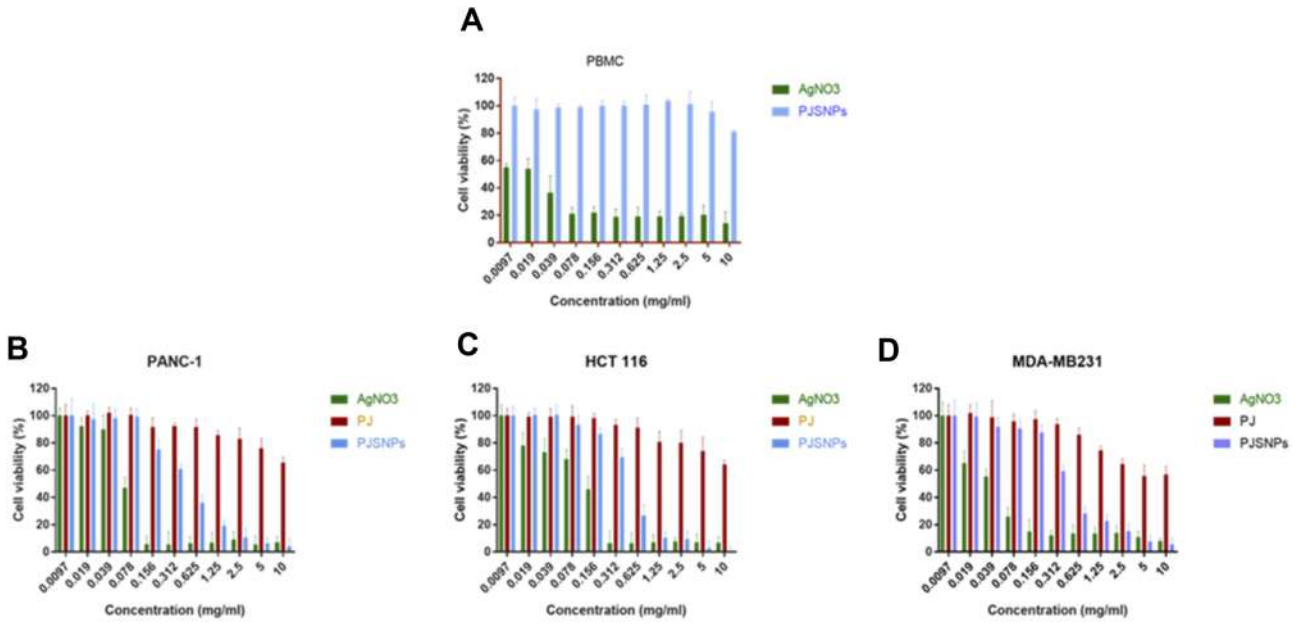

Figure 3 Comparative cytotoxicity of $AgNO_3$/PJSNPs on (**A**) PBMC (Peripheral Blood Mononuclear Cell as normal cell line); and $AgNO_3$/PJ/PJSNPs on (**B**) Pancreatic Carcinoma PANC-1; (**C**) Colon carcinoma HCT-116 and (**D**) Breast cancer MDA-MB 231 cell lines.

nanoparticles, high levels of ROS-mediated cytotoxicity were observed due to disruption of the electron-transfer chain.[59] However, in one of the studies, researchers reported a different mechanism which involves deactivation of enzymes by the formation of stable S-Ag bond with the thiol group of enzymes in the cell membrane; or denaturation of the DNA by breaking hydrogen bonds between nitrogen.[22] Some of the studies claim that the smaller the size of silver nanoparticles, the stronger is the cytotoxicity,[60,61] because the size has an effect on its uptake by the cells. We have also observed similar results in the present study that the small size (~8 ±2 nm) of PJSNPs may be the reason for better cellular activity of PJSNPs compared to PJ extract.

The cytotoxicity displayed by PJSNPs at lower concentrations might be linked to the phytoconstituents present in the plant extracts which are involved in AgNP formation.[62] Moreover, the cytotoxic effects of biosynthesized AgNPs against breast cancer MCF-7 cell line,[63] Hep-2 cancer cell line[64] and HeLa cell lines[65] also support our outcomes.

Apoptosis Induction

To find out if the mechanism of cell death is by apoptosis, the cancer cell lines were treated at IC_{50} concentration of PJSNPs. The results were evaluated by Annexin V-FITC/PI assay and DNA fragmentation assay.

(i) Annexin V-FITC/PI assay. Cell death induced by PJSNPs was investigated for apoptotic activity by monitoring Phosphatidylserine (PS) translocation using the Annexin V-FITC/PI assay. Early apoptosis is characterized by the translocation of PS from the inner layer of the plasma membrane to the outer surface.[66] Apoptotic cells are reflected by the quantification of Annexin V-FITC binding to externalized PS. In flow cytometer analysis, Annexin V/Propidium iodide (AnnV/PI) staining is based on the ability of the protein Annexin V to bind to Phosphatidylserine (PS), which is externalized in the outer cell membrane leaflet upon induction of apoptosis. In viable cells, PS is located in the inner-membrane leaflet, but upon induction of apoptosis, it is translocated to the outer-membrane leaflet and becomes available for Annexin V binding. The addition of PI enabled viable ($AnnV^-/PI^-$), early apoptotic ($AnnV^+/PI^-$), late apoptotic ($AnnV^+/PI^+$), and necrotic ($AnnV^-/PI^+$) cells to be distinguished.[67] The flow cytometry analysis of HCT-116, MDA-MB 231 and PANC-1 and cells showed that the cell population tended to shift from viable to apoptotic, on treatment with PJSNPs. After treatment with IC_{50} concentration of PJSNPs, the apoptotic cells were found higher in HCT-116 (71.5%), MDA-MB 231 (69.0%) and PANC-1 (76.8%) cells as compared to the respective control.

In contrast, the more number of live cells was found in untreated HCT-116 (87.2%), MDA-MB 231 (73.3%) and PANC-1 (99.1%) cells (Figure 4). In addition, the percent of dead (necrotic) cells observed in treated cells were 8.38, 1.18 and 3.78 in HCT-116, MDA-MB 231 and PANC-1, respectively (Figure 4). These results demonstrate the ability of PJSNPs to exert apoptosis in all the tested cancer cell lines.

(ii) DNA fragmentation assay. The DNA of HCT-116, PANC-1 and MDA-MB 231 cells treated with PJSNPs at IC_{50} concentration were extracted and loaded on the agarose gel. The results of DNA "laddering" pattern extracted from cells treated with PJSNPs are shown in Figure 5, (Supplementary Figure 1). The fragmentation pattern we observed was quite similar to that reported for cancer cell lines treated with silver nanoparticle.[68] It appears that during DNA fragmentation the silver particles accumulated inside the nucleus may possibly influence the DNA and cell division[69] by stimulating dose-dependent DNA damage, chromosomal aberrations, errors in chromosome segregation, sister chromatic exchanges and formation of micronuclei.[59,70] Consequently, it can be speculated that the similar pathways are pursued by PJSNPs to induce DNA fragmentation.

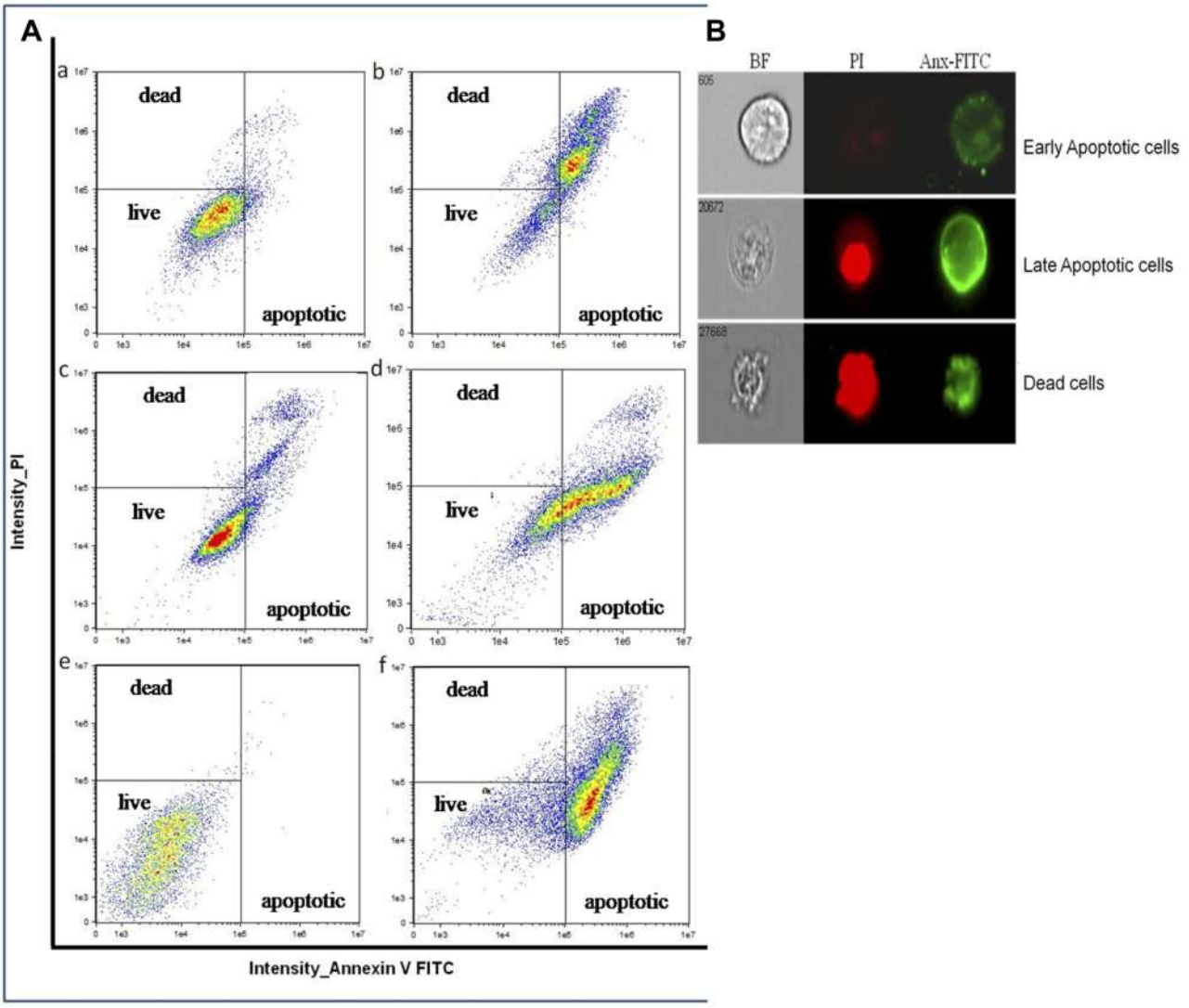

Figure 4 The PJSNPs induced apoptosis in three human cancer cell lines (HCT-116, MDA-MB 231 and PANC-1) after 24 h of incubation. Flow cytometer was used to collect 8000 cell count. Viable cells do not take any color (Annexin V^-/PI^-), early apoptotic cells (Annexin V^+/PI^-) are green, late apoptotic cells (Annexin V^+/PI^+) are green and red, and necrotic cells (Annexin V^-/PI^+) are red. (**A**) In the figure (a-b) represent HCT-116, (c-d) represent MDA-MB 231 cells and, (e-f) represent PANC-1 cells. (**B**) Figures represent fluorescence images obtained from the flow cytometer.

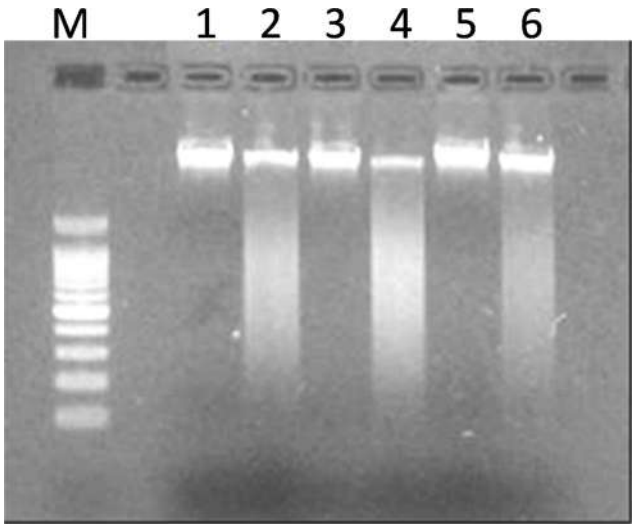

Figure 5 DNA ladder on agarose gel electrophoresis. Lane M: 100 bp ladder, L1: MDA-MB 231 control, L2: MDA-MB 231 treated, L3: HCT-116 control, L4: HCT-116 treated, L5: PANC-1 control, L6: PANC-1 treated.

Conclusion

Putranjiva roxburghii Wall. mediated silver nanoparticles (PJSNPs) were synthesized and characterized using various techniques. The silver nanoparticles were ~8± 2 nm spherical shaped, face-centered cubic having a negative charge. The small size and negative zeta potential could be the reasons that they are specifically taken up by the tumor cells. The biological studies indicated that aqueous extract of *Putranjiva roxburghii* Wall. seed was non-cytotoxic while the silver nanoparticles displayed weak cytotoxicity in the brine shrimp lethality assay. In MTT assay, PJSNPs displayed better cytotoxicity than PJ extract. However, $AgNO_3$ is toxic to normal cell also at the lowest tested concentration whereas PJSNPs showed no toxic effect at the same concentration. This reflects the importance of nanonization of $AgNO_3$ to PJSNP as the former is displaying toxic effect in normal cells also. In addition, the flow cytometric studies confirmed that the PJSNPs induced cell death via the apoptosis mechanism.

Thus, our findings propose the anticancer prospective of biosynthesized PJSNPs against human cancer cells and might play a significant role in the development of new and effective therapeutic agent for cancer treatment.

Acknowledgments

We are thankful to Patanjali Yogpeeth, Haridwar (India) for providing *Putranjiva roxburghii* Wall. seeds and to the Patanjali Ayurvedic Hospital, Haridwar (India) for providing blinded whole blood samples from healthy donors for the study. We also gratefully acknowledge UGC-DAE Consortium for Scientific Research, Indore (India) for providing the facilities for AFM, XRD and Raman, and the Indian Institute of Petroleum, Dehradun (India) for EDAX facility. The authors sincerely acknowledge Dr. L. N. Misra, Chief Research Advisor, Patanjali Research Foundation, Haridwar (India) for his suggestions and expert guidance in improving the quality of the paper.

Disclosure

The authors declare that they have no competing interests.

References

1. Lu W, Lieber CM. Nanoelectronics from the bottom up. *Nat Mater*. 2007;6:841–850. doi:10.1038/nmat2028
2. Shen Y, Friend CS, Jiang Y, et al. Nanophotonics: interactions, materials and applications. *J Phys Chem B*. 2000;104:7577–7587. doi:10.1021/jp0016131
3. Karni TC, Langer R, Kohane DS. The smartest materials: the future of nanoelectronics in medicine. *ACS Nano*. 2012;6:6541–6545. doi:10.1021/nn302915s
4. Nordberg G, Gerhardsson L. Silver. In: HG S, Sigel H, Sigel A, editors. *Handbook on Toxicity of Inorganic Compounds*. New York: Marcel Dekker; 1988:619–624.
5. Stark WJ, Stoessel PR, Wohlleben W, Hafner A. Industrial applications of nanoparticles. *Chem Soc Rev*. 2015;44(16):5793–5805. doi:10.1039/C4CS00362D
6. Jain S, Mehata MS. Medicinal plant leaf extract and pure flavonoid mediated green synthesis of silver nanoparticles and their enhanced antibacterial property. *Sci Rep*. 2017;7(1):15867. doi:10.1038/s41598-017-15724-8
7. Prow TW, Grice JE, Lin LL, et al. Nanoparticles and microparticles for skin drug delivery. *Adv Drug Deliv Rev*. 2011;63(6):470–491. doi:10.1016/j.addr.2011.01.012
8. Nair R, Varghese SH, Nair BG, Maekawa T, Yoshida Y, Kumar DS. Nanoparticulate material delivery to plants. *Plant Sci*. 2010;179(3):154–163. doi:10.1016/j.plantsci.2010.04.012
9. Bankura KP, Maity D, Mollick MM, et al. Synthesis, characterization and antimicrobial activity of dextran stabilized silver nanoparticles in aqueous medium. *Carbohydr Polym*. 2012;89(4):1159–1165. doi:10.1016/j.carbpol.2012.03.089
10. Kora AJ, Arunachalam J. Assessment of antibacterial activity of silver nanoparticles on Pseudomonas aeruginosa and its mechanism of action. *World J Microbiol Biotechnol*. 2011;27(5):1209–1216. doi:10.1007/s11274-010-0569-2
11. Abid JP, Wark AW, Brevet PF, Girault HH. Preparation of silver nanoparticles in solution from a silver salt by laser irradiation. *Chem Comm*. 2002;7:792–793. doi:10.1039/b200272h
12. Solano-Ruiz E, Sato Berrú R, Ocotlán-Flores J, Saniger JM. Synthesis of silver nanoparticles by sonochemical induced reduction application in SERS. *J Nanopart Res*. 2010;9:77–81. doi:10.4028/www.scientific.net/JNanoR.9.77
13. Maity D, Kanti Bain M, Bhowmick B, et al. In situ synthesis, characterization, and antimicrobial activity of silver nanoparticles using water soluble polymer. *J Appl Polym Sci*. 2011;122(4):2189–2196. doi:10.1002/app.34266
14. El-Rafie MH, El-Naggar ME, Ramadan MA, et al. Environmental synthesis of silver nanoparticles using hydroxypropyl starch and their characterization. *Carbohydr Polym*. 2011;86(2):630–635. doi:10.1016/j.carbpol.2011.04.088

15. Kalathil S, Lee J, Cho MH. Electrochemically active biofilm-mediated synthesis of silver nanoparticles in water. *Green Chem*. 2011;13:1482–1485. doi:10.1039/c1gc15309a
16. Zaarour M, El Roz M, Dong B, et al. Photochemical preparation of silver nanoparticles supported on zeolite crystals. *Langmuir*. 2014;30:6250–6256. doi:10.1021/la5006743
17. Kessler MT, Hentschel MK, Heinrichs C, Roitsch S, Prechtl MH. Fast track to nanomaterials: microwave assisted synthesis in ionic liquid media. *RSC Adv*. 2014;4:14149–14156. doi:10.1039/C3RA47801G
18. Adil SF, Assal ME, Khan M, Al-Warthan A, Siddiqui MRH, Liz-Marzán LM. Biogenic synthesis of metallic nanoparticles and prospects toward green chemistry. *Dalton Trans*. 2015;44:9709–9717. doi:10.1039/C4DT03222E
19. Otari S, Patil R, Waghmare S, Ghosh S, Pawar S. A novel microbial synthesis of catalytically active Ag–alginate biohydrogel and its antimicrobial activity. *Dalton Trans*. 2013;42:9966–9975. doi:10.1039/c3dt51093j
20. Ghaffari-Moghaddam M, Hadi-Dabanlou R, Khajeh M, et al. Green synthesis of silver nanoparticles using plant extracts. *Kr J Chem Eng*. 2014;31(4):548–557.
21. Shiv Shankar S, Rai A, Ahmad A, Sastry M. Rapid synthesis of Au, Ag, and bimetallic Au core–ag shell nanoparticles using neem (*Azadirachta indica*) leaf broth. *Colloid Interf Sci*. 2004;275(2):496–502. doi:10.1016/j.jcis.2004.03.003
22. Ahmed S, Ahmad M, Swami BL, Ikram S. A review on plants extract mediated synthesis of silver nanoparticles for antimicrobial applications: a green expertise. *J Adv Res*. 2016;7(1):17–28. doi:10.1016/j.jare.2015.02.007
23. Reanmongkol W, Noppapan T, Subhadhirasakul S. Antinociceptive, antipyretic, and anti-inflammatory activities of *Putranjiva roxburghii Wall*. Wall. leaf extract in experimental animals. *J Nat Med*. 2009;63:290–296. doi:10.1007/s11418-009-0336-6
24. Rajagopal PL, Kiron SS, Sreejith KR, Aneeshia S. Phytochemical, antioxidant and anti-inflammatory studies on the leaves of *Putranjiva roxburghii*. *Am J Pharm Tech Res*. 2014;4:429–435.
25. Sahni KC. *The Book of Indian Tree*. 2nd ed. Himalays Publishing House; 2009:285–289.
26. Singh A, Dubey NK. An ethnobotanical study of medicinal plants in Sonebhadra District of Uttar, Pradesh, India with reference to their infection by foliar fungi. *J Med Plants Res*. 2013;6(14):2727–2746.
27. Maurya R, Dongarwar N. Studies on the medicinal uses of wild trees of Nagpur district. *Int J Life Sci Pharma Res*. 2012;2:21–25.
28. Khan MZH, Tareq FK, Hossen MA, Roki MNAM. Green synthesis and characterization of silver nanoparticles using Coriandrum sativum leaf extract. *J Eng Sci Tech*. 2018;13(1):158–166.
29. Molaae N, Mosayebi G, Pishdadian A, Ejtehadifar M, Ganji A. Evaluating the proliferation of human peripheral blood mononuclear cells using MTT assay. *Int J Basic Sci Medi*. 2017;2(1):25–28. doi:10.15171/ijbsm.2017.06
30. Mosmann T. Rapid colorimetric assay for cellular growth and survival: application to proliferation and cytotoxicity assays. *J Immunol Method*. 1983;65(1–2):55–63. doi:10.1016/0022-1759(83)90303-4
31. Raman RP, Parthiban S, Srinithya B, et al. Biogenic silver nanoparticles synthesis using the extract of the medicinal plant Clerodendron serratum and its in-vitro antiproliferative activity. *Mat Lett*. 2015;160:400–403. doi:10.1016/j.matlet.2015.08.009
32. Prathna TC, Chandrasekaran N, Raichur AM, Mukherjee A. Biomimetic synthesis of silver nanoparticles by Citrus limon (lemon) aqueous extract and theoretical prediction of particle size. *Colloids Surf B Biointerf*. 2011;82:152–159. doi:10.1016/j.colsurfb.2010.08.036
33. Zaheer Z. Silver nanoparticles to self-assembled films: green synthesis and characterization. *Colloids Surf B Biointerf*. 2012;90:48–52. doi:10.1016/j.colsurfb.2011.09.037
34. Rahisuddin A. Extracellular synthesis of silver dimer nanoparticles using Callistemon viminalis (bottlebrush) extract and evaluation of their antibacterial activity. *Spec Lett*. 2016;49:268–275. doi:10.1080/00387010.2016.1140654
35. Martina I, Wiesinger R, Jembrih-Simbürger D, Scheiner M. Micro-raman characterisation of silver corrosion products: instrumental set up and reference database. *E-Preserv Sci*. 2012;9:1–8.
36. Liang H, Li Z, Wang W, et al. Highly surface-roughened "Flower-like" silver nanoparticles for extremely sensitive substrates of surface-enhanced Raman scattering. *Adv Mater Tech*. 2009;21(45):4614–4618. doi:10.1002/adma.v21:45
37. Chistensen L, Vivekanandhan S, Misra M, Mohanty AK. Biosynthesis of silver nanoparticles using *Murraya koenigii* (curry leaf): an investigation on the effect of broth concentration in reduction mechanism and particle size. *Adv Mater Lett*. 2011;2(6):429–434. doi:10.5185/amlett.2011.4256
38. Al-Harbi MS, El-Deeb BA, Mostafa N, Amer SA. Extracellular biosynthesis of SNPs by the bacterium Proteus mirabilis and its toxic effect on some aspects of animal physiology. *Adv Nanoparticles*. 2014;3(3):83. doi:10.4236/anp.2014.33012
39. Shaik MR, Khan M, Kuniyil M, et al. Plant-extract-assisted green synthesis of silver nanoparticles using origanum vulgare L. Extract and their microbicidal activities. *Sustainability*. 2018;10(4):913. doi:10.3390/su10040913
40. Tripathy A, Raichur AM, Chandrasekaran N, Prathna T, Mukherjee A. Process variables in biomimetic synthesis of silver nanoparticles by aqueous extract of Azadirachta indica (Neem) leaves. *J Nanopart Res*. 2010;12:237–246. doi:10.1007/s11051-009-9602-5
41. Shankar SS, Ahmad A, Sastry M. Geranium leaf assisted biosynthesis of silver nanoparticles. *Biotechnol Prog*. 2003;2003(19):1627–1631. doi:10.1021/bp034070w
42. Jang J, Lim B. Facile fabrication of inorganic-polymer core–shell nanostructures by a one-step vapor deposition polymerization. *Angewandte Chemie*. 2003;115(45):5758–5761. doi:10.1002/(ISSN)1521-3757
43. Vanaja M, Paulkumar K, Baburaja M, et al. Degradation of methylene blue using biologically synthesized silver nanoparticles. *Bioinorg Chem Appl*. 2014;2014.
44. Hanaor D, Michelazzi M, Leonelli C, Sorrell CC. The effects of carboxylic acids on the aqueous dispersion and electrophoretic deposition of ZrO_2. *J Eur Ceram Soc*. 2012;32:235–244. doi:10.1016/j.jeurceramsoc.2011.08.015
45. Honary S, Zahir F. Effect of zeta potential on the properties of nano-drug delivery systems-a review (Part 2). *Trop J Pharma Res*. 2013;12:265–273.
46. Kushwaha H, Malik C. Assessment of antibacterial and antifungal activities of silver nanoparticles obtained from the callus extracts (stem and leaf) of Tridax procumbens. *Ind J Biotechnol*. 2014;13:114–120.
47. He Y, Du Z, Lv H, et al. Green synthesis of silver nanoparticles by *Chrysanthemum morifolium* Ramat. extract and their application in clinical ultrasound gel. *Int J Nanomed*. 2013;8:1809–1815.
48. Philip D. Mangifera indica leaf-assisted biosynthesis of well-dispersed silver nanoparticles. *Spectrochim Acta a Mol Biomol Spectrosc*. 2011;78(1):327–331. doi:10.1016/j.saa.2010.10.015
49. Déciga-Campos M, Rivero-Cruz I, Arriaga-Alba M, et al. Acute toxicity and mutagenic activity of Mexican plants used in traditional medicine. *J Ethnopharmacol*. 2007;110:334–342. doi:10.1016/j.jep.2006.10.001
50. Bastos MLA, Lima M, Conserva LM, et al. Studies on the antimicrobial activity and brine shrimp toxicity of *Zeyheria tuberculosa* (Vell.) Bur. (Bignoniaceae) extracts and their main constituents. *Ann Clin Microbiol Antimicrob*. 2009;8:16–22. doi:10.1186/1476-0711-8-16
51. Kummara S, Patil MB, Uriah T. Synthesis, characterization, biocompatible and anti-cancer activity of green and chemically synthesized silver nanoparticles- A comparative study. *Biomed Pharmacother*. 2016;84:10–21. doi:10.1016/j.biopha.2016.09.003

52. Acharya B, Sharma N, Sharma VK, et al. Green synthesis, characterisation and biological studies of SNPs prepared using Shivlingi (*Bryonia laciniosa*) seed extract. *IET Nanobiotechnol*. 2017;12(3):371–375.
53. Sambale F, Wagner S, Stahl F, et al. Investigations of the toxic effect of silver nanoparticles on mammalian cell lines. *J Nanomater*. 2015;16(1):6.
54. Nel A, Xia T, Mädler L, Li N. Toxic potential of materials at the nanolevel. *Science*. 2006;311:622–627. doi:10.1126/science.1114397
55. Xia T, Kovochich M, Liong M, et al. Comparison of the mechanism of toxicity of zinc oxide and cerium oxide nanoparticles based on dissolution and oxidative stress properties. *ACS Nano*. 2008;2:2121–2134. doi:10.1021/nn800511k
56. Soenen SJ, Rivera-Gil P, Montenegro J-M, et al. Cellular toxicity of inorganic nanoparticles: common aspects and guidelines for improved nanotoxicity evaluation. *Nano Today*. 2011;6:446–465. doi:10.1016/j.nantod.2011.08.001
57. Smith KR, Klei LR, Barchowsky A. Arsenite stimulates plasma membrane NADPH oxidase in vascular endothelial cells. *Am J Physiol Lung Cell Mol Physiol*. 2001;280:L442–L449. doi:10.1152/ajplung.2001.280.3.L442
58. Xia T, Kovochich M, Brant J, et al. Comparison of the abilities of ambient and manufactured nanoparticles to induce cellular toxicity according to an oxidative stress paradigm. *Nano Lett*. 2006;6:1794–1807. doi:10.1021/nl061025k
59. AshaRani P, Low Kah Mun G, Hande MP, Valiyaveettil S. Cytotoxicity and genotoxicity of silver nanoparticles in human cells. *ACS Nano*. 2008;3:279–290. doi:10.1021/nn800596w
60. He D, Bligh MW, Waite TD. Effects of aggregate structure on the dissolution kinetics of citrate-stabilized silver nanoparticles. *Environ Sci Technol*. 2013;47:9148–9156. doi:10.1021/es400391a
61. Kittler S, Greulich C, Diendorf J, Köller M. Toxicity of silver nanoparticles increases during storage because of slow dissolution under release of silver ions. *Chem Mater*. 2010;22:4548–4554. doi:10.1021/cm100023p
62. Farah MA, Ali MA, Chen S-M, et al. Silver nanoparticles synthesized from adenium obesum leaf extract induced DNA damage, apoptosis and autophagy via generation of reactive oxygen species. *Colloids Surf B Biointerf*. 2016;141:158–169. doi:10.1016/j.colsurfb.2016.01.027
63. Vivek R, Thangam R, Muthuchelian K, et al. Green biosynthesis of silver nanoparticles from Annona squamosa leaf extract and its in vitro cytotoxic effect on MCF-7 cells. *Process Biochem*. 2012;47(12):2405–2410. doi:10.1016/j.procbio.2012.09.025
64. Jacob SJP, Finub JS, Narayanan A. Synthesis of silver nanoparticles using piper longum leaf extracts and its cytotoxic activity against Hep-2 cell line. *Colloids Surf B Biointerf*. 2012;91:212–214. doi:10.1016/j.colsurfb.2011.11.001
65. Suman TY, Radhika Rajasree SR, Kanchana A, et al. Biosynthesis, characterization and cytotoxic effect of plant mediated silver nanoparticles using Morinda citrifolia root extract. *Colloids Surf B Biointerf*. 2013;106:74–78. doi:10.1016/j.colsurfb.2013.01.037
66. Cury-Boaventura MF, Pompéia C, Curi R. Comparative toxicity of oleic acid and linoleic acid on Jurkat cells. *Clin Nutr*. 2004;23:721–732. doi:10.1016/j.clnu.2003.12.004
67. Baskić D, Popović S, Ristić P, Arsenijević NN. Analysis of cycloheximide-induced apoptosis in human leukocytes: fluorescence microscopy using annexin V/propidium iodide versus acridin orange/ethidium bromide. *Cell Biol Int*. 2006;30(11):924–932. doi:10.1016/j.cellbi.2006.06.016
68. Kalishwaralal K, Banumathi E, Pandian SRK, et al. Silver nanoparticles inhibit VEGF induced cell proliferation and migration in bovine retinal endothelial cells. *Colloids Surf B Biointerf*. 2009;73:51–57. doi:10.1016/j.colsurfb.2009.04.025
69. Wang J, Zhou G, Chen C, et al. Acute toxicity and bio distribution of different sized titanium dioxide particles in mice after oral administration. *Toxicol Lett*. 2007;168:176–185. doi:10.1016/j.toxlet.2006.12.001
70. Lu P-J, Ho I-C, Lee T-C. Induction of sister chromatid exchanges and micronuclei by titanium dioxide in Chinese hamster ovary-K1 cells. *Mutat Res Genet Toxicol Environ Mutagen*. 1998;414:15–20. doi:10.1016/S1383-5718(98)00034-5

Plant Cardenolides in Therapeutics

Article · September 2015

CITATION
1

READS
6,168

1 author:

Vinay Kumar Sharma
Patanjali Research Institute (PRI), Haridwar, India
58 PUBLICATIONS **1,757** CITATIONS

SEE PROFILE

Plant Cardenolides in Therapeutics

Acharya Bal Krishna
University of Patanjali, Haridwar, Uttarakhand - 249402, India
Email: acharyaji@divyayoga.com

Hemanth Kumar Manikyam
University of Patanjali, Haridwar, Uttarakhand - 249402, India
Email: phytochem2@gmail.com

Vinay K. Sharma
University of Patanjali, Haridwar, Uttarakhand - 249402, India
Email: vinay_sharma_2000@yahoo.com

Niti Sharma
University of Patanjali, Haridwar, Uttarakhand - 249402, India
Email: nitivinay@yahoo.co.in

ABSTRACT

Cardenolides have a long history of therapeutic relevance for treatment of heart failure and arrhythmia. Recently, they have emerged as promising agents in various diseases including cancer, cystic fibrosis, spinobulbar muscular atrophy and other polyglutamine-related diseases. The P glycoprotein inhibitory property of cardenolides makes them excellent targets to treat multidrug resistant cancers. In this review we have compiled the naturally occurring cardenolides from plants source and highlighted their multi-therapeutic role in treatment of various diseases which will be beneficial for future research.

Keywords- Cardenolides, Heart failure, Na^+/K^+-ATPase inhibitor, P Glycoprotein inhibition, NF- κB, Cancer**.**

Abbreviations: Na^+/K^+-ATPase, Sodium/Potassium-Adenosin Tri Phosphtase; NCX exchanger, Sodium Calcium Exchanger; SR, Sarcoplasmic Reticulum; SERCA2, Sarco/Endoplasmic Reticulum Ca^{2+}-ATPase; NF-kB, Nuclear Factor Kappa-light-chain-enhancer of activated B cells; bFGF, Basic Fibroblast Growth Factor; KLK, Kallikreins; FGF-2, Fibroblast Growth Factor-2; ROS, Reactive Oxygen Species

1. INTRODUCTION

Plants have been an integral part of primary health care since a very long time and are in use till today [1, 2]. In earlier times, mainly crude plant extracts were used for treating various ailments but later scientists started focusing on specific interactions between drug entity and biomolecules which developed the concept of "active constituent" leading to isolation of some of the early drugs from plants such as digitoxin and quinine [3-5]. Cardiac (from Greek word '*kardia*', meaning heart) glycosides are secondary plant metabolites which comprise of a potent group of naturally occurring drugs. On the basis of the structure they are classified as cardenolides and bufadienolides. The cardenolides have an unsaturated butyrolactone (5 membered) ring while the bufadienolides have a pyrone (6 membered) ring. The bufadienolides are characteristic features of some plants (members of Urginea) and toads' family Bufonidae, which are secreted as a defensive response to predators. Cardenolides, however, are produced almost exclusively by plants and serve to protect them from herbivory [2, 6-8]. This toxic attribute was exploited by humans to use them as arrow poisons [9, 10].

At low concentrations, cardenolides are priceless drugs for treating heart failure in humans. Oleandrin and oleandrigenin derived from *Nerium oleander* L. are used in the treatment of cardiac abnormalities in Russia and China for years [11]. The researchers have also conducted extensive pharmacological studies to prove cardiotonic activity of peruvoside [12, 13] on failing human heart. Another cardiac glycoside; tardigal, is used sometimes in place of digoxin as it has longer half-life than digoxin and is eliminated via the liver, unlike digoxin therefore could be used in patients with poor kidney function [14]. Many cardenolide have shown prominent anti-cancer activity [15-18]. Additionlly, cardenolides have role in treating various other diseases [19-22] and a number of cardenolides are marketed as drugs not only in US but also in several other countries**.**

Till date several reviews on cardiac glycosides have been published discussing cardenolides and bufadienolides together, describing their mechanism of action, structure-activity relationships, therapeutic applications and evolutionary ecology [20, 23-25]. However, a comprehensive review covering the latest studies on cardenolides alone is lacking. Therefore, in the current review article we have focused on the distribution, biosynthesis, mechanism of action and therapeutic applications of plant obtained cardenolides.

2. DISTRIBUTION OF CARDENOLIDES IN PLANTS

With a huge diversity of chemical forms, these secondary metabolites are sporadically distributed across various botanical families. Apocynaceae family has maximum number of cardenolides containing plants compared to other families. This family represents more than half of 55

cardenolide bearing genera, including the two genera (*Asclepias* and *Strophanthus*) with most cardenolide-bearing species [26]. Various plant families and the species containing cardenolides are Apocynaceae [6, 8, 27-73], Asparagaceae [74-79], Asteraceae [80], Brassicaceae [68, 81-88], Celastraceae [89-94], Combretaceae [95-97], Crassulaceae [98], Euphorbiaceae [99-101], Fabaceae [102, 103], Moraceae [104-113], Ranunculaceae [68, 114-117], Scrophulariaceae [36, 118], Solanaceae [119] and Malvaceae [120-125] **(Table 1)**. Cardenolides occur in all plant tissues though best studied in the leaves. After their synthesis they are either stored in cell vacuoles or loaded in the sieve tubes for transport to other sinks such as stem, leaves, flowers etc. A tissue specific expression of cardenolide was observed in Apocynaceae [26, 126-128] and Asparagaceae family [129]. The cardenolide concentration varies in different species of same genera. As among *Asclepias* species, *A. masonii* Woodson, *A. albicans* S. Watson, *A. viridis* Raf. and *A. erosa* Torr., have high cardenolide content while *A. incarnate* L., *A. tuberose* L. and *A. verticillata* L. are characterized by low cardenolide content. In fact, there is a remarkable difference in cardenolide content in various parts of same plant. For example, the relative concentrations of four cardenolides increase from the roots to leaves to stems to latex in *A. eriocarpa* Benth. [130]. A very high concentration of cardenolides was observed in latex of *A. humistrata* Walter compared to its leaves [131]. It is generally accepted that cardenolides are a potent chemical defense exhibited by the plants against various predators. In seeds of *A. syriaca* L., cardenolides are concentrated in the embryos; the parts on which Lygaeid bugs feed [132]. The high cardenolide in young leaves of *D. purpurea* L. protect the plant from grazing animals [133].Thus cardenolides have a significant role in providing chemical protection required for the plant survival.

Table 1 Some Cardenolides from Plants

S No.	Family	Species	Cardenolides (and Glycosides)
1	Apocynaceae	*Acokanthera schimperi* (A.DC.) Schweinf. *A. venenata* (Burm.f.) G.Don *A. deflersii* Schweinf. ex Lewin *A. longiflora* Stapf *A. spectabilis* (Sond.) Hook.f.	Ouabain (G-strophantin), Acovenoside A-C, Spectabilin [56]
		Adenium boehmanianum Schinz *A. somalense* Baif. *A. honghel* Lindl. *A. multiflorum* [*A. obesum* var. *multifiorum* (Klotsch) Codd]	Echujin, Hongheloside G (Somalin), Hongheloside A, C [60]
		Apocynum camrabinum L.	Cymarin [28]
		Cerbera odollam Gaertn.	Cerberin, beta-O-(2'-O-acetyl-l- thevetosyl)-15(14-->8)-abeo-5 beta-(8R)-14-oxo-card-20(22)-enolide (2'-O-acetyl cerleaside A, cerleaside A, 17 alpha-neriifolin, 17 beta- neriifolin [49]
		C. tanghin Hook.	Tanghinin
		C. mangus L.	Deacetyltanghinin, 17-α, 17-β Cerdollaside, 17-α, 17-β Solanoside, 17-α, 17-β Neriifolin, Cerberin, 12alpha-epoxy-(5beta,14beta,17betaH)-card-20 (22)-enolide, (-)-14-hydroxy-3beta-(3-O-methyl-6-deoxy-alpha-L-glucopyranosyl)-11alpha,12alpha-epoxy-(5beta,14beta,17betaH)-card -20(22)-enolide [31, 32, 45, 48]
		Nerium oleander L. *N. odorum* Lam. *N. indicum* Mill.	Oleandrin, Neriin, Neriantin, Neridiginoside, Nerizoside, Neritaloside, Odoroside-H, Cardenolides B, B-1 & B-2, Neriside, Odoroside A-B [30, 33, 43, 65, 66] 3beta-O-(beta-D-diginosyl)-14,15alpha-dihydroxy-5alpha-card-20(22)-enolide uzarigenin, cardenolide N-1 [64]

.		*Streptocaulon griffithii* J. D. Hooker	3beta,5beta,14beta-trihydroxyl-card-16,20(22)-dienolide, 3-O-beta-D-glucopyranosyl-5beta,14beta-dihydroxyl-card-16,20(22)-dienolide, digitogenin, 16-O-acetylgitoxigenin , periplogenin , 16-O-acetylperiplogenin, periplogenin digitoxoside , periplogenin-3-O-beta-D-glucopyranoside and periplogenin-3-O-beta-D-glucopyranosyl-(1-->4)-O-beta-D-digitoxopyranoside, 3-O(betaglucopyranosyl)acovenosigenin A, (17 alpha)-H-periplogenin-3-O-beta-D-glucopyranosyl-(1-4)-2-O-acetyl-3-O-methyl-beta-fucopyranoside [54,55]
		Streptocaulon tomentosum Wight & Arnott	Digitoxigenin 3-O-[O-β-D-glucopyranosyl-(1 → 4)-2-O-acetyl-β-D-digitalopyranoside] (1) and periplogenin 3-O-[O-β-D-glucopyranosyl-(1 → 4)-O-β-D-glucopyranosyl-(1 → 4)-β-D-cymaropyranoside [50]
		Streptocaulon juventas (Lour.) Merr.	1α, 14β-dihydroxy-5β-card-20 (22)-enolide 3-O-[O-β-D-glucopyranosyl-(1→2)-β-D-digitalopyranoside] , Acovenosigenin A 3-O-[O-β-D-glucopyranosyl-(1→4)-β-D-digitalopyranoside] , 16-O-acetyl-hydroxyperiplogenin 3-O-β-D-digitoxopyranoside , digitoxigenin 3-O-[O-β-D-glucopyranosyl-(1→6)-O-β-D-glucopyranosyl-(1→4)-2-O-acetyl-β-D-digitalopyranoside] , 16-O-acetyl-hydroxyacovenosigenin , 1β, 3β, 14β-trihydroxy-5β-card-16, 20 (22)-dienolide, Acovenosigenin A 3-O-beta-digitoxopyranoside , digitoxigenin gentiobioside , digitoxigenin 3-O-[O-beta-glucopyranosyl-(1-->6)-O-beta-glucopyranosyl-(1-->4)-3-O-acetyl-beta-digitoxopyranoside] (3), digitoxigenin 3-O-[O-beta-glucopyranosyl-(1-->6)-O-beta-glucopyranosyl-(1-->4)-O-beta-digitalopyranosyl-(1-->4)-beta-cymaropyranoside] , periplogenin 3-O-(4-O-beta-glucopyranosyl-beta-digitalopyranoside) [47,70,71]
		Strophantus gratus (Wall. and Hook.) Baill. *S. kombe* Oliver *S. hispidus* Stroph *S. sarmentosus* DC. *S. eminii* Asch. & Pax *S. boivinii* Baill.	Ouabain (G-strophantin), Cymarin, Sarmentocymarin, Periplocymarin, K-strophantin [6], Boivinide A-F [57]
		Thevetia neriifolia Juss. ex A.DC. *T. yecotli* A.DC.	Thevetin, Cerberin, Peruvoside Thevetosin, Thevetin A [27, 34] Neriifoside, Peruvoside and Lupeol acetate [39]
		Urechitis suberecta	Urechitin, Urechitoxin [6]

		Asclepias curassavica L.	Uzarigenin, Xysmalogenin, Coroglaucigenin , Gofruside , 6-O-(E-4-hydroxycinnamoyl)-desglucouzarin 6-O-sinapinoyl-desglucouzarin, Calactin , 16α-acetoxycalactin, Calotropin 16α-acetoxycalotropin , asclepin, 16α-hydroxyasclepin , 16α-acetoxyasclepin uscharin , 16α-hydroxyuscharin, uscharidin and 19-nor-16α-acetoxy-10β-hydroxyasclepin, 12beta,14beta-dihydroxy-3beta,19-epoxy-3alpha-methoxy-5alpha-card-20(22)-enolide, 12beta-hydroxycalotropin, 12beta-hydroxycoroglaucigenin, Calotropagenin , Desglucouzarin, 6'-O-feruloyl-desglucouzarin, Calotropin, Uscharidin , Asclepin [61, 62]
		A. eriocarpa Benth. *A. incarnate* L. *A. labriformis* M. E. Jones *A. syriaca* L. *A. tuberosa* L. *A. fruticosa* L.(syn. *Gomphocarpus fruticosus)* *Cryptostegia grandiflora* R. Br. *Oxystelma esculentum* R. Br.	Eriocarpin, Desglucosyrioside, Labriformin [8] Frugoside and Gofruside [46] Labriformin, Eriocarpin, Desglucosyrioside Syrioside, Syrioboside, Desglucosyrioside [36] Gomphoside, Afroside [227-229] 3'-spiro-linked thiazolidinone and S-oxythiazolidinone derivatives of delta5-Calotropin, 3'-O-beta-D-Glucopyranosyl delta5-calotropin, Cryptograndoside A-B [36, 44] Oxyline [38]
		Pergularia tomentosa L.	3'-O-beta-D-glucopyranosylcalactin 12-dehydroxyghalakinoside, 6'-dehydroxyghalakinoside, Ghalakinoside and Calactin, Pergulrotoside, Uscharidin, Calactin, 12 β-hydroxycalotropin, 6'-hydroxycalactin , and Galakinoside [37, 52, 72]
		Periploca graeca L. *P. nigrescens* Afzel. *P. forrestii* Schltr.	Periplocin [58] Strophantidin, Strophantidol, Nigrescin Periforosides D–H, Periforgenin C [63, 69]
		Xysmalobium undulatum	Xysmalobin, Uzarin.,Xysmalorin, Urezin, Uzaroside, Ascleposide, Glucoascleposide [68]
		Gomphocarpus fruticosus (syn. *Asclepias fruticosa*) (L.) W.T. Aiton *G. sinaicus* Boiss.	Uzarin,Uzarigenin, Gomphotin, Desglucouzarin, Gomphoside, Afroside [29, 35] 15 beta-hydroxycalotropin, 15 beta-hydroxy-7,8-dehydrocalotropin, Calotropin, 5,6-dehydrocalotropin, 3'-epi-afroside, 14 beta,17 alpha-epoxy-5,6-dehydrocalotropin, 15 beta-hydroxycalotropin, 15 beta-hydroxy-5,6 dehydrocalotropin, Coroglaucigenin-3-(6-deoxy-beta-D-allopyranoside)-19-acetate, 5,6-dehydrocalotropagenin and 16 alpha-hydroxy-5,6-dehydrocalotropin [40-42]
		Calotropis procera W.T. Aiton *C. gigantea* R. Br	Calotropin, Calactin, Uscharin, Calotoxin, 2''-Oxovoruscharin, Proceraside A [51, 68, 73] Asclepin [230, 231] 19-Nor- and 18,20-epoxy-cardenolides, Uscharin [53, 67]

2.	Asparagaceae	*Urginea fugax* (Moris) Steinh (syn. *Drimia fugax)* *Ornithogalum magnum* *O. thyrsoide* Jacq. *Convalaria majalis* L. *Tupistra chinensis* Baker.	Fugaxin [77] Ornithogalin [74] Ornithosaponin [78] Convalloside, Convallatoxin. Strophanthidin-3-O-6'-deoxy-beta-D-allosido-alpha-L-rhamnoside, Strophanthidin-3-O-6'-deoxy-beta-D-allosido-alpha-L-arabinoside, Srophanthidin-3-O-alpha-L-rhamnosido-2'-beta-D-glucoside, Cannogenol-3-O-6'-deoxy-beta-D-allosido-beta-D-glucoside, cannogenol-3-O-6'-deoxy-beta-D-allosido-alpha-L-rhamnoside, 19-hydroxy-sarmentogenin-3-O-alpha-L-rhamnoside, Sarmentogenin-3-O-6'-deoxy-beta-D-allosido-alpha-L-rhamnoside and Sarmentogenin-3-O-6'-deoxy-beta-D-guloside,Cannogenol-3-O-alpha-L-rhamnoside and Cannogenol-3-O-beta-D-allomethyloside [75,76] Tupichinolide [79]
3.	Asteraceae	*Saussurea stella* Maximowicz	3-O-beta-D-fucopyranosylstrophanthidin , 3-O-beta-D-quinovopyranosylperiplogenin and 3-O-beta-D-glucopyranosyl-(1 --> 4)-alpha- l-rhamnopyranosylcannogenin [80]
4.	Brassicaceae	*Erysimum cheiri* (syn. *Cheiranthus cheiri*) (L.) Crantz, *E. canescens* Roth *E. cheiranthoides* L. *E. inconspicuum* (S. Watson) MacMill *E. altaicum* Maxim *E. marschallianum* Andrz. ex M. Bieb. *E. nuratensae* Popov ex Botsch. & Vved. *Syrenia siliculosa* (M. Bieb.) Andrz *E. diffusum* Ehrh. *E. violascens* Popov *E. cuspidatum* (M.Bieb.) DC *Draba nemorosa* L. *Cheiranthus allioni* Hort	Cheiroside A, Cheirotoxin. Erysimoside, Glucoerysimoside, Erycanoside [68, 81] Cheiranthosides I-VII, Erysimoside and Erychroside [84-86] Strophanthidin, Uzarigenin [83] Erysimin and Erysimoside [82] Desglucocheirotoxin, Canescein, Erydiffuside Gypsobioside Cuspidoside [82] Corchoroside A , Helveticoside, cellobiosyldigigulomethyloside, Erysimoside [88] Cellobiosyldigigulomethyloside [87]
5.	Celastraceae	*Euonymus hamiltonianus* (syn. *E. sieboldianus*) Wall. *E. alatus* (Thunb.) Sieb. *Elaeodendron* sp. *Crossopetalum gaumeri* (Loes.) Lundell	Euonymoside A [89] Acovenosigenin A 3-O-alpha-L-ramnopyranoside , Euonymoside A and Euonymusoside A [90] Digitoxigeninglucoside , Quinovoside , Xyloside, Elaeodendrosides T and U, Elaeodendrosides A-C, F-G, K –S [92-94] Securigenin-3beta-O-beta-6-deoxyguloside,19-hydroxy-sarmentogenin-3beta-O-beta-6-deoxyguloside,Sarmentogenin-3beta-O-[alpha-allosyl-(1-->4)-beta-6-deoxy alloside], and Securigenin-3beta-O-[alpha-allosyl-(1-->4)-beta-6-deoxyal loside] [91]

6.	Combretaceae	*Terminalia arjuna* (Roxb.) Wight & Arn. *Terminalia bellerica* (Gaertn.) Roxb.	14,16 dianhydrogitoxigenin-3-beta-D-xylopyranosyl (1 -->2)- O-beta-D-galactopyranoside16,17-dihydroneridienone 3-O-beta-D-glucopyranosyl-(1-->6)-O-beta-D-galactopyranoside [95, 97] Cannogenol 3-O-beta-D-galactopyranosyl-(1-->4)-O-alpha-L-rhamnopyranoside [96]
7.	Crassulaceae	*Bryophyllum delagoense* (syn. *Kalanchoe tuberose*) H. Perrier	Kalantubolide A-B [98]
8.	Euphorbiaceae	*Mallotus philippinensis* Muell. Arg *Trewia nudiflora* L.	Coroglaucigenin, Coroglaucigenin L-rhamnoside L-rhamnoside, Corotoxigenin, Corotoxigenin L-rhamnoside CHO L-rhamnoside, Corotoxigenin L-rhamnoside and Corogl-aucigenin L-rhamnoside [99, 101] Trewianin and Trewioside [100]
9.	Fabaceae	*Coronilla* sp. *Tamarindus indica* L.	Alloglaucotoxin, Corotoxigenin, Frugoside, Glucocorotoxigenin, Coronillobioside Coroglaucin, Glaucorin, Hyrcanoside, Scorpioside [102] Uzarigenin-3-O-beta-D-xylopyranosyl (1 -->2)-alpha-L-rhamnopyranoside [103]
10.	Moraceae	*A. toxicaria* (Pers.) Lesch. (Var. *Antiaris africana* Engler)	Antiarin Alpha & Beta,Toxicarioside M, Toxicarioside H, Toxicarioside F –G, Antiarosides J-X, Antiarosides A-I, Antiarotoxinin A, Antiaritoxiosides A-G and Antiarotoxinin B, Periplogulcoside, Convallatoxin , Convallatoxol, Convalloside, 3-O-ß-D-Xylopyranosyl strophanthidin Glucostrosphanthidin, Strophanthidin [105-112] Toxicarioside D [104] Toxicarioside J-L, Glucostrophalloside [109] Strophalloside [113]
11.	Ranunculaceae	*Adonis vernalis* [Adon]. (syn. *A. apennina*) *A. aestivalis* L. *A. autumnalis* L. *A. flammea* Jacq. *A. amurensis* Regel & Radde	Strophanthidin digitaloside and Strophanthidin 6-deoxyguloside [114] Adonidin, Adonin, Cymarin, Adonitoxin [68] Strophanthidin-3-O-beta-D-digitoxosido-alpha-L-cymarosido-be ta-D-glucoside and strophanthidin-3-O-beta-D-digitoxosido-beta-D-digoxoside-bet a-D-diginosido-beta-D-glucoside, 3β,5α,14β,17β-tetrahydroxycard-20,22-enolide [115, 116] Amurensiosides L-P [117]
12.	Scrophulariaceae	*Digitalis purpurea* L. *D. lanata* L.	Digitoxin, Gitoxin, Gitalin, Digoxin, Glucodigifucoside , 3'-O-Acetylglucoevatromonoside , Digitoxigenin 3-O-β-D-glucopyranosyl-(1 → 4)-β-D-glucopyranosyl-(1 → 4)-3-O-acetyl-β-D-digitoxopyranoside, Purpureaglycoside A [118] F-gitonin, Digitonin, Lanatoside A-C [36]
13.	Solanaceae	*Nierembergia aristata* D. Don.	17-epi-11 alpha-hydroxy-6, 7-dehydrostrophanthidin-3-O-beta-boivinopyranoside, 6, 7-dehydrostrophanthidin-3-O-beta-boivinopyranoside , and 6,7-dehydrostrophanthidin-3-O-beta-oleandropyranoside [119]

14.	Malvaceae	*Corchorus aestuans* L. *C. olitorius* L. *C. trilocularis* L. *C. capsularia* L. *Reevesia formosana* Sprague	Cardenolides (glucoside A, B and C)[125] Cannogenol 3-O-beta-D-glucopyranosyl-(1-->4)-O-beta-D-boivinopyranoside, Periplogenin 3-O-beta-D-glucopyranosyl-(1-->4)-O-beta-D-digitoxopyranoside and Digitoxigenin 3-O-beta-D-glucopyranosyl-(1-->6)-O-beta-D-glucopyranosyl-(1-->4)-O-beta - D-digitoxopyranoside [122] Canarigenin 3-O-β-d-boivinoside, Corchoroside B [121] Corchortoxin, Corchorin(Stropanthidin)[120] Reevesioside A-I, Epi-reevesiosides F-I [123-124]

3. BIOSYNTHESIS OF CARDENOLIDES

Even though cardenolides have been used for centuries, still the exact biosynthetic pathway leading to 5 β-cardenolides is not yet clear and it is presumed that more than one pathway may be operative [134-135]. The "Pregnane pathway" include pregnenolone and progesterone whereas, in the "Norcholnic acid pathway" 23-nor-5,20(22)*E*-choldienic acid-3β-ol is the norcholnic acid equivalent of pregnenolone. The latter is operative only in the formation of fucose-type cardenolides. Nevertheless, a metabolic 'grid' instead of a linear biosynthetic pathway can better explain cardenolide biosynthesis as the intermediates of the pregnane pathway may serve as the substrates [136]. The different routes leading to final cardenolide are well described by Schebitz et al., [137] (**Fig. 1**). Cardenolide biosynthesis involves the transformation of sterols to pregnenolone. It is converted by Δ^5-3β-hydroxysteroid dehydrogenase (3βHSD; EC1.1.1.145) into isoprogesterone, which on isomerization forms progesterone. Progesterone 5β-reductase (P5βR; EC 1.3.1.3) catalyses 5β-reduction of progesterone to 5β-pregnan-3, 20-dione. As all cardenolides are 5β-configurated the stereospecific 5β-reduction of progesterone is a required step for cardiac glycoside biosynthesis in foxglove plants [138]. In a second stereospecific reaction, 3β-hydroxysteroid-5β-oxidoreductase converts 5β-pregnan-3,20-dione into 5β-pregnan- 3b-ol-20-one. Sequential hydroxylations at C14, C21 and the lactone ring formation at C17 lead to aglycone digitoxigenin. Stereospecific reactions determine that all the *Digitalis* cardenolides are β-configured at C3, C5, C14 and C17. The therapeutic role of cardenolides is based not only on the structure of aglycones, but also on the type and number of sugar units attached at C3. The secondary cardenolides (without sugar) are actively transported into the vacuole by a primary glycosidetranslocase after glucosylation by cytoplasmatic glucosyltransferases [139]. The polarity improves upon glucosyltion and therefore prevents its passive efflux out of the vacuole. The interconversion of primary to secondary cardenolides may be responsible for their existence in various plant tissues such as the latex [140] and the nectar of some milkweeds [141].

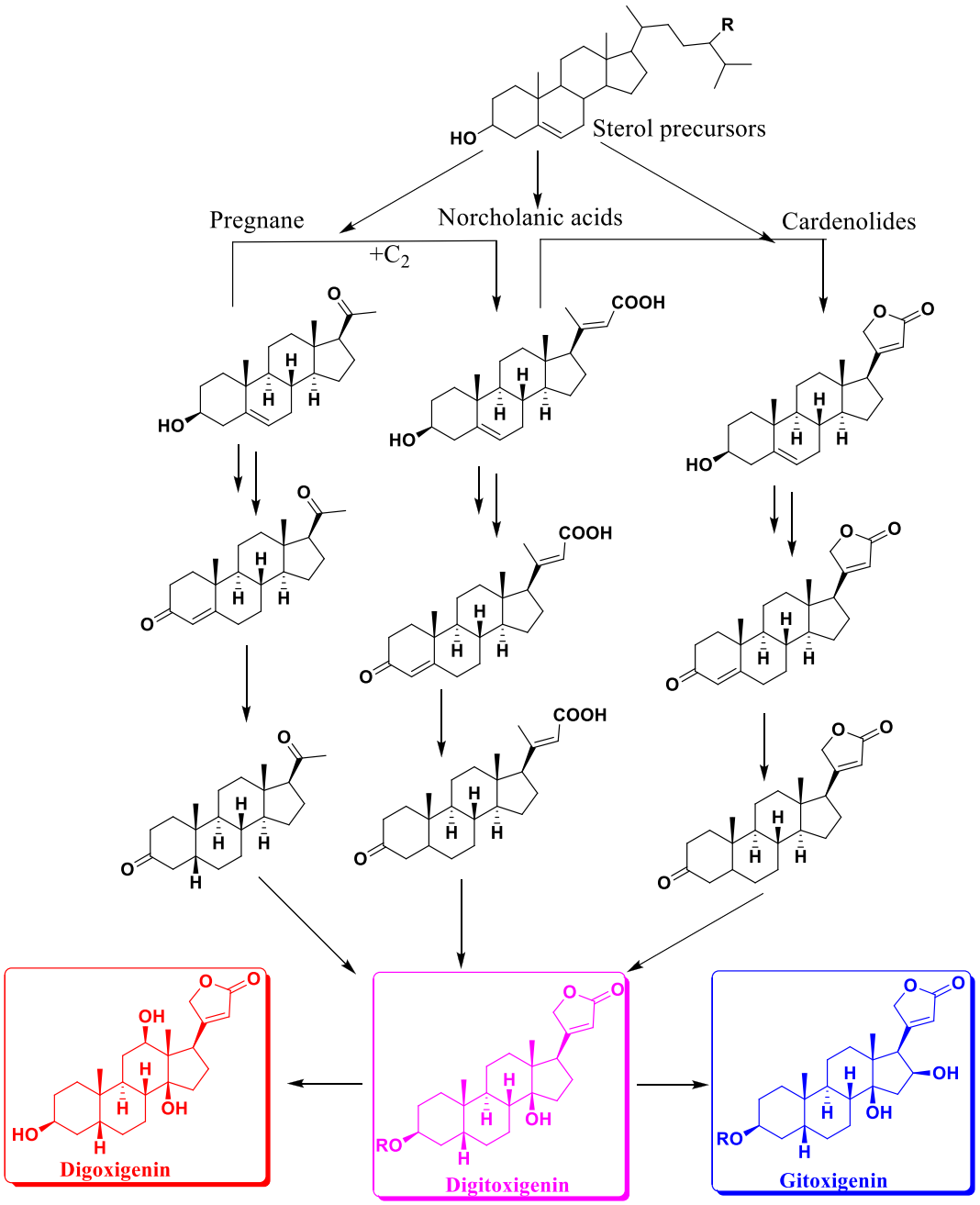

Figure 1 Proposed Pathways for the Preparation of Cardenolides, (i) Pregnane, (ii) Norcholanic acids, (iii) Cardenolides as per described by Schebitz et. al. [137]

3.1 Mechanism of Action of Cardenolides for their ATPase Activity

Cardiac glycosides are allosteric inhibitors of Na^+/K^+-ATPase [EC 3.6.3.9] [23]. The inhibition of Na^+/K^+-ATPase by cardiac glycosides is highly specific which implies that Na^+/K^+-ATPase is the receptor for cardiac glycosides. The catalytic site of the enzyme faces the intracellular matrix while the regulator site (cardiac glycoside binding site) is towards extracellular matrix. Sodium and potassium activates the enzyme at intracellular and extracellular site, respectively. During catalysis, the enzyme undergoes several conformational changes involving phosphorylation (activated by sodium) and dephosphorylation (activated by potassium). These steps lead to transport of ions (Na^+, K^+) across the membrane [142]. Inhibition of Na^+/K^+-ATPase results in high intracellular sodium concentration which in turn inhibits NCX exchanger (responsible for pumping calcium ions out of the cell and sodium ions in (3Na/Ca) as a result calcium ions build up inside the cell, as well. Increased cytoplasmic calcium concentrations cause increased calcium uptake into the sarcoplasmic reticulum via the SERCA2 transporter. Raised calcium stores in the SR allow for greater calcium release on stimulation, so the myocyte can accomplish faster and more potent

contraction by cross-bridge cycling **(Fig. 2)**. This affects the electrical physiology of the heart, blocking atrioventricular (AV) conduction and reducing the heart rate by enhancing vagal nerve activity (negative chronotropy). Thus, cardiac glycosides not only act on cardiac fibers but also on cardiac nerves, pulmonary circulations, and on autonomic reflex activity [143, 144]. The vagomimetic action (decreased conduction velocity through the AV node), baroreceptor sensitization (resulting in anti-sympathetic activity) and renin-angiotensin system (neurohormonal deactivating effect), results in slowing heart rate so tht it can pump more blood per beat through the body. The diastolic phase lasts longer, thus decreasing the heart rate. Raised extracellular potassium decreases binding of cardiac glycoside to Na^+/K^+-ATPase. As a consequence, increased toxicity of these drugs is observed in the presence of hypokalemia. Cardiac glycosides are prescribed in conditions of atrial flutter, atrial fibrillation, paroxysmal tachycardia, congestive heart failure that cannot be controlled by other medication [145].

Recently, Na^+/K^+-ATPase has emerged as a flexible signal transducer which can activate several downstream signaling pathways and thus may have role in regulating several other disease conditions [146].

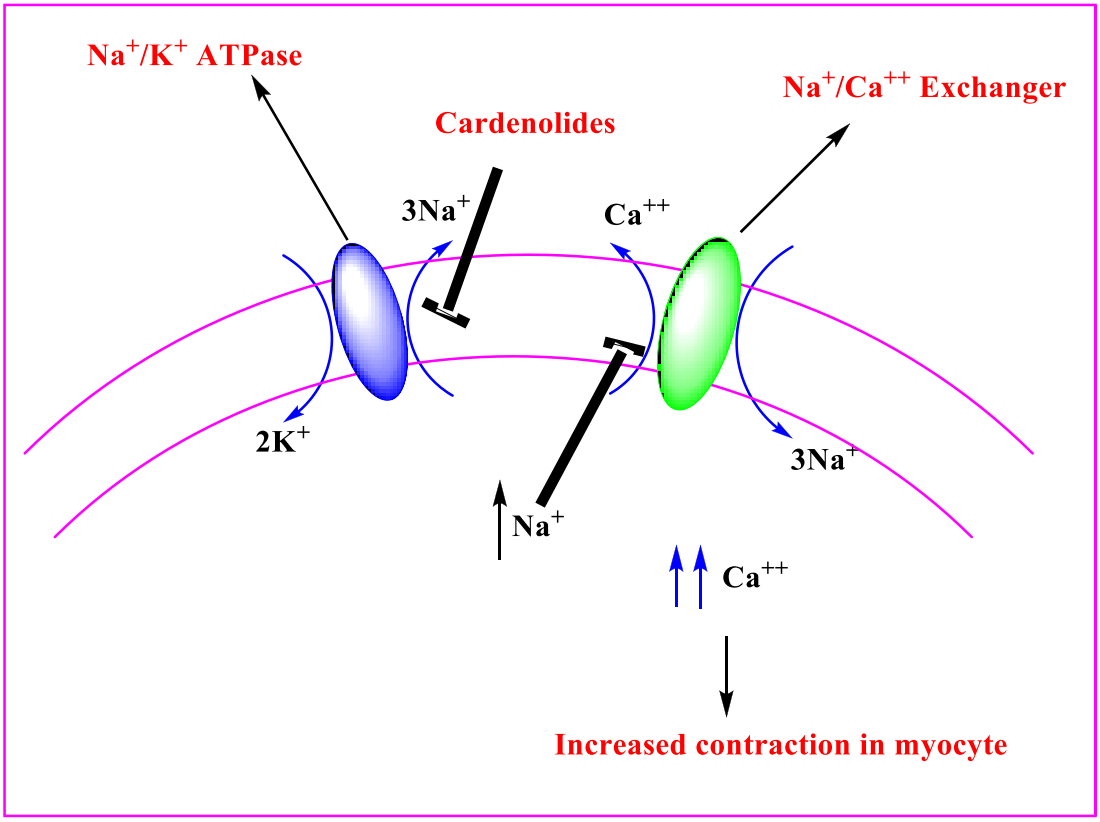

Figure 2 Mechanism of Action of Cardenolides

3.2 Structural Approach of Cardenolides towards their ATPase activity

The plants can synthesize both cardenolide type (e.g. *Convallaria majalis* L., *Antiaris toxicaria* Lesch, *Digitalis* L., *Nerium oleander* L., *Calotropis gigantea* (L.) W.T. Aiton) and bufadienolide type (e.g. *Drimia maritima* (L.) Stearn, *Kalanchoe* sp.) cardiac glycosides. Cardenolides are a group of remarkable steroidal glycosides derived from triterpenoids which possess a five-membered lactone group at C17, in the β position whereas the bufadienolides have a six-membered lactone ring at this position.

The cardenolides mainly have three key moieties which are crucial for their ATPase activity; the **steroidal moiety**: interacting at active site through hydrophobic binding, the **lactone ring** which has two interacting points (i.e. an electron-deficient β-Carbon atom and the carbonylic oxygen atom), and finally the **sugar moiety** which interact through hydrophobic bond and a hydrogen bond at C5' and C3'-OH, respectively [23] **(Fig. 3)**.The steroidal moiety is considered to be the pharmacophore for the activity of digitalis-like glycosides that is necessary for receptor recognition [147, 148]. In quantitative structure activity studies the energetic calculations between pharmacophore and the receptor interaction, the steroidal moiety have the high interaction energy which implies a strong binding with amino acids at the active site [149, 150].

The lactone ring at C17β is another key moiety, playing a crucial role in the ATPase activity of the cardenolides [151].This ring contains two oxygen atoms which create high negative potential and thus increase the directionality of bond formation [152, 153]. It was confirmed by another

research that on replacing other groups (except OH, OCOMe and COOMe) at C17β the interaction energy decreases [154]. This further elaborates the importance of lactone ring in cardenolides for their ATPase activity. In addition, some synthetic cardenolides were also designed by replacing lactone ring with their synthetic counterparts (pyridine or pyridazine, furan ring), but none of them showed good inhibition. Further replacing Oxygen by Nitrogen (furanone by pyrrolidone) or Sulphur decreases the activity. However, some research showed that simple lactone is not much responsible for the activity of cardenolides [155, 156].

Sugars attached to the steroid motif also plays a crucial role for the ATPase activity of cardenolides, similarly like lactone ring the sugar moiety also by themselves do not show any activity [157] but their presence makes some impact on the overall activity of cardenolides. The activity of cardenolides is increased by increasing the sugar moieties as monosaccharide-aglycone > disaccharide-aglycone > trisaccharide-aglycone >> aglycone. The sugar moieties in cardenolide vary from common glucose, galactose, mannose or rhamnose, to other uncommon sugars, as digitoxose, thevetose, cymarose, allose or altrose. Interestingly, the sugar moieties conferred by 6'-deoxysugars show maximum activity. In addition, equatorial 4'-OH proves far better than its counterpart 4'-OH axial group for potent activity.

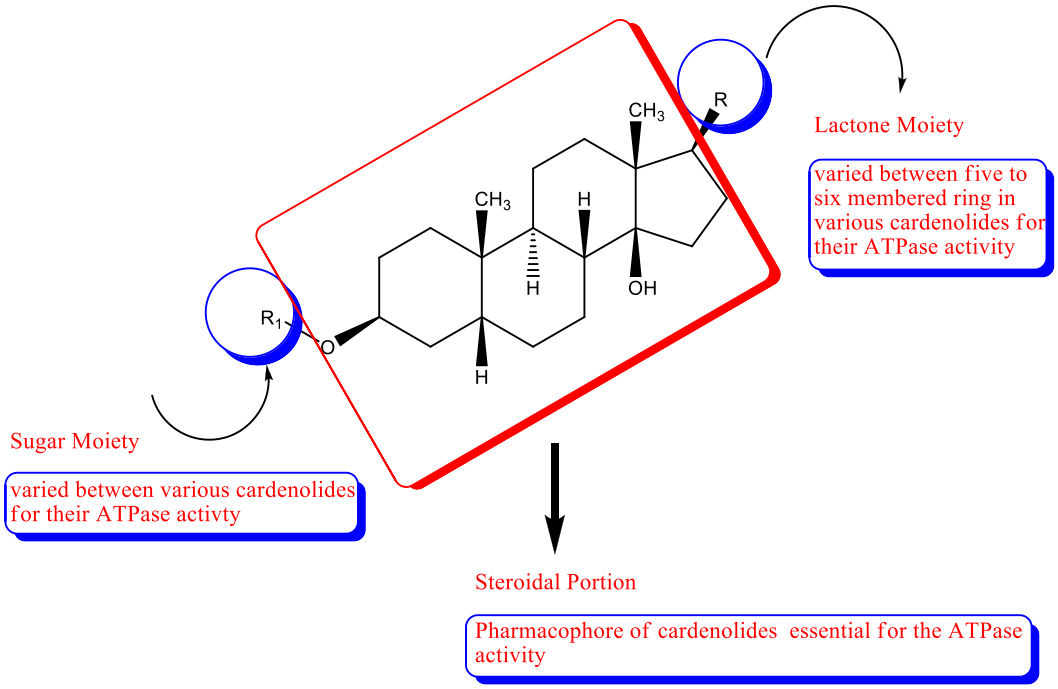

Figure 3 Key Structural Features of Cardenolides for ATPase Inhibitory Activity

3.3 Importance of Cardenolides as Heart Failure Drug

Cardiac glycosides have a long history in the treatment of cardiac disease. The digoxin and digitoxin are the two main cardenolides approved by US FDA for the treatment of heart failure **(Table 2).** The 1999 US consensus recommendations for the management of heart failure advocated administration of digoxin to improve the clinical status of patients with heart failure in combination with diuretics, an ACE inhibitor and a beta-blocker. They reported digoxin to be a favored drug in patients with rapid atrial fibrillation and to stop glycoside treatment in the case of considerable sinus or atrioventricular block [158].

The importance of digoxin in treating heart failure remain realistic as Digitalis Investigation Group (DIG) established that digoxin at low serum concentrations significantly reduced death rate in patients with chronic systolic and diastolic heart failure [159]. The drugs other than cardiac glycosides perform through calcium oscillations at concentrations that do not interfere with the pumping activity of Na^+/K^+-ATPase whereas cardiac-glycoside-based drugs preferentially activate the signaling properties of Na^+/K^+-ATPase which improves inotropy-to-toxicity ratio thus making them better drugs for the treatment of cardiac disorders [20]. Thus digoxin is the most acknowledged drug for rate control in atrial fibrillation, especially for heart failure patients [160].

Table 2. Cardenolide as Drugs Approved by various Countries

SNo	Compound	Structure	Brand*	Company/Country
1	**Acetyldigoxin ß-isomer**	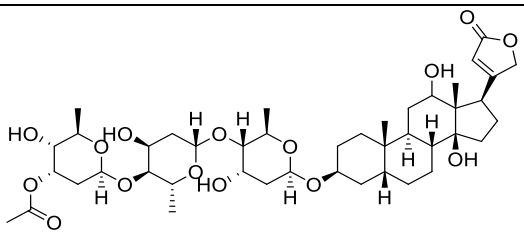	**β-Acetyldigoxin** **Digox-CT** **Digostada** **Novodigal** **Corotal** **Wabosan** **Lanatilin**	Ratiopharm, , Germany CT Arzneimittel Germany STADA Germany Mibe, Germany Austria Austria Unipharm, Bulgaria
2	**Calotropin**	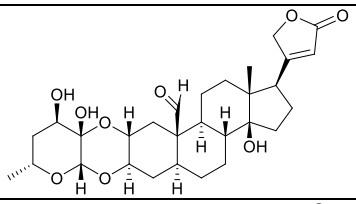		US Pharmacopeia
3	**Corglycon** (Convallotoxin)	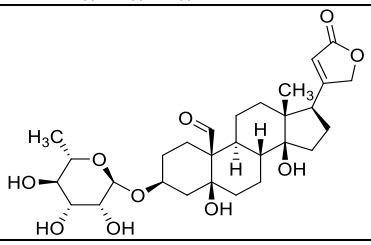	**Corglycon ®**	Arterium Co., Ukraine
4	**K-Strophanthin**	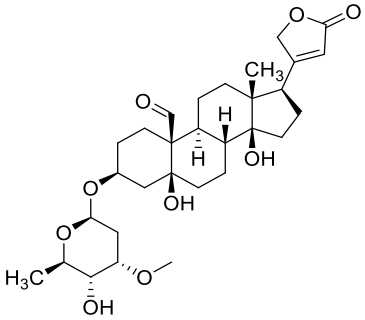	**Strophanthin K**	Double-Crane, China Halychpharm, Georgia
5	**Deslanoside**	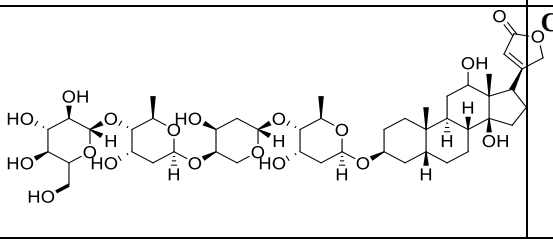	**Cedilanid-D**	Novartis, US

6	**Digitoxin**	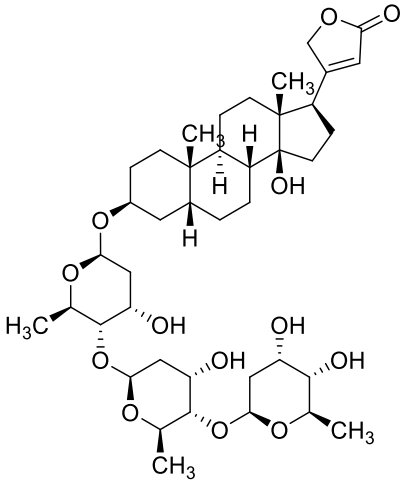	**Crystodigin** **Tardigal**	Lilly, US
7	**Digoxin**	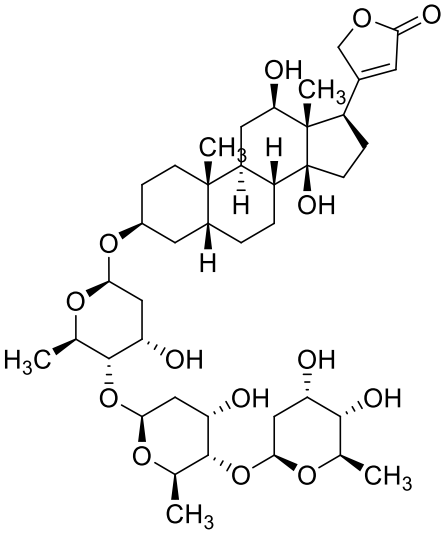	**Agoxin** **Apo-Digoxin** **Centoxin** **Cardiacin** **Cardiogoxin** **Cardiotoxin** **Celoxin** **Digacin** **Digocard-G** **Digoksino** **Digoregen** **Digosin** **Digosyp, Digox** **Digoxen** **Digoxicor** **Digoxin Alfresa** **Digoxin Alpharma**	Aristopharma, Bangladesh Apotex, Canada Opsonin, Bangladesh Center, Tiwan Medipharma, Argentina Oboi, Philippines Celon, India Mibe, Germany Klonal, Argentina; Medigroup, Peru Sanitas, Lithuania R.A.N., Germany Chugai Pharmaceutical, Japan; CJ Cheiljedang, South Korea Cadila, India Drug International, Bangladesh Briz, Latvia Alfresa Pharma, Japan Alpharma, Lithuania

			Digoxin Anfarm	Anfarm, Greece
			Digoxin Baxter	Baxter, United States
			Digoxin BioPhausia	BioPhausia, Sweden
			Digoxin Caraco	Caraco, United States
			Digoxin Dak	Nycomed, Denmark
			Digoxin Grindeks	Grindeks, Georgia; Grindeks, Latvia
			Digoxin Hospira	Hospira, United States
			Digoxin Impax	Impax, United States
			Digoxin Jugoremedija	Jugoremedija, Bosnia & Herzegowina
			Digoxin KY	Kyoto Yakuhin, Japan
			Digoxin Leciva	Zentiva, Czech Republic
			Digoxin NIHFI	NIHFI, Bulgaria
			Digoxin Nycomed	Nycomed, Estonia; Norway
			Digoxin Pasteur	Pasteur, Chile
			Digoxin R.A.N.	R.A.N., Germany
			Digoxin Richter	Gedeon Richter, Bulgaria
			Digoxin Roxane	Roxane, United States
			Digoxin SAD	SAD, Denmark
			Digoxin Sandoz	Sandoz, Canada;US
			Digoxin Sopharma	Sopharma, Bulgaria
			Digoxin Spofa	VUAB Pharma, Czech Republic
			Digoxin Stevens	JSP, United States
			Digoxin Taiyo	Taiyo Pharmaceutical, Japan

			Digoxin Teva **Digoxin West-Ward** **Digoxin WZF** **Digoxina, Lanoxin, Lanoxicaps, Lanoxin Lanicor**	Teva, Poland West-Ward, United States Polfa Warszawa, PolandGSK, US Roche, US
8	**Metildigoxin**	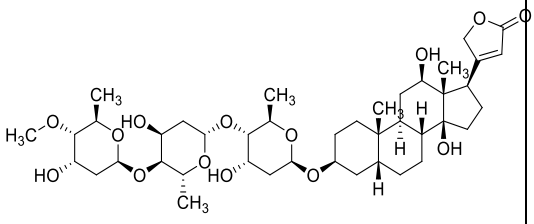	**Beikeli** **Bemecor** **Lanirapid** **Lanirapid** **Lanitop**	Sanofi Aventis, China Lek, Poland Chugai Pharmaceutical, Japan Kern, Spain Cheplapharm, Austria EuroCept, AGES, Austria Evolabis, Brazil Pharmakern, Portugal; Pliva, Croatia (Hrvatska); Slovenia Riemser, Bulgaria ; Czech Republic; Germany ; Greece ; Italy; Kenya Vargas, Venezuela
9	**Ouabain**	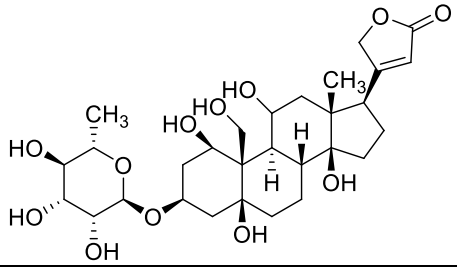	**Strodival** **Uabasin** **Ouabain**	Meda, Germany Taiwan Biotech, Taiwan Ta Fong, Taiwan.

3.4 Importance of Cardenolides in Cancer

There is a vast literature on cytotoxicity of cardenolides and numerous papers have been published describing the anti-cancer properties of these compounds *in vitro* the earliest report dating back to 1967 [161]. Since then, a number of experiments were conducted to establish anti proliferative effect of different cardenolides on various cancer cell lines, namely, leukaemia [162-164], breast [165-169], gastric [113], lung [70, 71, 170, 171], prostate [15, 73, 124], pancreatic [172, 173], melanoma [47, 88, 174, 175], neuroblastoma [176, 177], renal adenocarcinoma [118, 166, 178] and retinoblastoma [179]. Lower mortility rates have been observed in patients receiving cardenolide treatment though the exact mechanisms underlying these effects of cardenolides are not yet fully understood. Cardenolides works differently on normal and cancer cells [180-194] as at low serum concentrations cardenolides have shown to stimulate proliferation and inhibit cell death in normal cells. The cytoprotective effects might be useful in future therapies for the treatment of ischemic stroke and neurodegenerative diseases. On the other hand, cardenolides selectively induce death in cancer cells and are also reported to sensitize tumor cells to irradiation as reported for Ouabain [195, 196] which further enhances its therapeutic potential.

3.5 Mechanism of Action of Cardenolides for their Anti-Cancer Activity

Na+/K+-ATPase is an important target for anti-cancer treatment as its abnormal expression is reported in various types of cancer. Various researches have indicted a new role of sodium pump in cell adhesion and motility (for reviews [197-199]). In addition, the sodium pump interacts with neighbouring membrane proteins and get involved in different signalling pathways. As cardenolides are natural ligands for Na+/K+-ATPase, they interact with a number of signalling cascades ultimately affecting a variety of targets *e.g.* Toxicarioside A suppresses tumor growth through the endoglin/TGF-β signal pathway [16, 200, 201] while Calotropin does it by inhibiting Wnt signaling [202].

Strophalloside induces apoptosis through the mitochondrion-dependent Caspase-3 pathway [113] on the other hand, caspase-independent cell death was observed by Oubain [203]. Reevesioside A inhibits c-myc expression and down-regulates the expression of various cyclins leading to decreased RB phosphorylation and G1 arrest [124]. Cardenolides also work by inhibiting kallikreins (KLK, the serine proteases) [204] and fibroblast growth factor-2 (potent angiogenesis promoting substances) [205]. In an experiment, Anvirzel and Oleandrin were found to reduce the amount of FGF-2 to half in prostate cancer cells [206]. However, detailed studies on explaining the role of carenolides in regulating the activities of KLK and FGF-2 are presently under investigation.

The role of Oleandrin cannot be neglected in cancer research as it a potent antiproliferative agent in a wide variety of cancers [174, 207-211]. As a cytotoxic agent, it produces reactive oxygen species (ROS) and stimulates apoptosis. This may be due to its potential to inhibit P-glycoprotein [212]. The first cardenolide based anti-cancer drug, Anvirzel is under clinical trial for cancer [213] which is a patented extract from the *Nerium oleander* L. by Ozelle Pharmaceuticals Inc. **(Fig. 4)**. The supercritical CO_2 extract of *Nerium* (PBI 05204) is in Phase I clinical trial for the treatment of solid tumor [207]. To date three cardiac glycosides have been developed for treatment of cancer and are tested in a phase 1 clinical trial. The mechanisms of these anticancer effects may include decrease of intracellular K^+ and increase of Na^+ and Ca^{2+}; intracellular acidification; inhibition of IL-8 production, TNF-α/NF-κB pathway and DNA topoisomerase II; activation of the Src kinase pathway [214, 215]. Overexpression of P-glycoprotein (ABCB1, MDR1) is noted in certain cancer cells which may cause failure of chemotherapy leading to multidrug resistant cancers. Fortuntely, some cardenolides have been successfully screened for P-glycoprotein inhibitory activity. These novel compounds may serve as candidates to reverse doxorubicin resistance in leukemia cells [216, 217]. The modification of the sugar moiety of cardenolides can also alter the anti-cancer effect of these compounds [218, 219]. Such studies have opened new avenues for anti-cancer research and development of more effective drugs for the same.

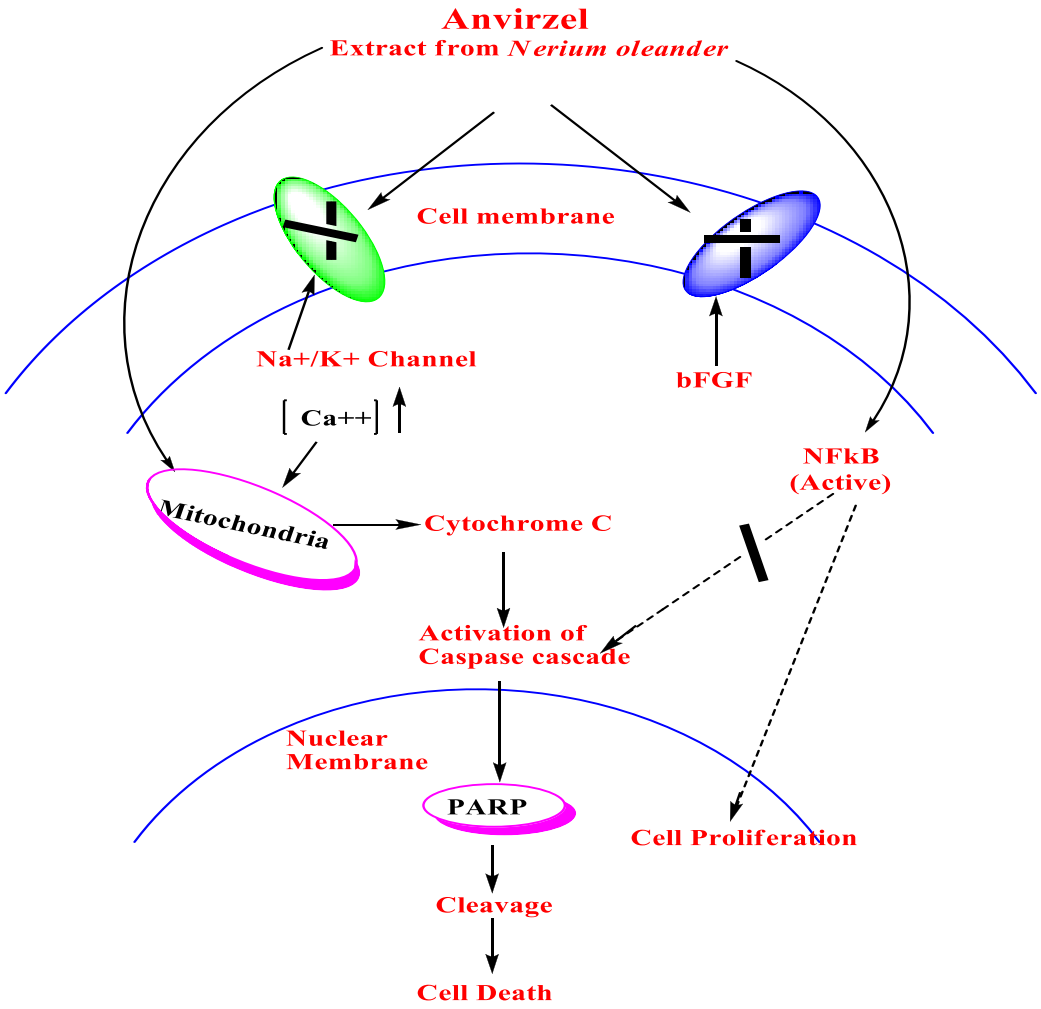

Figure 4 The Cardenolide based Anti-cancer Drug, Anvirzel showed a Distinctive way of Killing Tumor Cells as it (i) Activate Caspase Cascade, (ii) Inhibit Transport of bFGF, (iii) Blocks Na^+/K^+ Channel, (iv) Blocks the Activation of a Potent Signal (NF-kB) that leads to Tumor Cell Proliferation and Metastases [213]

3.5 Role of Cardenolides in other Diseases

Since centuries cardenolides were only reported for the treatment of heart disease, but recently a number of researchers reported their role in other diseases too. The potential application of cardiac glycosides for the treatment of cystic fibrosis was also reported [220]. The profound lung inflammation that characterizes cystic fibrosis is mainly attributed to an overproduction of IL-8 in the lungs. Oleandrin has shown to inhibit IL-8 mediated biological responses in diverse cell types by modulating IL-8 receptors through altering membrane fluidity and micro viscosity. A new link between cardiac glycosides and neurodegenerative diseases has been suggested [221]. A library of over one thousand FDA-approved drugs was screened for their ability to inhibit polyglutamine-dependent CASP3 activation. Interestingly, three of the four hits identified belong to the cardiac glycoside family (digitoxin, neriifolin and peruvoside) which suggests a new therapeutic role of these drugs for spinobulbar muscular atrophy and other polyglutamine-related diseases. Later, in a different study neriifolin, digoxin, digitoxin and ouabain were identified as the potent neuro-protective compounds [222]. Low concentrations of cardiac glycosides trigger downstream signaling cascades that can prevent apoptosis and induce proliferation [16, 69-71, 223]. These effects underlie possible therapeutic uses of cardiac glycosides in the context of ischaemic stroke. The protection of ischaemic heart tissue in rat by ouabain suggested the therapeutic potential of the mitochondrial ATP-sensitive potassium channels (K-ATP) in treating ischemic heart [224]. Anti-herpes activity of glucoevatromonoside, a cardenolide isolated from a Brazilian cultivar of *Digitalis lanata* is recently detected. The synergistic antiviral effects with acyclovir and anti-Na^+/K^+ATPase activity, suggests role of cellular electrochemical gradient alterations in the mechanism of viral inhibition thus, cardenolides might be promising for future antiviral drug design [225]. Also, the effectiveness of Anvirzel, on HIV infection of human peripheral blood mononuclear cells was studied and it was found as a novel candidate for anti-HIV therapeutic [22, 226]. Collectively, these data highlight a potential multi-therapeutic character for these compounds.

4. DISCUSSION & CONCLUSION

Cardenolides have a long history of therapeutic relevance for treatment of heart failure and are now emerging as promising agents in various diseases, especially cancer. Their main target is Na^+/K^+-ATPase, a membrane protein involved in cellular ion homeostasis and plays an important role in cancer biology by influencing numerous signaling pathways in both sensitive and drug-resistant cancer cells.The plant based cardiac-glycoside-based drugs preferentially activate the signaling properties of Na^+/K^+-ATPase which improves inotropy-to-toxicity ratio thus making them better drugs for the treatment of cardiac disorders. The recently discovered P-glycoprotein inhibitory property of cardenolides makes them excellent targets to treat multidrug resistant cancers.

As toxicity narrows the therapeutic window of cardenolides, more research is required to identify new naturally occurring cardenolides and design better cardenolides analoges on the basis of structure-activity relationship studies to limit the cardiovascular side-effects and improve the anti-cancer activity.

Conflict of interest

We wish to confirm that there are no known conflicts of interest associated with this publication and there has been no significant financial support for this work that could have influenced its outcome.

REFERENCES

[1] Patwardhan, B., et al., (2004), "Ayurveda and natural products drug discovery", Current Science, 86, pp 789-799.

[2] Lahlou, M., (2007), "Screening of natural products for drug discovery", Expert Opinion on Drug Discovery, 2, pp 697-705.

[3] Newman, D. J., et al., (2000), "The influence of natural products upon drug discovery", Natural Product Reports, 17, pp 215– 234.

[4] Butler, M.S., (2004), "The role of natural product chemistry in drug discovery", Journal of Natural Products, 67, pp 2141– 2153.

[5] Samuelsson, G., (2004), "Drugs of Natural Origin", a Textbook of Pharmacognosy, 5th Swedish Pharmaceutical Press, Stockholm.

[6] Watt, J. M., and Breyer-Brandwijk, M. G., (1962), **"**The medicinal and poisonous plants of southern and eastern Africa", E. & S. Livingstone, London, UK, 2nd edition.

[7] J. M. Benson, et al., , "Studies on the toxic principle of *Asclepias eriocarpa* and *A. labriformis*" in Effects of Poisonous Plants on Livestock, R. F. Keeler, K. R. Van Kampen, L. F. James, Eds. New York: Academic Press, 1978, pp. 273-284.

[8] Seiber, J. N., et al., (1978), "Three new cardenolides from the milkweeds *Asclepias eriocarpa* and *A. labriformis",* Phytochemistry, 17, pp 967–970.

[9] Bisset, N. G., (1989), "Arrow and dart poisons", Journal of Ethnopharmacology, 25, pp 1-41.

[10] Neuwinger, H. D., (1996), "African ethnobotany. Poisons and drugs. Chemistry, Pharmacology, Toxicology. Chapman & Hall, London.

[11] Hung, K. C., (1999), "The Pharmacology of Chinese Herbs," Boca Raton, FL. CRC Press, Inc., pp 53.

[12] Bhatia, M. L., et al. (1970), "Haemodynamic studies with peruvoside in human congestive

heart failure", British Medical Journal, 26, pp 740-743.

[13] Imai, S., et al., (1972), "A quantitative comparison of the cardiac actions of peruvoside with those of G-strophanthin and proscillaridin", Tohoku Journal of Experimental Medicine, 108, pp 389-399.

[14] Martindale, (1993), "The Extra Pharmacopoeia", Reynolds, J. E. F.(Ed). The Pharmaceutical Press, London, 30th Edition.

[15] Platz, E. A., et al., (2011), "A novel two-stage, transdisciplinary study identifies digoxin as a possible drug for prostate cancer treatment", Cancer Discovery, 1, pp 68-77.

[16] Li, Y. N., (2012a) "Toxicarioside A, isolated from tropical *Antiaris toxicaria*, blocks endoglin/TGF-β signaling in a bone marrow stromal cell line", Asian Pacific Journal of Tropical Medicine, 5, pp 91-97.

[17] Montano, C. J. M., et al., (2014), "Evaluating the cancer therapeutic potential of cardiac glycosides", Journal of Biomedical Research International, pp 1-9.

[18] Babula, P., et al., (2013), "From Na+/K+-ATPase and cardiac glycosides to cytotoxicity and cancer treatment", Anticancer Agents Med Chem, 13, pp 1069-87.

[19] Newman, R. A., et al., (2008), "Cardiac glycosides as novel cancer therapeutic agents", Journal of Molecular Interventions, 8, pp 36-49.

[20] Prassas, .I, and Diamandis, E. P., (2008), "Novel therapeutic applications of cardiac glycosides", Nature Reviews Drug Discovery, 7, pp 926-935.

[21] Anderson, E. S., et al., (2012), "The cardiotonic steroid digitoxin regulates alternative splicing through depletion of the splicing factors SRSF3 and TRA2B", RNA, 18, pp 1041-1049.

[22] Singh, S., et al., (2013), "*Nerium oleander* derived cardiac glycoside oleandrin is a novel inhibitor of HIV infectivity", Fitoterapia, 84, pp 32-39.

[23] Melero, C. P., et al., (2000), "A short review on cardiotonic steroids and their aminoguanidine analogues", Molecules, 5, pp 51-81.

[24] Dostanic-Larson, I., et al., (2006), "Physiological role of the alpha1- and alpha2-isoforms of the Na+-K+-ATPase and biological significance of their cardiac glycoside binding site", American Journal of Regulatory, Integrative and Comparative Physiology, 290, pp R524-8.

[25] Agrawal, A. A., et al., (2012), "Toxic cardenolides: chemical ecology and coevolution of specialized plant–herbivore interactions", New Phytologist, 194, pp 28–45.

[26] S. B. Malcolm, "Cardenolide-mediated interactions between plants and herbivores", in Herbivores: their interactions with secondary plant metabolites, 2nd edn, Vol. I: The chemical participants, G. A. Rosenthal, M. R. Berenbaum, Eds. San Diego, CA, USA: Academic Press, 1991, pp 251–296.

[27] Lang, H. –Y., and Sun, N. C., (1964), "The cardiac glycoside of *Thevetia peruviana* II. Isolation and identification of cerberin, ruvoside and a new cardiac glycoside.perusitin", Yao Hsueh Hsueh Po, 11, pp 464-472.

[28] Gerlach, H., et al., (1965), "On the cardiac glycosides from the roots of *Apocynum cannabinum* L. Isolation and separation of glycosides", Pharmazie, 20, pp 450-455.

[29] Chernobai, V. T., and Komissarenko, N. F., (1971), "Cardenolides of Gomphocarpus fruticosus and the partial synthesis of uzarigenin glycosides", Chemistry of Natural Compounds, 7, pp 421-424.

[30] Yamauchi, T., et al., (1976), "Cardiac glycosides of the root bark of *Nerium odorum*", Phytochemistry, 15, pp 1275–1278.

[31] Yamauchi, T., et al., (1987a), "Polar cardenolide glycosides from the leaves of *Cerbera odollam* and *Cerbera manghas* (III)", Chemical and Pharmaceutical Bulletin, 35, pp 2744-2749.

[32] Yamauchi, T., et al., (1987b), "Studies on Cerbera. IV. Polar cardenolide glycosides from the leaves of *Cerbera odollam* and *Cerbera manghas*", Chemical and Pharmaceutical Bulletin, 35, pp 4813-4818.

[33] Yamauchi, T., and Abe, F., (1978), "Neriaside, a 8, 14-seco-cardenolide", Tetrahedron Letters, 19, pp 1825–1828.

[34] Some, N., and Pousset, J. L., (1981), "African medicinal plants. IV. Technic for the extraction of thevetine from *Thevitia neriifolia*. Preparation of a cardiotonic drug", Dakar Medical, 26, pp 226.-233.

[35] Mutlib, A. E., et al., (1987), "*In vivo* and *in vitro* metabolism of gomphoside, a cardiotonic steroid with doubly linked sugar" Journal of Steroid Biochemistry, 28, pp 65–75.

[36] Fenwick, G. R., et al. (1989), "Toxicants of Plant Origin: Glycosides" CRC Press Inc, Florida.

[37] Hifnawy, M. S., et al., (1990), "Pergularotoside, a new cardiac glycoside from *Pergularia tomentosa* L", Al-Azhar Journal of Natural Products, 5, pp 186-197.

[38] Srivastava, S., et al., (1991), "A cardenolide tetraglycoside from *Oxystelma esculentum*", Phytochemistry, 30, pp 301-303.

[39] Siddiqui, S., et al., (1992), "Cardenolides and triterpenoids of the leaves of *Thevetia neriifolia*", Phytochemistry, 31, pp 3541–3546.

[40] El-Askary, H., et al. (1993), "Cardenolide glycosides with doubly linked sugars from *Gomphocarpus sinaicus*", Phytochemistry, 34, pp 1399-1402.

[41] El-Askary, H., et al. (1995), "Cardenolide glycosides from *Gomphocarpus sinaicus*", Phytochemistry, 38, pp 943-946.

[42] Abdel-Azim, N. S., (1998), "A cardenolide glycoside from *Gomphocarpus sinaicus*", Phytochemistry, 49, pp 273-275.

[43] Begum, S., et al., (1999), "Bio-active cardenolides from the leaves of *Nerium oleander*", Phytochemistry, 50, pp 435-438.

[44] Abe, F., and Yamauchi, T., (2000), "An Androstane Bioside and 3'-Thiazolidinone Derivatives of Doubly-linked Cardenolide Glycosides from the Roots of *Asclepias tuberosa*", Chemical & Pharmaceutical Bulletin, 48, pp 991-993.

[45] Chang, L. C., et al. (2000), "Activity-guided isolation of constituents of *Cerbera manghas* with antiproliferative and antiestrogenic activities", Bioorganic & Medicinal Chemistry Letters, 10, pp 2431-2434.

[46] Warashina, T., and Noro, T., (2000), "Cardenolide and oxypregnane glycosides from the root of *Asclepias incarnata L*", Chemical & Pharmaceutical Bulletin, 48, pp 516-524.

[47] Ueda, J. Y., (2003), "Antiproliferative activity of cardenolides isolated from *Streptocaulon juventas*", Biological and Pharmaceutical Bulletin, 26, pp 1431-1435.

[48] Cheenpracha, S., et al., (2004), "New Cytotoxic Cardenolide Glycoside from the Seeds of *Cerbera mangha*", Chemical & Pharmaceutical Bulletin, 52, pp 1023-1025.

[49] Laphookhieo, S., et al., (2004), "Cytotoxic cardenolide glycoside from the seeds of *Cerbera odollam*", Phytochemistry, 65, pp 507-510.

[50] Myint-Khine, M., et al., (2004), "New cardenolides from roots of *Streptocaulon tomentosum*", Fitoterapia, 75, pp 779-781.

[51] Van Quaquebeke, E., et al., (2005), "Identification of a novel cardenolide (2"-oxovoruscharin) from *Calotropis procera* and the hemisynthesis of novel derivatives displaying potent in vitro antitumor activities and high in vivo tolerance: structure-activity relationship analyses", Journal of Medicinal Chemistry, 48, pp 849-856.

[52] Hamed, A. I., et al., (2006), "Cardenolide glycosides from *Pergularia tomentosa* and their proapoptotic activity in Kaposi's sarcoma cells" , Journal of Natural Product, 69, pp 1319-1322.

[53] Lhinhatrakool, T., and Sutthivaiyakit, S., (2006), "19-Nor- and 18,20-epoxy-cardenolides from the leaves of *Calotropis gigantean*", Journal of Natural Products, 69, pp 1249-1251.

[54] Zhang, L., et al., (2006), "Two New cardenolides from the roots of *Streptocaulon griffithii*", Journal of Asian Natural Product Research, 8, pp 613-617.

[55] Zhang, X. H., et al., (2007), "Cytotoxic cardenolides from *Streptocaulon griffithii*", Chemistry & Biodiversity, 4, pp 998-1002.

[56] O. Bethwell, "*Acokanthera oppositifolia* (Lam.) Codd," in Medicinal plants/Plantes médicinales, G.H. Schmelzer, A. Gurib-Fakim, Eds. Netherlands: PROTA, Wageningen, 2007.

[57] Karkare, S., et al., (2007), "Cytotoxic cardenolide glycosides of *Roupellina (Strophanthus) boivinii* from the Madagascar rainforest", Journal of Natural Product, 70, pp 1766-1770.

[58] Spera, D., et al., (2007), "Antiproliferative cardenolides from *Periploca graeca*", Planta Medica, 73, pp 384-387.

[59] Zhao, M., et al., (2007), "Bioactive cardenolides from the stems and twigs of *Nerium oleander",* Journal of Natural Product, 70, pp 1098–1103.

[60] Schmelzer, G. H., Gurib-Fakim, A., Arroo, R., Bosch, C. H., de Ruijter, A., Simmonds, M. S. J., (Eds.), (2008), "Plant Resources of Tropical Africa 11(1) – Medicinal Plants 1", Backhuys Publishers, Wageningen, Netherlands.

[61] Warashina, T., et al., (2008), "New cardenolide and acylated lignan glycosides from the aerial parts of Asclepias curassavica", Chemical & Pharmaceutical Bulletin, 56, pp 1159-1163.

[62] Li, J. Z., et al., (2009), "Cytotoxicity of cardenolides and cardenolide glycosides from Asclepias curassavica", Bioorganic Medicinal Chemistry Letters, 19, pp 1956-1959.

[63] Oliver-Bever, B., (2009), "Medicinal plants in tropical west Africa", Cambridge University Press, Cambridge, UK.

[64] Wang, X. B., et al., (2009), "Nematicidal cardenolides from *Nerium indicum* Mill", Chemistry & Biodiversity, 6, pp 431-436.

[65] Bai, L., et al., (2010), "Three new cardenolides from methanol extract of stems and twigs of

Nerium oleander", Chemical & Pharmaceutical Bulletin, 58, pp 1088-1092.

[66] Bai, Y., et al. (2011), "The biological activities of cardenolide triglycosides from stems, twigs, and leaves of *Nerium oleander*", Journal of Wood Science, 57, pp 56-65.

[67] Jacinto, S. D., et al., (2011), "Cytotoxic cardenolide and sterols from *Calotropis gigantean*", Natural Product Communication, 6, pp 803-806.

[68] Singh, A., (201l) Herbalism, Phytochemistry and Ethnopharmacology. Boca Raton, FL, Enfield, N. H. CRC Press, Science Publishers.

[69] Li, Y., et al., (2012b), "Cytotoxic cardenolides from the stems of *Periploca forrestii*", Steroids, 77, pp 375–381.

[70] Xue, R., et al., (2013a), "Cytotoxic Cardiac Glycosides from the Roots of *Streptocaulon juventas*", Planta Medica, 79, pp 157-162.

[71] Xue, R., et al., (2013b), "Cardenolide glycosides from root of *Streptocaulon juventas*", Phytochemistry, 88, pp 105-111.

[72] Babaamer, Z., et al., (2014), "Isolation of Cardenolide glycosides from *Pergularia tomentosa* L. and their Antioxidant activities", Annales des Science et Technologie, 6, pp 123-128.

[73] Ibrahim, S. R., et al., (2014), "Proceraside A, a new cardiac glycoside from the root barks of *Calotropis procera* with in vitro anticancer effects", Natural Product Research, 28, pp 1322-1327.

[74] Komissarenko, N. F., (1971), "Ornithogalin — A cardenolide glycoside from *Ornithogalum magnum*", Chemistry of Natural Compounds, 7, pp 33-35.

[75] Schenk, B., et al., (1980), "Cannogenol-3-O-alpha-L-rhamnoside and cannogenol-3-O-beta-D-allomethyloside, two new cardiac glycosides from *Convallaria majalis*", Planta Medica, 40, pp 1-11.

[76] Kopp, B., and Kubelka, W., (1982), "New cardenolides from *Convallaria majalis*", Planta Medica, 45, pp 195-202.

[77] Krenn, L., et al., (2004), "Chemotaxonomic relevance of cardenolides in *Urginea fugax*", Phytochemistry, 65, pp 2881-2884.

[78] Kuroda, M., et al., (2006), "Ornithosaponins A-D, four new polyoxygenated steroidal glycosides from the bulbs of *Ornithogalum thyrsoides*", Steroids, 71, pp 199-205.

[79] Pan, Z. H., et al.,(2012), "A cytotoxic cardenolide and a saponin from the rhizomes of *Tupistra chinensis*", Fitoterapia, 83, pp 1489-1493.

[80] Wang, T. M., et al., (2007), "Cardenolides from *Saussurea stella* with cytotoxicity toward cancer cells", Journal of Natural Product, 70, pp 1429-1433.

[81] Nover, L., (1967), "On the structure of erycanoside, a cardenolide glycoside from *Erysimum cancescens* Roth", Archives Pharmaceutical Ber Dtsch Pharm Ges, 300, pp 1022-1026.

[82] Maslennikova, V. A, et al., (1967), "Glycosides of Erysimum", Chemistry of Natural Compounds, 3, pp 143-146.

[83] Piatak, D. M., et al., (1985), "Constituents of *Erysimum inconspicuum*. Two sulfur-containing lactone compounds", Journal of Natural Products, 48, pp 424-428.

[84] Huang, X., et al., (1993), "A chemical basis for differential acceptance of *Erysimum cheiranthoides* by two Pieris species", Journal of Chemical Ecology, 19, pp 195-210.

[85] Lei, Z. H., et al., (1996), "Cardenolides from *Erysimum cheiranthoides*", Phytochemistry, 41, pp 1187-1189.

[86] Lei, Z. H., et al., (2000), "Cardiac glycosides from *Erysimum cheiranthoides*", Chemical & Pharmaceutical Bulletin, 48, pp 290-292.

[87] Makarevich, I. F., et al., (1996), "Cardenolide glycosides of *Cheiranthus allioni*. XVI. Neoevonoside and cellobiosyldigigulomethyloside", Chemistry of Natural Compounds, 32, pp 53-55.

[88] Moon, S. S., et al., (2010), "Kaempferol glycosides and cardenolide glycosides, cytotoxic constituents from the seeds of *Draba nemorosa* (Brassicaceae)", Archives of Pharmacal Research, 33, pp 1169-1173.

[89] Baek, N. I., et al., (1994), "Euonymoside A: a new cytotoxic cardenolide glycoside from the bark of *Euonymus sieboldianus*", Planta Medica, 60, pp 26-29.

[90] Kitanaka, S., et al., (1996), "Cytotoxic cardenolides from woods of *Euonymus alata*", Chemical and Pharmaceutical Bulletin (Tokyo), 44, pp 615-617.

[91] Ankli, A., et al., (2000), "Cytotoxic cardenolides and antibacterial terpenoids from *Crossopetalum gaumeri*", Phytochemistry, 54, pp 531-537.

[92] Cao, S., et al., (2007), "Antiproliferative cardenolides of an *Elaeodendron* sp. from the

Madagascar rain forest (1)", Journal of Natural Product, 70, pp 1064-1067.

[93] Butler, M. S., et al., (2014), "Cardenolide glycosides from *Elaeodendron australe* var. *integrifolium*", Phytochemistry, 98, pp 160-163.

[94] Osorio, A. A., et al., (2014), "Elaeodendron orientale as a source of cytotoxic cardenolides", Phytochemistry, 105, pp 60-67.

[95] Yadava, R. N., and Rathore, K., (2000), "A new cardenolide from the seeds of *Terminalia arjuna* (W&A)", Journal of Asian Natatural Product Research, 2, pp 97-101.

[96] Yadava, R. N., and Rathore, K., (2001), "New cardenolide from the seeds of *Terminalia bellerica*", Fitoterapia, 72, pp 310-312.

[97] Yadav, R. N., and Rathore, K., (2001), "A new cardenolide from the roots of *Terminalia arjuna*", Fitoterapia, 72, pp 459-461.

[98] Huang, H. C., et al., (2013), "Cardenolides and bufadienolide glycosides from *Kalanchoe tubiflora* and evaluation of cytotoxicity", Planta Medica, 79, pp 1362-1369.

[99] Roberts, K. D., et al., (1963), "Glycosides and aglycons. CCLII. Cardenolides of the seed of *Mallotus philippinensis*", Helvetica Chimica Acta, 46, pp 2886–2893.

[100] Shilpi, J. A., et al., (2010), "New cardenolides from the stem bark of *Trewia nudiflora*", Fitoterapia, 81, pp 536-539.

[101] Gangwar, M., et al., (2014), "*Mallotus philippinensis* Muell. Arg (Euphorbiaceae): Ethnopharmacology and Phytochemistry Review", BioMed Research International, 2014, pp 1-13.

[102] Komissarenko, N. F., (1969), "Scorpioside—A cardenolide glycoside from *Coronilla scorpioides*", Chemistry of Natural Compounds, 5, pp 317-320.

[103] Yadava, R. N., and Yadav, S., (1999), "A new cardenolide uzarigenen-3-O-beta-D-xylopyranosyl (1-->2)-alpha-L-rhamnopyranoside", Journal of Asian Natural Product Research, 1, pp 245-249.

[104] Jiang, M. M., et al., (2008), "Cardenolides from *Antiaris toxicaria* as potent selective Nur77 modulators", Chemical & Pharmaceutical Bulletin (Tokyo), 56, pp 1005-1008.

[105] Dai, H. F., et al. (2009a), "A new cytotoxic 19-nor-cardenolide from the latex of *Antiaris toxicaria*", Molecules, 14, pp 3694-3699.

[106] Dai, H. F., et al. (2009b), "Two new cytotoxic cardenolides from the latex of *Antiaris toxicaria*", Journal of Asian Natural Product Research, 11, pp 832-837.

[107] Shi, L. -S., et al., (2010), "Cardiac glycosides from *Antiaris toxicaria* with potent cardiotonic activity", Journal of Natural Product, 73, pp 1214–1222.

[108] Shi, L. S., et al., (2014), "Cytotoxic cardiac glycosides and coumarins from *Antiaris toxicaria*", Bioorganic Medicinal Chemistry, 22, pp 1889-1898.

[109] Dong, W. H., et al., (2011), "Cytotoxic cardenolide glycosides from the seeds of *Antiaris toxicaria*", Planta Medica, 77, pp 1730-1734.

[110] Levrier, C., et al., (2012), "Toxicarioside M, a new cytotoxic 10β-hydroxy-19-nor-cardenolide from *Antiaris toxicaria*", Fitoterapia, 83, pp 660-664.

[111] Liu, Q., et al., (2013), "Antiproliferative cardiac glycosides from the latex of *Antiaris toxicaria*", Journal of Natural Product, 76, pp 1771-1780.

[112] Wu, X. L., et al., (2014), "A new periplogenin cardenolide from the seeds of *Antiaris toxicaria*", Journal of Asian Natural Product Research, 16, pp 418-421.

[113] Zhang, X. J., et al., (2015), "Strophalloside Induces Apoptosis of SGC-7901 Cells through the Mitochondrion-Dependent Caspase-3 Pathway", Molecules, 20, pp 5714-5728.

[114] Wichtl, M., and Junior, P., (1977), "Strophanthidin digitaloside and strophanthidin 6-deoxyguloside, two new cardenolide glycosides from *Adonis vernalis* L", Arch Pharm (Weinheim) 310, pp 905-910.

[115] Kopp, B., (1992), "Cardenolides from *Adonis aestivalis*", Phytochemistry, 31, pp 3195-3198.

[116] Kubo, S., et al., (2012), "New cardenolides from the seeds of *Adonis aestivalis*", Chemical & Pharmaceutical Bulletin, 60, pp 1275-1282.

[117] Kubo, S., et al., (2015), "Amurensiosides L-P, five new cardenolide glycosides from the roots of *Adonis amurensis*", Natural Product Communications, 10, pp 27-32.

[118] Fujino, T., et al., (2015), "Cardenolide glycosides from the seeds of *Digitalis purpurea* exhibit carcinoma-specific cytotoxicity toward renal adenocarcinoma and hepatocellular carcinoma cells", Bioscience Biotechnology and Biochemistry, 79, pp 177-184.

[119] Gil, R. R., et al., (1995), "Cardenolides from *Nierembergia aristata*", Journal of Natural Products, 58, pp 848-856.

[120] Sen, N. K., et al., (1957), "Glycosides and aglycones. CLXXXIV. Glycosides of the jute

seeds of Corchorus *capsularis* and *C.olitorius*. Identification of corchorin, corchorigenin, and corchsularin with strophanthidin", Helvetica Chimica Acta, 40, pp 588-592.

[121] Rao, D. V., and Rao, E. V., (1975), "New cardenolides from seeds of *Corchorus trilocularis*", Phytochemistry, 14, pp 533-537.

[122] Nakamura, T., et al., (1998), "Cardenolide glycosides from seeds of *Corchorus olitorius*", Phytochemistry, 49, pp 2097-2101.

[123] Chang, H. S., et al., (2013), "Cytotoxic cardenolide glycosides from the root of *Reevesia formosana*", Phytochemistry, 87, pp 86-95.

[124] Leu, W. -J., et al., (2014), "Reevesioside A, a cardenolide glycoside, induces anticancer activity against human hormone-refractory prostate cancers through suppression of c-myc expression and induction of g1 arrest of the cell cycle", PLoS One, 9, pp e87323.

[125] CRGAE(http://publish.plantnetproject.org/project/riceweeds_en/collection/collection/information/details/CRGAE) Date accessed March, 2015.

[126] Isman, M. B., et al., (1977), "Variation in cardenolide content of lygaeid bugs, Oncopeltus fasciatus and Lygaeus kalmii and of their milkweed hosts (*Asclepias* spp) in central California", Journal of Chemical Ecology, 3, pp 613–624.

[127] Abe, F., and Yamauchi, T., (1994), "Cardenolide glycosides from the roots of *Apocynum cannabinum*", Chemical and Pharmaceutical Bulletin, 42, pp 2028–2031.

[128] Rasmann, S., and Agrawal, A. A., (2011), "Latitudinal patterns in plant defense: evolution of cardenolides, their toxicity and induction following herbivory", Ecology Letters, 14, pp 476–483.

[129] Schrutka-Rechtenstamm, R., (1985), "Origin of cardenolides in rhizomes and roots of *Convallaria majalis* L. Biogenesis in situ or transport from leaves?", Zeitschrift Fur Naturforschung, C 40, pp 627–630.

[130] Nelson, C. J., et al., (1981), "Seasonal and intraplant variation of cardenolide content in the California milkweed *Asclepias eriocarpa*, and implications for plant defense", Journal of Chemical Ecology, 7, pp 981–1010.

[131] Zalucki, M. P., et al., (2001), "Detrimental effects of latex and cardiac glycosides on survival and growth of first-instar monarch butterfly larvae *Danaus plexippus* feeding on the sandhill milkweed *Asclepias humistrata*", Ecological Entomology, 26, pp 212–224.

[132] Vaughan, F. A., (1979), "Effect of gross cardiac glycoside content of seeds of common milkweed, *Asclepias syriaca*, on cardiac glycoside uptake by the milkweed bug *Oncopeltus fasciatus*", Journal of Chemical Ecology, 5, pp 89–100.

[133] Van Baalen, J., and Prins, E. G. M., (1983), "Growth and reproduction of *Digitalis purpurea* in different stages of succession", Oecologia, 58, pp S. 84–91.

[134] Maier, M. S., et al., (1986), "Biosynthesis of the butenolide ring of cardenolides in *Digitalis purpurea*", Phytochemistry, 25, pp 1327-1329.

[135] Kreis, W., et al., (1998), "Cardenolide biosynthesis in foxglove", Planta Medica, 64, pp 491–499.

[136] W. Kreis, and F. Mu¨ller-Uri, "Biochemistry of sterols, cardiac glycosides, brassinosteroids, phytoecdysteroids and steroid saponins," in Biochemistry of plant Secondary metabolism. M. Wink, Ed. Sheffield, UK: CRC Press, 2010, pp. 304–63.

[137] Schebitz, P., et al., (2010), "Norcholanic acids as substrates for recombinant 3β-hydroxysteroid dehydrogenase and progesterone 5β-reductase, enzymes of the 5β-cardenolide biosynthesis", Tetrahedron Letters, 51, pp 367-370.

[138] Pedro Perez-Bermudez, P., et al., (2010), "*Digitalis purpurea* P5bR2, encoding steroid 5β-reductase, is a novel defense-related gene involved in cardenolide biosynthesis", New Phytologist, 185, pp 687–700.

[139] Luckner, M., and Wichtl, M., (2000), "Digitalis", Wissenschaftliche Verlagsgesellschaft., Stuttgart, Germany.

[140] Agrawal, A. A., et al., (2008), "Evolution of latex and its constituent defensive chemistry in milkweeds (Asclepias): a test of phylogenetic escalation", Entomologia Experimentalis Et Applicata, 128, pp 126–138.

[141] Manson, J. S., et al., (2012), "Cardenolides in nectar may be more than a consequence of allocation to other plant parts: a phylogenetic study of *Asclepias*", Functional Ecology, 26, pp 1100–1110.

[142] Godfraind T., (1984), "Mechanism of action of cardiac glycosides", European Heart Journal, 5, pp 303-308.

[143] Smith, T. W., and Braunwald, E., (1980), "The management of heart failure," in Cardiovascular diseases, E. Braunwald Eds. Philadelphia: Saunders, pp 509-570.

[144] B. F. Hoffman and J. T. Bigger, Jr., "Digitalis and allied cardiac glycosides," in The pharmacological basis of therapeutics, A. G.

Gilman, L. S. Goodman, T. Rall, F. Murad, Eds. New York: MacMillan, 1985, pp716–747.

[145] Longhurst, J. C., and Ross, J., (1985), "Extra cardiac and coronary vascular effects of digitalis", Journal of the American College of Cardiology, 5, pp 99-105.

[146] Aperia, A., (2007), "New roles for an old enzyme: Na, K-ATPase emerges as an interesting drug target", Journal of Internal Medicine, 261, pp 44–52.

[147] Repke, K., (1985), "New developments in cardiac glycoside structure–activity relationships", Trends in Pharmacological Sciences, 6, pp 275–278.

[148] Schönfeld, W., et al., (1985), "The lead structure in cardiac glycosides is 5 beta, 14 beta-androstane-3 beta 14-diol", Naunyn-Schmiedeberg's Archives of Pharmacology, 329, pp 414-426.

[149] Schönfeld, W., et al., (1986), "Origin of differences of inhibitory potency of cardiac glycosides in Na^+/K^+-transporting ATPase from human cardiac muscle, human brain cortex and guinea-pig cardiac muscle", Biochemical Pharmacology, 35, pp 3221-3231.

[150] Burt, S. K., et al., "Computer-Aided Drug Design: Methods and Applications," New York: Marcel Dekker, 1989, pp 55-91.

[151] Smith, P., et al., (1982), "Cardenolide analogues. Synthesis and biological activity of glucosides of c17b-modified derivatives of digitoxigenin", Journal of Medicinal Chemistry, 25, pp 1222-1226.

[152] Bohl, M., and Süssmilch, R., (1986), "Calculations on molecular structure and electrostatic potentials of cardiotonic steroids", European Journal of Medicinal Chemistry, 21, pp 193-198.

[153] Boobbyer, D. N. A., et al., (1989), "New hydrogen-bond potentials for use in determining energetically favorable binding sites on molecules of known structure", Journal of Medicinal Chemistry, 32, pp 1083-1094.

[154] Thomas, R. E.,"Cardiac Drugs," in Burger's Medicinal Chemistry and Drug Discovery, Wolff, M. Ed. New York: John Wiley & Sons, 1996, pp 153-261.

[155] Guzmán, A., et al., (1981), "Replacement of the butenolide moiety of digitoxigenin by cyclic Michael acceptor systems", Canadian Journal of Chemistry, 59, pp 3241- 3247.

[156] Schönfeld, W., and Repke, K. R. H., (1988), "A Free-Wilson Analysis of 5.beta, 14.beta.-Androstane derivatives inhibiting the Na/K-ATPase from human heart", Quantitative Structure-activity Relationships, 7, pp 160-165.

[157] T. Akera, "Cardiac Glycosydes, Part I," in Experimental Pharmacology, K. Greeff, Ed. Berlin: Springer, 1981, pp 287-336.

[158] Chavey , W. E., et al. (2001), "Guideline for the Management of Heart Failure Caused by Systolic Dysfunction: Part II", Treatment.American Family Physician, 64, pp 1045-1055.

[159] Ahmed, A., (2008), "Effects of digoxin at low serum concentrations on mortality and hospitalization in heart failure: A propensity matched study of the DIG trial", International Journal of Cardiology, 123, pp 138–146.

[160] Maury, P., et al., (2014), "Role of digoxin in controlling the ventricular rate during atrial fibrillation: a systematic review and a rethinking", Research Reports in Clinical Cardiology, 5, pp 93-101.

[161] Shiratori, O., (1967), "Growth inhibitory effect of cardiac glycosides and aglycones on neoplastic cells: *in vitro* and *in vivo* studies", Japanese Journal of Cancer Research Gann, 58, pp 521–528

[162] Xu, J. W., et al., (2009), "Effects of ouabain at different concentrations on growth of leukemia cells", Zhongguo Dang Dai Er Ke Za Zhi, 11, pp 259-262.

[163] Hallböök, H., et al., (2011), "Ex vivo activity of cardiac glycosides in acute leukaemia", PLoS One, 6, pp 15718.

[164] Kuroda, M., et al., (2013), "New cardenolide glycosides from the seeds of *Digitalis purpurea* and their cytotoxic activity", Bioscience, Biotechnology, and Biochemistry, 77, pp 1186-1192.

[165] Stenkvist, B., (1999), "Is digitalis a therapy for breast carcinoma?", Oncology Reports, 6, pp 493-496.

[166] López-Lázaro, M., et al., (2005), "Digitoxin inhibits the growth of cancer cell lines at concentrations commonly found in cardiac patients", Journal of Natural Product, 68, pp 1642-1645.

[167] Bielawski, K., et al., (2006), "Inhibition of DNA topoisomerases I and II, and growth inhibition of breast cancer MCF-7 cells by ouabain, digoxin and proscillaridin A", Biological and Pharmaceutical Bulletin, 29, pp 1493–1497.

[168] Menger, L., et al., (2012), "Cardiac glycosides exert anticancer effects by inducing immunogenic cell death", Science Translational Medicine, 4, pp 143ra99.

[169] Siddiqui, B. S., et al., (2012), "Flavonoid and cardenolide glycosides and a pentacyclic triterpene from the leaves of *Nerium oleander* and evaluation of cytotoxicity," Phytochemistry, 77, pp 238-244.

[170] Li, X. S., et al., (2014), "Cardiac glycosides from the bark of *Antiaris toxicaria*", Fitoterapia, 97, pp 71-77.

[171] Van Khang, P., et al., (2014), "Cardenolides from the bark of *Calotropis gigantean*", Natural Product Research, 28, pp 1191-1196.

[172] Newman, R. A., et al., (2007), "Autophagic cell death of human pancreatic tumor cells mediated by oleandrin, a lipid-soluble cardiac glycoside", Integrative Cancer Therapies, 6, pp 354-364.

[173] Yang, P., et al., (2009), "Oleandrin-mediated inhibition of human tumor cell proliferation: importance of Na,K-ATPase alpha subunits as drug targets", Molecular Cancer Therapeutics, 8, pp 2319-2328.

[174] Newman, R. A., et al., (2006), "Oleandrin-mediated oxidative stress in human melanoma cells", Journal of Experimental Therapeutics and Oncology, 5, pp 167-181.

[175] Joshi, A. L., et al., (2015), "Calotropis procera extract induces apoptosis and cell cycle arrest at G2/M phase in human skin melanoma (SK-MEL-2) cells" , Natural Product Research, pp 1-4.

[176] Svensson, A., et al., (2005), "Digoxin inhibits neuroblastoma tumor growth in mice", Anticancer Research, 25, pp 207-212.

[177] Kulikov, A., et al., (2007), "Ouabain activates signaling pathways associated with cell death in human neuroblastoma", Biochimica et Biophysica Acta, 1768, pp 1691-1702.

[178] López-Lázaro, M., et al., (2003), "Anti-tumour activity of *Digitalis purpurea* L. subsp. *Heywoodii*", Planta Medica, 69, pp 701-704.

[179] Antczak, C., et al., (2009), "Revisiting Old Drugs as Novel Agents for Retinoblastoma: *In vitro* and *In vivo* Antitumor Activity of Cardenolides", Investigative ophthalmology & visual science, 50, pp 3065–3073.

[180] Xie, Z., and Askari, A., (2002), "Na+/K+-ATPase as a signal tranducer", European Journal of Biochemistry, 269, pp 2434–2439.

[181] Mijatovic, T., et al., (2007), "The α1 subunit of the sodium pump could represent a novel target to combat non-small cell lung cancers', The Journal of Pathology, 212, pp 170–179.

[182] Xie, Z., and Cai, T., (2003), "Na+/K+-ATPase-mediated signal transduction: from protein interaction to cellular function, Molecular Interventions, 3, pp 157–168.

[183] McConkey, D. J., et al., (2000), "Cardiac glycosides stimulate Ca2+ increases and apoptosis in androgenindependent, metastatic human prostate adenocarcinoma cells", Cancer Research, 60, pp 3807–3812.

[184] Trevisi, L., B. Visentin, F. Cusinato, I. Pighin, S. Luciani et al., (2004), "Antiapoptotic effect of ouabain on human umbilical vein endothelial cells", Biochemical Biophysical Research Communications, 321, pp 716–721.

[185] Taurin, S., et al., (2002), "c-Fos expression in ouabain-treated vascular smooth muscle cells from rat aorta: evidence for an intracellular-sodiummediated, calcium-independent mechanism", Journal of Physiology, 15, pp 835–847.

[186] Mijatovic, T., et al., (2006), "Cardenolide-induced lysosomal membrane permeabilization contributes therapeutic benefits in experimental human non-small-cell-lung cancers", Neoplasia, 8, pp 402–412.

[187] Lin, H., et al., (2004), "Involvement of Cdk5/p25 in digoxintriggered prostate cancer cell apoptosis", The Journal of Biological Chemistry, 279, pp 29302–29307.

[188] Haux, J., (1999), "Digitoxin is a potential anticancer agent for several types of cancer", Medical Hypotheses, 153, pp 543–548.

[189] Huang, Y.T., et al., (2004), "Investigation of ouabaininduced anticancer effect in human androgen-independent prostate cancer PC-3 cells", Biochemical Pharmacology, 67, pp 727–733.

[190] Yeh, J. H., et al., (2001), "Inhibitory effects of digitalis on the proliferation of androgen dependent and independent prostate cancer cells", The Journal of Urology, 166, pp 1937–1942.

[191] Yeh, J. H., et al., (2003), "Effects of bufalin and cinobufagin on the proliferation of androgen dependent and independent prostate cancer cells", Prostate, 54, pp 112–124.

[192] Frese, S., et al., (2006), "Cardiac glycosides initiate Apo2L/TRAIL-induced apoptosis in non-small cell lung cancer cells by up-regulation of death receptors 4 and 5", Cancer Research, 66, pp 5867–5874.

[193] Pathak, S., et al., (2000), "Anvirzel, an extract of Nerium oleander, induces cell death in human but

not murine cancer cells", Anticancer Drugs, 11, pp 455–463.

[194] Sreenivasan, Y., et al., (2006), "Oleandrin-mediated expression of Fas potentiates apoptosis in tumor cells", Journal of Clinical Immunology, 26, pp 308–322.

[195] Verheye-Dua, F., and Bohm, L., (1996), "Influence of ouabain on cell inactivation by irradiation", Strahlentherapie und Onkologi, 172, pp 156–161.

[196] Verheye-Dua, F., and Bohm, L., (1998), "Na+,K+-ATPase inhibitor, ouabain accentuates irradiation damage in human tumour cell lines", Radiation Oncology Investigations, 6, pp 109–119.

[197] Rajasekaran, S. A., et al., (2001), "Na,K-ATPase betasubunitis required for epithelial polarization, suppression of invasion, and cell motility", Molecular Biology of the Cell, 12, pp 279–295.

[198] Rajasekaran, A. K., and Rajasekaran, S. A., (2003), "Role of Na-K-ATPase in the assembly of tight junctions", American journal of physiology:Renal physiology, 285, pp F388–F396.

[199] Rajasekaran, S. A., et al., (2005), "Multiple functions of Na,K-ATPase in epithelial cells", Seminars in Nephrology, 25, pp 328–334.

[200] Guo, J. L., et al., (2012), "Toxicarioside A inhibits SGC-7901 proliferation, migration and invasion via NF-κB/bFGF signaling", World Journal of Gastroenterology, 18, pp 1602-1609.

[201] Huang, F. Y., et al., (2012), "Toxicarioside A inhibits tumor growth and angiogenesis: involvement of TGF-β/endoglin signaling", PLoS One, 7, pp e50351.

[202] Park, H. Y., et al., (2014), "Calotropin: a cardenolide from calotropis gigantea that inhibits Wnt signaling by increasing casein kinase 1α in colon cancer cells", Chembiochem, 15, pp 872-878.

[203] Trenti, A., et al., (2014), "Cardiac glycoside ouabain induces autophagic cell death in non-small cell lung cancer cells via a JNK-dependent decrease of Bcl-2", Biochemical Pharmacology, 89, pp 197-209.

[204] Prassas, I., et al., "High-throughput screening for modulators of tissue-kallikrein expression", American Association for Cancer Research (AACR) Annual Meeting, Los Angeles, USA, April 14- 18th, 2007.

[205] Florkiewicz, R. Z., et al., (1998), "The inhibition of fibroblast growth factor-2 export by cardenolides implies a novel function for the catalytic subunit of Na+,K+-ATPase", The Journal of Biological Chemistry, 273, pp 544–551.

[206] Smith, J. A., et al., (2001), "Inhibition of export of fibroblast growth factor-2 (FGF-2) from the prostate c ancer cell lines PC3 and DU145 by Anvirzel and its cardiac glycoside component, oleandrin", Biochemical Pharmacology, 62, pp 469–472.

[207] Lin, Y., et al., (2008), "Determinants of human and mouse melanoma cell sensitivities to oleandrin", Journal of Experimental Therapeutics and Oncology, 7, pp 195-205.

[208] Felth, J., et al., (2009), "Cytotoxic effects of cardiac glycosides in colon cancer cells, alone and in combination with standard chemotherapeutic drugs", Journal of Natural Products, 72, pp 1969-1974.

[209] Hong, D. S., et al., (2014), "First-in-human study of pbi-05204, an oleander-derived inhibitor of akt, fgf-2, nf-κB and p70s6k, in patients with advanced solid tumors", Investigational New Drugs, 32, pp 1204-1212.

[210] Yang, P., et al., (2014), "Cellular location and expression of Na+, K+ -ATPase α subunits affect the anti-proliferative activity of oleandrin", Molecular Carcinogenesis, 53, pp 253-263.

[211] Pan, Y., et al., (2015), "PBI-05204, a supercritical CO2 extract of *Nerium oleander*, inhibits growth of human pancreatic cancer via targeting the PI3K/mTOR pathway", Investigational New Drugs, 33, pp 271-279.

[212] Kumar, A., et al., (2013), "Oleandrin: A cardiac glycosides with potent cytotoxicity", Pharmacognosy Reviews, 7, pp 131-139.

[213] Neriumbiotech (http://www.neriumbiotech.com/cancer_research.htm) Date accessed February, 2015

[214] Slingerland, M., et al., (2013), "Cardiac glycosides in cancer therapy: from preclinical investigations towards clinical trials", Investigational New Drugs, 31, pp 1087-1094.

[215] Okina, Y., et al., (2015), "Cardenolide aglycones inhibit tumor necrosis factor α-induced expression of intercellular adhesion molecule-1 at the translation step by blocking Na^+/K^+-ATPase", Biological and Pharmaceutical Bulletin, 38, pp 39-47.

[216] Zeino, M., et al., (2015a), "Cytotoxicity of cardiotonic steroids in sensitive and multidrug-resistant leukemia cells and the link with Na(+)/K(+)-ATPase", The Journal of Steroid Biochemistry and Molecular Biology, 150, pp 97-111.

[217] Zeino, M., et al., (2015b), "Identification of new P-glycoprotein inhibitors derived from cardiotonic steroids", Biochemical Pharmacology, 93, pp 11-24.

[218] Wang, H. Y. L., et al., (2011a), "C5′-Alkyl Substitution Effects on Digitoxigenin alpha-L-Glycoside Cancer Cytatoxicity", ACS Medicinal Chemistry Letters, 2, pp 259–263.

[219] Wang, H. Y. L., et al., (2011b), "Synthesis and Evaluation of the alpha-D-/alpha-L-Rhamnosyl and Amicetosyl Digitoxigenin Oligomers as Antitumor Agents", ACS Medicinal Chemistry Letters, 2, pp 264–269.

[220] Manna, S. K., et al., (2006), "Cardiac glycoside inhibits IL-8-induced biological responses by down regulating IL-8 receptors through altering membrane fluidity", Journal of Cellular Physiology, 207, pp 195–207.

[221] Piccioni, F., et al., (2004), "A screen for drugs that protect against the cytotoxicity of polyglutamine-expanded androgen receptor", Human Molecular Genetics, 13, pp 437–446.

[222] Wang, J. K T., et al., (2006), "Cardiac glycosides provide neuroprotection against ischemic stroke: discovery by a brain slice-based compound screening platform", Proceedings of the National Academy of Sciences USA, 103, pp 10461–10466.

[223] Li, J., et al., (2006), "Low doses of ouabain protect from serum deprivation-triggered apoptosis and stimulate kidney cell proliferation via activation of NF-κB", Journal of the American Society of Nephrology, 17, pp 1848–1857.

[224] Pierre, S. V., et al., (2007), "Ouabain triggers preconditioning through activation of the Na+, K+-ATPase signaling cascade in rat hearts", Cardiovascular Research, 73, pp 488–496.

[225] Bertol, J. W., et al., (2011), "Antiherpes activity of glucoevatromonoside, a cardenolide isolated from a Brazilian cultivar of *Digitalis lanata*", Antiviral Research, 92, pp 73-80.

[226] Mekhail, T., et al., (2006), "Phase 1 trial of Anvirzel in patients with refractory solid tumors", Investigational New Drugs, 24, pp 423–427.

[227] Watson, T. R., and Wright, S. E., (1956), "The Cardiac Glycosides of *Gomphocarpus fruticosus* (R.Br.) I. Afroside", Australian Journal of Chemistry, 9, pp 497-511.

[228] Watson, T. R., and Wright, S. E., (1957), "The Cardiac Glycosides of *Gomphocarpus fruticosus* (R.Br.) II. Gomphoside", Australian Journal of Chemistry, 10, pp 79-84.

[229] Coombe, R. G. and Watson, T. R., (1964), "The Cardiac Glycosides of *Gomphocarpus fruticosus* (R. Br.) III. Gomphoside", Australian Journal of Chemistry, 17, pp 92-100.

[230] Singh, B., and Rastogi, R. P., (1969), "Chemical investigation of *Asclepias curassavica* Linn", Indian Journal of Chemistry, 7, pp 1105-1110.

[231] Singh, B., and Rastogi, R. P., (1972), "Structure of ascelpin and some observations on the NMR spectra of *Calotropis* glycosides", Phytochemistry, 11, pp 757-762.

frontiers in Pharmacology

ORIGINAL RESEARCH
published: 11 October 2019
doi: 10.3389/fphar.2019.01186

Cytokines Driven Anti-Inflammatory and Anti-Psoriasis Like Efficacies of Nutraceutical Sea Buckthorn (*Hippophae rhamnoides*) Oil

*Acharya Balkrishna[1,2], Sachin Shridhar Sakat[1], Kheemraj Joshi[1], Kamal Joshi[1], Vinay Sharma[1], Ravikant Ranjan[1], Kunal Bhattacharya[1] and Anurag Varshney[1,2]**

[1] Drug Discovery and Development Division, Patanjali Research Institute, Haridwar, India, [2] Department of Allied Sciences, University of Patanjali, Patanjali YogPeeth, Haridwar, India

OPEN ACCESS

Edited by:
Maura Palmery, Sapienza University of Rome, Italy

Reviewed by:
Marika Cordaro, Università degli Studi di Messina, Italy
Tania Silvia Frode, Federal University of Santa Catarina, Brazil
Yucui Li, Guangzhou University of Chinese Medicine, China
Eduardo Dalmarco, Federal University of Santa Catarina, Brazil

***Correspondence:**
Anurag Varshney
anurag@prft.co.in

Specialty section:
This article was submitted to Inflammation Pharmacology, a section of the journal Frontiers in Pharmacology

Received: *07 February 2019*
Accepted: *13 September 2019*
Published: *11 October 2019*

Citation:
Balkrishna A, Sakat SS, Joshi K, Joshi K, Sharma V, Ranjan R, Bhattacharya K and Varshney A (2019) Cytokines Driven Anti-Inflammatory and Anti-Psoriasis Like Efficacies of Nutraceutical Sea Buckthorn (Hippophae rhamnoides) Oil. Front. Pharmacol. 10:1186. doi: 10.3389/fphar.2019.01186

Psoriasis is a chronic inflammatory skin disease characterized by circumscribed, red, thickened plaques with overlying silvery white scales. It is associated with the release of pro-inflammatory mediators that lead to the development of edema and distress. Here we show the anti-inflammatory and anti-psoriatic efficacies of a neutraceutical sea buckthorn oil (SBKT) derived from the fruit pulp of *Hippophae rhamnoide*s. Chemical analysis of the SBKT showed the presence of 16 major saturated, mono-, and polyunsaturated fatty acids components, imparting significant nutritional values. Efficacy of the SBKT in modulating psoriasis and associated inflammation was first tested *in vitro* using human monocytic (THP-1) cells. SBKT induced cytotoxicity at a dose of ≥25 µl/ml. Treatment of the lipopolysaccharide-stimulated THP-1 cells with SBKT subdued the enhanced release of intracellular reactive nitrogen species and expression of NF-κB protein, in a concentration-dependent manner. This was accompanied by a reduction in the release of downstream pro-inflammatory cytokines: Interleukin-1β and interleukin-6. Tumor necrosis factor-α released in the stimulated THP-1 cells were also inhibited by SBKT dose of 5 µl/ml. *In vivo* oral and topical treatment with SBKT in the Carrageenan-stimulated paw edema model, showed a significant decrease in paw volume and edema. In the 12-O tetradecanoyl phorbol 13-acetate (TPA) stimulated CD-1 mice psoriasis-like model, concurrent oral and tropical SBKT treatments substantially reduced ear edema and ear biopsy weights. Histopathologically, significant reduction in ear epidermal thickness and skin lesion scores was observed in the SBKT-treated animals. In conclusion, SBKT showed anti-inflammatory and anti-psoriasis-like efficacies in healing chemical-induced inflammation and psoriasis. The possible mode of action of SBKT was found through inhibition of reactive nitrogen species, and downregulation of NF-κB protein and pro-inflammatory cytokines. Thus, the present data suggest that Sea buckthorn oil can be used as an anti-inflammatory and anti-psoriatic nutraceutical.

Keywords: sea buckthorn oil, nutraceutical, anti-inflammatory activity, paw edema, psoriasis, 12-O-tetradecanoyl phorbol-13-acetate, THP-1, cytokines

INTRODUCTION

Inflammation is induced as a response by the immune system to stimulations by invading foreign pathogens or by endogenous signals originating from damaged cells. While the primary function for pro-inflammatory cells is to counter the inducer and perform damage repair, sustained and unchecked inflammation can lead to the development of pathologies and induction of chronic diseases. Psoriasis is one such chronic inflammatory disease of skin and joints that affects 2–3% of the population of the world at the age of <40 years (Lebwohl, 2003; Wagner et al., 2010; World Health Organization, 2016). General symptoms of the psoriasis are circumscribed, red, and thickened plaques with an overlying silver-white scale(s) inducing itching, burning, and irritation.

Pathological signatures for psoriasis development include enhanced keratinocyte proliferation in the basal and suprabasal epidermal regions, the diminished thickness of the stratum granulosum, hyperkeratosis, and parakeratosis (Gudjonsson and Elder, 2008). Critical inflammatory cells such as macrophages, dendritic cells, neutrophils, lymphocytes, and T helper (T_H) cells infiltrate the psoriasis lesions, and along with the stressed keratinocytes produce reactive oxygen and nitrogen species, and pro-inflammatory cytokines and chemokines (Liu, 2005; Richardson and Gelfand, 2008; Wagner et al., 2010). Currently, there are no permanent treatments for psoriasis, and anti-inflammatory drugs are topically applied during the flaring of the disease.

The term "nutraceutical" has been derived from the combination of "nutrition" and "pharmaceutical" to describe a nutritional product with pharmaceutical effects (Das et al., 2012). Nutraceuticals application includes a range of therapeutic areas like skin diseases, sleeping disorders, osteoporosis, metabolic disorders, etc. Sea buckthorn [*Hippophae rhamnoide*s L.; sea buckthorn oil (SBKT)] belongs to the plant family Elaeagnaceae. It is a medium-sized, thorny plant grows in the cold arid regions of Europe and Asia. Medicinal applications of these plants have been mentioned in the ancient Greek and Tibetan medicinal texts. Due to its wide medicinal applications, SBKT has also been named as a "wonder plant." Different parts of the SBKT plants (berries, leaves, young shoots, roots, and bark) have been used in therapeutic purposes (Redei et al., 2018). In modern times, the SBKT plant and its parts have been studied for their therapeutic applications in cardiovascular, gastrointestinal, liver, and skin diseases (Zeb, 2004; Ganju et al., 2005; Gupta et al., 2005; Suchal et al., 2016; Hou et al., 2017). The oil content of the dried fruit pulp of SBKT is about 20–25%. The oil obtained from the pulp of the SBKT plant is composed of sterols, saturated and unsaturated fatty acids, tocopherols, tocotrienols, and carotenoids (Zeb, 2006; Bal et al., 2011; Bonesi et al., 2016; Zielinska and Nowak, 2017). Presence of high quantities of these biomolecules along with mineral elements like Ca, P, Fe, and K; vitamins like C, B1, B2, and K; and sugars like glucose and fructose, effectively presents the SBKT plant as a valuable source for human nutrition (Christaki, 2012). Omega-3 and omega-6 fatty acids have positive effects on neurological disorders, with observed anti-inflammatory and anti-oxidant activities (Kumar et al., 2011). Acute and sub-chronic toxicity studies in animals have also shown that SBKT is non-toxic up to 90 days of repeated dosing in rats (Zhao et al., 2017).

In the present study, we performed the chemical analysis of SBKT and tagged those findings with its observed biological efficacies. We also investigated the mechanism of action for the SBKT in its anti-inflammatory and anti-psoriasis-like activities in bacterial lipopolysaccharide (LPS)-stimulated human monocyte (THP-1) cells under *in vitro* conditions. Finally, we validated the efficacy of SBKT administered at a human equivalent dosage, in modifying Carrageenan-induced paw inflammation in Wistar rats, and in ameliorating 12-O-tetradecanoyl phorbol-13-acetate (TPA)-induced skin psoriasis in CD-1 mice.

Abbreviations: SBKT, sea buckthorn oil; TNF-α, tumor necrosis factor-α; IL-6, interleukin-6; IL-1β, interleukin-1β; LPS, lipopolysaccharides; ELISA, enzyme-linked immunosorbent assay; RPMI, Roswell Park Memorial Institute 1640 Medium; FBS, fetal bovine serum; RNS, reactive nitrogen species; CPCSEA, Committee for the Purpose of Control and Supervision of Experiments on Animals; IAEC, Institutional Animal Ethical Committee; DEXA, dexamethasone; Na CMC, sodium carboxy methyl cellulose; ANOVA, analysis of variance; NC, normal control; TPA, 12-O-tetradecanoyl phorbol-13-acetate; VC, vehicle control; TPA CON, TPA control; INDO, indomethacin; T.A., topical application; SFA, saturated fatty acids; MUFA, monounsaturated fatty acids; PUFA, polyunsaturated fatty acids.

MATERIALS AND METHODS

Chemicals and Reagents

SBKT, isolated from the pulp, was obtained from Food and Herbal Park, Patanjali Ayurveda Limited, Haridwar, India. Culture media RPMI-1640, fetal bovine serum, and antibiotic/anti-mycotic mixture were obtained from Gibco. Cytokines interleukin 1-beta (IL-1β), IL-6, and tumor necrosis factor-α (TNF-α) ELISA kits were purchased from BD Biosciences. LPS, TPA, λ-Carrageenan, indomethacin (INDO), and dexamethasone (DEXA) were purchased from Sigma-Aldrich (St. Louis, MO, USA). Hematoxylin, potassium aluminium sulfate dodecahydrate, and mercury (II) oxide red were purchased from Merck India Pvt. Ltd, Mumbai, India. Eosin yellow and ferric chloride were purchased from Hi-Media Laboratories, Mumbai, India. All the other chemicals and reagents purchased for the study were of the highest commercial grade.

Fatty Acid Profiling of SBKT

The saturated, polyunsaturated, and monounsaturated fat in SBKT were determined by gas chromatography–flame ionized detector (GC–FID) using AOAC Method 996.01 (AOAC, 2000). SBKT mixture was refluxed for 10 min after adding 10 ml methanolic NaOH solution. The mixture was again refluxed for an additional 5 min after the addition of 10 ml BF_3 reagent. n-Heptane (10 ml) was added through the top of the condenser and refluxed for 1 min, and the reaction mixture was kept for 10 min at ambient temperature. The entire mixture was transferred to the centrifuge tube, mixed with 5 ml NaCl solution using a vortex at a low speed, and allowed to separate into multiple layers. One milliliter of the upper layer containing fatty acid methyl esters was transferred to GC vial and further used for the gas chromatography (AOAC, 2000).

For the GC–FID analysis of the SBKT fatty acid content, a 7890B gas chromatograph (Agilent Technologies) equipped with flame ionization detector and non-bonded 90% cyanopropyl and 10% phenyl siloxane capillary column was used. Measurements were obtained following the GC–FID operational parameters of injector temperature of 250°C, detector temperature of 275°C, H flow of 34 ml/min, air flow of ca. 300 ml/min, split ratio of 100:1, carrier gas of helium, linear velocity of 21 cm/s at 175°C, initial temperature of 120°C (hold 4 min), rate of 5°C/min, final temperature of 230°C, and final time of 5 min. Fatty acid methyl ester (FAME) mix was used in the identification and quantification of individual fatty acids. For GC–FID analysis, FAME was reconstituted with 10 ml of n-hexane (AOAC, 2000).

Cell Culture for *In Vitro* Experiments

THP-1 cell line was obtained from the National Centre for Cell Science, Pune, India, and cultured in RPMI-1640 media, supplemented with 10% heat-inactivated fetal bovine serum in the presence of penicillin–streptomycin (100 U/ml), sodium pyruvate (1 mM), and L-glutamine (4 mM). The cells were grown at 37°C in a 5% CO_2 in a sterile environment.

Cell Viability Analysis

SBKT oil was prepared as an emulsion in incomplete culture media (RPMI-1640). THP-1 cells were plated in a 96-well plate at a concentration of 10,000 cells per well in a 96-well plate. The cells were pre-incubated overnight and exposed to the SBKT oil at concentrations of 0.0, 1.56, 3.12, 6.25, 12.5, 25, and 50 µl/ml for a period of 24 h. At the end of the exposure time, cells were washed with 100 µl PBS. One hundred microliters of 0.5 mg/ml 3-(4,5-dimethylthiazol-2-yl)-2,5-diphenyltetrazolium bromide was added to each well, and the plates were incubated for 3 h at 37°C. At the end of the exposure period, the dye was removed. One hundred microliters of dimethyl sulfoxide (DMSO) was added, and the plates were placed on a shaker for 10 min. Absorbance of each well was read using the PerkinElmer Envision microplate reader at 595-nm wavelength, and cell viability percentage was calculated.

Reactive Nitrogen Species Measurement

THP-1 cells were seeded in 96-well culture plates at a density of 2×10^5 cells/ml. Cells were treated with different concentrations of SBKT oil emulsion made in incomplete RPMI-1640 media and incubated for 1 h. Cells were stimulated with LPS (500 ng/ml) and incubated for an additional 24 h at 37°C in CO_2 incubator. The reactive nitrogen species (RNS) release in the culture media was determined using modified Griess reagent (Sigma), following the manufacturer's protocol. Absorbance was recorded at 540 nm using Envision Microplate reader (PerkinElmer).

Cytokines Level Measurement

THP-1 cells were seeded in 24-well culture plates at a density of 5×10^5 cells/well. For the experiment, SBKT oil was prepared as an emulsion and mixed with the cell culture media at different concentrations: 1.25, 2.5, and 5 µl/ml. THP-1 cells were pre-incubated with the SBKT containing media for 1 h before addition of 1 µg/ml (final concentration) LPS. No LPS was added to the negative control cells. Cell culture supernatants were collected after 24 h, and different pro-inflammatory cytokines IL-1β, IL-6, and TNF-α were measured using ELISA kits (BD Biosciences) following the manufacturer's protocol. Absorbance was recorded at 450 nm using the Envision microplate reader (PerkinElmer).

Luciferase Reporter NF-κB Gene Assay

THP-1 cells were transiently transfected with luciferase reporter vector with NF-κB promoter sequence upstream of the luciferase gene. Transfection was performed following the manufacturer's instruction in 96-well plates using Lipofectamine 3000 (Invitrogen, USA). Two days after transfection, the experiment was performed as described by Ishimoto et al. (2015) with the following modifications. Used media was replaced with media containing test compound and control. After 1 h, LPS was added at a concentration of 500 ng/ml, where required and incubated further for 12 h. D-Luciferin salt (PerkinElmer) at a final concentration of 150 µg/ml was added to the cells and incubated at 37°C, protected from light. Relative percentage changes in light emission intensity were measured from each well and calculated, and LPS alone was measured as 100% activity of the NF-κB reporter gene.

Experimental Animals

CD-1 male mice (6–8 weeks) were procured from a Charles River Laboratory-licensed supplier, Hylasco Biotechnology Pvt. Ltd, Hyderabad, India. Male Wistar rats (8 to 10 weeks) were procured from Liveon Biolabs Pvt. Ltd, Bangalore, India. All the animals were placed under a controlled environment with a relative humidity of 60–70% and 12:12-h light and dark cycle in a registered animal house (1964/PO/RC/S/17/CPCSEA) of Patanjali Research Institute, India. The animals were fed a standard pellet diet (Golden Feed, India) and sterile-filtered water *ad libitum*. The study protocol was approved by the Institutional Animal Ethical Committee (IAEC) of Patanjali Research Institute vide approval numbers: PRIAS/LAF/IAEC-008 and PRIAS/LAF/IAEC-022. All the experiments were performed in accordance with relevant guidelines and regulations described by the ethical committees.

Evaluation of *In Vivo* Anti-Inflammatory and Anti-Psoriasis-Like Efficacies

Carrageenan-Induced Rat Paw Edema Model

Carrageenan-induced paw edema test was performed according to the modified methods described earlier (Sakat et al., 2014). Wistar rats were divided into different groups of eight animals each based on basal paw volume (0 h), measured using Plethysmometer (Ugo Basile, Italy). Inflammation was induced by the subcutaneous injection of λ-Carrageenan (0.1 ml of 1% solution in normal saline) into the plantar side of the left hind paw. The paw was marked with ink at the level of the lateral malleolus, and the volume was measured up to the mark at 1, 2, 3, 4, and 5 h after carrageenan injection for all the animals. Further, animals were treated orally with SBKT [100 mg/kg p.o. + 40 µl/paw topical application (T.A.)] or INDO at 10 mg/kg (p.o.), 1 h before carrageenan challenge. Paw edema was calculated by subtracting the 0-h (basal) paw volume from the respective paw volumes at 1,

2, 3, 4, and 5 h. The anti-inflammatory activity (%) was calculated for each animal using the following formula: [Mean paw edema of control animals (ml) − paw edema of each test animals (ml)]/[Mean paw edema of control animals (ml)] × 100.

TPA-Induced Psoriasis-Like Lesion Mouse Model

Anti-psoriatic-like effects of SBKT were examined on the TPA-induced skin inflammation model as described previously with a slight modification (Goto et al., 2010). Briefly, 20 µl of TPA solution (2.5 µg/ear of TPA in acetone) was applied topically on the right ear of CD-1 mice on days 0, 2, 4, 6, 8, and 10. The left ear was served as the vehicle control and treated with 20 µl of acetone on the same days. Ear thickness was measured every day using a digital Vernier caliper (Mitutoyo, Tokyo, Japan). An increase in ear thickness was determined by subtracting the ear thickness of day 0 (before TPA or acetone application) from the respective time point thickness. Animals were treated with a vehicle or SBKT (at 100 mg/kg p.o. + 20 µl T.A and 200 mg/kg p.o. + 20 µl T.A.) or DEXA (0.2 mg/ear T.A.) throughout the study. The anti-psoriasis activity (%) was calculated for each animal on day 10 (D10), using the following formula: [Mean ear edema of TPA control mice − ear edema of each mouse of test or DEXA-treated mouse]/[Mean ear edema of TPA control mice] × 100.

Histopathological Analysis

CD-1 mice were humanely euthanized on day 10 after 6 h of the last drug treatment. Ear biopsy samples were weighed and fixed in 10% (v/v) neutral-buffered formalin, embedded in paraffin, and sectioned at 3–5 µm. The sections were then stained with hematoxylin and eosin. By using a bright-field microscope, low-magnification and high-magnification histology images of the ear biopsy samples were obtained at 100× and 400×, respectively. The thickness of the epidermis (from the basal layer to the stratum corneum) was measured by MagVision image analysis software using the Magcam DC5 microscopic camera and calibration by a stage micrometer. The severity of the observed lesions was recorded as NAD = no abnormality detected, 1 = minimal (<1%), 2 = mild (1–25%), 3 = moderate (26–50%), 4 = moderately severe/marked (51–75%), and 5 = severe (76–100%). Distribution of the lesions was recorded as focal, multifocal, and diffused. The different parameters like the extent of the lesion, severity of hyperkeratosis, number and size of pustules, epidermal hyperplasia (measured in the interfollicular epidermis), the severity of inflammation in the dermis and soft tissue, and any other lesion(s) were considered for histopathological examination and scoring.

Statistical Analysis

The data are expressed as mean ± SEM for each group. Statistical analysis was done using GraphPad Prism version 7.03 software. Two-way ANOVA followed by Newman–Keuls multiple comparison test was used to calculate the statistical difference in absolute paw volume, paw edema, and ear edema. A one-way ANOVA followed by Dunnett's multiple comparison post hoc test was used to calculate the statistical difference in cytokine(s) analysis, ear biopsy weights, epidermal thickness, and lesion scores. The values of $p < 0.05$ were considered statistically significant.

RESULTS

Chemical Profiling of SBKT Components Using GC–FID

GC–FID technique-based chemical analysis of the SBKT showed the presence of 16 major fatty acid peaks and several minor peaks (**Figure 1A**). Saturated fatty acid content represented the highest quantity of fatty acids (57.06%) present in the SBKT, followed by monounsaturated (23.31%) and polyunsaturated (19.64%) fatty acids (**Table 1** and **Figure 1B**). FAME-based GC–FID analysis of the SBKT for the identification and quantification of individual fatty acids showed the presence of palmitic acids (26.30%), cis-9 oleic acid (13.66%), linoleic acid (9.31%), lignoceric acid (9.16%), myristic acid (8.40%), palmitoleic acid (8.10%), stearic acid (7.45%), tricosanoic acid (1.97%), henicosadienoic acid (1.55%), alpha-linolenic acid 1.53%), heptadecanoic acid (1.31%), butyric acids (1.12%), pentadecanoic acid (0.81%), and arachidic acid (0.54%) (**Table 1**). Several other fatty acid components were also detected in the SBKT, but their quantities were relatively low (<0.10%) (**Table 1**).

In Vitro Anti-Inflammatory Activity of SBKT

Traditional use of SBKT in reducing gastric ulcers as an anti-inflammatory mediator has been attributed to the modulation of pro-inflammatory mediators (Xing et al., 2002). SBKT was found to induce significant ($p < 0.01$) loss of cell viability in the normal THP-1 cells at concentrations ≥25 µl/ml (**Figure 2A**). Therefore, 10 µl/ml was taken as the maximum test dose for subsquent *in vitro* assessments. Analysis of the RNS production in the LPS-stimulated THP-1 cells showed a significant ($p < 0.001$) increase as compared to the normal cells. SBKT treatment of the stimulated THP-1 cells led to a reduction in the cellular RNS levels ($p < 0.01$) in a concentration-dependent manner (**Figure 2B**). Treatment of the THP-1 cells with LPS also stimulated the expression of inflammatory NF-κB protein (**Figure 2C**). This stirred-up increase in the NF-κB protein expression was ameliorated by SBKT treatment. Increase in the NF-κB protein expression was also associated with a significant increase in the release of the pro-inflammatory cytokines: IL-1β ($p < 0.001$), IL-6 ($p < 0.001$), and TNF-α ($p < 0.001$) (Figures 2D, E, F). Treatment of the THP-1 cells with SBKT emulsion significantly reduced the LPS-stimulated release levels of IL-1β [5 µl/ml ($p < 0.05$), 2.5 µl/ml ($p < 0.01$), and 1.25 µl/ml ($p < 0.05$)] and IL-6 [5 µl/ml ($p < 0.001$), 2.5 µl/ml ($p < 0.01$), and 1.25 µl/ml ($p < 0.001$)] from the THP-1 cells (**Figures 2D**, **E**). A reducing trend in TNF-α cytokine release in the THP-1 cells treated with SBKT and LPS was observed at 24 h, with a significant reduction occurring at the highest test concentration of the oil (5 µl/ml; $p < 0.01$) (**Figure 2F**).

In Vivo Anti-Inflammatory Effects of SBKT

Subplantar injection of λ-Carrageenan (0.1 ml of 1% solution in normal saline) in the Wistar rats induced a time-dependent increase in both the absolute paw volume and paw edema (**Figures 3A**, **B**). Post-treatment of the Carrageenan-stimulated Wistar rats with 10 mg/kg of standard anti-inflammatory drug

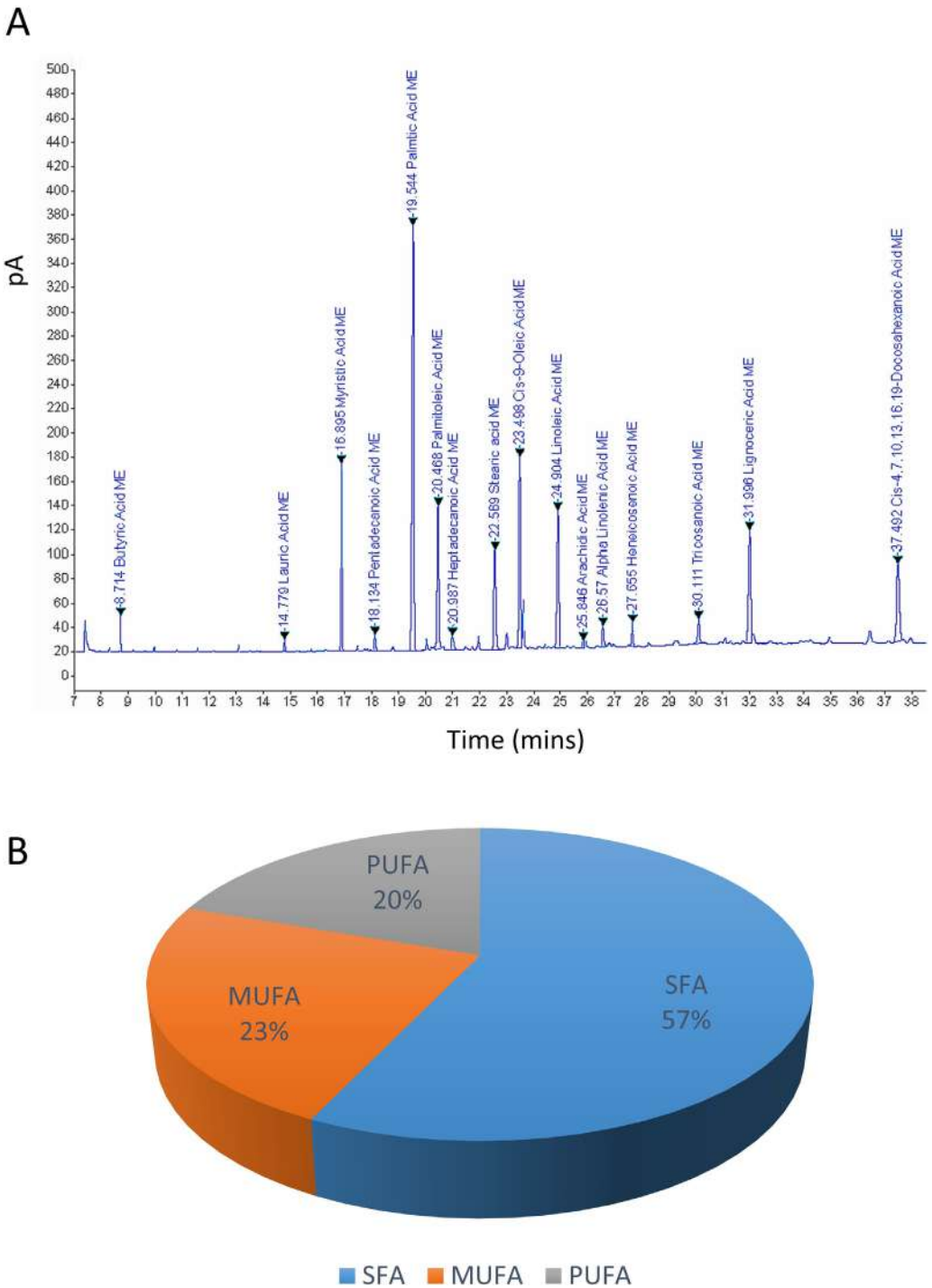

FIGURE 1 | Gas chromatography–flame ionized detector (GC–FID) chromatogram of sea buckthorn oil (SBKT). **(A)** The fatty acid composition of the SBKT was determined using the GC–FID methodology. Individual fatty acids were identified and quantified using fatty acid methyl ester methodology. Chromatography analysis identified 16 major fatty acids. **(B)** Pie-diagram represents the percentage of three categories of fatty acids identified in the SBKT—saturated fatty acids (SFA), monounsaturated fatty acids (MUFA), and polyunsaturated fatty acids (PUFA) (also see **Table 1**).

INDO exhibited a significant reduction of absolute paw volume ($p < 0.001$) and paw edema ($p < 0.001$) (**Figures 3A**, **B**). Oral (100 mg/kg: calculated from a human equivalent dose of 2000 mg/day, for rats) and topical (40 µl/paw) treatment of the Carrageenan-stimulated rats with SBKT induced an observable decrease in both the paw absolute volume and paw edema (statistically significant at 4 h; $p < 0.05$), compared to the disease control animals (**Figures 3A**, **B**).

TABLE 1 | Gas chromatography–flame ionized detector analysis of sea buckthorn oil (SBKT) fatty acid contents.

Fatty acid name	Chemical structure	Content (%)
Palmitic acid ME ($C_{16}H_{32}O_2$; mol wt. 256.43; SFA)	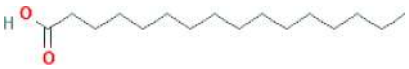	26.30
Lignoceric acid ME ($C_{24}H_{48}O_2$; mol wt. 368.63; SFA)		9.16
Myristic acid ME ($C_{14}H_{28}O_2$; mol wt 228.37; SFA)		8.40
Stearic acid ME ($C_{18}H_{36}O_2$; mol wt. 284.48; SFA)		7.45
Tricosanoic acid ME ($C_{23}H_{46}O_2$; mol wt. 354.61; SFA)		1.97
Butyric acid ME ($C_4H_8O_2$; mol wt. 88.11; SFA)	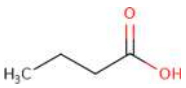	1.12
Heptadecanoic acid ME ($C_{17}H_{34}O_2$; mol wt 270.45; SFA)	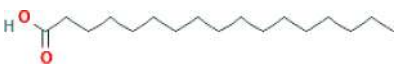	1.31
Pentadecanoic acid ME ($C_{15}H_{30}O_2$; mol wt. 242.39; SFA)	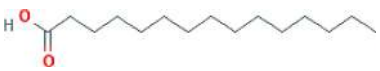	0.81
Arachidic acid ME ($C_{20}H_{40}O_2$; mol wt. 312.53; SFA)		0.54
Cis-9 Oleic acid ME ($C_{18}H_{34}O_2$; mol wt. 282.47; MUFA)	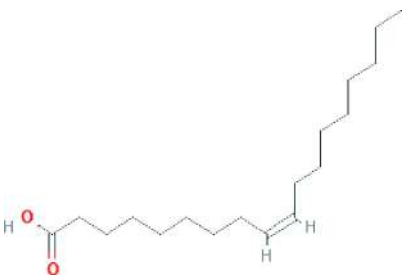	13.66
Palmitoleic acid ME ($C_{16}H_{30}O_2$; mol wt. 254.41; MUFA)	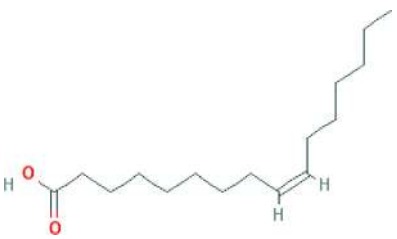	8.10
Henicosadienoic acid ME ($C_{21}H_{38}O_2$; mol wt. 322.53; MUFA)	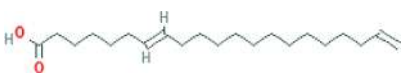	1.55
Linoleic acid ME ($C_{18}H_{32}O_2$; mol wt. 280.44; PUFA)	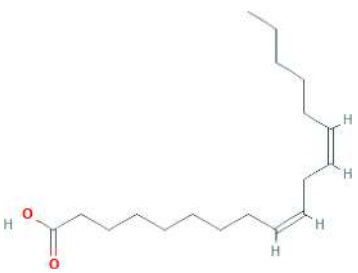	9.31

(Continued)

TABLE 1 | Continued

Docosahexaenoic acid ME ($C_{22}H_{32}O_2$; mol wt 328.48; PUFA)	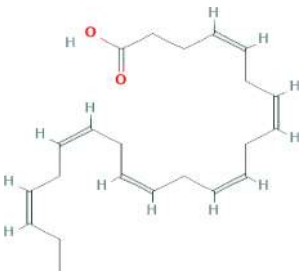	8.80
Alpha-linolenic acid ME ($C_{18}H_{30}O_2$; mol wt. 278.43; PUFA)	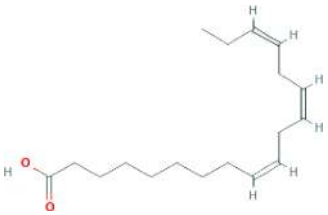	1.53

*Quantified fatty acid methyl esters (ME) have been listed in the descending order of contents (%) for saturated fatty acids (SFA), monounsaturated fatty acids (MUFA), and polyunsaturated fatty acids (PUFA), in SBKT (also see **Figure 1**). The following fatty acid MEs were found to be <0.10% quantitatively: caproic acid ME, cis-10-penta decanoic acid ME, cis-10-heptadecanoic acid ME, trans-9 elaidic acid ME, linolelaidic acid ME, myristoleic acid ME, cis-11-eicosenoic acid ME, caprylic acid ME, cis-11,14 eicosadienoic acid ME, behenic acid ME, cis 8,11,14 eicosatrienoic acid ME, erucic acid ME, cis 11,14,17 eicosatrienoic acid, capric acid ME, lauric acid ME, tridecanoic acid ME, EPA ME, gamma-linolenic acid ME, arachidonic acid ME, cis 13,16 docosadienoic acid ME, and nervonic acid ME.*

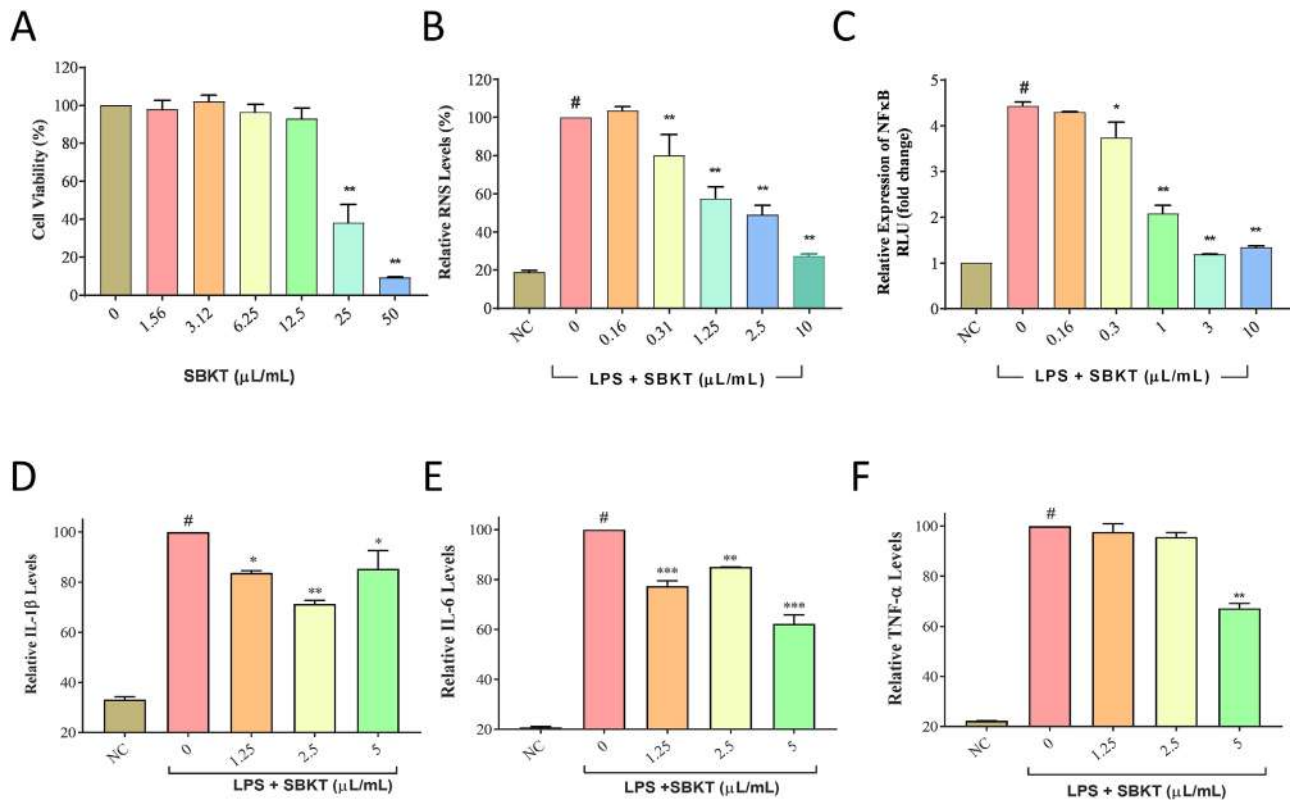

FIGURE 2 | *In vitro* anti-inflammatory potentials of the SBKT. **(A)** Treatment of THP-1 cells with SBKT induced loss of cell viability at concentrations ≥25 µl/ml. Treatment of the lipopolysaccharide (LPS)-stimulated THP-1 cells with the non-cytotoxic doses of SBKT showed amelioration in the production of **(B)** reactive nitrogen species (RNS) and **(C)** NF-κB. Downstream reduction in the release of pro-inflammatory cytokines: **(D)** interleukin-1β (IL-1β), **(E)** interleukin-6 (IL-6), and **(F)** tumor necrosis factor-α (TNF-α) was observed in the LPS-stimulated THP-1 cells treated with different concentrations of SBKT. These experiments were performed thrice in triplicates. One-way ANOVA followed by Dunnett's post hoc test was performed to calculate statistical significance. $^{\#}p < 0.001$ (LPS-stimulated *versus* normal control cells); $^{*}p < 0.05$, $^{**}p < 0.01$, $^{***}p < 0.001$ (LPS only stimulated cells *versus* LPS + SBKT-treated cells).

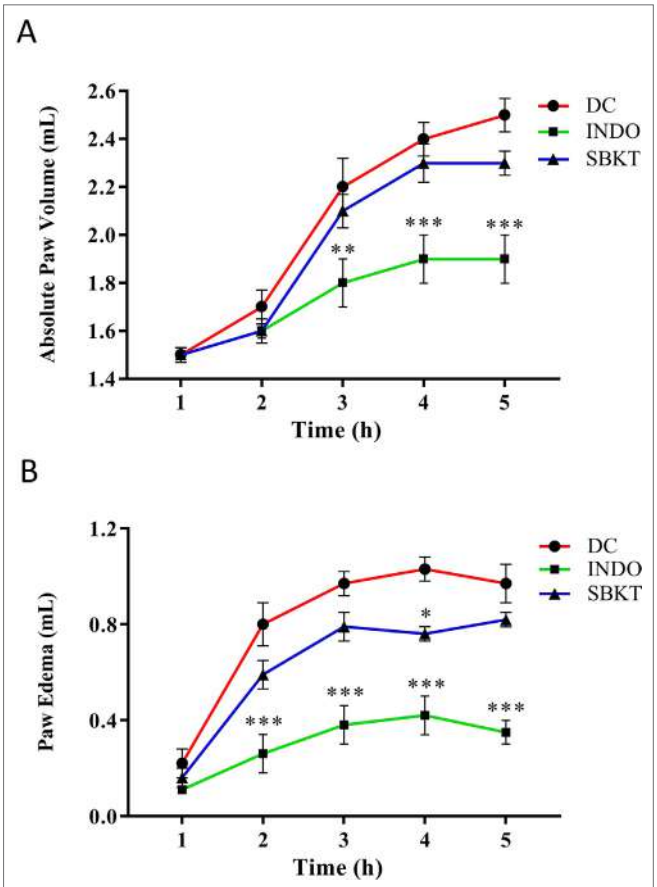

FIGURE 3 | Effect of SBKT on λ-Carrageenan-induced paw rat edema model. Co-treatment of carrageenan-stimulated Wistar rats with SBKT [100 mg/kg; p.o. and 40 µl topical application (T.A.)] or with INDO (10 mg/kg; p.o.) led to a considerable reduction in their **(A)** absolute paw volume and **(B)** paw edema. Statistical analysis of the treatments was performed using two-way ANOVA followed by Newman–Keuls multiple comparison test (n = 7 animals). *p < 0.05, **p < 0.01, ***p < 0.001 (DC *versus* SBKT; DC *versus* INDO-treated animals). DC, disease control, SBKT, sea buckthorn oil; INDO, indomethacin.

In Vivo Anti-Psoriatic Activity of SBKT

TPA formulated in acetone was applied on the CD-1 mouse ear (2.5 µg/ear) for induction of psoriasis-like disease. Topical application of TPA significantly induced ear edema in the control (TPA CON) animals ($p < 0.001$) (**Figure 4A**). Topical treatment of the psoriatic ear with the standard anti-inflammatory drug DEXA (0.2 mg/ear) significantly reduced the ear edema from day 2 onward ($p < 0.001$) (**Figure 4A**). Similarly, concurrent oral (100 and 200 mg/kg) and topical (20 µl) treatment of the SBKT in the psoriatic animals significantly reduced ear edema from day 2 onwards. In these test parameters, no significant variation in the responses was observed in the animals treated with 100 and 200 mg/kg-dose of SBKT. For mice, 200 mg/kg is the calculated human equivalent dose (2000 mg/day), as per body weights and surface area conversions. The percent inhibition (at D-10) in the ear edema of DEXA and SBKT 100 and 200 mg/kg treated mice was found to be 70.05 ± 6.25%, 34.05 ± 7.65%, and 30.45 ± 8.90%, respectively, in comparison to TPA CON mice (**Figure 4B**).

Effect of SBKT on Psoriatic Ear Biopsy Weight and Epidermal Thickness

Increased ear biopsy weight was detected in the TPA CON CD-1 mice after 10 days' treatment showing inflammatory effects ($p < 0.001$) (**Figures 5A**, **B**). Treatment of the psoriatic animals with DEXA (0.2 mg/ear) significantly reduced the elevated ear biopsy weight ($p < 0.001$) (**Figure 5A**). Oral (100 and 200 mg/kg) and topical (20 µl) treatment of the SBKT also significantly reduced the inflammation-induced biopsy weight ($p < 0.001$) compared to the TPA CON animal (**Figure 5A**).

Similarly, histopathological evaluation of psoriatic ear punch biopsy (TPA CON) showed a significant ($p < 0.001$) increase in epidermal thickness (54.42 ± 12.20 µm) as compared to the normal control (NC) animals (8.26 ± 1.07 µm) (**Figure 5B**). Treatment of the TPA-induced psoriatic ear with the topical application of DEXA significantly ($p < 0.001$) reduced the epidermal layer thickness (15.53 ± 4.10 µm). Similarly, concurrent oral (100 and 200 mg/kg) and topical (20 µl) treatment of the SBKT also significantly ($p < 0.001$) reduced the ear epidermal thickness (31.80 ± 6.90 µm and 21.91 ± 5.07 µm, respectively), indicating the anti-inflammatory and anti-psoriatic efficacies of SBKT (**Figure 5B**).

Effect of SBKT on Inflammatory Lesion Scores

Histopathological analysis of the TPA-stimulated mice ear showed a significant increase in inflammatory lesions score such as epidermal hyperkeratosis and infiltration of inflammatory cells in the dermal region (**Figures 6A**, **C**). No such changes were observed in the tissue of the mouse ears treated with vehicle control (**Figure 6B**). Treatment of the TPA-stimulated ear with DEXA reduced the influx of inflammatory cells but continued to show the signs of persisting hyperkeratosis lesions and hyperplasticity in the epidermis (**Figure 6D**). Concurrent oral (100 and 200 mg/kg) and topical (20 µl) application of the SBKT on the psoriatic mice ear also reduced signs of hyperkeratosis and hyperplasticity in the skin epidermis but sustained the presence of inflammatory cells in the dermal region (**Figures 6E**, **F**).

Individual scoring through histopathological analysis further confirmed the efficacy of SBKT. Results suggested an elevation in the lesion score of hyperkeratosis, epidermal hyperplasia, pustule formation, and inflammatory cell infiltration in the epidermal and dermal regions of the TPA CON animals (**Figures 7A–D**). Treatment of the psoriatic ear with oral and topical (20 µl) application of the SBKT exhibited a significant reduction in the lesion scores [hyperkeratosis: SBKT 200 mg/kg ($p < 0.05$); hyperplasia: SBKT 200 mg/kg ($p < 0.001$); pustule formation and epidermal inflammation: SBKT 100 mg/kg ($p < 0.01$) and SBKT 200 mg/kg ($p < 0.001$); inflammatory cells infiltration] (**Figures 7A–D**). DEXA topical treatment also reduced the observed individual lesion scores and infiltration of inflammatory cells (**Figures 7A–D**), as expected. Total lesion score analysis and % inhibition (activity) calculation showed a significant decrease in the overall inflammation in the SBKT ($p < 0.01$ at 100 mg/

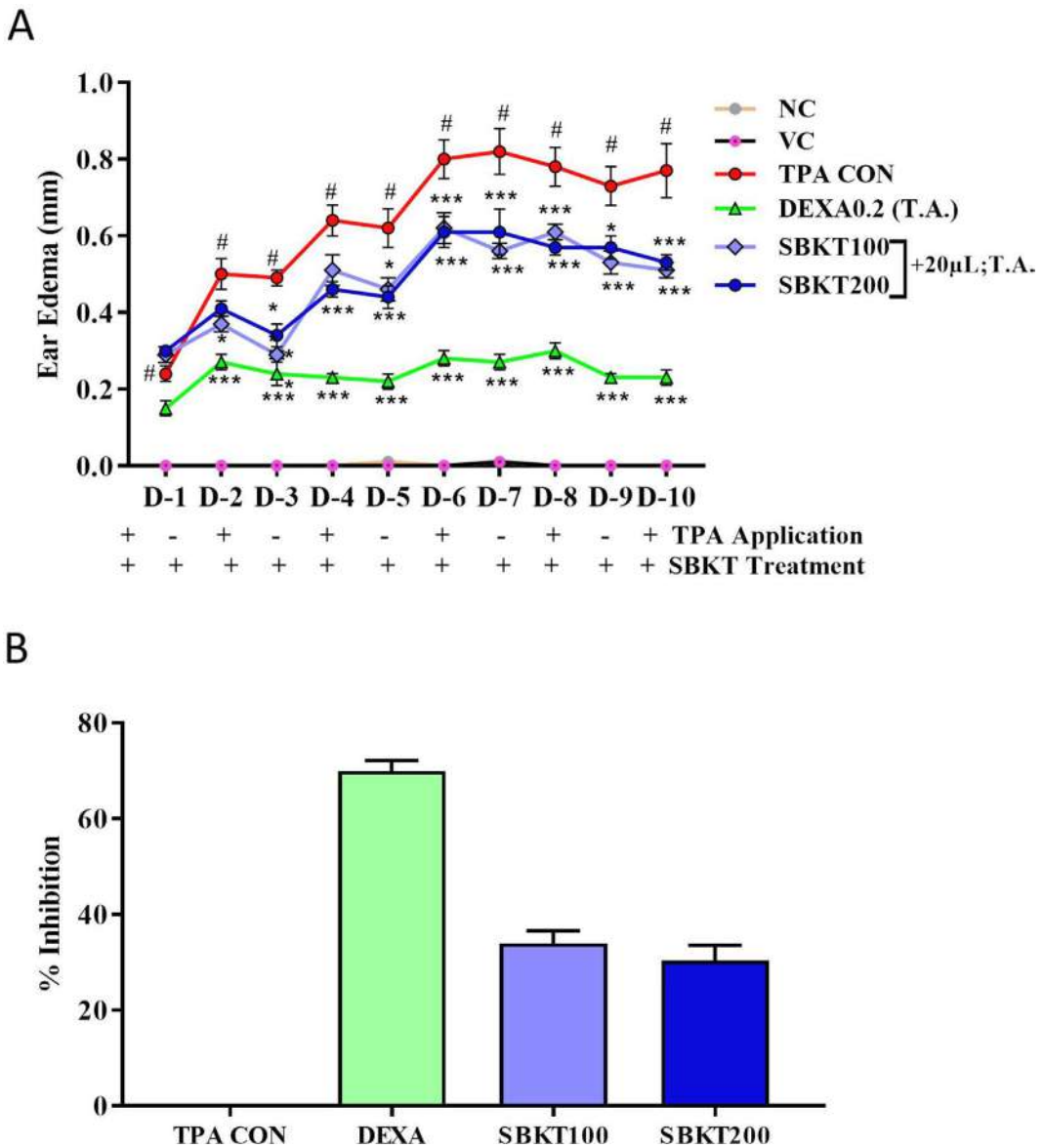

FIGURE 4 | Effect of SBKT on TPA-induced ear edema in mice. **(A)** Co-treatment of the TPA-stimulated psoriatic ear (TPA CON) with SBKT (100 and 200 mg/kg; p.o. and 20 µl T.A.) or with DEXA (0.2 mg/ear; T.A.) significantly reduced ear edema. **(B)** Represents percent ear edema inhibition (activity) calculated in comparison to TPA CON animals at D10. This panel represents % inhibition (activity) of SBKT 100, SBKT 200, and DEXA individually. Statistical analysis was performed using two-way ANOVA followed by Newman–Keuls multiple comparison test (n = 8 animals). $^{\#}p < 0.001$ (NC *versus* TPA CON); NS $p > 0.05$ (NC versus VC) $^{*}p < 0.05$, $^{**}p < 0.01$, $^{***}p < 0.001$ (TPA CON *versus* SBKT; TPA CON *versus* DEXA). NC, normal control; VC, vehicle control; TPA CON, 12-O-tetradecanoyl phorbol-13-acetate; DEXA, dexamethasone; SBKT, sea buckthorn oil.

kg; $p < 0.001$ at 200 mg/kg) and DEXA ($p < 0.001$) treated TPA-stimulated mice (**Figures 7E**, **F**).

DISCUSSION

Psoriasis a common skin systemic inflammatory disease leading to the development of dermal changes such as itching, burning, and soreness (Lowes et al., 2007; Wagner et al., 2010). During the onset of disease, the affected keratinocytes and pro-inflammatory immune cell cross-talk to release soluble pro-inflammatory mediators such as IL-1β, TNF-α, IL-6, and IL-8. So far, there is no permanent cure for psoriasis, and the disease can undergo cyclic evolution with periods of flaring for weeks or months, and then becoming dormant for a significant amount of time.

SBKT has been used as a good source of nutrition for centuries (see Krejcarová et al., 2015, for the detailed review), with defined medicinal uses like cardioprotective, antidiabetic, hepatoprotective, and anti-carcinogenic activities. In the present study, we investigated the SBKT extracted from the fruit pulp for its

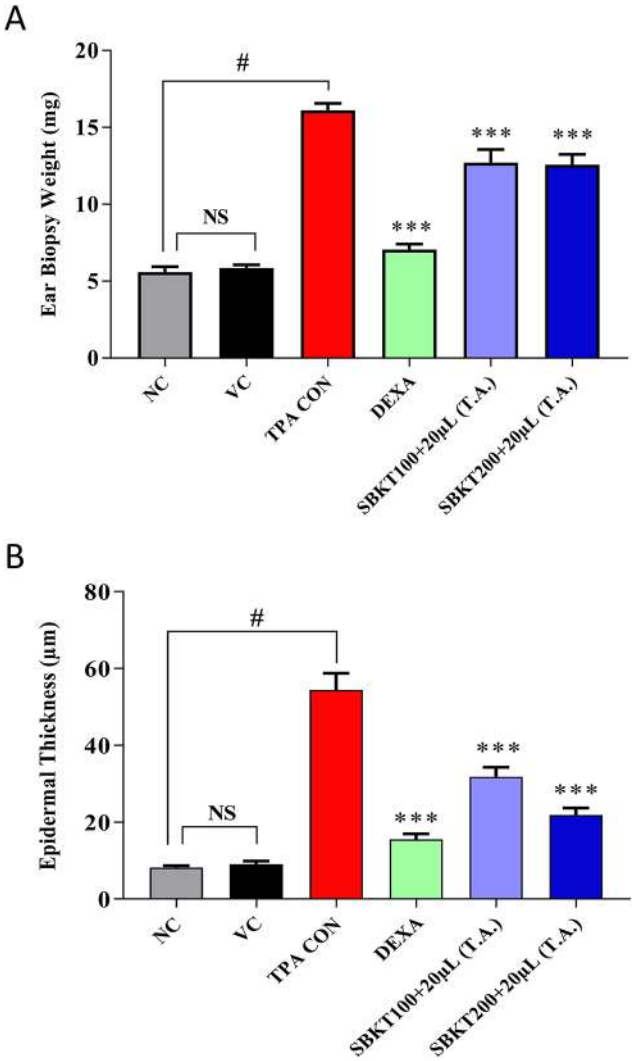

FIGURE 5 | Effect of SBKT on TPA-induced ear biopsy weight in mice. Co-treatment of the psoriatic ear with SBKT (100 and 200 mg/kg; p.o. and 20 µl T.A.) or with DEXA (0.2 mg/ear; T.A.) significantly reduced the **(A)** ear biopsy weight and **(B)** ear epidermal thickness. Statistical analysis was performed using one-way ANOVA method followed by Dunnett's multiple comparison *t* test (n = 8 animals). $^{\#}p < 0.001$ (NC *versus* TPA CON); NS p>0.05 (NC versus VC); ***p < 0.001 (TPA CON *versus* SBKT; TPA CON *versus* DEXA). NC, normal control; VC, vehicle control; TPA CON, 12-O-tetradecanoyl phorbol-13-acetate; DEXA, dexamethasone; SBKT, sea buckthorn oil.

anti-inflammatory and anti-psoriatic roles. Initial chemical analysis of the fatty acid content of the SBKT using GC–FID revealed the presence of high quantities of saturated, monounsaturated, and polyunsaturated fatty acids along with smaller factions of several other fatty acids. Presence of most of these fatty acids in the SBKT has been reported earlier by Zielinska and Nowak and correlates well with our findings (Zielinska and Nowak, 2017). Fatty acids such as palmitic acid, oleic acid, palmitoleic acid, stearic acid, and the linoleic acid identified in the SBKT act as major constituents of the human epidermis (Kim et al., 2010). Palmitoleic acid also promotes wound healing and diminishes inflammation through modulation of pro-inflammatory cytokines (Bal et al., 2011; Kumar et al., 2011; Shi et al., 2017; Souza et al., 2017). Omega-3 (α-linolenic acid) and omega-6 (linoleic acids) fatty acids present in the SBKT have been identified as essential components of the body and help in the translocation of the fat-soluble vitamins (A, D, E, and K) and wound healing (Lee et al., 2006; Cupara et al., 2011; Ito et al., 2014; Calder, 2017). Omega-3 (α-linolenic acid), omega-6 (linoleic acid), and omega-9 (oleic acid) fatty acids also help in forming a protective barrier against trans-epidermal water loss (Zielinska and Nowak, 2017). Therefore, the presence of these saturated, monounsaturated, and polyunsaturated fatty acid components in the SBKT along with other bioactive compounds helps in forming a protective barrier for the skin and helps in the skin wound healing and repair.

Inflammation plays a major role in the development of psoriasis. Initiation of psoriasis is associated with the infiltration of the pro-inflammatory cells such as, monocytes, neutrophils, and T cells (Ogawa et al., 2018). These cells boost the development of inflammation and oxidative stress through the release of pro-inflammatory cytokines and reactive oxygen and nitrogen species. Our initial *in vitro* screening for the anti-inflammatory behavior of SBKT was done using LPS-stimulated THP-1 cells. Treatment of the THP-1 cells with SBKT showed that it is capable of inducing cytotoxicity at a dose of 25 µl/ml. Applying a non-cytotoxic dose, SBKT was found capable of ameliorating LPS-induced inflammation in the THP-1 cells through the reduction of pro-inflammatory RNS levels and NF-κB protein expression. Both the RNS and NF-κB have been reported as critical components involved in the induction of psoriasis (Bruch-Gerharz et al., 1998; Goldminz et al., 2013; Moorchung et al., 2014). Hence, modulation of both these markers of inflammation by SBKT indicated its anti-inflammatory capabilities. Analysis of the NF-κB protein downstream expression of the pro-inflammatory cytokines IL-1β, IL-6, and TNF-α showed a modulation via SBKT treatment in the stimulated THP-1 cells. This finding holds importance since the onset of psoriasis disease involves the increased expression of NF-κB and release of the pro-inflammatory mediators and RNS (Kupper and Fuhlbrigge, 2004).

An anti-inflammatory activity study of the SBKT was performed using the λ-Carrageenan-stimulated Wistar rat inflammation model and the TPA-stimulated CD-1 mice psoriasis-like model. The TPA-stimulated CD-1 mice psoriasis-like model is well-established for studying the disease-modulating efficacy of test compounds (Madsen et al., 2016; Ma et al., 2018; Yang et al., 2018). Treatment of the Carrageenan-stimulated Wistar rats with a human equivalent dose of SBKT showed a significant decrease in the drug-induced paw volume increase and edema in the rats. Similarly, SBKT treatment at a human equivalent dose in the TPA-stimulated CD-1 mice revealed a modulation of the psoriasis-like inflammation and associated lesions in the mice ear. Reduction in the inflammatory lesions can be well correlated with the anti-inflammatory activity of the SBKT observed in the LPS-stimulated THP-1 cells, showing downregulation of inflammatory mediators.

Earlier studies have also shown the SBKT to possess anti-inflammatory properties through the modulation of pro-inflammatory cytokines, cyclooxygenase-2, inducible nitric oxide synthase, and inflammasome-associated IKK-β/NF-κB

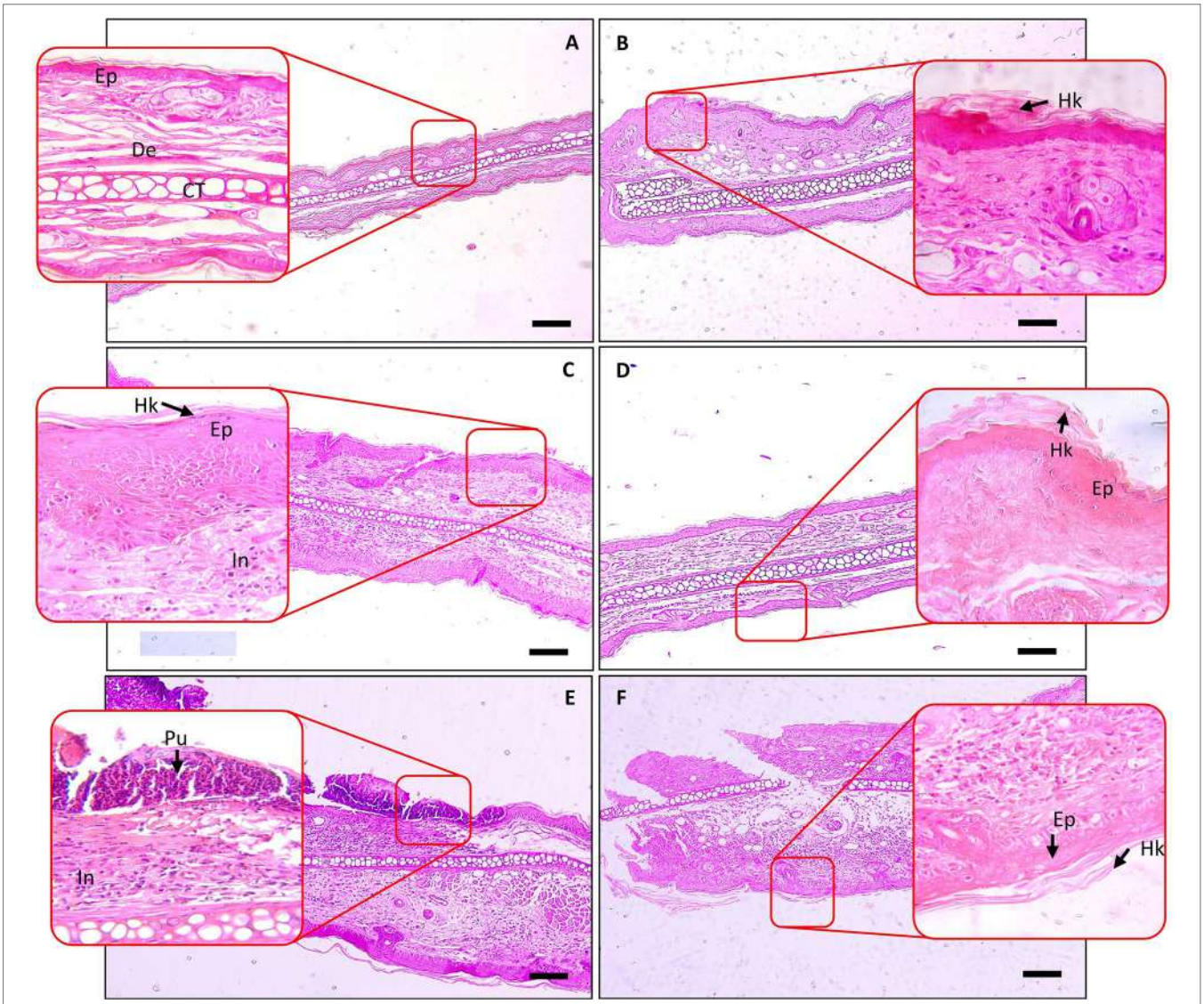

FIGURE 6 | Histopathological analysis of SBKT treatment on TPA-induced ear psoriasis in mice**.** Histopathological analysis of mice ear tissue was performed following fixation and hematoxylin and eosin staining. Low-magnification images were obtained at 100×, and the higher-magnification image was obtained at 400×. **(A)** Normal control: represents normal epidermis (Ep), dermis (De), sebaceous gland (Sg), cartilage (CT). **(B)** Vehicle control (acetone) treated ear: represents normal epidermis (Ep), dermis (De), sebaceous gland (Sg), cartilage (CT). **(C)** TPA-CON: represents hyperkeratosis (Hk) and hyperplastic epidermis (Ep), presence of inflammatory cells (In) in the dermis region. **(D)** TPA and DEXA (0.2 mg/ear) treated ear: reduced hyperplastic epidermis (Ep), absence of inflammatory cells in the dermis region. **(E)** TPA and SBKT (100 mg/kg; p.o. and 20 µl; T.A.) treated ear: reduced hyperkeratosis (Hk) and hyperplastic epidermis (Ep), reduced presence of inflammatory cells (In) in the dermis region. **(F)** TPA and SBKT (200 mg/kg; p.o. and 20 µl; T.A.) treated ear: reduced hyperkeratosis (Hk) and hyperplastic epidermis (Ep). The scale represents 100 µm (n = 8 animals).

pathways (Jayashankar et al., 2012; Jayashankar et al., 2014; Suchal et al., 2016; Shi et al., 2017; Tanwar et al., 2018). The anti-inflammatory property of the SBKT can be related to the presence of fatty acids, such as polyunsaturated and omega-3 fatty acid components. These fatty acids have been reported to inhibit LPS-stimulated inflammation in inflammatory cells through modulation of Toll-like receptor 4, NF-κB, Nod-like receptor protein 3, cyclooxygenase-2, JAK, and P38 pathways and associated release of pro-inflammatory cytokines (Lee et al., 2003; Martínez-Micaelo et al., 2016; Hou et al., 2017). Hence, in our study, the presence of these fatty acids can be correlated with modulation of the NF-κB and pro-inflammatory cytokine inhibition observed in the stimulated THP-1 cells when treated with SBKT and inhibition of inflammation in the *in vivo* studies. Blocking of the TNF-α, the NF-κB pathways have been a focus of the anti-psoriasis treatments as it leads to the reduction in the inflammasome activation and downregulation of the cytokine such as IL-1β (Goldminz et al., 2013; Moorchung et al., 2014).

Traditionally, the SBKT plant has been called as the "wonder plant" for its therapeutic applications in several diseases. While our study demonstrated loss of cell viability in the THP-1 cells under *in vitro* conditions at higher doses. Similarly, using *in vivo* models,

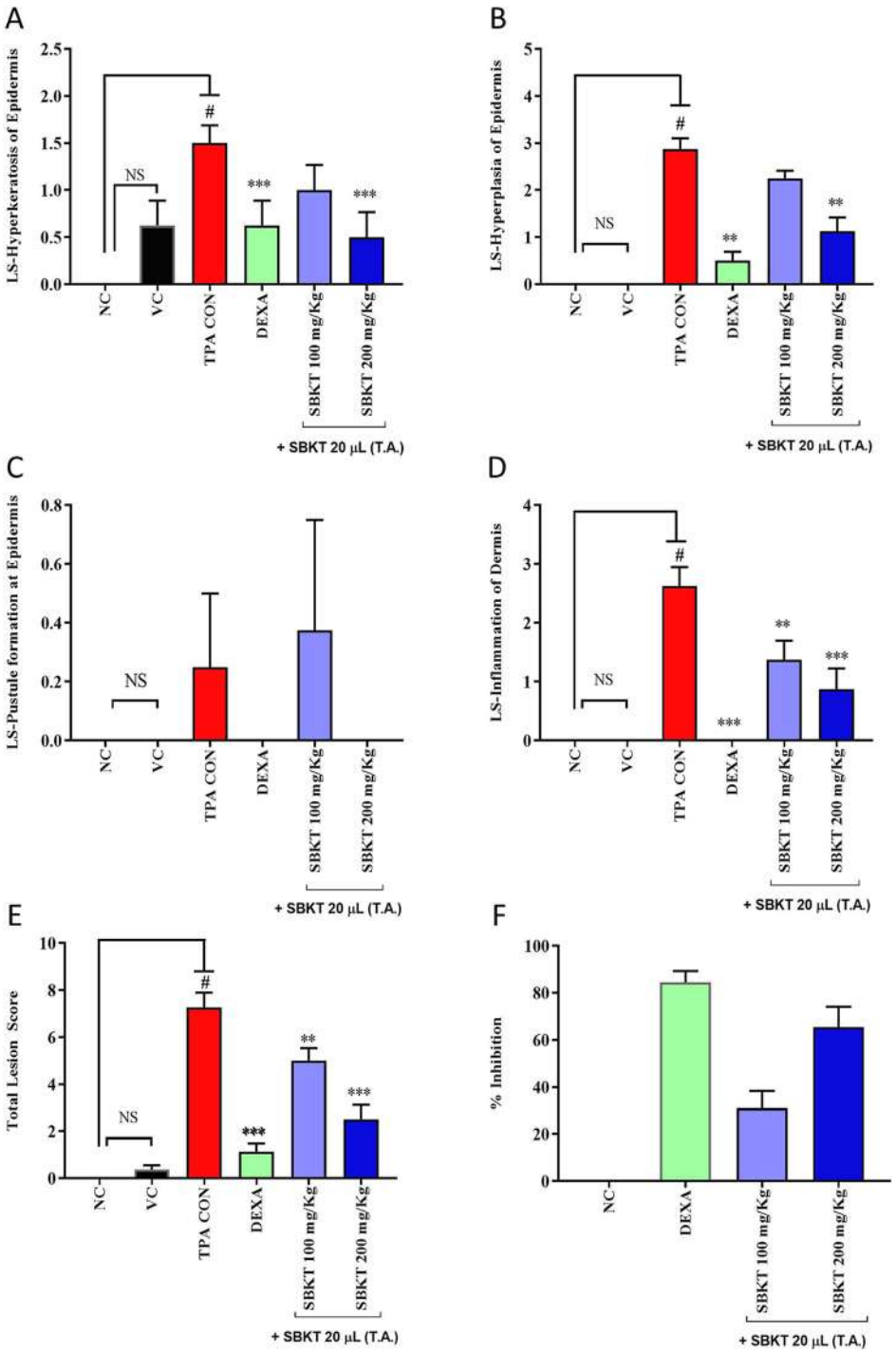

FIGURE 7 | Effect of SBKT on TPA-induced inflammatory lesions in mice ear. Mice co-treated with TPA and DEXA or SBKT showed a reduction in histopathological lesions viz. **(A)** Hyperkeratosis of the epidermis. The data clearly demonstrated the considerable decrease in hyperkeratosis score by SBKT at 100 and 200 mg/kg ($p < 0.001$) in comparison to TPA CON. **(B)** Hyperplasia of the epidermis. Results showed a decrease in hyperplasia score by SBKT at 100 and 200 mg/kg ($p < 0.001$). **(C)** Pustule formation at the epidermis. Only SBKT at 200 mg/kg ($p < 0.001$) was found to reduce pustule formation in comparison to TPA CON. **(D)** Inflammation of the dermis. A significant decrease in dermal inflammation score was observed following treatment with SBKT at 100 ($p < 0.01$) and 200 mg/kg ($p < 0.001$). **(E)** Results showed a significant decrease in total lesion score at 100 ($p < 0.01$) and 200 mg/kg ($p < 0.001$). Represents percentage inhibition of total lesion score. % Inhibition data have not been statistically compared between SBKT 100 and SBKT 200 with DEXA. This panel represents % inhibition (activity) of SBKT 100, SBKT 200, and DEXA individually. **(F)** Percentage inhibition of total lesion score. High activity in inhibiting inflammatory lesions was observed in the SBKT at 200 mg/kg followed by 100 mg/kg in comparison to TPA CON. Statistical analysis was performed using one-way ANOVA followed by Dunnett's multiple comparisons *t* test (n = 8 animals). #$p < 0.001$ (NC *versus* TPA CON), NS $p > 0.05$ (NC *versus* VC), **$p < 0.01$, ***$p < 0.001$ (TPA CON *versus* SBKT; TPA CON *versus* DEXA). NC, normal control; VC, vehicle control; TPA CON, TPA control; SBKT, sea buckthorn oil; DEXA, dexamethasone.

no toxicity has been reported for this plant's part extracts and oils. Acute and sub-chronic toxicity studies performed in Wistar rats have shown no signs of toxicity and reported a no-observed-adverse-effect level of 10 ml/kg body weight (Zhao et al., 2017). Furthermore, no mutagenicity was observed from the SBKT exposure in histidine-dependent *Salmonella typhimurium* stain (Wen et al., 2018), suggesting no induction of genotoxicity by SBKT. Exposure to SBKT also did not induce any changes in sperm morphology and micronucleus formation rate in polychromatic erythrocytes obtained from mice orally treated with the oil (Wen et al., 2018). In the present study, we have not seen any change in the animal weights, food, or water consumption (data not shown). In a recently published article, clinical application of the SBKT extract in 10 psoriatic patients showed a significant reduction in their Psoriasis Area Severity Index scores and in Dermatology Life Quality Index scores within 4–8 weeks' treatment, compared to placebo-treated patients who showed worsening signs in 4 weeks' trial period (Boca et al., 2019). In another study, obese children aged 10–18 years treated with SBKT (800 mg/day) for 60 days were found with reduced levels of total cholesterol, triglyceride, leptin, fasting C peptide, oxidative stress, and carotid artery intima–media thickness, at the end of the treatment period (Virgolici et al., 2013). These clinical outcomes bode very well with the results reported here, suggesting an overall efficacy of SBKT in the treatment of psoriasis and general inflammations.

Besides having high nutritional and therapeutic values, SBKT can have other applications such as the development of lipid-based nano-drug-delivery vehicle as well as its incorporation into capsules, gelatine, and oral liquids as an emulsifier (Yang and Kallio, 2002). In our present study, it was observed that there is very little that SBKT, the wonder plant, cannot be used for. The present study adds a pharmacological body of evidence to its tradition-rich nutritional usage—natural nutraceutical—indeed.

CONCLUSION

Finally, our study provided scientific evidence to the traditional wisdom that the SBKT obtained from the pulp of the seabuck thorn berries can be used as a therapeutic agent in subduing systemic inflammations and psoriasis-like lesions. Presence of high levels of saturated, monounsaturated, and polyunsaturated fatty acids along with other biomolecules in the oil significantly increases its values as a nutraceutical. In addition, the presence of high levels of clinically relevant lipids provides the opportunity to further explore the commercial and pharmaceutical applications of SBKT.

ETHICS STATEMENT

The animal study protocol was approved by the Institutional Animal Ethical Committee of Patanjali Research Institute vide IAEC approval numbers: PRIAS/LAF/IAEC-008 and PRIAS/LAF/IAEC-022. All the experiments were performed in accordance with relevant guidelines and regulations.

AUTHOR CONTRIBUTIONS

AB provided a broad direction for the study, identified the test formulation, generated resources, and gave final approval for the manuscript. SS conducted the *in vivo* study, analyzed the data, and helped in manuscript writing and reviewing. KhJ assisted in animal handling and in performing *in vivo* studies. KaJ prepared the histopathological slides. RR performed the *in vitro* experiments. VS and KB performed data curing and wrote the manuscript. AV supervised overall research project planning, generated resources, and reviewed and finally approved the manuscript.

FUNDING

This presented work has been conducted using research funds from Patanjali Research Foundation Trust, Haridwar, India.

ACKNOWLEDGMENTS

We are indebted to Param Shradhey Swami Ramdev ji for his financial and institutional supports to accomplish this research work. We also acknowledge support from Mr. Rajendra Shukla, Patanjali Ayurveda Limited, Haridwar, India, and from Professor Paran Gowda, University of Patanjali, Haridwar, India. We would also like to appreciate Mr. Bhanu Pratap, Mr. Pushpendra Singh, Mr. Vipin Kumar, and Mr. Sonit Kumar for the excellent animal handling and maintenance. We extend our gratitude to Ms. Babita Chandel, Mr. Brij Kishore, Mr. Pradeep Nain, Mr. Gagan Kumar, and Mr. Lalit Mohan for their swift administrative support. This presented work has been conducted using research funds from Patanjali Research Foundation Trust, Haridwar, India.

REFERENCES

AOAC (2000). *"Official Methods of Analysis: Method 996.01"*. 17th Ed., AOAC International Gaithersburg, MD.

Bal, L. M., Meda, V., Naik, S. N., and Satya, S. (2011). Sea buckthorn berries: a potential source of valuable nutrients for nutraceuticals and cosmeceuticals. *Food Res. Int.* 44 (7), 1718–1727. doi: 10.1016/j.foodres.2011.03.002

Boca, A. N., Ilies, R. F., Saccomanno, J., Pop, R., Vesa, S., Tataru, A. D., et al. (2019). Sea buckthorn extract in the treatment of psoriasis. *Exp. Ther. Med.* 17 (2), 1020–1023. doi: 10.3892/etm.2018.6983

Bonesi, M., Loizzo, M. R., Provenzano, E., Menichini, F., and Tundis, R. (2016). Anti-psoriasis agents from natural plant sources. *Curr. Med. Chem.* 23 (12), 1250–1267. doi: 10.2174/0929867323666160321121819

Bruch-Gerharz, D., Ruzicka, T., and Kolb-Bachofen, V. (1998). Nitric oxide in human skin: current status and future prospects. *J. Invest. Dermatol.* 110 (1), 1–7. doi: 10.1046/j.1523-1747.1998.00084.x

Calder, P. C. (2017). Omega-3 fatty acids and inflammatory processes: from molecules to man. *Biochem. Soc. Trans.* 45 (5), 1105–1115. doi: 10.1042/BST20160474

Christaki, E. (2012). Hippphae Rhamnoides L. (Sea Buckthorn): a potential source of neutraceuticals. *Food Public Health* 2 (3), 69–72. doi: 10.5923/j.fph.20120203.02

Cupara, S. M., Ninkovic, M. B., Knezevic, M. G., Vuckovic, I. M., and Jankovic, S. M. (2011). Wound healing potential of liquid crystal structure emulsion with sea buckthorn oil. *HealthMED.* 5 (5), 1218–1223.

Das, L., Bhaumik, E., Raychaudhuri, U., and Chakraborty, R. (2012). Role of nutraceuticals in human health. *J. Food Sci. Technol.* 49 (2), 173–183. doi: 10.1007/s13197-011-0269-4

Ganju, L., Padwad, Y., Singh, R., Karan, D., Chanda, S., Chopra, M. K., et al. (2005). Anti-inflammatory activity of Seabuckthorn (*Hippophae rhamnoides*) leaves. *Int. Immunopharmacol.* 5 (12), 1675–1684. doi: 10.1016/j.intimp.2005.03.017

Goldminz, A. M., Au, S. C., Kim, N., Gottlieb, A. B., and Lizzul, P. F. (2013). NF-κB: an essential transcription factor in psoriasis. *J. Dermatol. Sci.* 69 (2), 89–94. doi: 10.1016/j.jdermsci.2012.11.002

Goto, M., Kadoshima-Yamaoka, K., Murakawa, M., Yoshioka, R., Tanaka, Y., Inoue, H., et al. (2010). Phosphodiesterase 7A inhibitor ASB16165 impairs proliferation of keratinocytes *in vitro* and *in vivo*. *Eur. J. Pharmacol.* 633 (1-3), 93–97. doi: 10.1016/j.ejphar.2010.01.024

Gudjonsson, J. E., and Elder, J. T. (2008). *Fitzpatrick's Dermatology in General Medicine 7th edn*. New York: McGraw-Hill.

Gupta, A., Kumar, R., Pal, K., Banerjee, P. K., and Sawhney, R. C. (2005). A preclinical study of the effects of seabuckthorn (*Hippophae rhamnoides* L.) leaf extract on cutaneous wound healing in albino rats. *Int. J. Low Extrem. Wounds* 4 (2), 88–92. doi: 10.1177/1534734605277401

Hou, D. D., Di, Z. H., Qi, R. Q., Wang, H. X., Zheng, S., Hong, Y. X., et al. (2017). Sea Buckthorn (*Hippophae rhamnoides* L.) Oil Improves Atopic Dermatitis-Like Skin Lesions *via* Inhibition of NF-κB and STAT1 Activation. *Skin Pharmacol. Physiol.* 30 (5), 268–276. doi: 10.1159/000479528

Ishimoto, T., Azechi, K., and Mori, H. (2015). Identification of a Novel Protein Kinase A Inhibitor by Bioluminescence Based Screening. *Biol. Pharm. Bull.* 38, 1969–1974. doi: 10.1248/bpb.b15-00566

Ito, H., Asmussen, S., Traber, D.L., Cox, R.A., Hawkins, H.K., Connelly, R., et al. (2014) Healing efficacy of sea buckthorn (Hippophae rhamnoides L.) seed oil in an ovine burn wound model. *Burns* 40 (3), 511–519. doi: 10.1016/j.burns.2013.08.011

Jayashankar, B., Mishra, K. P., Kumar, M. S., Udayasankar, K., Misra, K., Ganju, L., et al. (2012). A supercritical CO_2 extract from seabuckthorn leaves inhibits pro-inflammatorymediators *via* inhibition of mitogen activated protein kinase p38 and transcription factor nuclear factor-κB. *Int. Immunopharmacol.* 13 (4), 461–467. doi: 10.1016/j.intimp.2012.05.011

Jayashankar, B., Mishra, K. P., Ganju, L., and Singh, S. B. (2014). Supercritical extract of Seabuckthorn Leaves (SCE200ET) inhibited endotoxemia by reducing inflammatory cytokines and nitric oxide synthase 2 expression. *Int. Immunopharmacol.* 20 (1), 89–94. doi: 10.1016/j.intimp.2014.02.022

Kim, E. J., Kim, M. K., Jin, X. J., Oh, J. H., Kim, J. E., and Chung, J. H. (2010). Skin aging and photoaging alter fatty acids composition, including 11,14,17-eicosatrienoic acid, in the epidermis of human skin. *J. Korean Med. Sci.* 25 (6), 980–983. doi: 10.3346/jkms.2010.25.6.980

Krejcarová, J., Straková, E., Suchý, P., Herzig, I., and Karásková, K. (2015). Sea buckthorn (*Hippophae rhamnoides* L.) as a potential source of nutraceutics and its therapeutic possibilities - A review. *Acta Vet. Brno* 84, 257–268. doi: 10.2754/avb201584030257

Kumar, R., Kumar, G. P., Chaurasia, O. P., and Singh, S. B. (2011). Phytochemical and pharmacological profile of Seabuckthorn oil: a review. *Res. J. Med. Plant* 5, 491–499. doi: 10.3923/rjmp.2011.491.499

Kupper, T. S., and Fuhlbrigge, R. C. (2004). Immune surveillance in the skin: mechanisms and clinical consequences. *Nat. Rev. Immunol.* Mar4 (3), 211–222. doi: 10.1038/nri1310

Lebwohl, M. (2003). Psoriasis. *Lancet* 361 (9364), 1197–1204. doi: 10.1016/S0140-6736(03)12954-6

Lee, J. Y., Plakidas, A., Lee, W. H., Heikkinen, A., Chanmugam, P., Bray, G., et al. (2003). Differential modulation of Toll-like receptors by fatty acids: preferential inhibition by n-3 polyunsaturated fatty acids. *J. Lipid Res.* 44 (3), 479–486. doi: 10.1194/jlr.M200361-JLR200

Lee, S., Gura, K. M., Kim, S., Arsenault, D. A., Bistrian, B. R., and Puder, M. (2006). Current clinical applications of Ω-6 and Ω-3 fatty acids. *Nutr. Clin. Pract.* 21 (4), 323–341. doi: 10.1177/0115426506021004323

Liu, Y. J. (2005). IPC: professional type 1 interferon-producing cells and plasmacytoid dendritic cell precursors. *Annu. Rev. Immunol.* 23, 275–306. doi: 10.1146/annurev.immunol.23.021704.115633

Lowes, M. A., Bowcock, A. M., and Krueger, J. G. (2007). Pathogenesis and therapy of psoriasis. *Nature* 445 (7130), 866–873. doi: 10.1038/nature05663

Ma, N., Tang, Q., Wu, W. T., Huang, X. A., Xu, Q., Rong, G. L., et al. (2018). Three Constituents of *Moringa oleifera* seeds regulate expression of Th17-relevant cytokines and ameliorate TPA-induced psoriasis-like skin lesions in mice. *Molecules* 23 (12), E3256. doi: 10.3390/molecules23123256

Madsen, M., Hansen, P. R., Nielsen, L. B., Hartvigsen, K., Pedersen, A. E., Christensen, J. P., et al. (2016). Effect of 12-O-tetradecanoylphorbol-13acetate-induced psoriasis-like skin lesions on systemic inflammation and atherosclerosis in hypercholesterolaemic apolipoprotein E deficient mice. *BMC Dermatol.* 16, 9. doi: 10.1186/s12895-016-0046-1

Martínez-Micaelo, N., González-Abuín, N., Pinent, M., Ardévol, A., and Blay, M. (2016). Dietary fatty acid composition is sensed by the NLRP3 inflammasome: omega-3 fatty acid (DHA) prevents NLRP3 activation in human macrophages. *Food Funct.* 7 (8), 3480–3487. doi: 10.1039/C6FO00477F

Moorchung, N., Kulaar, J. S., Chatterjee, M., Vasudevan, B., Tripathi, T., and Dutta, V. (2014). Role of NF-κB in the pathogenesis of psoriasis elucidated by its staining in skin biopsy specimens. *Int. J. Dermatol.* 53 (5), 570–574. doi: 10.1111/ijd.12050

Ogawa, E., Sato, Y., Minagawa, A., and Okuyama, R. (2018). Pathogenesis of psoriasis and development of treatment. *J. Dermatol.* 45 (3), 264–272. doi: 10.1111/1346-8138.14139

Redei, D., Kusz, N., Jedlinszki, N., Blazso, G., Zupko, I., and Hohmann, J. (2018). Bioactivity-Guided Investigation of the Anti-Inflammatory Activity of *Hippophae rhamnoides* Fruits. *Planta Med.* 84 (1), 26–33. doi: 10.1055/s-0043-114424

Richardson, S. K., and Gelfand, J. M. (2008). Update on the natural history and systemic treatment of psoriasis. *Adv. Dermatol.* 24, 171–196. doi: 10.1016/j.yadr.2008.09.006

Sakat, S. S., Mani, K., Demidchenko, Y. O., Gorbunov, E. A., Tarasov, S. A., Mathur, A., et al. (2014). Release-active dilutions of diclofenac enhance anti-inflammatory effect of diclofenac in carrageenan-induced rat paw edema model. *Inflammation* 37 (1), 1–9. doi: 10.1007/s10753-013-9705-0

Shi, J., Wang, L., Lu, Y., Ji, Y., Wang, Y., Dong, K., et al. (2017). Protective effects of seabuckthorn pulp and seed oils against radiation-induced acute intestinal injury. *J. Radiat. Res.* 58 (1), 24–32. doi: 10.1093/jrr/rrw069

Souza, C. O., Teixeira, A. A., Biondo, L. A., Silveira, L. S., Calder, P. C., and Rosa Neto, J. C. (2017). Palmitoleic acid reduces the inflammation in LPS-stimulated macrophages by inhibition of NFkappa-B, independently of PPARs. *Clin. Exp. Pharmacol. Physiol.* 44 (5), 566–575. doi: 10.1111/1440-1681.12736

Suchal, K., Bhatia, J., Malik, S., Malhotra, R. K., Gamad, N., Goyal, S., et al. (2016). Seabuckthorn pulp oil protects against myocardial ischemia-reperfusion injury in rats through activation of Akt/eNOS. *Front Pharmacol.* 7, 155. doi: 10.3389/fphar.2016.00155

Tanwar, H., Shweta, Singh, D., Singh, S. B., and Ganju, L. (2018). Anti-inflammatory activity of the functional groups present in *Hippophae rhamnoides* (Seabuckthorn) leaf extract. *Inflammopharmacology* 26 (1), 291–301. doi: 10.1007/s10787-017-0345-0

Virgolici, B., Lixandru, D., Casariu, E. D., Stancu, M., Greabu, M., Totanet, A., et al. (2013). Sea buckthorn pulp oil treatment prevents atherosclerosis in obese children. *ISRN Oxid. Med.* 164941, 9. doi: 10.1155/2013/164941

Wagner, E. F., Schonthaler, H. B., Guinea-Viniegra, J., and Tschachler, E. (2010). Psoriasis: what we have learned from mouse models. *Nat. Rev. Rheumatol.* 6 (12), 704–714. doi: 10.1038/nrrheum.2010.157

Wen, P., Zhao, P., Qin, G., Tang, S., Li, B., Zhang, J., et al. (2018). Genotoxicity and teratogenicity of seabuck thorn (*Hippophae rhamnoides* L.) berry oil. *Drug Chem. Toxicol.* 1, 7. doi: 10.1080/01480545.2018.1497047

World Health Organization. (2016). Global report on psoriasis. World Health Organization, Geneva, Switzerland. http://www.who.int/iris/handle/10665/204417.

Xing, J., Yang, B., Dong, Y., Wang, B., Wang, J., and Kallio, H. P. (2002). Effects of sea buckthorn (*Hippophae rhamnoides* L.) seed oil on burn wounds in rats. *Food Chem. Toxicol.* 47, 1146–1153. doi: 10.1016/j.fct.2009.02.002

Yang, B., and Kallio, H. (2002). Composition and physiological effects of sea buckthorn (Hippophae) lipids. *Trends Food Sci. Technol.* 13, 160–167. doi: 10.1016/S0924-2244(02)00136-X

Yang, G., Li, S., Yang, Y., Yuan, L., Wang, P., Zhao, H., et al. (2018). Nobiletin and 5-hydroxy-6,7,8,3',4'-pentamethoxyflavone ameliorate 12-O-Tetradecanoylphorbol-13-acetate- induced psoriasis-like mouse skin lesions by regulating the expression of Ki-67 and proliferating cell nuclear antigen and the differentiation of $CD4_+$ T cells through mitogen-activated protein kinase signaling pathways. *J. Agric. Food Chem.* 66 (31), 8299–8306. doi: 10.1021/acs.jafc.8b02524

Zeb, A. (2004). Important therapeutic ues of Sea Buckthorn (Hippophae): a review. *J. Biol. Sci.* 4 (5), 687–693. doi: 10.3923/jbs.2004.687.693

Zeb, A. (2006). Anticarcinogenic potential of lipids from Hippophae–evidence from the recent literature. *Asian Pac. J. Cancer Prev.* 7 (1), 32–35.

Zhao, P., Wang, S., Liang, C., Wang, Y., Wen, P., Wang, F., et al. (2017). Acute and subchronic toxicity studies of seabuckthorn (*Hippophae rhamnoides* L.) oil in rodents. *Regul. Toxicol. Pharmacol.* 91, 50–57. doi: 10.1016/j.yrtph.2017.10.002

Zielinska, A., and Nowak, I. (2017). Abundance of active ingredients in sea-buckthorn oil. *Lipids Health Dis.* 16 (1), 95. doi: 10.1186/s12944-017-0469-7

Conflict of Interest: The authors declare that the research was conducted in the absence of any commercial or financial relationships that could be construed as a potential conflict of interest.

IET Nanobiotechnology

Research Article

IET Journals
The Institution of Engineering and Technology

Green synthesis, characterisation and biological studies of AgNPs prepared using Shivlingi (*Bryonia laciniosa*) seed extract

ISSN 1751-8741
Received on 18th May 2017
Revised 10th November 2017
Accepted on 28th November 2017
E-First on 23rd February 2018
doi: 10.1049/iet-nbt.2017.0099
www.ietdl.org

Acharya Balkrishna[1,2], Niti Sharma[1] ✉, Vinay Kumar Sharma[1], Nayan Deep Mishra[1], Chandra Shekhar Joshi[1]

[1]*Drug Discovery & Development Division, Patanjali Research Foundation, Haridwar, Uttarakhand, India*
[2]*University of Patanjali, Haridwar, Uttarakhand, India*
✉ *E-mail: nitivinay@yahoo.co.in*

Abstract: Green synthesis of silver nanoparticles (AgNPs) using Shivlingi (*Bryonia laciniosa*) seed extract was carried out. Characterisation of synthesised nanoparticles was accomplished through the optical absorption and photoluminescence spectrum, X-ray diffraction (XRD), transmission electron microscopy (TEM), scanning electron microscopy (SEM), Fourier transform infrared spectroscopy (FTIR) and Raman spectroscopy. The XRD analysis further confirmed the size of nanoparticles ∼15 nm. TEM images revealed homogeneous spherical ∼10 nm *Bryonia* extract capped AgNPs. The biological studies indicated that both *Bryonia* seed extract and the nanoparticles lack anti-microbial activity; however, the nanoparticles had better cytotoxicity and total antioxidant activity. The Lethal concentration $(LC)_{50}$ value of water extract and the nanoparticles were found to be 1091 and 592 µg/ml, respectively. The lower LC_{50} of nanoparticles indicates that it is more cytotoxic than the crude extract. The results indicate that the *Bryonia* seed is safe to be used as a medicine and the formation of their nanoparticle has further enriched the chemical reactivity, energy absorption and biological mobility.

1 Introduction

Shivlingi known as *Bryonia laciniosa* Linn. (Cucurbitaceae) is categorised as *Vrishyarasayana* (for maintaining fertility and sexual performance) in Ayurveda. The seeds of *B. laciniosa* are important constituent of Ayurvedic formulation '*Striravallabhpugpak*' described in the ancient text to improve sexual behaviour and are traditionally being used as an aphrodisiac and reproductive tonic [1] and also possesses anti-inflammatory, anti-diabetic, anti-microbial, analgesic and anti-pyretic activities [2–5].

Green synthesis of nanoparticles is in vogue these days and the micro-organisms and plants are replacing expensive, energy consuming and potentially toxic chemical/physical methods for the production of nanoparticles. Plant synthesised green silver nanoparticles (AgNPs) are widely accepted as they are cost effective, bio-compatible and eco-friendly. The plant extracts contain various bio-molecules, which are relentlessly busy in the redox reactions. These reactions act as bio-reductants for metal ions or provide a platform to direct the formation of metallic nanoparticles in the solution after which the colour of solution changes. This is attributed to the surface plasmon resonance (SPR) phenomenon [6]. Owing to their distinctive properties, nanoparticles have a significant role in the field of medicine, biology, material science, physics and chemistry [7]. During last decade a number of research papers have been published on green AgNPs synthesised using various plants such as *Azadirachta indica* [8], *Cymbopogon flexuosus* [9], *Aloe vera* [10], *Camellia sinensis* [11], *Jatropha curcas* [12], *Acalypha indica* [13] as well as various other plant extracts [14].

B. laciniosa seeds have important medicinal properties as an Ayurvedic medicine but till date they have not been characterised in detail. Thus, in the present paper, we have synthesised the AgNPs using *B. laciniosa* seed extract and characterised them using optical absorption, photoluminescence, X-ray diffraction (XRD), scanning electron microscopy (SEM), transmission electron microscopy (TEM), Fourier transform infrared spectroscopy (FTIR) and Raman spectroscopy. The biological activity was also accessed to compare its anti-microbial as well as cytotoxic potential in both aqueous extract as well as in the synthesised nanoparticles.

2 Material and methods

2.1 Material

The seeds of *B. laciniosa* were gifted by Divya Pharmacy, Haridwar, India and stored in ambient conditions for further study. The other solvents and chemicals were purchased from Sigma-Aldrich and S.D. Fine Chemicals, India.

2.2 Methods

2.2.1 Preparation of extract: About 10 g of seeds were milled into a fine powder and boiled for 2 h in 100 ml of deionised water. The extract was filtered and refrigerated (4°C) for further experiments. In each and every step of the experiment, sterility conditions were maintained for the accuracy of the results.

2.2.2 Synthesis of AgNPs: In a typical reaction procedure, 5 ml of seed extract was added to 20 ml of 10^{-2} M aqueous Ag nitrate ($AgNO_3$) solution, the mixture was heated at 80°C for 1 h. Complete reduction of $AgNO_3$ to Ag^+ ions resulted in the colour change from yellowish to colloidal brown. The precipitate was collected by filtration, washed with deionised water several times and finally air dried at 60°C for 6 h.

2.2.3 Characterisation of nanoparticles: The prepared AgNPs were analysed and characterised using optical absorption (Shimadzu UVPC-1601 spectrophotometer, Japan), photoluminescence spectrum (PerkinElmer LS-55 luminance spectrophotometer, USA), crystalline metallic Ag was examined by XRD (Bruker D8 diffractometer, USA), scanning electron microscopy (SEM) (MIRA 3, TESCAN), TEM (TEM-TECHANI-20-G2), FTIR (Agilent Technologies Cary 630) and Raman spectroscopy (Deitanu Rock Hound Nuspec 2.0, USA).

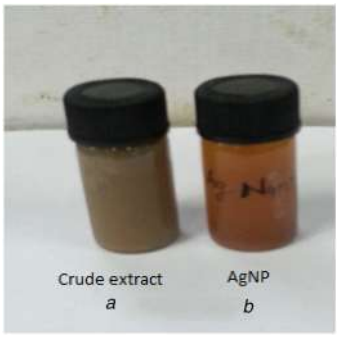

Fig. 1 *Colour change after the formation of AgNPs*
(a) *B. laciniosa* seed extract ***(b)*** After the formation of AgNPs

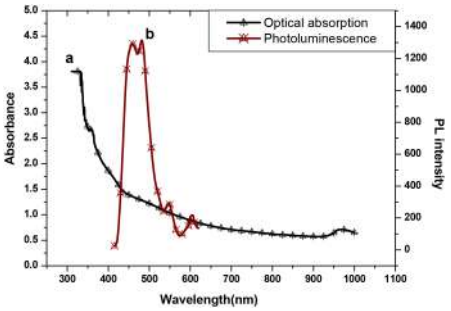

Fig. 2 *Optical absorption and photoluminescence spectrum*
(a) Optical absorption spectrum ***(b)*** Photoluminescence spectrum of AgNPs prepared using the aqueous seed extract of *B. laciniosa*

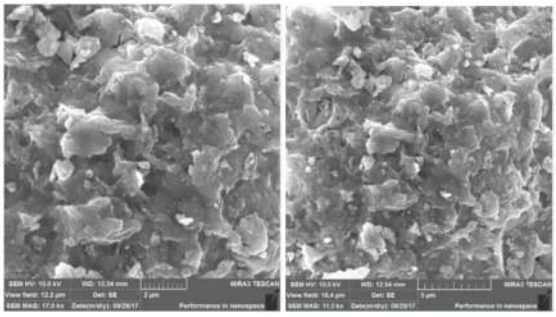

Fig. 3 *SEM image of AgNP clusters synthesised using B. laciniosa*

2.2.4 Anti-microbial activity: Test micro-organisms: The micro-organism used for the test were *Escherichia coli* (MCC226), *Pseudomonas aeruginosa* (MCC2035), *Staphylococcus aureus* (MCC2408), *Bacillus cereus* (MCC2128), *Aspergillus niger* (MCC1074) and *Candida albicans* (MCC1151) procured from NCL (Pune, India).

Experimentation: Nutrient agar plates were prepared and swabbed with bacterial strains by using sterilised cotton swabs. Sample loaded discs were placed on the bacterial strain containing nutrient agar plates. The plates were allowed for diffusion for 30 min and incubated for 24 h. Both positive control (PC) (tetracycline 100 mg/ml) and negative control (distiled water) were placed along with the sample loaded disc. After 24 h, inhibition zones were measured around the sample discs.

2.2.5 Total antioxidant activity: The total antioxidant capacity of the plant extract/fraction was evaluated as described [15]. The diluted sample solution was mixed with 3.0 ml of the reagent solution (600 mM sulphuric acid, 28 mM sodium phosphate and 4 mM ammonium molybdate). The reaction mixture was incubated at 95°C for 60 min and the absorbance was measured at 695 nm against a reagent blank.

2.2.6 Brine shrimp lethality assay: Brine shrimp (BS) eggs were obtained from the Lucky Extra^{TM} Artemia Cysts. The brine solution was prepared (3.8% sea salt solution) for hatching the shrimp eggs. The brine solution was put in a small plastic container with a partition for dark (covered) and light areas. The shrimp eggs were added to the dark side of the chamber. After 2 days, when the shrimp larvae (nauplii) were ready, brine and 15 BSs were introduced into each vial. The volume was adjusted to 5 ml with the brine and the vials were left uncovered under the lamp. The number of surviving shrimps was counted and recorded after 24 h [16].

The percentage mortality (%M) = number of dead nauplii/total number of nauplii × 100.

3 Result and discussion

3.1 Characterisation of AgNPs

The possible reason for bio-reduction of Ag^+ into metallic Ag might be its reaction with different bio-molecules present in the plant extract (e.g. reducing sugars, proteins, terpenoids, phenolic compounds etc.) [17]. The colour of the reaction mixture changed from yellowish to colloidal brown due to excitation of SPR vibration of AgNPs [6] (Fig. 1).

3.2 Optical absorption and photoluminescence spectrum

The optical absorption and photoluminescence spectrum of Ag nano-crystals were observed using the aqueous seed extract of *B. laciniosa* (Fig. 2). Curve (a) shows intense absorption peak of Ag nano-crystals at ∼420 nm with signs of surface plasmon states ∼ 460 nm. The peak positions of AgNPs in curve (b) exhibited a size dependent red shift but the surface state emission at wavelength ∼580 nm. The excitation wavelength for a AgNP with seed extract at 380 nm. The red shift indicates that the thin film of AgNPs consists of nano-crystals with an average radius smaller than the Bohr excitation radius. It means that the sample has a relatively narrow size distribution of ∼15 ± 5 nm [18].

3.3 Scanning electron microscopy analysis

Each of the colloidal solution containing AgNPs was centrifuged at 4000 rpm for 15 min, and the pellet was discarded and the supernatants were again centrifuged at 25,000 rpm for 30 min. This time, the supernatants were discarded and the final pellets were dissolved in 0.1 ml of deionised water. The pellet was mixed properly and carefully placed on a glass cover slip followed by air drying. The cover slip itself was used in Scanning electron microscopy analysis. The details regarding applied voltage, magnification used and size of the contents of the images were implanted on the images itself. The self-organised AgNP thin film gave rise to another interesting feature with smooth surface cluster (Fig. 3). The average smallest cluster size was measured as ∼400 nm, which is in good agreement with XRD and optical absorption spectroscopy results.

3.4 X-ray diffraction analysis

X-ray diffraction analysis of the prepared sample of AgNPs was done using a Bruker D8 diffractometer, Cu-Kα X-rays of wavelength $\lambda = 1.54056$ Å and data was taken for the 2θ range of 35–70° with a step of 0.02°. The X ray diffraction patterns of synthesised AgNPs revealed a crystalline, face-centred cubic geometry **(**Fig. 4**)**. The diffraction peaks obtained at $2\theta = 38.04°$ (111), 46.14° (200) and 63.13° (220) are identical with those reported for standard Ag metal (JCPDS, USA). Similarly, the diffraction pattern of AgNPs revealed the existence of peaks (111), (200) and (220) matched with the standard JCPDS data file # 04784 [19]. The synthesised AgNP had a normal size distribution of ∼15 ± 5 nm using Scherrer equation.

3.5 Transmission electron microscopy

A typical dark and bright field image of nano-crystals have been shown in Figs. 5*a* and *b*. The average particle size of the nano-crystals was estimated as ∼10 ± 2 nm, which is in good agreement with the XRD analysis results. The size distribution histogram of

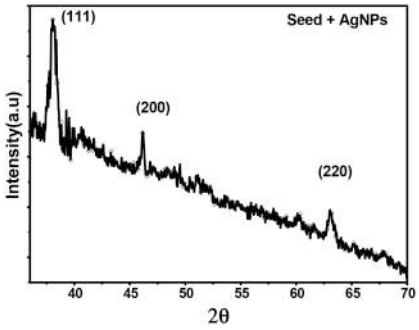

Fig. 4 *XRD patterns of AgNPs synthesised using B. laciniosa*

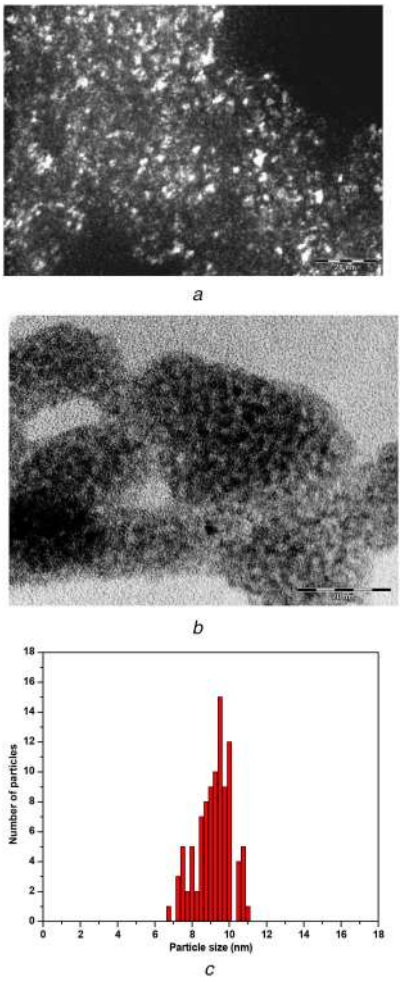

Fig. 5 *TEM image of AgNPs synthesised using B. laciniosa*
(a) Dark field TEM image, ***(b)*** Bright field TEM image, ***(c)*** Particle size distribution histogram of 8 nm AgNPs

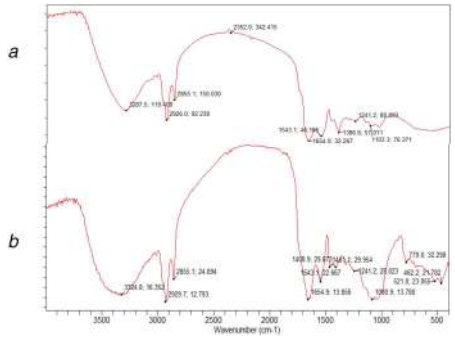

Fig. 6 *Fourier transformation infrared spectra*
(a) AgNPs derivatised *B. laciniosa* seed extract, ***(b)*** *B. laciniosa* seed extract

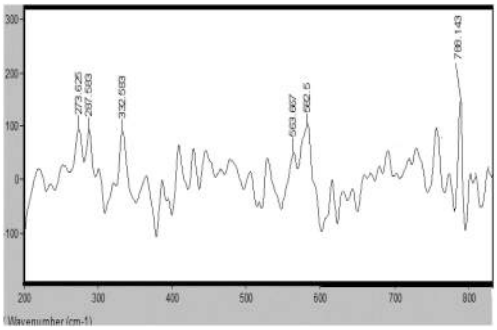

Fig. 7 *Raman Spectra of AgNPs synthesised by treating B. laciniosa seed extract with aqueous 10^{-2} M $AgNO_3$ solution*

nano-crystals has been shown in Fig. 5*c*. The TEM image revealed the homogeneous spherical shape of *Bryonia* extract (BE) capped AgNPs. It could be possible because of the capping agent that these AgNPs are showing spherical and clustered shape geometry [20].

3.6 Fourier transform infrared spectroscopy

The FTIR measurement was studied to identify the possible bio-molecules responsible as capping and reducing agent for the AgNPs synthesised by the extract (Fig. 6). The intense broad bands at 3324 and 2929 cm^{-1} are probably due to the O–H and C–H stretching modes, respectively. The AgNP derivatised extract did not show any band at 1080 cm^{-1}, whereas the original extract showed the prominent band at the same frequency indicating that the AgNPs have stabilised through the C–O bond. Similarly, the absence of a peak at 1408 cm^{-1} (C=C group) in the AgNP derivatised extract is probably due to the reduction of $AgNO_3$ to Ag [21].

3.7 Raman spectroscopic analysis

As an important technique Raman spectroscopy (Deitanu Rock Hound Nuspec 2.0) can be used to study chemical identification, characterisation of molecular structures, effects of bonding, environment and stress of the compounds. In Raman spectrum of the AgNP derivatised with *Bryonia* seeds, four intense peaks centred at 2 ± 7, 332, 582 and 788 cm^{-1} are evident (Fig. 7). Annealing at a high temperature induces dissolution of oxygen in the Ag. The peak at 560 cm^{-1} can be assigned to dissolve atomic oxygen in AgNPs. The bands at 582 and 788 cm^{-1} can be ascribed to the ν(Ag–O) vibrations for sub-surface species and ν(O–O) mode for adsorbed molecular oxygen.

Although, sub-surface species might promote adsorption of molecular oxygen, it could also be a probable consequence of surface restructuring in AgNPs [19, 20, 22].

3.8 Anti-microbial activity

Water extract and AgNPs of *B. laciniosa* seeds were analysed for anti-microbial activity using different bacterial and fungal strains. However, no clear zone of inhibition was observed in either case. This suggests that *B. laciniosa* seed extract lacks anti-microbial activity (Tables 1a and b). Similar results were obtained for seeds when researchers compared the anti-microbial activity of various parts of *B. laciniosa* [23]. The results obtained were in good agreement with Minimum Inhibitory Concentration (MIC)/ Minimum Bactericidal Concentration (MBC) tests, where the clear zone of inhibition was observed for AgNPs up to 10 nm size but not for larger nanoparticles [24]. Moreover, the release of Ag from large nanoparticles is stated to be lower in the solid culture media [25].

3.9 Total antioxidant activity

The total antioxidant activity of *B. laciniosa* seed extract was increased from 2.087 ± 1.02 to 3.33 ± 0.22 mg by the formation of AgNPs. The increased antioxidant activity of nanoparticles as

Table 1a Anti-microbial activity of *B. laciniosa* seed extract.

Micro-organism	Concentration (mg/ml)							
	10		30		60		100	
	BE (mm)	PC (mm)	BE (mm)	PC (mm)	BE (mm)	PC (mm)	BE (mm)	PC (mm)
E. coli	nil	31.9	nil	22.9	nil	26.0	nil	21.4
P. aeruginosa	nil	43.6	nil	45.6	nil	20.8	nil	37.4
S. aureus	nil	39.8	nil	38.2	nil	42.0	nil	35.2
B. cereus	nil	42.8	nil	40.7	nil	32.0	nil	41.8
A. niger	nil	42.5	nil	39.3	nil	32.6	nil	40.1
C. albicans	nil	16.6	nil	12.0	nil	9.2	nil	11.0

Table 1b Anti microbial activity of nanoparticles prepared using *B. laciniosa* seed extract.

Micro-organism	Concentration (mg/ml)							
	10		30		60		100	
	NP (mm)	PC (mm)	NP (mm)	PC (mm)	NP (mm)	PC (mm)	NP (mm)	PC (mm)
E. coli	nil	39.5	nil	35.0	nil	37.0	nil	38.5
P. aeruginosa	nil	42.3	nil	37.5	nil	40.0	nil	25.3
S. aureus	nil	46.4	nil	42.9	nil	36.3	nil	38.0
B. cereus	nil	41.3	nil	41.0	nil	40.4	nil	35.6
A. niger	nil	36.6	nil	44.4	nil	51.3	nil	46.7
C. albicans	nil	9.5	nil	11.5	nil	8.9	nil	8.9

BE = *Bryonia* extract; PC = positive control (tetracycline 100 mg/ml); NP = nanoparticle.

compared with the crude extract has been observed in a number of studies [26, 27]. AgNPs might act as electron donors, which transforms free radicals to the more stable product. Also, the reducing power of Ag nanoparticles is associated with the radical scavenging activity [28].

3.10 BS lethality assay

To study the pharmacological properties of *B. laciniosa* seed extract, BS lethality bioassay was performed which is based on the ability to kill laboratory cultured BS. In the present paper, different concentrations of *B. laciniosa* seed extract, as well as the synthesised nanoparticles, were used to access their cytotoxicity using BS lethality assay. The LC_{50} values of water extract (1091 μg/ml) and the nanoparticles (592 μg/ml) were calculated using Probit analysis. The lower LC_{50} of nanoparticles indicates that it is more cytotoxic than the crude extract. The criteria of toxicity followed was LC_{50} values >1000 μg/ml (non-toxic), ≥500≤1000 μg/ml (weak toxicity) and <500 μg/ml (toxic) [29, 30]. A significant lethality in BS assay is an indicator of effective cytotoxic constituents in the extract [31]. However, to explore the mechanism of cytotoxicity, various bio-active constituents have to be identified.

4 Conclusion

We have synthesised the AgNPs using the aqueous seed extract of *B. laciniosa* and characterised them using various techniques. All the analyses (optical absorption and photoluminescence spectrum, SEM, XRD, TEM, FTIR and Raman) confirmed the formation of AgNPs. The optical absorption showed an intense peak of Ag nano-crystals at 420 nm with signs of surface plasmon states near 460 nm. The self-organised AgNP thin film has indicated the smooth surface cluster having an average smallest cluster size of 400 nm. The XRD analysis further confirmed the size to be ∼15 ± 5 nm. TEM images revealed homogeneous ball shaped ∼10 ± 2 nm BE capped AgNPs. The Raman spectroscopy indicated that the bands at 582 and 788 cm^{-1} are due to the stretching of ν(Ag–O) vibrations for sub-surface species and stretching ν(O–O) mode for adsorbed molecular oxygen, which endorses the formation of AgNPs. The biological studies indicated that both *Bryonia* seed extract and the nanoparticles lack anti-microbial activity; however, the nanoparticles had better cytotoxicity and total antioxidant activity. The LC_{50} value of water extract and the nanoparticles were found to be 1091 and 592 μg/ml, respectively. The lower LC_{50} of nanoparticles indicates that it is more cytotoxic than the crude extract. This will be advantageous if it is ingested as a drug, because it may not harm microbial flora of the gut. In addition, the better total antioxidant activity and cytotoxicity of the nanoparticles to seed extract suggest an important role of nanoparticles in anticancer drug development.

5 Acknowledgments

We are thankful to Divya Pharmacy, Haridwar (India) for providing *Bryonia laciniosa* seeds for the study. We also gratefully acknowledge UGC-DAE Consortium for Scientific Research, Indore (India) for providing the facilities of recording the SEM, TEM, XRD and Raman spectra. Authors sincerely acknowledge Dr. L.N. Misra, Chief Research Advisor, Patanjali Research Foundation, Haridwar for his suggestions and expert guidance in improving the quality of the paper.

6 References

[1] Chauhan, N.S., Dixit, V.K.: 'Effects of *Bryonia laciniosa* seeds on sexual behaviour of male rats', *Int. J. Impot. Res.*, 2010, **22**, (3), pp. 190–195

[2] Gupta, M., Mazumdar, U.K., Sivakumar, T., *et al.*: 'Evaluation of anti-inflammatory activity of chloroform extract of *Bryonia laciniosa* in experimental animal models', *Biol. Pharm. Bull.*, 2013, **26**, (9), pp. 1342–1344

[3] Sivakumar, T., Perumal, P., Kumar, R.S., *et al.*: 'Evaluation of analgesic, antipyretic activity and toxicity study of *Bryonia laciniosa* in mice and rats', *Am. J. Chin. Med.*, 2004, **32**, (4), pp. 531–539

[4] Singh, V., Malviya, T., Tripathi, D.N., *et al.*: 'An *Escherichia coli* antimicrobial effect of arabinoglucomannan from fruit of *Bryonia laciniosa*', *Carbohydr. Polym.*, 2009, **75**, (3), pp. 534–537

[5] Patel, S.B., Santani, D., Patel, V., *et al.*: 'Anti-diabetic effects of ethanol extract of *Bryonia laciniosa* seeds and its saponins rich fraction in neonatallystreptozotocin-induced diabetic rats', *Pharmacognosy Res.*, 2015, **7**, pp. 92–99

[6] Ahmed, S., Ahmad, M., Swami, B.L., *et al.*: 'A review on plants extract mediated synthesis of silver nanoparticles for antimicrobial applications: a green expertise', *J. Adv. Res.*, 2016, **7**, (1), pp. 17–28

[7] Yokoham, K., Welchons, D.R.: 'The conjugation of amyloid beta protein on the gold colloidal nanoparticles surfaces', *Nanotechnology*, 2007, **18**, (10), pp. 105101–105107

[8] Shiv Shankar, S., Rai, A., Ahmad, A., *et al.*: 'Rapid synthesis of Au, Ag, and bimetallic Au core–Ag shell nanoparticles using neem (*Azadirachtaindica*) leaf broth', *Colloid Interface Sci.*, 2004, **275**, (2), pp. 496–502

[9] Shiv Shankar, S., Rai, A., Ahmad, A., *et al.*: 'Controlling the optical properties of lemongrass extract synthesized gold nano-triangles and potential application in infrared-absorbing optical coatings', *Chem. Mater.*, 2005, **17**, (3), pp. 566–572

[10] Chandran, S.P., Chaudhary, M., Pasricha, R., *et al.*: 'Synthesis of gold nano triangles and silver nanoparticles using *Aloe vera* plant extract', *Biotechnol. Prog.*, 2006, **22**, (2), pp. 577–583

[11] Vilchis-Nestor, A.R., Sánchez-Mendieta, V., Camacho-López, M.A., *et al.*: 'Solventless synthesis and optical properties of Au and Ag nanoparticles using *Camellia sinensis* extract', *Mater. Lett.*, 2008, **62**, (17–18), pp. 3103–3105

[12] Bar, H., Bhui, D.K., Sahoo, G.P., *et al.*: 'Green synthesis of silver nanoparticles using latex of *Jatropha curcas*', *Colloids Surf. A*, 2009, **339**, (1–3), pp. 134–139

[13] Krishnaraj, C., Jagan, E.G., Rajasekar, S., *et al.*: 'Synthesis of silver nanoparticles using *Acalyphaindica* leaf extracts and its antibacterial activity against water borne pathogens', *Colloids Surf B.*, 2010, **76**, (1), pp. 50–56

[14] Ghaffari-Moghaddam, M., Hadi-Dabanlou, R., Khajeh, M., *et al.*: 'Green synthesis of silver nanoparticles using plant extracts', *Korean J. Chem. Eng.*, 2014, **31**, (4), pp. 548–557

[15] Prieto, P., Pineda, M., Aguilar, M.: 'Spectrophotometric quantitation of antioxidant capacity through the formation of phosphomolybdenum complex: specific application to determination of vitamin E', *Anal. Biochem.*, 1999, **269**, pp. 337–341

[16] Lilybeth, F., Olowa, M., Olga, M.: 'Brine shrimp lethality assay of the ethanolic extracts of three selected species of medicinal plants from iligan city. Phil', *Int. Res. J. Biol. Sci.*, 2013, **2**, pp. 74–77

[17] Cooper, K.E.: 'The theory of antibiotic inhibition zones', in Kavanageh, F. (Ed.): '' (Academic Press, New York, 1963), pp. 1–86

[18] Wang, R.P., Xu, G., Jin, P.: 'Size dependence of electron-phonon coupling in ZnO nanowires', *Phy. Rev. B.*, 2004, **69**, pp. 113303–113306

[19] Liang, H., Li, Z., Wang, W., *et al.*: 'Highly surface-roughened flower-like silver nanoparticles for extremely sensitive substrates of surface-enhanced Raman scattering', *Adv. Mater.*, 2009, **21**, (45), pp. 4614–4618

[20] de Álvaro, J., Ruíz, B., Simón, Y., *et al.*: 'Green synthesis of silver nanoparticles using a *Melissa officinalis* leaf extract with antibacterial properties', *Results Phys.*, 2017, **7**, pp. 2639–2643

[21] Yan, H., Zhiyun, D., Huibin, L.V., *et al.*: 'Green synthesis of silver nanoparticles by *Chrysanthemum morifolium* Ramat. Extract and their application in clinical ultrasound gel', *Int. J. Nanomed.*, 2013, **8**, pp. 1809–1815

[22] Ethiraj, A.S., Jayanthi, S., Ramalingam, C., *et al.*: 'Control of size and antimicrobial activity of green synthesized silver nanoparticles', *Mater. Lett.*, 2016, **185**, pp. 526–529

[23] Ehsan, B.R., Vital, A., Bipinraj, N.K.: 'Antimicrobial activity of the ethanolic extract of *Bryonopsislaciniosa* leaf, stem, fruit and seed', *Afr. J. Biotechnol.*, 1972, **8**, (15), pp. 3565–3567

[24] Agnihotri, S., Mukherji, S.: 'Size-controlled silver nanoparticles synthesized over the range 5–100 nm using the same protocol and their antibacterial efficacy', *RSC Adv.*, 2014, **4**, pp. 3974–3983

[25] Xiu, Z.M., Zhang, Q.B., Puppala, H.L., *et al.*: 'Negligible particle-specific antibacterial activity of silver nanoparticles', *Nano. Lett.*, 2012, **12**, pp. 4271–4275

[26] Dipankar, C., Murugan, S.: 'The green synthesis, characterization and evaluation of the biological activities of silver nanoparticles synthesized from *Iresineherbstii* leaf aqueous extracts', *J. Colloids Surf. B, Biointerfaces*, 2012, **98**, pp. 112–119

[27] Velavan, S., Arivoli, P., Mahadevan, K.: 'Biological reduction of silver nanoparticles using *Cassia auriculata* flower extract and evaluation of their *in vitro* antioxidant activities', *Nanosci. Nanotechnol., Int. J.*, 2012, **2**, (4), pp. 30–35

[28] Khan, A.U., Wei, Y., Khan, Z.U.H., *et al.*: 'Electrochemical and antioxidant properties of biogenic silver nanoparticles', *Int. J. Electrochem. Sci.*, 2015, **10**, pp. 7905–7916

[29] Bastos, M.L.A., Lima, M.R.F., Conserva, L.M., *et al.*: 'Studies on the antimicrobial activity and brine shrimp toxicity of *Zeyheria tuberculosa* (Vell.) Bur. (Bignoniaceae) extracts and their main constituents', *Ann. Clin. Microbiol. Antimicrob.*, 2009, **28**, pp. 16–22

[30] Déciga-Campos, M., Rivero-Cruz, I., Arriaga-Alba, M., *et al.*: 'Acute toxicity and mutagenic activity of Mexican plants used in traditional medicine', *J. Ethnopharmacol.*, 2007, **110**, pp. 334–342

[31] Meyer, B.N., Ferrigni, N.R., Putnam, J.E., *et al.*: 'Brine shrimp; a convenient general bioassay for active plant constituents', *Plant Med.*, 1982, **45**, pp. 31–34